Genetic and chemogenetic investigation of the circuits underlying schizophrenia-related behaviours in mice

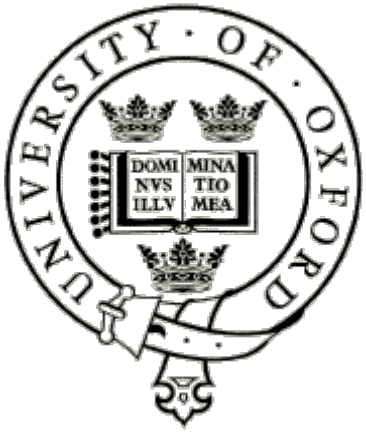

ALEXEI BYGRAVE

A thesis submitted for the degree of Doctor of Philosophy

Department of Physiology, Anatomy and Genetics

Wolfson College

University of Oxford

Michaelmas Term, 2016

For Ayesha

Abstract

Alexei Bygrave, Wolfson College, D.Phil, Michaelmas Term, 2016

Genetic and chemogenetic investigation of the circuits underlying schizophrenia-related behaviours in mice

Multiple neurotransmitter systems have been implicated in the pathophysiology of schizophrenia. In particular, changes in the GABAergic and glutamatergic system could be upstream to changes in the dopamine system, and also responsible for the cognitive and negative symptoms of the disease.

This thesis has utilised genetic models of glutamatergic dysfunction, both globally in mice lacking the GluA1 AMPAR subunit (*Gria1* KO), and in a circuit specific manner in mice lacking the NR1 NMDAR subunit specifically in parvalbumin (PV) positive interneurons (*Grin1*$^{\Delta PV}$). In addition, the chemogenetic DREADD silencer hM4Di was used to transiently and specifically silence PV positive interneurons *in vivo*. These genetic and chemogenetic manipulations have been used in combination with behavioural assays that could assess schizophrenia-relevant behaviours in rodents.

Grin1$^{\Delta PV}$ animals were found to be largely normal when tested for schizophrenia-relevant behavioural abnormalities. However, when *Grin1*$^{\Delta PV}$ animals were challenged with the NMDAR antagonist MK-801 (commonly used to pharmacologically model glutamatergic dysfunction) there was clear behavioural divergence between *Grin1*$^{\Delta PV}$ and control animals. In contrast to previous reports, *Grin1*$^{\Delta PV}$ mice appeared to be sensitised to the effects of MK-801. This has important implications for the understanding of how NMDAR antagonists can induce schizophrenia-relevant behavioural deficits in rodents.

Hypofunction of PV interneurons, particularly in the hippocampus, is predicted to underlie schizophrenia-relevant behavioural deficits. To directly test this, hM4Di was expressed in PV interneurons in the dorsal or ventral hippocampus, preferentially in area CA1. Despite the fact that hM4Di was capable of reducing the excitability of PV interneurons *in vitro*, there was no evidence that silencing of PV interneurons in CA1 *in vivo* could induce the predicted behavioural deficits.

Gria1 KO mice have a well established behavioural phenotype that could be relevant to schizophrenia. A viral-rescue approach was utilised to reintroduce GluA1 preferentially into area CA3 of the hippocampus of *Gria1* KO animals. This was sufficient to rescue novelty induced hyperactivity and spatial novelty preference but not spatial working memory in *Gria1* KO animals. Recordings of local field potentials (LFP) in the dorsal hippocampus revealed enhanced theta power oscillations in *Gria1* KO mice. This elevated theta power was also rescued by GluA1 re-introduction into area CA3 of *Gria1* KO mice.

Together these experiments question the hypothesis that NMDAR antagonists preferentially exert their effects through NMDARs on PV interneurons. In addition, with respect to schizophrenia-related behavioural deficits, hypofunction of PV interneurons in area CA1 of the hippocampus might not be be as critical as hypofunction of PV interneurons in other circuits. Finally, area CA3 of the hippocampus is implicated as a brain region in which GluA1 expression appears particularly important for some behaviours relevant to schizophrenia.

Acknowledgements

The work in this thesis would not have been possible if it were not for the support I have received during the last 4 years. In particular, I would like to thank my three D.Phil. supervisors; David Bannerman (Oxford), Dennis Kätzel (Oxford, now Ulm) and Dimitri Kullmann (UCL). I am also incredibly grateful to the Wellcome Trust and the OXION studentship that has funded this project.

I thank David for his constant support throughout my D.Phil. project and for always finding the time to discuss ideas and issues that I have had along the way. I owe all of my (limited!) knowledge of behavioural testing to you!

I thank Dennis for the limitless enthusiasm, energy and also financial contribution he has brought to this project. I have never met somebody as hard working as Dennis and without his contribution and encouragement far less would have been achieved during my D.Phil. project.

I would also like to thank Amy Wolff for her support, scientific contribution to this project and establishment of the lifeline that is the “T-maze sanity” Spotify playlist. But more importantly for the friendship and support she has given me throughout my time in Oxford, especially during my write up process.

I would like to thank members of the Bannerman lab for their support during my D.Phil. In particular Amy Taylor, for teaching me how to conduct behavioural experiments, Steve McHugh for scientific input and advice, Thomas Jahans-Price for help with electrophysiology analysis and Marios Panagi for advice about statistics.

I would also like to say a special thanks to Thomas Börner for his friendship and constant source of optimism (sorry I could not resist…) throughout my D.Phil. and more importantly(!) for originally introducing me to the wonders of the T-maze.

I am grateful to members of the Behavioural Neuroscience Unit, in particular to Katie Hewitt for accommodating my frequent last minute room bookings! I would also like to thank the BSB animal technicians and NACWOs, in particular Carol and Debbie.

I also thank Elizabeth Nicholson, Simonas Masiulis, Michelle Berkemann for their contribution to the work presented in chapters 2 and 3. In addition, I am also very grateful to Chris Barkus, for his advice regarding many of the behavioural tasks used in this thesis.

I would also like to thank Ed Mann and Pantelis Antonoudiou for their help and advice. Pantelis performed the patch clamp recordings presented in chapter 4 to validate the hM4Di DREADD construct for which I am very grateful.

I thank Paul Harrison for his input into this project, particularly in helping turn chapters 2 and 3 into a manuscript.

I thank Thomas Akam for his scientific input and advice but also for introducing me to bouldering!

I thank Luiz Guidi for being an all round good guy and helping with all things antibody related!

I thank Louise Upton for teaching me immunohistochemistry, for scientific discussions and for being supportive throughout my time in Oxford.

I thank Dimitrios Kotzadimitriou for discussions about all things PV and NMDAR related!

I would like to thank my family for their constant support and encouragement throughout my life.

Finally, I would like to thank my girlfriend Ayesha Sengupta. You can’t know how much your love and support has helped me over the years, and I can’t express how lucky I am to have you in my life.

Table of contents

ABSTRACT ..... **III**

ACKNOWLEDGEMENTS ..... **V**

TABLE OF CONTENTS ..... **VI**

ABBREVIATIONS ..... **XI**

TABLE OF FIGURES ..... **XIII**

GENERAL INTRODUCTION **1**

1.1 SCHIZOPHRENIA **1**

1.1.1 Prevalence of schizophrenia *1*

1.1.2 Symptoms of schizophrenia *1*

1.1.3 Genetics of schizophrenia *2*

1.1.4 How to study schizophrenia? *3*

1.2 NEUROBIOLOGY OF SCHIZOPHRENIA **4**

1.2.1 Dopamine hypothesis of schizophrenia *4*

1.2.2 Glutamate hypothesis of schizophrenia *6*

1.2.3 GABAergic hypothesis of schizophrenia *8*

1.3 OSCILLATIONS AND SYNCHRONY **11**

1.3.1 Importance of gamma oscillations *11*

1.3.2 Generation of gamma oscillations *12*

1.3.3 Long range synchrony in neuronal oscillations *13*

1.3.4 Slow oscillations and schizophrenia *15*

1.4 THE HIPPOCAMPUS **16**

1.4.1 The Hippocampus and schizophrenia *16*

1.4.2 Hippocampal formation circuitry *16*

1.4.3 What is the function of the hippocampus? *18*

1.5 IONOTROPIC GLUTAMATE RECEPTORS IN THE CNS **20**

1.5.1 Structure of NMDARs *20*

1.5.2 NMDAR subunits and stoichiometry *21*

1.5.3 Alternative splicing of NMDARs *22*

1.5.4 NMDARs and synaptic plasticity *22*

1.5.5 NMDAR antagonists *24*

1.5.6 Structure of AMPARs *24*

1.5.7 Alternative splicing of AMPARs *25*

1.5.8 RNA editing of AMPAR subunits *26*

1.5.9 Subunit stoichiometry of AMPARs *27*

1.5.10 AMPARs and synaptic plasticity *27*

1.6 BEHAVIOURAL TESTS IN RODENTS RELEVANT TO SCHIZOPHRENIA **29**

1.6.1 Behavioural tasks in rodents relevant to positive symptoms *29*

1.6.2 Behavioural tasks in rodents relevant to negative symptoms *30*

1.6.3 Behavioural tasks in rodents relevant to cognitive symptoms *32*

1.7 GENETIC STRATEGIES TO STUDY GENE FUNCTION **35**

1.8 "ANIMAL MODELS" OF SCHIZOPHRENIA **37**

1.8.1 Dopamine based animal "models" *38*

1.8.2 Glutamate based genetic animal "models" *39*
1.8.3 Glutamate based pharmacological animal "models" *41*
1.8.4 GABAergic based animal "models" *43*

1.9 TOOLS FOR MANIPULATING NEURONAL ACTIVITY **46**

1.10 VIRAL APPROACHES TO TARGET NEURONAL CIRCUITS **47**
1.10.1 Using adeno-associated viruses to target neurons *48*

1.11 AIMS OF THE THESIS **49**
1.11.1 Chapter 2 aims *49*
1.11.2 Chapter 3 aims *50*
1.11.3 Chapter 4 aims *51*
1.11.4 Chapter 5 aims *51*

2 BEHAVIOURAL PHENOTYPE OF *GRIN1*$^{\Delta PV}$ MICE **54**

2.1 INTRODUCTION **54**
2.1.1 The Lisman/Grace model *54*
2.1.2 Testing the Lisman/Grace model *57*
2.1.3 Chapter 2 experimental aims *59*

2.2 METHODS **60**
2.2.1 Breeding of animals *60*
2.2.2 Immunohistochemistry *61*
2.2.3 In vitro patch clamp recordings *63*
2.2.4 Behavioural studies *63*
2.2.5 Novelty-induced locomotor activity *64*
2.2.6 Pre-pulse inhibition *64*
2.2.7 Elevated plus maze *65*
2.2.8 Sucrose preference *66*
2.2.9 Nest building *66*
2.2.10 Social recognition memory *67*
2.2.11 Novel object recognition (object short-term memory) *68*
2.2.12 Spatial novelty preference *68*
2.2.13 Rewarded alternation on the T-maze *69*
2.2.14 Spatial reference memory and reversal learning *70*
2.2.15 Statistical analysis *71*

2.3 RESULTS **72**
2.3.1 Efficient and specific targeting of PV interneurons *72*
2.3.2 Validation of NMDAR ablation in Grin1$^{\Delta PV}$ *knockouts* *73*
2.3.3 Age-dependent novelty-induced hyperactivity in Grin1$^{\Delta PV}$ *mice* *74*
2.3.4 Normal pre pulse inhibition in Grin1$^{\Delta PV}$ *mice* *76*
2.3.5 Normal sucrose preference in Grin1$^{\Delta PV}$ *mice* *77*
2.3.6 Reduced anxiety in young Grin1$^{\Delta PV}$ *mice* *79*
2.3.7 Normal nest building in Grin1$^{\Delta PV}$ *mice* *81*
2.3.8 Normal social interaction and social memory in Grin1$^{\Delta PV}$ *mice* *82*
2.3.9 Intact novel object recognition in Grin1$^{\Delta PV}$ *mice* *84*
2.3.10 Normal spatial novelty preference in Grin1$^{\Delta PV}$ *mice* *86*
2.3.11 Normal spatial working memory in Grin1$^{\Delta PV}$ *mice* *89*
2.3.12 Intact spatial reference memory and reversal learning in Grin1$^{\Delta PV}$ *mice* *93*

2.4 DISCUSSION **96**
2.4.1 Grin1$^{\Delta PV}$ *mice and positive symptoms* *97*
2.4.2 Grin1$^{\Delta PV}$ *mice and cognitive symptoms* *98*

2.4.3 Grin1$^{\Delta PV}$ mice and negative symptoms 102
2.4.4 Conclusions 103

3 NMDAR ANTAGONIST STUDIES IN *GRIN1*$^{\Delta PV}$ MICE 106

3.1 INTRODUCTION 106
3.1.1 Disinhibition following NMDAR challenge 106
3.1.2 PV NMDAR KO protects from MK-801-induced hyperactivity 107
3.1.3 Chapter 3 experimental aims 108

3 METHODS 110
3.2.1 Breeding of animals 110
3.2.2 Drugs 110
3.2.3 Locomotor activity: MK-801 challenge 110
3.2.4 Motor coordination: MK-801 challenge 111
3.2.5 Spatial working memory: MK-801 challenge 111
3.2.6 Sucrose preference: MK-801 challenge 112
3.2.7 Surgery for electrode implantation 112
3.2.8 Electrophysiology: MK-801 challenge 113
3.2.9 Electrophysiology recordings 113
3.2.10 Histology 114
3.2.11 Statistical analysis 114

3.3 RESULTS 115
3.3.1 Grin1$^{\Delta PV}$ mice show an attenuated locomotor response to acute MK-801 challenge 115
3.3.2 Grin1$^{\Delta PV}$ mice display a pronounced flat-posture and stereotypies following MK-801 challenge 121
3.3.3 Grin1$^{\Delta PV}$ mice are sensitised to MK-801 induced motor coordination impairments 123
3.3.4 Grin1$^{\Delta PV}$ mice are sensitised to anhedonia induced by MK-801 128
3.3.5 Grin1$^{\Delta PV}$ mice are sensitised to MK-801 induced SWM deficits 131
3.3.6 Induction of prominent 3-5 Hz oscillations in Grin1$^{\Delta PV}$ mice following MK-801 challenge 136

3.4 DISCUSSION 141
3.4.1 MK-801-induced hyperlocomotion in control and Grin1$^{\Delta PV}$ mice 141
3.4.2 MK-801-induced flat-state and stereotypies in Grin1$^{\Delta PV}$ mice 141
3.4.3 Impaired motor coordination in MK-801-challenged Grin1$^{\Delta PV}$ mice 143
3.4.4 Grin1$^{\Delta PV}$ mice are sensitised to MK-801 induced anhedonia 143
3.4.5 Grin1$^{\Delta PV}$ mice are sensitised to cognitive impairing effects of MK-801 144
3.5.6 Induction of slow oscillations in Grin1$^{\Delta PV}$ mice 145
3.5.7 Conclusions 146

4 CHEMOGENETIC SILENCING OF PARVALBUMIN POSITIVE INTERNEURONS 149

4.1 INTRODUCTION 149
4.1.1 GABAergic dysfunction in schizophrenia 149
4.1.2 Circuit based models of GABAergic dysfunction 150
4.1.3 Tools to study neuronal circuits 151
4.1.4 Chapter 4 experimental aims 153

4.2 METHODS 154
4.2.1 Breeding of animals 154
4.2.2 Virus constructs 154
4.2.3 Surgery 154
4.2.4 Immunohistochemistry 155

4.2.5 In vitro patch clamp recordings 156
4.2.6 Drugs 157
4.2.7 Behavioural testing 157

4.3 RESULTS 158
4.3.1 Successful targeting of PV neurons with hM4Di 159
4.3.2 Expression of hM4Di in dorsal or ventral CA1 160
4.3.3 Efficient targeting of PV interneurons at the virus injection site 163
4.3.4 In vitro validation of DREADD mediated PV interneuron silencing 165
4.3.5 Silencing of PV interneurons in dorsal and ventral hippocampus does not induce hyperactivity 168
4.3.6 Silencing of PV interneurons in dorsal and ventral hippocampus does not impair spatial novelty preference 170
4.3.7 Silencing of PV interneurons in dorsal or ventral hippocampus does not impair spatial working memory 172
4.3.8 Silencing PV interneurons throughout the hippocampus can induce seizures 175

4.4 DISCUSSION 177
4.4.1 hM4Di is able to reduce the excitability of PV interneurons in vitro 177
4.4.2 hM4Di-mediated PV interneuron silencing in dorsal or ventral CA1 does not induce hyperactivity 179
4.4.3 hM4Di-mediated PV interneuron silencing in dorsal or ventral CA1 does not induce cognitive deficits 180
4.4.4 Targeting of PV interneurons in the dorsal and ventral hippocampus cohorts 183
4.4.5 Do PV interneurons outside of the hippocampus contribute to schizophrenia like behavioural deficits? 184
4.4.6 Conclusions 185

5 RESCUE OF BEHAVIOURAL AND PHYSIOLOGICAL ABNORMALITIES IN *GRIA1* KO MICE WITH GLUA1 RE-INTRODUCTION TO AREA CA3 186

5.1 INTRODUCTION 186
5.1.1 Role of Gria1 for plasticity 186
5.1.2 Gria1 and schizophrenia 186
5.1.3 Synaptic plasticity and behaviour of Gria1 KO mice 187
5.1.4 Gria1 KO as a mouse model of psychological processes relevant to schizophrenia 188
5.1.5 Where in the brain is GluA1 needed for short term memory? 190
5.1.6 In vivo electrophysiology in Gria1 KO animals 191
5.1.7 Chapter 5 experimental aims 192

5.2 METHODS 193
5.2.1 Generation of Gria1 KO mice 193
5.2.2 Design and synthesis of Gria1 rescue virus 193
5.2.3 Surgery (virus injection and electrode implantation) 194
5.2.4 Immunohistochemistry 196
5.2.5 Locomotor activity testing 197
5.2.6 Electrophysiology recordings 197
5.2.7 Calculation of theta power 198
5.2.8 T-maze rewarded alternation test 198
5.2.9 Y-maze novelty preference test 199

5.3 RESULTS 200
5.3.1 Viral re-introduction of GluA1 was limited to area CA3 of the hippocampus 200
5.3.2 Viral re-introduction of GluA1 to area CA3 throughout the hippocampus 203
5.3.3 Hyperactivity is rescued in Gria1 KO rescue mice 204

5.3.4 Enhanced theta power in the dorsal hippocampus of Gria1 KO mice is rescued with re-introduction of GluA1 to area CA3 206
5.3.5 Re-introduction of GluA1 to area CA3 in Gria1 KO mice does not rescue SWM on the T-maze 211
5.3.6 Re-introduction of GluA1 to area CA3 rescues spatial novelty preference in Gria1 KO mice 214

5.4 DISCUSSION 219
5.4.1 Preference of AAV5-hSyn-GluA1 virus for area CA3 220
5.4.2 Viral re-introduction of GluA1 to area CA3 of Gria1 KO mice rescues novelty induced hyperactivity 221
5.4.3 Viral re-introduction of GluA1 to area CA3 of Gria1 KO mice fails to rescue SWM on the T-maze 222
5.4.4 Viral re-introduction of GluA1 to area CA3 of Gria1 KO mice rescues spatial novelty preference. 223
5.4.5 Viral re-introduction of GluA1 to area CA3 of Gria1 KO mice normalises theta power 225
5.4.6 Conclusions 227

6 GENERAL DISCUSSION 229
6.1 Chapter 2 summary: "Normal" phenotype of Grin1$^{\Delta PV}$ mice 229
6.2 Chapter 3 summary: Grin1$^{\Delta PV}$ mice appear sensitised to the effects of MK-801 232
6.3 Chapter 4 summary: Acute silencing of PV interneurons does not induce schizophrenia-relevant behavioural deficits 235
6.4 Chapter 5 summary: re-introduction of GluA1 to area CA3 of Gria1 KO mice rescues some schizophrenia-relevant behaviours 237
6.5 How do experiments in this thesis fit within the Lisman/Grace framework? 239
6.6 General considerations for the role of NMDARs on PV interneurons for gamma oscillation generation 241
6.7 Do PV interneurons contribute to gamma oscillations in area CA1? 242
6.8 Conclusions 244

7 APPENDIX 245

7.1 SPECIFICITY TESTING OF PPP1R2^{CRE} DRIVER LINE 245
7.1.1 Ppp1r2^{cre} line targets pyramidal neurons as early as 16 weeks of age 245

7.2 NMDAR ANTAGONIST STUDIES IN *GRIN1*$^{\Delta PV}$ MICE 247
7.2.1 MK-801 influence on choice latency on the T-maze in control and Grin1$^{\Delta PV}$ mice 247
7.2.2 Location of electrodes in Grin1$^{\Delta PV}$ mice 250

7.3 ELECTROPHYSIOLOGY AND BEHAVIOUR IN *GRIA1* KO MICE 251
7.3.1 Electrode placements in prefrontal cortex and ventral hippocampus 251
7.3.2 Potential rescue of SWM in female Gria1 KO rescue animals 252

8 BIBLIOGRAPHY 255

Abbreviations

AAV	Adeno-associated virus
ADAR2	Adenosine deaminase acting on RNA 2
AIS	Axon initial segment
AMPAR	α-amino-3-hydroxy-5-methyl-4-isoxazolepropionic acid receptor
AP5	2-amino-5-phosphonopentanoic acid
ASR	Auditory startle response
BDNF	Brain derived neurotrophic factor
BOLD	Blood oxygen level-dependent
CA	*Cornu ammonis*
CaMKII	Ca^{2+}/calmodulin-dependent protein kinase II
CNO	Clozapine-N-oxide
CNS	Central nervous system
DG	Dentate gyrus
DLPFC	Dorsal lateral prefrontal cortex
Dox	Doxycycline
DREADDs	Designer receptors activated exclusively by designer drugs
EEG	Electroencephalogram
ES	Embryonic stem
GABA	Gamma-aminobutyric acid
GAD67	Glutamic acid decarboxylase isoform 67
GAT1	GABA membrane transporter 1
GFP	Green fluorescent protein
GlyT1	Glycine transporter 1
GPCRs	G-Protein Coupled Receptors
GWAS	Genome wide association study
hSyn	Human synapsin 1
ING	Interneuron network gamma
KO	Knockout
LFP	Local field potentials
LSD	Least significant difference
LTD	Long term depression
LTP	Long term potentiation
MAM	Methylazoxymethanol acetate
MK-801	Dizocilpine
MRI	Magnetic resonance imaging
MS	Medial septum
MWM	Morris water maze
NAA	M-acetyl aspartate
NAAG	N-acetylaspartylglutamte
neo	Neomycin
NMDAR	N-Methyl-D-Aspartate receptor
NOR	Novel object recognition
PB	Phosphate buffer
PBS	Phosphate buffered saline

PCP	Phencyclidine
PCR	Polymerase chain reaction
PING	Pyramidal interneuron network gamma
PKA	Protein kinase A
PV	Parvalbumin
PVBC	Parvalbumin positive basket cell
PVChC	Parvalbumin positive chandelier cell
SDS-PAGE	Sodium dodecyl sulfate - polyacrylamide gel electrophoreses
SNP	Spatial novelty preference
SRM	Spatial reference memory
STP	Short term potentiation
SWM	Spatial working memory
TrkB	Tropomyosin-related kinase B
TTX	Tetrodotoxin
UR	Unconditioned response
UTR	Untranslated region
VTA	Ventral tegmental area
WPRE	Woodchuck hepatitis virus post- transcriptional regulatory element

Table of figures

FIGURE 1.1: SCHEMATIC EXPLANATION OF THE THETA/GAMMA CODE 12
FIGURE 1.2: PRINCIPLE OF NEURONAL "COMMUNICATION THROUGH COHERENCE" 13
FIGURE 1.3: TRI-SYNAPTIC CIRCUITRY OF THE HIPPOCAMPUS 17
FIGURE 1.4: SCHEMATIC REPRESENTATION OF THE STRUCTURE OF AN NMDAR 21
FIGURE 1.5: SCHEMATIC REPRESENTATION OF AN INDIVIDUAL AMPAR SUBUNIT AND THE ASSEMBLED CHANNEL 25
FIGURE 1.6: SCHEMATIC DEMONSTRATION OF *CRE/LOXP* MEDIATED GENE DELETION 36
FIGURE 2.1: SPECIFICITY TESTING OF PV^{CRE} DRIVER LINE 73
FIGURE 2.2: CONFIRMATION OF NMDAR ABLATION *IN VITRO* 74
FIGURE 2.3: AGE DEPENDENT NOVELTY INDUCED HYPERACTIVITY IN *GRIN1*$^{\Delta PV}$ MICE 76
FIGURE 2.4: NORMAL PRE PULSE INHIBITION IN *GRIN1*$^{\Delta PV}$ MICE 77
FIGURE 2.5: NORMAL SUCROSE PREFERENCE IN *GRIN1*$^{\Delta PV}$ MICE 79
FIGURE 2.6: REDUCED ANXIETY IN YOUNG *GRIN1*$^{\Delta PV}$ MICE 81
FIGURE 2.7: NORMAL NEST BUILDING IN *GRIN1*$^{\Delta PV}$ MICE 82
FIGURE 2.8: NORMAL SOCIAL INTERACTION AND SOCIAL MEMORY IN *GRIN1*$^{\Delta PV}$ MICE 83
FIGURE 2.9: INTACT NOVEL OBJECT RECOGNITION IN *GRIN1*$^{\Delta PV}$ MICE 86
FIGURE 2.10: NORMAL SPATIAL NOVELTY PREFERENCE IN *GRIN1*$^{\Delta PV}$ MICE 88
FIGURE 2.11: LARGELY NORMAL SPATIAL WORKING MEMORY IN *GRIN1*$^{\Delta PV}$ MICE 92
FIGURE 2.12: NORMAL SPATIAL REFERENCE MEMORY AND REVERSAL LEARNING IN *GRIN1*$^{\Delta PV}$ MICE 95
FIGURE 3.1: ATTENUATED LOCOMOTOR RESPONSE IN $GRIN1^{\Delta PV}$ MICE FOLLOWING MK-801 CHALLENGE 120
FIGURE 3.2: INDUCTION OF STEREOTYPIES AND FLAT-STATE IN *GRIN1*$^{\Delta PV}$ MICE FOLLOWING MK-801 CHALLENGE 122
FIGURE 3.3: MK-801 IMPAIRS MOTOR COORDINATION IN $GRIN1^{\Delta PV}$ MICE 127
FIGURE 3.4: *GRIN1*$^{\Delta PV}$ MICE ARE SENSITISED TO ANHEDONIA INDUCING EFFECTS OF MK-801 130
FIGURE 3.5: *GRIN1*$^{\Delta PV}$ MICE ARE SENSITISED TO THE COGNITIVE IMPAIRING EFFECTS OF MK-801 134
FIGURE 3.6: INDUCTION OF SLOW OSCILLATIONS IN *GRIN1*$^{\Delta PV}$ MICE FOLLOWING MK-801 CHALLENGE 139
FIGURE 4.1: SUCCESSFUL TARGETING OF PV NEURONS WITH HM4DI 160
FIGURE 4.2: TARGETING OF DORSAL HIPPOCAMPUS WITH HM4DI-MCHERRY 161
FIGURE 4.3: TARGETING OF VENTRAL HIPPOCAMPUS WITH HM4DI-MCHERRY 163
FIGURE 4.4: EFFICIENT TRANSFECTION OF PV INTERNEURONS AT THE VIRUS INJECTION SITE 165
FIGURE 4.5: HM4DI CAN REDUCE EXCITABILITY OF PV INTERNEURONS *IN VITRO* 167
FIGURE 4.6: SILENCING OF PV INTERNEURONS IN DORSAL AND VENTRAL HIPPOCAMPUS DOES NOT INDUCE HYPERACTIVITY 169
FIGURE 4.7: SILENCING OF PV INTERNEURONS IN DORSAL OR VENTRAL HIPPOCAMPUS DOES NOT IMPAIR SPATIAL NOVELTY PREFERENCE 172
FIGURE 4.8: SILENCING OF PV INTERNEURONS IN THE DORSAL OR VENTRAL HIPPOCAMPUS DOES NOT IMPAIR SPATIAL WORKING MEMORY 175
FIGURE 4.9: EXPRESSION OF HM4DI-MCHERRY IN PV INTERNEURONS THROUGHOUT THE HIPPOCAMPUS 176
FIGURE 5.1: GLUA1 VIRUS CAN REINTRODUCE GLUA1 IN AN AREA CA3 SPECIFIC MANNER IN *GRIA1* KO MICE 202
FIGURE 5.2: VIRAL EXPRESSION OF GLUA1 THROUGHOUT THE HIPPOCAMPUS OF A *GRIA1* KO MOUSE 204
FIGURE 5.3: VIRAL EXPRESSION OF GLUA1 PREFERENTIALLY INTO AREA CA3 OF *GRIA1* KO MICE RESCUES NOVELTY INDUCED HYPERACTIVITY 205
FIGURE 5.4: ELEVATED THETA POWER IN DORSAL HIPPOCAMPUS OF *GRIA1* KO MICE IS RESCUED WITH AREA CA3 RE-INTRODUCTION OF GLUA1 210
FIGURE 5.5: RE-INTRODUCTION OF GLUA1 TO AREA CA3 OF *GRIA1* KO MICE DOES NOT RESCUE SWM ON THE T-MAZE 212
FIGURE 5.6: AREA CA3 RE-INTRODUCTION OF GLUA1 IN *GRIA1* KO MICE RESTORES SHORT TERM SPATIAL NOVELTY PREFERENCE 217
FIGURE 7.1: RECOMBINATION IN PYRAMIDAL NEURONS IN 16 WEEKS OLD PPP1R2-AI9 MICE 246
FIGURE 7.2: CHOICE TRIAL LATENCIES ON THE T-MAZE FOLLOWING MK-801 CHALLENGE 249
FIGURE 7.3: ESTIMATES OF ELECTRODE PLACEMENT IN CONTROL AND *GRIN1*$^{\Delta PV}$ MICE 250
FIGURE 7.4: ESTIMATES OF ELECTRODE PLACEMENT IN CONTROL AND *GRIA1* KO MICE 252
FIGURE 7.5: SWM COULD BE PARTIALLY RESCUED IN FEMALE *GRIA1* KO RESCUE ANIMALS 253

General introduction

1.1 Schizophrenia

1.1.1 Prevalence of schizophrenia

Schizophrenia is a debilitating disease that affects around 1% of the population (Picchioni and Murray, 2007). The disease has a huge cost, both to the quality of the patients' life, and also economically to society (Wu et al. 2005). Diagnosis of schizophrenia is based on symptoms rather than biological changes, largely because we **do not** understand the underlying biology in the disorder. This lack of understanding probably explains why we have not seen significantly improved antipsychotic drugs for over 50 years (Carpenter and Davis, 2012; Hyman, 2012).

1.1.2 Symptoms of schizophrenia

Symptoms of schizophrenia have been categorised into three main groups, consisting of positive, negative, and cognitive symptoms (Mueser and McGurk, 2004). Positive symptoms of schizophrenia are so named because they are *additional* to what is present in healthy individuals. Positive symptoms include hallucinations and delusions. Negative symptoms are so named because they are *lacking* in schizophrenia patients compared to healthy individuals. Negative symptoms include blunted affect (reduced emotional response), anhedonia (inability to find pleasure from activities that are usually pleasurable) and a lack of motivation. Cognitive symptoms include deficits in working memory, attention and cognitive flexibility. Phenotypically there is a large overlap between symptoms of schizophrenia, autism and bipolar disorder and it has been suggested that the diagnostic boundaries separating these psychiatric disorders are largely arbitrary (Carroll and Owen, 2009). In addition, genetic studies indicate that there is considerable overlap between schizophrenia,

autism and bipolar disorders raising the possibility that common biological pathways are involved in the disorders (Carroll and Owen, 2009).

Current antipsychotic drugs can help to alleviate positive symptoms of schizophrenia in some, but not all, patients. However, antipsychotic drugs are generally considered to be less efficacious at treating negative and cognitive symptoms (Hill et al. 2010; King et al. 1998). Interestingly, cognitive impairments can be observed long before diagnosis of schizophrenia (O`Carroll, 2000). Since cognitive symptoms of schizophrenia correlate with the functional outcome of the disease (O`Carroll, 2000), there remains an urgent need for improved treatments in this domain.

1.1.3 Genetics of schizophrenia

A clear genetic component of schizophrenia exists. The risk of developing schizophrenia is increased to 6.5 % in first degree relatives of patients (Kendler et al., 1993), and this risk is increased to 40 % in identical (monozygotic) twins (Picchioni and Murray, 2007). The genetic component of schizophrenia has been assessed with many genome wide association studies (GWAS). The most notable being a GWAS study in 2014 that assessed over 36,000 schizophrenia cases and over 113,000 controls (Ripke et al., 2014, 2013). Interestingly, of the 108 loci that were found to be significantly associated with schizophrenia, a number are located close to genes that relate to synaptic plasticity and glutamatergic and dopaminergic systems (Ripke et al., 2014). Such GWAS studies highlight the heterogeneity of schizophrenia, with identified single nucleotide polymorphism each conferring only a small increased risk of the disease (Harrison, 2015). It is clear that mutations in single genes do not lead to schizophrenia, so these genetic studies do not provide us with single genes in which to target. However, the convergence of risk factors associated with particular signalling pathways (i.e. glutamatergic signalling) highlight potential opportunities for therapeutic

intervention at “druggable” targets within these signalling pathways (Harrison, 2015). Changes in the glutamatergic system that could be relevant to schizophrenia is a main focus of this thesis.

1.1.4 How to study schizophrenia?

Schizophrenia is a highly complex disease. To better understand the underlying pathophysiology of schizophrenia we need to study the disease at various different levels, from molecular and cellular changes through to dysfunction of neuronal circuits and behaviour. Beyond that we want to understand the psychological processes that are driving the symptoms of the disease. Whilst we cannot replicate schizophrenia as such in rodents, we *can* study basic mechanisms relating to molecular, cellular, neuronal circuit and behavioural changes. This thesis is interested in how molecular changes in the glutamate system can give rise to altered neuronal circuit function, and ultimately changes in behaviours that are thought to rely on psychological processes relevant to schizophrenia.

This introduction will start by summarising the main hypotheses of schizophrenia, based on different neurotransmitter systems. Then neuronal circuit dysfunction in schizophrenia will be discussed in the context of abnormal local field potential oscillations and neuronal synchrony between brain regions. The function of the hippocampus will then be covered, as this is a brain region which could be particularly relevant in schizophrenia. Zooming in to the molecular level, ionotropic glutamate receptors will be discussed in detail as molecular changes in these receptors have been reported in schizophrenics. Rodent behavioural tests that are relevant to schizophrenia will then be scrutinised, followed by an explanation of different genetic strategies available for generating mutant mice to study gene function. The concept of animal models of schizophrenia will then be explored, with examples given based on

the different hypotheses of schizophrenia. Additional tools available to study the function of neuronal circuits will then be discussed, including the use of viruses to express transgenes in rodents. Finally, the aims of this thesis will be outlined.

1.2 Neurobiology of schizophrenia

The neurobiology of schizophrenia is poorly understood and is thought to involve multiple neurotransmitter systems (Howes and Kapur, 2009; Lisman et al., 2008). Hypotheses involve the dopamine, glutamate and GABAergic systems will be discussed in turn.

1.2.1 Dopamine hypothesis of schizophrenia

The dopamine hypothesis of schizophrenia has been revised several times over the years. Initial excitement about the role of dopamine in schizophrenia came from the observation that neuroleptic (antipsychotic) drugs used in the treatment of schizophrenia, have in common that they act upon dopamine receptors, especially those of type 2 (D2). In 1975, the stimulated release of dopamine from acute striatal slices (from rat brain) was assessed, with and without incubation of a variety of neuroleptic drugs. Such drugs were shown to block dopamine release from brain slices (Seeman and Lee, 1975). The IC_{50} of each drug (the concentration of drug required to block dopamine release by 50%) was strongly correlated with the clinical dose at which each neuroleptic drug is effective (Seeman and Lee, 1975). The fact that all known antipsychotic drugs blocked dopamine receptors, whilst improving some symptoms of the disease, strongly suggested that a hyperdopaminergic state was, at least partly, involved in the pathophysiology of schizophrenia (Seeman et al., 1976; Seeman and Lee, 1975). This formed the basis of the original dopamine hypothesis of schizophrenia.

This basic model was then revised and regional specificity was assigned to changes in dopamine levels. A hyperdopaminergic state was assigned to the striatum but a hypodopaminergic state was attributed to the frontal cortex (Davis et al., 1991). Cortical *hypodopaminergia*, as it became known, was argued to underlie the negative deficits in schizophrenia, whilst striatal *hyperdopaminergia* was linked to positive symptoms of the disease (Davis et al., 1991).

In 2009, the dopamine hypothesis was revisited again and a new proposal made by Howes and Kapur (Howes and Kapur, 2009). The article was entitled "The dopamine hypothesis of schizophrenia: version III- The final common pathway", but the authors concede a suitable title would also have been "Dopamine hypothesis of psychosis-in-schizophrenia". In this model, the idea that dopamine is responsible for all facets of schizophrenia is dropped, and the importance of other neurotransmitter systems, such as glutamate and gamma-aminobutyric acid (GABA), is highlighted, especially with respect to cognitive and negative symptoms (Howes and Kapur, 2009). The evidence remains strong for striatal hyperdopaminergia, but this is considered in the context of psychosis, rather than schizophrenia as a whole. There is good evidence that psychosis correlates with elevated striatal dopamine. However, schizophrenia is not characterised by psychosis alone (Howes and Kapur, 2009).

Dopamine has been proposed to mediate the salience of stimuli which when dysfunctional could underlie psychosis (Kapur, 2003). In 2003, Kapur proposed that psychosis arises due to aberrant salience, as a consequence of a hyperdopaminergic state (Kapur, 2003). When aberrant salience occurs, stimuli (both external and internal), that under normal circumstances would not be considered motivationally important, have abnormal additional salience befitted upon them. This can be a gradual process, which likely progresses through the prodromal phase of

schizophrenia (Kapur, 2003). The consequence of these aberrant saliences can be delusions, as a result of the patient trying to make sense of these stimuli that now carry additional motivational salience (Kapur, 2003). Antipsychotic drugs are proposed to dampen down this “aberrant salience”, and as a result decrease positive symptoms of the disease (Howes and Kapur, 2009).

To summarise, the latest version of the dopamine hypothesis of schizophrenia states that striatal hyperdopaminergia is important in the development of psychosis, likely due to its role in the attribution of aberrant salience to stimuli (Howes and Kapur, 2009). The hypothesis also highlights that there are a number of environmental and biological “risk factors” for striatal hyperdopaminergia, accounting for the accumulating evidence of environmental risk factors in schizophrenia (Howes and Kapur, 2009). In fact, “the final common pathway” element of the hypothesis suggests the convergence of number of risk factors/primary insults that together can induce striatal hyperdopaminergia. The hypothesis also suggests other neurotransmitter systems are likely involved, especially with regard to negative and cognitive symptoms of the disease (Howes and Kapur, 2009).

1.2.2 Glutamate hypothesis of schizophrenia

The glutamate hypothesis of schizophrenia, or more commonly, the *N-methyl-D-aspartate receptor* (*NMDAR) hypofunction* hypothesis of schizophrenia, was established after observations that abuse of the NMDAR antagonist phencyclidine (PCP) can induce symptoms similar to those observed in schizophrenia (Luby et al., 1959; Javitt and Zukin, 1991). In later studies, healthy volunteers challenged with ketamine (another NMDAR antagonist) also developed acute symptoms similar to the positive, negative and cognitive symptoms of schizophrenia (Krystal et al., 1994). In addition (in a seemingly unethical study), ketamine challenge to schizophrenia

patients (whose condition was stabilised with antipsychotic drugs), caused reinstatement of their symptoms (Lahti et al., 1995). Together, these studies established that NMDAR hypofunction was likely involved in the pathophysiology of schizophrenia.

Post mortem studies have found evidence for elevated levels of N-acetylaspartylglutamate (NAAG) in the brains of schizophrenia patients (Tsai et al., 1995). NAAG is an endogenous antagonist of NMDARs, thus an increase in NAAG is consistent with hypofunction of NMDARs (Tsai et al., 1995). Interestingly, another endogenous antagonist of NMDARs, known as kynurenic acid, is also elevated in the brains of schizophrenia patients (Schwarcz et al., 2001). In addition, in the prefrontal cortex there is evidence for reduced expression of the NMDAR subunit GluN2A (previously referred to as NR2A) in parvalbumin (PV) positive interneurons (Bitanihirwe et al., 2009).

Taken together, there is substantial evidence for NMDAR hypofunction in schizophrenia. This has prompted a number of clinical trials with agents to boost NMDAR function but although some have shown promising signs of improving treatment resistant negative symptoms, as of yet none have made it to the clinic (Coyle, 2012). One such example is the development of glycine transporter 1 (GlyT1) inhibitors (Harvey and Yee, 2013). Glycine is a co-agonist at NMDARs and is required (in combination with glutamate) to activate NMDARs (see **1.5.2**). GlyT1 re-uptakes glycine from the synapse, maintaining sub-saturating synaptic concentrations and thus limiting NMDAR mediated neurotransmission (Harvey and Yee, 2013). Inhibition of GlyT1 could therefore boost NMDAR transmission. Clinical trials with GlyT1 inhibitors are currently ongoing (Harvey and Yee, 2013). The most advanced candidate drug, bitopertin, was successful in Phase II trials, but failed to reduce negative symptoms

significantly in two subsequent Phase III trials, after which the remaining Phase III trials in schizophrenia were cancelled (Bugarski-Kirola et al., 2014; Umbricht et al., 2014).

It would be incomplete to discuss NMDAR hypofunction in schizophrenia without mention of the special role that inhibitory interneurons might play. This is central to the Lisman/Grace model of the pathophysiology of schizophrenia, and is discussed in detail later (see **1.8.3** and **2.1.1**).

Non-NMDA glutamate receptors have also been implicated in schizophrenia. For example, the α-amino-3-hydroxy-5-methyl-4-isoxazolepropionic acid receptor (AMPAR) subunit GluA1 was recently linked to schizophrenia in the largest GWAS study to date (Ripke et al., 2014, 2013). Identification via GWAS does not provide evidence that the biological function of GluA1 is changed. However, previous post-mortem work has also indicated that the expression of GluA1 is decreased in the hippocampus of schizophrenic patients, independent of effects of neuroleptic treatment (Eastwood et al., 1997, 1995). Therefore, there is growing evidence that changes in the glutamatergic system, both NMDAR- and AMPAR-related, occur in schizophrenia. Animal studies have also helped to bolster the glutamate hypothesis of schizophrenia. Data from animal studies are discussed in detail later (see **1.8.2** and **1.8.3**).

1.2.3 GABAergic hypothesis of schizophrenia

Gamma-aminobutyric acid (GABA) is the main inhibitory neurotransmitter in the CNS. There is post mortem evidence for changes in the GABAergic system in schizophrenia. A key idea is that there could be reduced GABAergic signalling from particular populations of interneurons.

One of the most consistent post mortem findings in schizophrenia is reductions in glutamic acid decarboxylase isoform 67 (GAD67), an enzyme involved in the synthesis of GABA (Akbarian et al., 1995). In particular, loss of GAD67 seems to occur in parvalbumin (PV) positive interneurons (Hashimoto et al., 2003). PV is a calcium (Ca^{2+}) binding protein, which "buffers" the intracellular levels of Ca^{2+}. The reuptake of GABA could also be compromised, as levels of GABA membrane transporter 1 (GAT1) are also reduced in the brains of schizophrenics (Volk et al., 2001). After release, GABA is recycled into the neuron terminal by GAT1, so loss of GAT1 is expected to increase levels of GABA at the synapse. This has been proposed to be a compensatory mechanism through which GABAergic signalling can be increased (Lewis et al. 2005). Loss of GAD67 and GAT1 would therefore compromise both the synthesis and re-uptake of GABA respectively. In addition, there also seems to be a reduction in the expression of PV in schizophrenics, whilst the absolute number of PV interneurons remains unchanged (Hashimoto et al., 2003). The decrease in PV expression is expected to decrease the activity of the interneuron, by decreasing the amount of PV there is to buffer intracellular Ca^{2+} (Lisman et al., 2008). Decreased expression of GAD67 has mostly been reported in the dorsal lateral prefrontal cortex (DLPFC), but has also been found in the hippocampus (Benes et al., 2007).

GABAergic synapses onto excitatory pyramidal neurons also seem to differ in schizophrenia. Fast inhibition is mediated by ionotropic $GABA_A$ receptors (Jacob et al., 2008). The $\alpha 2$ subunit is of particular interest, since it forms $GABA_A$ receptors with particularly fast kinetics, that are enriched in synapses onto the axon initial segment (AIS) of pyramidal neurons (Jacob et al., 2008; Nusser et al., 1996). Interestingly, in the DLPFC, there is a large increase in the immunoreactivity of the $\alpha 2$ subunit in schizophrenia (Volk et al., 2002). Changes in the expression of the $\alpha 2$ subunits have

been attributed to compensatory mechanisms, where the postsynaptic neuron is trying to boost GABAergic signalling in the environment of compromised GABAergic neurotransmission (Lewis et al., 2005). These postsynaptic changes in $GABA_A$ receptor expression seem to be specific to GABAergic synapses onto pyramidal neurons from chandelier neurons, which are PV positive, and provide inhibition to the AIS (Somogyi et al., 1985).

What causes the loss of GAD67 in schizophrenia? There are different hypotheses for how this could occur. The expression of GAD67 is activity dependent (Lau and Murthy, 2012), so reduced excitatory input to PV interneurons could explain the decreased expression observed in schizophrenia. The Lisman/Grace model argues that NMDAR hypofunction specifically on PV interneurons reduces excitatory drive onto these cells (Lisman et al., 2008; see **2.1.1**). However, alternative explanations exist, where decreased excitation of DLPFC could stem from reduced excitatory input from the mediodorsal thalamus or hippocampus (Lewis et al., 2005). Indeed, in an animal "model" of schizophrenia in which the ventral hippocampus is lesioned in neonatal rodents, there is reduced expression of GAD67 in the PFC (Lipska et al., 2003). Another possible mechanism through which GAD67 levels could be decreased is via reduced tropomyosin-related kinase B (TrkB) signalling (Lewis et al., 2005). TrkB signalling, activated by brain derived neurotrophic factor (BDNF), increases the expression of GAD67, GAT1 and also parvalbumin (Lewis et al., 2005; Yamada et al., 2002). Levels of BDNF and TrkB appear to be reduced in the DLPFC in schizophrenics, providing a possible mechanism for the reduced expression of GAD67, GAT1 and PV (Hashimoto, 2005; Weickert et al., 2003). It is interesting that PV expressing interneurons seem to be affected in schizophrenia, since these neurons are thought to play a critical role in the generation of fast (30 – 100 Hz)

oscillations in the local field potential (LFP) known as gamma oscillations (see **1.3.1** and **1.3.2**).

1.3 Oscillations and synchrony

1.3.1 Importance of gamma oscillations

The transmembrane flow of ions leads to voltage fluctuations that can be measured extracellularly as changes in the local field potential (LFP). Synaptic activity is a major contributor to the LFP, but it is important to highlight that **any** flow of ions (independent of the kinetics) will contribute to the LFP (Buzsáki et al., 2012). Rhythmic oscillations in the LFP reflect the coordinated activity of neurons and can be observed at frequencies that span many orders of magnitude. These include delta oscillations (1 - 4 Hz), theta oscillations (5 - 12 Hz) and fast gamma oscillations (30 - 80 Hz).

Gamma oscillations are thought to be important for a number of cognitive processes (Lisman, 2005; Lisman and Jensen, 2013) and are known to be disrupted in schizophrenia. In particular, altered gamma oscillations potentially underlie cognitive deficits of the disease (Gandal et al., 2012; Lisman, 2005; Uhlhaas and Singer, 2010). The power of gamma oscillations has been shown to positively correlate with working memory load in humans (Howard et al., 2003). In addition, a “theta/gamma code” has been proposed, whereby gamma oscillations (30 - 100 Hz) are nested within slower theta (5 - 12 Hz) cycles (Lisman, 2005; Lisman and Jensen, 2013). The theta/gamma code enables the packaging of information into discrete gamma cycles. For example, an ensemble of neurons that encode “item A” will fire during a different gamma cycle compared to neurons encoding “item B” (see **figure 1.1**) (Lisman and Jensen, 2013).

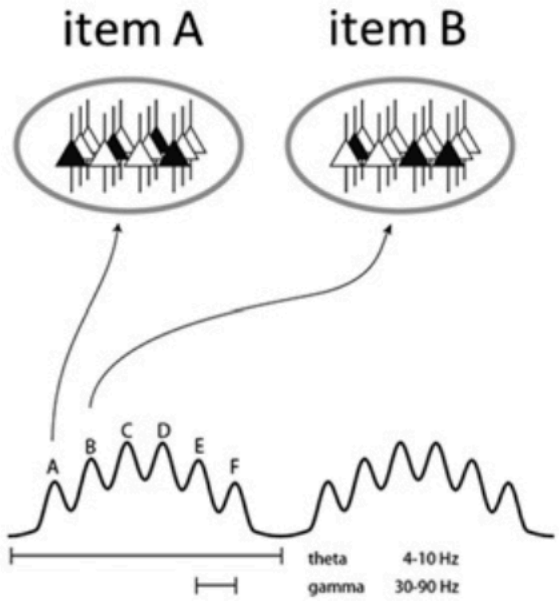

Figure 1.1: Schematic explanation of the theta/gamma code
Gamma oscillations are nested within slower theta oscillations. The gamma cycles per theta cycle are labelled (a-f). These individual cycles could help to segregate the encoding of information. For example, an ensemble of neurons that encode item A (indicated by black shaded cell bodies) fire on a different gamma cycle to those that encode item B. Figure taken from Lisman and Jensen 2013.

1.3.2 Generation of gamma oscillations

The generation of gamma oscillations requires coordinated activity between excitatory and inhibitory neurons. Mechanisms of gamma oscillations have been extensively studied both *in vivo* and *in vitro*.

Fast perisomatic inhibition of pyramidal neurons by PV positive basket cells is known to play a critical role in the generation of gamma oscillations *in vitro* (Mann et al., 2005). Furthermore, artificially driving PV neurons (using optogenetic activation) in cortical circuits has been shown to entrain the network with gamma oscillations *in vivo* (Cardin et al., 2009). This was not the case when excitatory pyramidal neurons were artificially driven at the same frequency (Cardin et al., 2009). In a complementary study, optogenetic silencing of PV neurons significantly reduced the power of gamma

oscillations in the cortex (Sohal et al., 2009). Together, these studies provide powerful evidence for the role of PV neurons in the generation of gamma oscillations.

1.3.3 Long range synchrony in neuronal oscillations

Network oscillations could play an important role in aiding the communication between different brain structures. When two populations of neurons oscillate, with a fixed phase shift, they are said to be coherent. Oscillations transiently modulate the excitability of neurons, making them more or less sensitive to input, and influencing their ability to spike, providing a mechanism which could be used to selectively route information flow (Fries, 2005).

Neurons are hardwired to a complex network of other neurons via fixed anatomical connections. How can a neuron communicate preferentially with a particular subgroup of neurons to which it is anatomically connected? The basic principle is that coherence creates brief windows where the presynaptic neuron (the sender) can transmit information when the postsynaptic neuron (the receiver) is maximally excitable, and poised to receive the message (Fries, 2005; see **figure 1.2**).

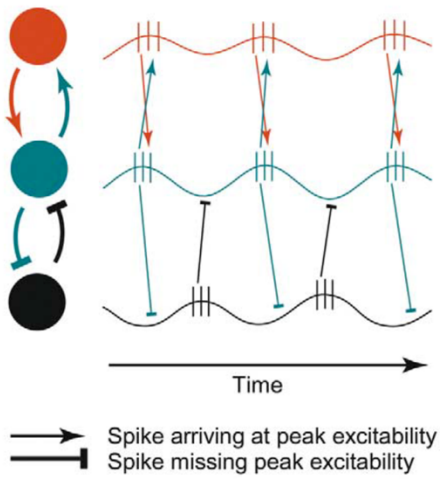

Figure 1.2: Principle of neuronal "communication through coherence"

This schematic shows three neurons (red, green, black), with pairs that are connected reciprocally. The oscillation of each neuron is indicated via the sigmoidal lines, with spikes shown by vertical lines. In this example the red and green neurons are able to effectively communicate with one another, since their spikes arrive when the other neuron is at its peak excitability (indicated by arrows). In contrast, the green and black neurons are unable to effectively communicate with each other, as their spikes arrive as the other neuron is at its least excitable (blunt arrows). Taken from Fries *et al.* 2005.

Theta frequency coherence has been implicated in routing information between the medial prefrontal cortex and hippocampus (Jones and Wilson, 2005), two brain regions known to be important in spatial working memory (SWM) in rodents (Deacon et al., 2002; Floresco et al., 1997; Wang and Cia, 2006). During performance of a SWM task in rodents, theta frequency coherence between the medial prefrontal cortex and dorsal hippocampus is prominent and increases at the choice point where animals have to make a decision (Jones and Wilson, 2005; O'Neill et al., 2013; Sigurdsson et al., 2010).

Anatomically the human neocortex is conventionally divided into four "lobes". These consist of the frontal lobe, parietal lobe, occipital lobe and temporal lobe. Long range synchrony between frontal and temporal lobes is reduced in schizophrenia patients whilst talking (Ford et al., 2002). In addition, there is impaired prefrontal to hippocampal coherence in several rodent "models" of schizophrenia (Dickerson et al., 2010; Sigurdsson et al., 2010). Decreased prefrontal-hippocampal coherence at theta and gamma frequency is correlated with deficits in spatial working memory (SWM) performance (Sigurdsson et al., 2010) and impaired pre-pulse inhibition (PPI) (Dickerson et al., 2010) respectively. Thus, disrupted long range synchrony in animal "models" of schizophrenia correlates with behavioural performance and replicates observations of decreased coherence in schizophrenia patients (Ford et al., 2002).

1.3.4 Slow oscillations and schizophrenia

In addition to changes in high frequency (gamma) oscillations, slow (1 - 5 Hz) delta oscillations also appear to be dysregulated in schizophrenia. A meta analysis identified increased power of delta oscillations in schizophrenia that were also present in non-medicated patients (Boutros et al., 2008; Galderisi et al., 2009). Delta oscillations are most prominent during non-rapid eye movement sleep, and are thought to arise from the highly coordinated transitions of cortical neurons between UP (periods of depolarisation, with irregular firing of neurons) and DOWN (periods of hyperpolarisation, where firing of neurons is ceased) states (Vyazovskiy et al., 2007). As delta oscillations are associated with sleep, their increased prominence in schizophrenia has led to the suggestion that the brain enters an "inactive sleep-like state" whilst patients are awake (Lisman, 2012). The increased slow-oscillations are most prominent in the medial ventral prefrontal cortex (Schulman et al., 2011). Delta oscillations are thought to reduce metabolic demand, so it is interesting that the blood oxygenation level-dependent (BOLD) signal in healthy volunteers administered with ketamine also decreases in the medial ventral prefrontal cortex (Deakin et al., 2008). This is in contrast to other regions of the brain in which NMDAR antagonists such as ketamine increase the BOLD signal, consistent with the hypothesis that NMDARs antagonists lead to an overall increase in glutamate release (Deakin et al., 2008). In an imaging study by Deakin *et al.*, the ketamine-induced BOLD signal decrease in the medial ventral prefrontal cortex correlated with symptoms of schizophrenia in the volunteers (Deakin et al., 2008). Interestingly, NMDARs antagonists have been shown to induce delta oscillations *in vitro* (Zang et al., 2009), indicating that NMDAR hypofunction could also underlie the increased delta oscillations observed in schizophrenia (Lisman, 2012).

1.4 The hippocampus

1.4.1 The Hippocampus and schizophrenia

Morphological and molecular abnormalities have been found in the hippocampus of schizophrenic patients (Harrison, 2004; Harrison and Weinberger, 2005; Weinberger, 1999). Meta-analysis of magnetic resonance imaging (MRI) studies indicate a small, but consistent, decrease in hippocampal volume in schizophrenic patients (Wright et al., 2000). In addition, post mortem studies of gene expression indicate that levels of synaptic proteins are dysregulated in the hippocampus of schizophrenics (Harrison, 2004; Weinberger, 1999). It is interesting that these post mortem changes include reductions in glutamate receptor numbers, such as the GluA1 AMPAR subunit which has recently been associated with schizophrenia in the largest GWAS study to date (Eastwood et al., 1995; Harrison and Weinberger, 2005; Ripke et al., 2013, 2014). Hippocampal dysfunction is central to the Lisman/Grace hypothesis of schizophrenia, in which increased glutamatergic output from the hippocampus drives a hyperdopaminergic state (Lisman et al., 2008). Overall, there is strong evidence for hippocampal dysfunction in schizophrenia and it is possible that changes in glutamate receptors contribute to this hippocampal dysfunction.

1.4.2 Hippocampal formation circuitry

The hippocampal formation consists of the dentate gyrus (DG), the different *cornu ammonis* (CA) subfields including CA3 and CA1, and the entorhinal cortex (Andersen et al., 2007). The classic tri-synaptic circuitry of the hippocampus is described below and depicted schematically in **figure 1.3**.

The DG sends projections to CA3, via collaterals known as the mossy fibers (Andersen et al., 2007). The CA3 subfield contains recurrent collaterals (it innervates itself), and

also sends projections to the CA1 subfield, via the Shaffer collaterals (Andersen et al., 2007). Area CA1 sends output to deep layers of the entorhinal cortex and the subiculum. The subiculum is the main source of output from the hippocampus.

The majority of input to the hippocampus comes through the perforant and temporoammonic pathways (Andersen et al., 2007). The perforant pathway arises from the entorhinal cortex layer II, and directly innervates the DG and also CA3. The temporoammonic pathway also arises from the entorhinal cortex, but from layer III, and directly innervates CA1.

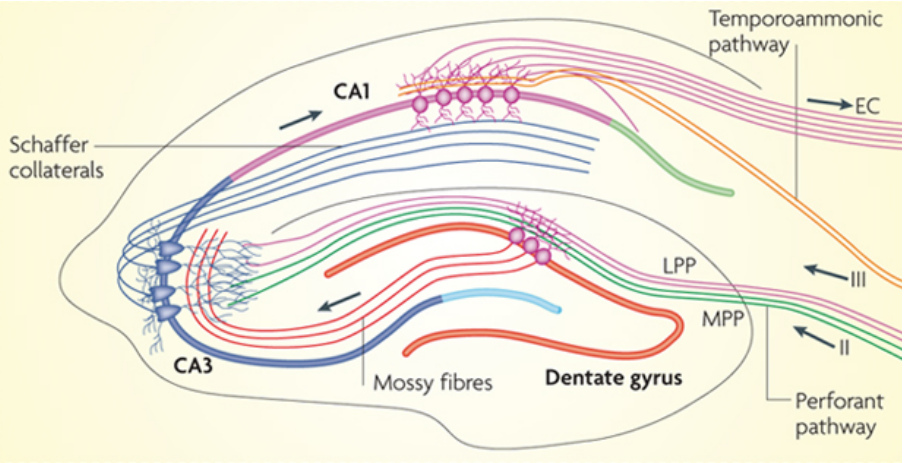

Figure 1.3: Tri-synaptic circuitry of the hippocampus
Schematic representation of the basic hippocampal circuitry. Information flow in the hippocampus is from DG to CA3 (via mossy fibres), then from CA3 to CA1 (via Shaffer collaterals), and finally from CA1 to entorhinal cortex (EC) and subiculum. The main input to the hippocampus is via the entorhinal cortex via the perforant pathway and temporoammonic pathway from the EC layer II and III respectively. The perforant pathway sends input to the dentate gyrus and CA3, whereas the temporoammonic pathway sends input directly to area CA1. Taken from Deng et al. 2010.

1.4.3 What is the function of the hippocampus?

The hippocampus is thought to be required for episodic memory in humans (Bird and Burgess, 2008). Evidence for this has come from patients who have had portions of the temporal lobe, including parts of the hippocampus, surgically removed. Such patients show profound memory deficits (e.g. Scoviille and Milner, 1957). Our understanding of the hippocampus has increased with studies in rodents with lesions or genetic mutations to hippocampal circuits. Here, discussion of the hippocampus will be focused on rodent studies.

Undoubtedly, in the rodent literature the most influential hypothesis of hippocampus function is the “cognitive map” theory proposed by O’Keefe and Nadal in 1978. This hypothesis came to light after the observations of hippocampal “place cells”, neurons which preferentially fire when an animal is in a particular spatial location (O’Keefe and Dostrovsky, 1971). Place cells are proposed to underlie spatial navigation, by providing a spatial representation of the environment (Moser et al., 2008). Having a representation of space is important for encoding “where”, which is an important component of episodic memory.

Although the “cognitive map” hypothesis has been widely accepted, and forms the “textbook view” of hippocampus function, there are problems with this concept. In particular, the hippocampus is known to play an important role in non-spatial memory tasks and emotional processing, particularly in anxiety (Bannerman et al., 2003, 2014), which is not accounted for by a purely spatial, or even a purely mnemonic, account of hippocampal function. For example, transient inactivation of the hippocampus of mice can impair performance of a context independent variation of the novel object recognition task (Cohen et al., 2013). In addition, lesions of the ventral hippocampus have been found to decrease measures of anxiety in rats, highlighting another

important role of the hippocampus (Bannerman et al., 2003). In fact, an interesting dissociation exists between the effects of lesions of the dorsal or ventral hippocampus in rats. Lesion of the dorsal hippocampus impair spatial memory, but not not influence anxiety. In contrast, lesions of the ventral hippocampus spare spatial memory performance but cause reduced anxiety (Bannerman et al., 2002, 2014).

An alternative suggestion is that the hippocampus is actually providing a means of disambiguating between competing response options and/or the memories that support them (Gray and McNaughton, 1982; Gray and McNaughton, 2000; Bannerman et al., 2014). Evidence for this comes, at least in part, from studies with genetic mutants that lack long term potentiation (LTP; see **1.5.4** and **1.5.10** below) in hippocampal circuits due to deletion of NMDARs from area CA1 and DG (Bannerman et al., 2012). LTP is thought to provide a putative mechanism for the storage of memories (Bliss and Collingridge, 1993). These mutants can, however, form normal long-term spatial associations (i.e. spatial reference memory (SRM); see **1.6.3**) despite lacking hippocampal LTP (Bannerman et al., 2012). However, the mice show impairments when faced with ambiguous cues that have opposing or different outcomes associated with them, suggesting the NMDARs in the hippocampus could be important for disambiguating overlapping/similar memories (Bannerman et al., 2012; discussed extensively in **1.5.4**).

In addition, mutant mice that lack the GluA1 AMPAR subunit (*Gria1* KO; see **1.5.6** below) have dramatic disruptions to their place fields when running on a linear track (Resnik et al., 2012), despite showing normal (Zamanillo et al., 1999), or under certain conditions, enhanced (Sanderson et al., 2009a), long term spatial associative memory. This highlights that the relationship between the integrity of place cell fields, and spatial memory performance, is unclear. Therefore, the function(s) of the

hippocampus are still being contested, and almost certainly are not limited to the "cognitive map" hypothesis.

1.5 Ionotropic glutamate receptors in the CNS

Glutamate receptor dysfunction could be relevant to the pathophysiology of schizophrenia, particularly as glutamate receptors are critical for synaptic plasticity and deficits in synaptic plasticity are thought to be central to schizophrenia (Crabtree and Gogos, 2014). In the mammalian central nervous system (CNS) glutamate is the major excitatory neurotransmitter, which acts on both metabotropic and ionotropic receptors. Ionotropic glutamate receptors in the CNS include AMPARs, NMDARs and kainate receptors. The AMPAR subunit GluA1, and the NMDAR subunit NR2A (also known as GluN2A), have been linked to schizophrenia in the largest GWAS to date (Ripke et al., 2013, 2014). The structure and function of NMDARs and AMPARs will be discussed in greater detail below.

1.5.1 Structure of NMDARs

NMDARs are tetrameric ion channels activated by the excitatory neurotransmitter glutamate. In addition to glutamate, activation of NMDARs is also dependent on the co-agonist glycine (Johnson and Ascher, 1987). NMDARs are cation channels, permeable to Na^+ and Ca^{2+}, and have the unique property of a magnesium (Mg^{2+}) block at resting membrane potentials (Mayer et al., 1984). Subunits of NMDARs all have three transmembrane portions and one re-entry loop, such that the N-terminus is extracellular and the C-terminus is intracellular. A schematic representation of the subunit arrangements is shown below (see **figure 1.4**).

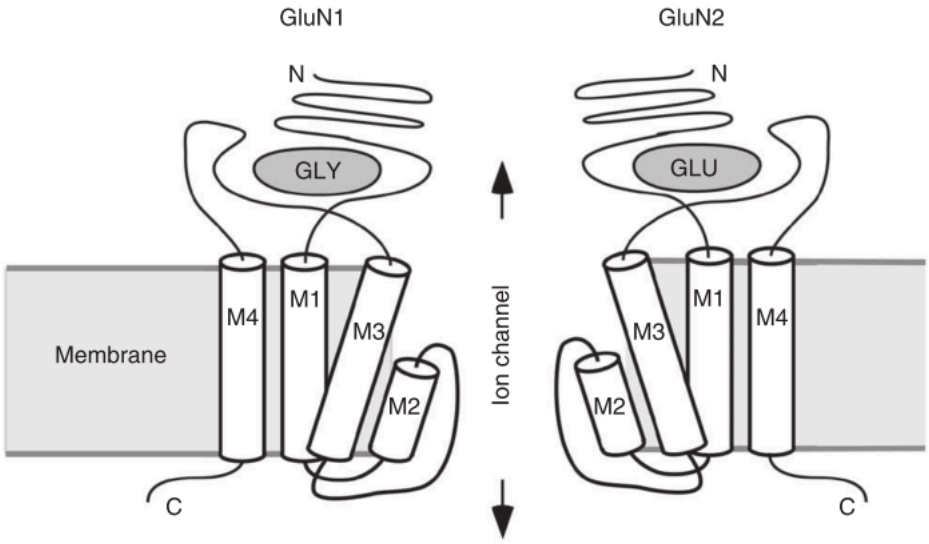

Figure 1.4: Schematic representation of the structure of an NMDAR
Glutamate (GLU) and the co-agonist glycine (GLY) bind to extracellular N-terminal domains of NR2 (GluN2) and NR1 (GluN1) subunits respectively. The transmembrane portions are labelled M1, M3 and M4 along with the re-entry loop (M2). It is the re-entry loops of the subunits that come together to form the ion channel pore. Taken from Retchless *et al.* 2012.

1.5.2 NMDAR subunits and stoichiometry

There are seven NMDAR subunits, that assemble in different combinations as tetramers, with different kinetic and pharmacological properties (Lee et al., 2014). The seven subunits are; NR1, NR2A, NR2B, NR2C, NR2D, NR3A and NR3B. The NR1 subunit is obligatory (i.e. an essential component of all NMDARs), and gene deletion of *Grin1*, that encodes NR1, leads to a complete loss of NMDARs and neonatal death (Forrest et al., 1994). NR1 subunits contain the glycine binding site (Kuryatov et al., 1994), and the NR2A-D subunits contain the glutamate binding site (Laube et al., 1997). As the NR1 subunit is obligatory, deletion of NR1 has been used as a way of functionally removing all NMDARs (see **1.5.4** and **1.8.2**).

NR1 is expressed in neurons throughout the brain but other subunits show regional, developmental and cell type specific expression patterns (Monyer et al., 1994, 1992).

For example, in excitatory pyramidal neurons of the hippocampus, levels of NR2A and NR2B are enriched (Monyer et al., 1994). In contrast, expression of NR2C and NR2D appears to be largely limited to interneurons (Monyer et al., 1994).

NR3A and NR3B subunits were identified later and add further complexity to the combinations and properties of NMDARs. In tri-heteromeric receptors (consisting of NR1, NR2 and NR3 subunits), the addition of NR3A or NR2B subunits appears to exert a dominant negative effect on NMDAR conductance (Chatterton et al., 2002; Henson et al., 2010; Sucher et al., 1995). In contrast, di-heteromeric receptors (consisting of NR1 and NR3 subunits) have unique properties and are actually considered to be excitatory glycine receptors that are no longer sensitive to glutamate (Chatterton et al., 2002).

1.5.3 Alternative splicing of NMDARs

The NR1 NMDAR subunit exists as 8 alternative splice variants (Hollmann et al., 1993; Laurie and Seeburg, 1994). The expression of splice variants varies throughout the brain and could regulate the surface expression of NR1 (Laurie and Seeburg, 1994; Okabe et al., 1999). A full review of how alternative splicing influences NMDAR function is beyond the scope of this thesis, but it does highlight the incredible layers of complexity present in NMDARs. NMDARs are important for synaptic plasticity and this will be discussed below.

1.5.4 NMDARs and synaptic plasticity

Synaptic plasticity has been extensively studied since the first report of synaptic potentiation by Bliss and Lomo in 1973 (Bliss and Lomo, 1973). A pivotal discovery was that NMDAR antagonists can block the induction of LTP (Bliss and Collingridge, 1993; Collingridge et al., 1983).

To study NMDAR dependent LTP, and its relation to behaviour, genetic mutants have been generated where NMDARs have been ablated selectively from the hippocampus. The first of these studies conditionally ablated NMDARs from area CA1 excitatory neurons (Tsien et al., 1996b). LTP was completely abolished in the CA3 to CA1 Shaffer collaterals pathway and mice were found to have impaired spatial reference memory (SRM), assessed in the Morris water maze (Tsien et al., 1996b). However, the specificity of this line for area CA1, and therefore the validity of the conclusions have been questioned, following observations that NR1 was also deleted from deep cortical layers (Fukaya et al., 2003; Rondi-Reig, 2006).

In a later study, where NR1 was ablated selectively from area CA1 and DG excitatory neurons (hereafter referred to as *Grin1*$^{\Delta CA1/DG}$), similar deficits in LTP were observed, but behavioural perturbations were much more subtle (Bannerman et al., 2012). *Grin1*$^{\Delta CA1/DG}$ animals showed normal acquisition of SRM in the Morris water maze but were impaired when tested for SRM on the radial maze (Bannerman et al., 2012). Although these tasks both assess SRM, they may require different psychological processes. In the radial maze there are many, identical looking arms that the animals have to differentiate between. Thus, there is potentially a higher degree of ambiguity in the radial maze. To explore this MWM-normal and radial maze-impaired SRM dissociation, a variation of the water maze task was used, with one escape platform, and two identical visible beacons (one directly above the escape platform and the other in the opposite quadrant of the maze acting as a decoy) designed to increase the ambiguity in the task (i.e. the visible beacon becomes associated with both escape and no escape). When presented with the two visibly identical beacons, *Grin1*$^{\Delta CA1/DG}$ animals made significantly more errors and often swam towards the decoy beacon, despite having knowledge of the true spatial location of the platform based on

performance during “probe” trials where the sunken platform is removed from the maze with no beacons present (Bannerman et al., 2012). Therefore, NMDARs in the hippocampus could be responsible for resolving ambiguity, rather than encoding spatial information *per se* (Bannerman et al., 2012, 2014).

1.5.5 NMDAR antagonists

A number of antagonists for NMDARs have been discovered, which has dramatically facilitated our understanding of their role in physiology and behaviour. Examples of frequently used antagonists and their mechanism of action are given below in **table 1.1**.

Antagonist	Mechanism of action	Notes
2-amino-5-phosphonopentanoic acid (**AP5**)	Competitive antagonist	Frequently used *in vitro* to study NMDAR function
Dizocilpine (**MK-801**)	Uncompetitive	Frequently used *in vivo* in animal models to study NMDAR function
Phencyclidine (**PCP**)	Uncompetitive	Drug of abuse, known as “angel dust” Frequently used *in vivo* in animal models
Ketamine	Non-competitive	Drug of abuse. Used *in vivo* to study NMDAR function in humans

Table 1.1: Commonly used NMDAR antagonists and their mechanism of action

1.5.6 Structure of AMPARs

AMPARs are the other major ionotropic glutamate subtype responsible for excitatory neurotransmission in the CNS. AMPARs are tetrameric ion channels composed of the GluA1-4 subunits, encoded by *Gria1-4* genes. Each subunit contains 4 membrane segments but the C-terminus is actually intracellular because the second membrane segment forms a re-entry loop and does not completely span the membrane (see **figure 1.5**). The consequence of this is highly important, as the intracellular C-terminal

domain of AMPARs regulates receptor trafficking and is implicated in plasticity processes (Shepherd and Huganir, 2007). For example, the dynamic insertion and removal of AMPARs from the post synaptic membrane are thought to underlie LTP and LTD respectively (Malinow and Malenka, 2002).

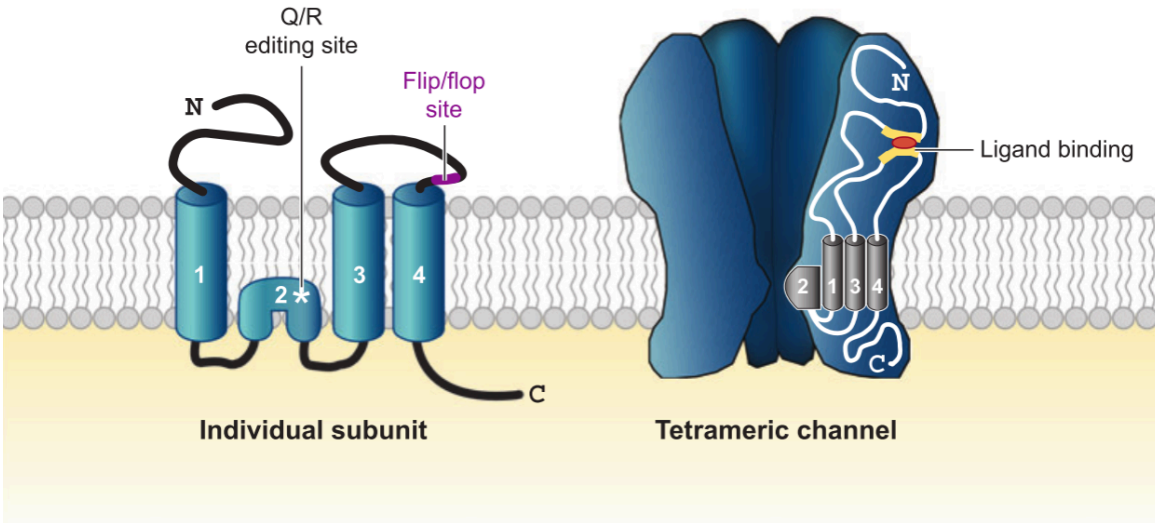

Figure 1.5: Schematic representation of an individual AMPAR subunit and the assembled channel
Each individual AMPAR subunit consists of 3 transmembrane segments (labelled 1,3 and 4) and one re-entry loop (labelled 2). In the assembled tetramer, the re-entry loops form the ion channel pore. Within the re-entry loop of the GluA2 subunit is the Q/R editing site (indicated with a *) which regulates the Ca^{2+} permeability of the assembled receptor. The "flip/flop" alternative splicing site is present in all subunits, and can alter receptor kinetics and assembly (see text). Figure taken from Huganir and Shepherd, 2007.

1.5.7 Alternative splicing of AMPARs

The different AMPAR subunits are highly similar, except for their C-terminus (Shepherd and Huganir, 2007). GluA1 exists only with a long cytoplasmic tail, and GluA3 exists only with a short cytoplasmic tail. GluA2 and GluA4, in contrast, have two alternative splice variants with long or short cytoplasmic tails (Shepherd and Huganir, 2007). In addition, all AMPAR subunits exist as alternative "flip" or "flop"

splice variants (Sommer et al., 1989). “Flip/flop” alternative splicing alters a region of the receptor that forms the ligand binding domain (LBD), located in the extracellular loop (see **figure 1.5**). “Flip” and “flop” splice variants are developmentally regulated (Monyer et al., 1991), and change the kinetic properties of AMPARs. For example, the “flip” splice variants show slower receptor desensitisation properties (Sommer et al., 1989). In addition, activity levels can dynamically regulate “flip/flop” alternative splicing, resulting in AMPARs with different properties that could be important for the process of homeostatic plasticity (Penn et al., 2012).

1.5.8 RNA editing of AMPAR subunits

AMPAR subunits are subject to RNA editing by enzymes that target mRNA before it is translated. The most striking RNA editing event occurs exclusively in the GluA2 subunit. Here, RNA that encodes the amino acid glutamine (Q) is edited to encode for arginine (R) at the Q/R site (Greger and Esteban, 2007). This RNA editing event renders all AMPARs containing the GluA2 subunit impermeable to Ca^{2+}, and is faithfully carried out 99% of the time (Higuchi et al., 2000). In fact, genetic deletion of **a**denosine **d**eaminase **a**cting on **R**NA 2 (ADAR2), the enzyme responsible for this RNA editing event, is lethal with mice showing epilepsy and premature death due to excitotoxicity, presumably due to an abundance of Ca^{2+} permeable AMPARs (Higuchi et al., 2000). Interestingly, the phenotype of ADAR2 KO mice can be rescued by genetically encoding arginine at the Q/R site of GluA2 (Higuchi et al., 2000).

Another RNA editing site exists in GluA2-4 subunits, where RNA encoding for an arginine (R) is edited to encode for glycine (G). Again, RNA editing at this site can change receptor kinetic properties and has also been shown to alter receptor biogenesis, influencing the stoichiometry of AMPARs (Greger and Esteban, 2007).

1.5.9 Subunit stoichiometry of AMPARs

In excitatory hippocampal pyramidal neurons, AMPARs are thought to consist largely of GluA1/2 or GluA2/3 hetero-tetramers (Henley and Wilkinson, 2016; Lu et al., 2009). Levels of GluA4 are high during early development but decrease over time and are very low in adult excitatory neurons (Zhu et al., 2000). The inclusion of the GluA2 subunit (edited at the Q/R site, see **1.5.8**), renders the majority of AMPARs in excitatory pyramidal neurons calcium impermeable. The stoichiometry of AMPARs in inhibitory interneurons, such as PV interneurons, is different to that of excitatory pyramidal neurons. For example, PV interneurons express mainly GluA1 and GluA4 AMPAR subunits (Fuchs et al., 2007; Geiger et al., 1995).

1.5.10 AMPARs and synaptic plasticity

Synaptic plasticity underlies the strengthening (potentiation) and weakening (depression) of synaptic transmission between neurons. AMPARs are thought to play a critical role in both long term potentiation (LTP) and long term depression (LTD) (Henley and Wilkinson, 2016; Huganir and Nicoll, 2013; Shepherd and Huganir, 2007). The role of AMPARs in LTP will be briefly discussed below, with focus on the GluA1 subunit.

LTP at glutamatergic synapses onto excitatory pyramidal neurons occurs when post-synaptic depolarisation is paired with synaptic input. Coincident glutamate release and depolarisation of the post synaptic neuron is critical to release the Mg^{2+} block of NMDARs present at resting membrane potentials. The subsequent influx of Ca^{2+} through NMDARs initiates a cascade of events leading to potentiation of the specific synapse (Nicoll et al., 1988). AMPAR trafficking and insertion into the postsynaptic membrane is thought to be critical for this potentiation of synapses, and is dependent on phosphorylation of AMPARs. In animals where phosphorylation sites on the GluA1

subunit are mutated such that phosphorylation is no longer possible, LTP was impaired, along with the retention of spatial reference memory tested in the MWM (Lee et al., 2003). The importance of the GluA1 subunit for LTP was also highlighted following the generation of *Gria1* KO mice, which globally lack GluA1 (Zamanillo et al., 1999). Certain forms of LTP are absent or abnormal in *Gria1* KO mice (Hoffman et al., 2002; Romberg et al., 2009; Zamanillo et al., 1999).

Deficits in short-term synaptic plasticity could be highly relevant in schizophrenia (Crabtree and Gogos, 2014) which is especially interesting since risk genes for schizophrenia include those known to be involved in regulating synaptic plasticity (Barkus et al., 2014; Ripke et al., 2013, 2014). The GluA1 AMPAR subunit is thought to play a particularly important role in short term synaptic plasticity, so it is of great interest that levels of GluA1 appear to be decreased in the hippocampus of schizophrenics (Eastwood et al., 1995, 1997). The phenotype of *Gria1* KO mice and how this could be relevant to schizophrenia will be discussed in detail later (see **5.1**).

1.6 Behavioural tests in rodents relevant to schizophrenia

It is important to stress that behavioural tests in rodents, for obvious reasons, are largely unable to replicate the nature of tests used in humans. However, a combination of behavioural tests can provide information about the psychological processes that could be disrupted or altered in various models. These psychological processes, e.g. short-term habituation, could be relevant to schizophrenia. Thus, rodent models allow us to probe how risk genes, pharmacological challenges, or direct circuit manipulations can manipulate the psychological processes that are relevant to schizophrenia. In the following section some common rodent assays used to measure deficits that correlate with the positive, negative and cognitive symptom domains of schizophrenia will be discussed.

1.6.1 Behavioural tasks in rodents relevant to positive symptoms

Positive symptoms are uniquely human in nature and therefore very hard to model in animals. For example, we do not know when rodents are, or even if they are, capable of experiencing hallucinations or delusions. That said, there are rodent behavioural assays that are known to be sensitive to elevated levels of dopamine, a neurotransmitter that could be very important in the expression of positive symptoms in humans (see **1.2.1** and also Howes and Kapur, 2009). Thus, rodent behavioural tests of positive symptoms could be considered as tests that can reveal hyperdopaminergic states, thought to be associated with positive symptoms in schizophrenia.

Locomotor activity evoked by novelty or psychostimulants

Locomotor activity is quick and simple to test in rodents and has been used extensively as an assay to identify potential antipsychotic drugs. Locomotor activity in rodents is sensitive to dopamine levels. For example, drugs that increase dopamine signalling, such as amphetamine, also increase locomotor activity (Yates et al., 2007). Therefore, locomotor activity is thought to provide a readout of mesolimbic dopamine levels (Pratt et al., 2012). In addition, NMDAR antagonists, commonly used to acutely model elements of schizophrenia, are also able to induce hyperactivity in rodents (Brigman et al., 2010; Gilmour et al., 2009; Pratt et al., 2012).

Pre-pulse inhibition

A sudden loud sound (startle pulse) induces an auditory startle response (ASR). This ASR can be reduced by presentation of a weaker pre-pulse preceding the startle pulse. This process is known as pre pulse inhibition (PPI), and has been found to be impaired in schizophrenia (Perry et al., 1999). As the ASR is present across species, PPI can be readily tested in rodents, using very similar paradigms to those used in humans. PPI is sensitive to manipulation of the dopamine system. For example, amphetamine challenge (inducing a hyperdopaminergic state) can lead to PPI deficits in rodents (Ralph-Williams et al., 2002). A number of animal models relevant to schizophrenia show impaired PPI (Belforte et al., 2010; Wolff and Bilkey, 2010).

1.6.2 Behavioural tasks in rodents relevant to negative symptoms

It is a challenging to measure rodent correlates of negative symptoms of schizophrenia, specifically, discriminating them from rodent forms of depression or autism. Essentially, rodent assays of this domain are identical to behavioural tests of depression. So the specificity of assays for schizophrenia is not clear.

Anhedonia

Anhedonia, the inability to feel pleasure from activities that are usually pleasurable, is considered a negative symptom of schizophrenia. In rodents, anhedonia is tested using the sucrose preference test, in which animals are given a choice between standard drinking water and water containing sucrose. Wildtype animals show a strong preference for the pleasurable sucrose-containing water, while animals exhibiting anhedonia do not show such a preference. Sucrose preference is frequently tested in animal models relevant to schizophrenia (Arguello and Gogos, 2006; Brigman et al., 2010).

Social behaviours

In rodents, impaired social interaction, is often proposed to represent a negative symptom of schizophrenia, potentially modelling social withdrawal seen in patients (Arguello and Gogos, 2006). However, it is unclear how deficits in social behaviour in animals parallel social withdrawal in schizophrenia (Pratt et al., 2012). Schizophrenia related animal models often observe reduced social interactions (Belforte et al., 2010; Tatard-Leitman et al., 2014). The common rodent tests of reciprocal and non-reciprocal social interaction are equally interpreted as indicators of depression, autism, and schizophrenia, even though the underlying causes of social withdrawal are likely distinct in those human diseases.

Nest building

Nest building can be readily tested in rodents (Deacon, 2006), and has been proposed to reflect an important social behaviour of rodents (Powell and Miyakawa, 2006), or, more generally, a social, cognitive and motivational capacity to organise daily living (Deacon, 2006). Mice challenged with the NMDAR antagonist phencyclidine (PCP) sub-chronically (based on the glutamatergic hypothesis of schizophrenia) show impaired nest building (Pedersen et al., 2014). Interestingly, PCP-induced nest

building deficits are rescued by treatment with an agonist of nicotinic α7 receptors which has been indicated to have beneficial effects on negative symptoms in schizophrenia patients (Lieberman et al., 2013), but not with the atypical antipsychotic drug risperidone (Pedersen et al., 2014). This suggests that nest building, in combination with a NMDAR hypofunction "model" of schizophrenia, has some predictive validity for drugs that could improve negative and/or cognitive symptoms of schizophrenia.

1.6.3 Behavioural tasks in rodents relevant to cognitive symptoms

Cognitive symptoms in schizophrenia include deficits in working memory, attention and cognitive flexibility. There are a number of behavioural assays to test working memory in rodents, so in principle working memory can be tested in both humans and rodents. In humans, working memory is often tested with the N-back test. In this test subjects are presented with a series of stimuli and have to respond when the stimulus matches that of *n* steps before. The higher the value of *n* then the greater the working memory load of the test. In rodents, working memory is frequently tested on win-shift maze tasks, designed to assess spatial working memory (SWM). It should be noted that SWM in rodents may well be different to working memory tested in humans (Sanderson and Bannerman, 2012). It is important to clarify some terminology when referring to rodent "working memory", and to highlight the potential role of stimulus specific short-term habituation. When a stimulus (spatial or other) is presented it will generate an unconditioned exploratory response (UR). Repeated presentation of the same stimulus will lead to a reduction in the UR to that stimulus. The psychological process underlying this process is known as habituation. In the literature maze-based (i.e. T-maze and radial maze) alternation (win-shift) performance is generally referred to as SWM, but it would perhaps be better to refer to this as short-term memory.

Bannerman and Sanderson have argued that maze-based working memory tasks (such as the T-maze and radial maze) may actually assess a form of stimulus specific short-term habituation with animals choosing between arms based on their relative familiarity (Sanderson and Bannerman, 2012).

For consistency with the wider literature, this thesis will use either the term spatial working memory (SWM) or spatial working/short-term memory. But the reader is urged to consider that short-term habituation could contribute to the psychological processes required for task performance. Schizophrenia has been associated with deficits in habituation (Ludewig et al., 2003), so rodent assays that assess habituation directly could also be very useful tools in schizophrenia research (e.g. spatial novelty preference on the Y-maze; Barkus et al., 2014).

T-maze alternation

SWM can be assessed on the T-maze (Deacon and Rawlins, 2006). Animals can be tested with spontaneous or rewarded alternation protocols. Each trial of alternation performance (spontaneous or rewarded) is split into a sample and choice run. During the sample run the animals are forced (in rewarded) or allowed to choose (in spontaneous) one of the goal arms. Then after a delay (intra-trial interval) animals are returned to the maze and given a free choice of both goal arms. In both cases a "correct" decision would be to pick the arm that was not visited in the sample run (i.e. to alternate). The "working memory" component comes from the delay period (intra-trial interval) where animals have to remember the location of the arm visited during the sample run and flexibly vary their choice between one trial and another based on trial specific information (but see the short-term habituation account above).

With rewarded alternation more trials can be run per block as animals are more motivated to run on the maze which is particularly useful for drug studies where it is

desirable to run a large number of trials following injection of drug. The task difficulty can be manipulated by changing the inter- and intra-trial interval periods. By having multiple trials close together (short inter-trial interval/massed trials) proactive interference (i.e. memory from a previous, but no longer informative, trial) is increasingly making the task more difficult (Deacon and Rawlins, 2006). Lengthening the time between the sample and choice trials (intra-trial interval) increases the difficulty of the task as animals are required to remember the location of the arm in the sample run for longer (Deacon and Rawlins, 2006).

Y-maze spatial novelty preference

Spatial novelty preference assesses the innate preference animals show for a previously unvisited, and hence "novel" arm of a Y-maze. During the exposure (or sample) phase, animals will explore two arms of the maze, and presumably habituate to this portion of the maze as it becomes familiar. This will then drive exploration of the third, previously unvisited arm when animals are returned to the maze in the choice phase and given a choice of all three arms.

Spatial reference memory

Spatial reference memory (SRM) tests the ability of animals to form associative memories with particular spatial locations. SRM is classically tested in the Morris water maze (MWM), in which animals are placed in a circular pool of water and have to swim to find a submerged (and therefore not visible) platform, onto which they can climb in order to escape from the water. The platform is kept in the same place but the release site of animals is varied on each trial. Animals that learn the spatial location of the platform will swim directly towards the escape platform. Memory can then be tested on probe trials, during which the platform is removed from the maze. Animals that have

learnt the spatial location of the platform will then spend more time searching where the platform *was* located during training (despite it no longer being there).

Spatial memory and the hippocampus

T-maze alternation, spatial novelty preference and SRM are all acutely sensitive to hippocampal lesions (Deacon et al., 2002; Deacon and Rawlins, 2006; Morris et al., 1982; Sanderson and Bannerman, 2012). Despite all of the above tasks being sensitive to lesions of the hippocampus there are interesting dissociations in animals lacking different glutamate receptor subunits. For example, animals that lack the GluA1 AMPAR subunit (*Gria1* KO) display impaired SWM but have normal SRM (Reisel et al., 2002). Thus, although all the tasks require intact hippocampal circuitry, there is differential sensitivity to "genetic lesions". Although, in the case of *Gria1*$^{-/-}$ animals it is important to stress that GluA1 is absent throughout the brain, so the lack of GluA1 in cortical circuits could also contribute to this behavioural phenotype.

1.7 Genetic strategies to study gene function

In order to study gene function, genes of interest can be completely knocked out (KO) from the genomes of model organisms. In the case of mice, this process involves targeting of embryonic stem cells (ES cells) with DNA constructs, and the hijacking of a DNA repair process known as homologous recombination (Hall et al., 2009). The process of homologous recombination can lead to switching of genomic DNA with DNA from the targeting construct. The targeting construct is designed in such a way so as to block gene expression (often by deleting a critical exon or by inserting a STOP codon). Modified ES cells are then injected into a mouse blastocyst and transplanted into a pseudo-pregnant mouse. Resulting offspring are chimeras (i.e. their bodies contain a mixture of some cells which contain the wildtype (WT) DNA and others the modified DNA from the targeting construct). When bred together some offspring will

have germ cells contain the mutation, so that it can be stably inherited over the next generations (Hall et al., 2009). *Gria1* KO mice used in this thesis were generated in this way (Zamanillo et al., 1999; for specific details see **5.2.1**).

KO mice are undoubtedly useful tools to study gene functions but animals generated in this way do have some limitations. For example, the gene is completely ablated throughout the organism, so gene function is not assessed in a region or cell-type specific manner. In addition, it is often not known how gene deletion might affect developmental processes. So it can be impossible to differentiate whether gene deletion is leading to a particular behavioural phenotype due to an absence during development or a role in adulthood (Tsien et al., 1996). To gain cell-type specificity and regional and temporal control of gene KO the *Cre/LoxP* system (Sauer and Henderson, 1988) is frequently used in rodents (see **figure 1.6**).

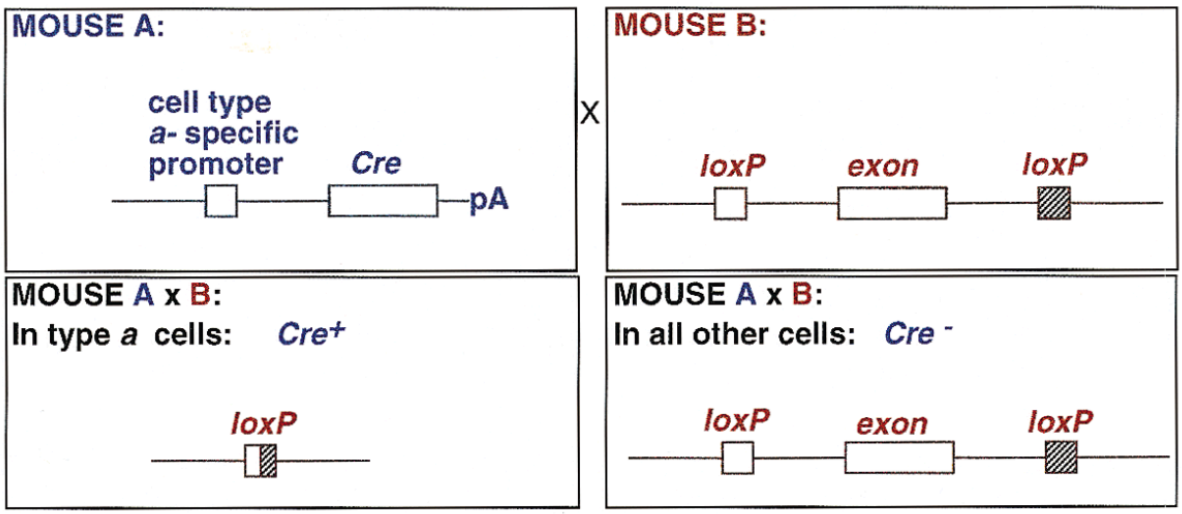

Figure 1.6: Schematic demonstration of *Cre/LoxP* mediated gene deletion
Demonstration of *Cre/LoxP* mediated gene deletion. In this example mouse A expresses *Cre* under a cell type specific promoter. Mouse B contains a target gene which is "Floxed". A critical exon of the gene has been flanked by two *loxP* sites. These two animals can be bred together to give double transgenic animals (i.e. mouse AxB). In *Cre* positive cells the "floxed" exon will be deleted. In all *Cre* negative cells the "floxed" exon will not be deleted, and will be expressed as normal. Taken from Tsien *et al.* 1996.

This was first demonstrated using the T 29-1 *Cre* line that was originally reported to selectively target area CA1 of the hippocampus (Tsien et al., 1996; but see **1.5.4**). When crossed with a mouse harbouring a "floxed" exon critical for the expression of *Grin1* (encoding NR1) this led to cell type specific (i.e. area CA1 excitatory pyramidal neurons) deletion of NMDARs (Tsien et al., 1996). Since these pioneering studies, the technology has also been used to study gene function in different subpopulations of neurons by using different cell-type specific *Cre* lines. This thesis has utilised the *Cre/LoxP* technology to generate animals that lack NMDARs selectively on PV interneurons (see **2.2.1**). In addition, the *Cre*/*LoxP* technology was used in this thesis to selectively target virus expression to PV interneurons (see **4.3.1**).

Recently, the CRISPR/Cas9 technology has emerged and is likely to revolutionise the generation of genetically modified model organisms (Yang et al., 2014). The technology highjacks a bacterial system that protects the host cell from foreign nucleic acids (Yang et al., 2014). The Cas9 protein (a nuclease that introduces double stranded DNA breaks) can be directed to specific DNA sequences with the help of single-guide RNAs, so double stranded DNA breaks can be precisely targeted in the genome of the target organism. A major strength of the CRISPR/Cas9 system is the possibility to "multiplex" and edit many genes in one go, a process that would be extremely time consuming using traditional methods (Yang et al., 2014).

1.8 "Animal models" of schizophrenia

Schizophrenia is a human disease and it is important to stress that schizophrenia, in its full human form, cannot be modelled in mice. However, endophenotypes are useful when trying to understand complex diseases such as schizophrenia (Kellendonk et al., 2009; Walters and Owen, 2007). Defined as "individual measured traits", endophenotypes model elements of a complex disease that, in isolation, will often be

sub-clinical (Kellendonk et al., 2009). The idea behind endophenotypes is that the underlying genetics is simpler and therefore more accessible. For example, in schizophrenia working memory has been proposed to be an endophenotype (Kellendonk et al., 2009). Alone, a working memory deficit would not lead to a diagnosis of schizophrenia but studying the genetics (or neuronal circuits) associated with working memory is a more manageable task than trying to understand the disease as a whole.

Animal models provide a means to test specific hypotheses about schizophrenia, in ways that would be technically impossible and also unethical in humans. It is also possible to explore how risk genes for schizophrenia impact upon the physiology and behaviour of genetically modified mice. Or to test the effects of drugs such as NMDAR antagonists (that induce schizophrenia-like phenotypes in human volunteers), on the behaviour and physiology of rodents. Genetic and pharmacological "models" based on the dopamine, glutamate and GABAergic hypotheses of schizophrenia will be discussed in turn.

1.8.1 Dopamine based animal "models"

The dopamine theory of schizophrenia suggests that a hyperdopaminergic state in the striatum could be involved in the pathophysiology of schizophrenia (Howes and Kapur, 2009). This is backed up by the fact that current antipsychotic drugs all block D2 dopamine receptors (Seeman and Lee, 1975). To model this in mice, the D2 dopamine receptor was selectively overexpressed in the striatum, in a manner where overexpression of the transgene could be switched on and off under the control of doxycycline (*Dox*) (Kellendonk et al., 2006). When the D2 receptor was overexpressed throughout life, mice displayed deficits in SWM performance when tested on the T-maze and radial maze (Kellendonk et al., 2006). Interestingly, even if overexpression

of the D2 receptor was stopped in adulthood the cognitive impairment was not reversed, suggesting that developmental overexpression of D2 changes the network in ways that persist into adulthood (Kellendonk et al., 2006).

1.8.2 Glutamate based genetic animal “models”

The glutamate hypothesis of schizophrenia emerged following observations that drugs that block NMDARs, such as PCP, can induce behavioural states similar to those seen in schizophrenia (Javitt and Zukin, 1991). Since then, rodent models have been extensively used to explore NMDAR hypofunction using both pharmacological and genetic manipulations.

The first genetic study investigating NMDAR hypofunction in mice used mutants that expressed NR1 to just 5-10% of the levels in WTs (hereafter referred to as hypomorph mice) (Mohn et al., 1999). Complete deletion of NR1 is lethal (Forrest et al., 1994), but hypomorph animals express enough NR1 for survival (Mohn et al., 1999). Hypomorph mice display pronounced hyperactivity, that was reversed with the antipsychotic drugs haloperidol and clozapine (Mohn et al., 1999). The hypomorph mice were later tested through an extensive test battery including cognitive tasks (Barkus et al., 2012). In every cognitive task tested, the hypomorph mice were severely impaired, even on simple visual discrimination tasks (Barkus et al., 2012). Therefore, the hypomorph animals were concluded to exhibit behavioural deficits far more extensive and unspecific than what would be expected in a useful model of schizophrenia (Barkus et al., 2012).

Recently, mice with NR1 deletion specifically from forebrain excitatory neurons (hereafter referred to as *Grin1*$^{\Delta CaMKII}$) have been generated (Tatard-Leitman et al., 2014). *Grin1*$^{\Delta CaMKII}$ mutants showed a wide range of deficits that could be relevant to schizophrenia, including hyperactivity, deficits in nest building, social interaction and

working memory (Tatard-Leitman et al., 2014). When baseline and auditory evoked potentials were assessed via electroencephalogram (EEG) recordings, *Grin1*$^{\Delta CaMKII}$ mice were found to display enhanced gamma power under baseline conditions, and reduced evoked gamma power (Tatard-Leitman et al., 2014). The strong behavioural deficits in *Grin1*$^{\Delta CaMKII}$ mice are interesting but the study did not report any control tasks that the mice could perform. Thus, similar to the NR1 hypomorph animals, their behavioural deficits could extend to all cognitive tasks making them less appealing as a "model" of schizophrenia (Tatard-Leitman et al., 2014). However, the changes in gamma oscillations are particularly interesting, and mirror the elevated baseline and reduced evoked gamma oscillations found in schizophrenia (Gandal et al., 2012; Uhlhaas and Singer, 2010).

In addition, animals have been generated in which NR1 is selectively ablated from PV interneurons. These will be discussed later (see **1.8.4**)

As mentioned previously, non-NMDA glutamate receptors have also been linked to schizophrenia (see **1.2.2**). In particular the GluA1 AMPAR subunit seems to be expressed at reduced levels in schizophrenia (Eastwood et al., 1995, 1997). Mice that globally lack the GluA1 AMPAR subunit (*Gria1* KO) were originally generated to study the role that GluA1 plays in plasticity processes such as LTP (see **1.5.10**). However, after extensive behavioural characterisation of *Gria1* KO mice, and renewed evidence that GluA1 could be associated with schizophrenia (Ripke et al., 2014, 2013), the behavioural phenotype of *Gria1* KO animals has been suggested to be relevant to the psychological processes affected in schizophrenia (Barkus et al., 2014; Barkus et al., 2012; Fitzgerald et al., 2010; Wiedholz et al., 2008). In particular, *Gria1* KO mice are thought to display impaired stimulus-specific short-term habituation (Sanderson et al., 2009b; Sanderson and Bannerman, 2012), and under certain conditions stimulus-

specific sensitisation (Sanderson et al., 2011b). The behavioural phenotype of *Gria1* KO animals (discussed in greater detail later see **5.1.3**) could provide a means to explore how changes in the glutamatergic system can alter psychological processes such as habituation (Ludewig et al., 2003) and sensitisation which are thought to be a driver of aberrant salience and thus relevant to schizophrenia (Barkus et al., 2014).

1.8.3 Glutamate based pharmacological animal "models"

The observation that NMDAR antagonists, such as PCP, can induce a wide range of schizophrenia like symptoms in humans (Javitt and Zukin, 1991) prompted NMDAR antagonists to be given to rodents to study mechanisms linking glutamatergic dysfunction to schizophrenia-relevant behaviours. Central to NMDAR hypofunction models is the prediction that NMDAR hypofunction could be upstream of changes in the dopamine system (i.e. striatal *hyperdopaminergia*) (Bubeníková-Valesová et al., 2008; Lisman et al. 2008).

Administration of the NMDAR antagonist 2-amino-5-phosphonopentanoic acid (AP5), can lead to excessive glutamate release *in vivo* (measured with micro dialysis), in the hippocampus and striatum of freely moving rats (Liu and Moghaddam, 1995). Later, NMDAR challenge (with ketamine) was also shown to elevate levels of glutamate and also dopamine in the prefrontal cortex (PFC) of freely moving rats (Moghaddam et al., 1997). Interestingly, doses of ketamine (30 mg/kg) that increased dopamine in the PFC, also impaired SWM performance when rats were tested on the T-maze (Moghaddam et al., 1997). The elevated levels of glutamate triggered by ketamine challenge could stimulate glutamatergic transmission through AMPA and kainate receptors (Moghaddam et al., 1997). When rats were pre-treated with an AMPA and kainate receptor antagonist, ketamine (30mg/kg) was unable to induce deficits in

SWM, and the increase in PFC dopamine was attenuated (but not abolished) (Moghaddam et al., 1997).

MK-801 is a uncompetitive NMDAR antagonist (it does not compete with glutamate for the glutamate binding site) that binds to the ion channel pore and blocks the movement of ions through the channel (Lee et al., 2014; Olney et al., 1989). When rats are challenged with MK-801 they display impaired alternation performance on the T-maze (Jackson et al., 2004). When single units were recorded in the PFC of MK-801 challenged rats, the average firing rate was increased (Jackson et al., 2004). This complements the observation that NMDARs increase the excitability of the network, previously observed as an increase in the levels of glutamate in the PFC (Liu and Moghaddam, 1995; Moghaddam et al., 1997).

These changes are somewhat paradoxical. How can blockade of excitatory NMDARs lead to an overall increase in network activity? One possibility is through disinhibition of excitatory pyramidal neurons following the decreased excitation of inhibitory interneurons. When putative excitatory and inhibitory neurons were recorded in the PFC of rats challenged with MK-801, there was an increase and decrease in the average firing rates of putative excitatory and inhibitory neurons respectively (Homayoun and Moghaddam, 2007). Thus, it appears that inhibitory interneurons are more sensitive to NMDAR challenge than excitatory neurons (at least with lower doses of NMDAR antagonists), and a decrease in inhibitory neuron excitation can initiate disinhibition in the network, releasing inhibition onto excitatory neurons. This will be discussed in depth later (see **3.1.1** and **3.4**).

A variety of different NMDAR antagonists have been used to “model” elements of schizophrenia in both humans and rodents. Whist it is compelling that a number of different NMDAR antagonists, with different mechanisms of action, can all induce

behavioural and physiological changes potentially relevant to schizophrenia, it also creates a problem of translatability. For example, in the majority of cases the same NMDAR antagonists have not been used in human and rodent studies, raising questions about the translational validity of the different studies. This was demonstrated in a study that tested the behaviour of rats challenged with 8 different NMDAR antagonists (Gilmour et al., 2009). The results of the different NMDAR antagonists were highly variable, even when looking at basic locomotor activity following drug challenge (Gilmour et al., 2009). There were striking differences in the locomotor activity of rats challenged with MK-801 vs ketamine, which is potentially of concern since many human studies have been conducted with ketamine, while MK-801 is commonly used in rodents (Gilmour et al., 2009). Thus, caution needs to be taken when assessing the translational value of rodent NMDAR antagonist studies.

1.8.4 GABAergic based animal "models"

Circuit-based models suggest that NMDAR hypofunction, specifically on inhibitory interneurons, could be central to the pathophysiology of schizophrenia (Jiang et al., 2013; Lisman et al., 2008; Nakazawa et al., 2012). This forms the basis of the "Lisman/Grace" model that is central to a significant part of this thesis. In particular, PV interneurons have been suspected to be dysfunctional in schizophrenia (Lewis et al., 2012; Lisman et al., 2008; Nakazawa et al., 2012). To test this circuit-based model, mice lacking NMDARs specifically from different populations of interneurons have been generated.

The first study published early in 2010 used a *Cre* driver line that targeted a population of corticolimbic interneurons, of which a large proportion were PV positive, combined with two different "floxed" NR1 lines with differential spacing ("short" and "long") between *loxP* sites (Belforte et al., 2010). In neocortex, 92% of the neurons targeted

by the line were GABAergic (i.e. GAD67-positive) and >70 % PV-positive, with around 24% Reelin-positive, and around 15% NPY-positive. Counting in reverse, the line covered 40-50% of cortical interneurons and around 75% of the PV-positive and 30% of the Reelin-positive populations. When the “short” floxed NR1 line was crossed with that *Cre* line, recombination and subsequent NR1 deletion were predicted to occur during adolescence (Belforte et al., 2010). In contrast, the “long” floxed NR1 line was predicted to produce the majority of NR1 deletion in adulthood (Belforte et al., 2010). Adolescent, but not adult, NR1 KO animals displayed behavioural abnormalities that could be relevant to the positive (hyperlocomotion and PPI deficits), negative (social interaction, nest building and sucrose preference deficits), and cognitive (SWM deficits) symptoms of schizophrenia (Belforte et al., 2010a). In fact, adolescent NR1 KO animals were impaired on all tasks tested, raising questions about the specificity of the observed behavioural deficits (Belforte et al., 2010). Interestingly, adult NR1 KO animals were not impaired when assessed for PPI and social interactions although performance on other tasks were not reported (Belforte et al., 2010). This suggests that NMDARs on PV interneurons might be essential during development rather than adulthood. However, it is worth noting that a couple of tasks were conducted after long-term social isolation, a factor that likely exacerbated or provoked deficits, as the same group showed in a follow-up study (Jiang et al. 2013).

Later the same year, PV specific NR1 KO animals (hereafter referred to as *Grin1*$^{\Delta PV}$ mice) were generated using a *Cre* line selective for PV interneurons that also preferentially targeted the hippocampus (Korotkova et al., 2010). These animals, although not proposed as a model of schizophrenia *per se*, did show some relevant behavioural deficits, including a profound deficit in SWM assessed on the T-maze but normal SRM (Korotkova et al., 2010). Interestingly, *Grin1*$^{\Delta PV}$ mice were found to have

reduced theta oscillation power and increased gamma oscillation power under baseline conditions in the hippocampus (Korotkova et al., 2010).

In 2012, another *Grin1*$^{\Delta PV}$ mouse was generated using a PV *Cre* driver line that targeted PV interneurons throughout the brain (Carlén et al., 2012). Surprisingly, considering PV neurons were being targeted throughout the brain and not just the hippocampus, these *Grin1*$^{\Delta PV}$ animals displayed only the most subtle SWM deficit when tested on the T-maze (Carlén et al., 2012), in contrast to the strong deficits reported with the hippocampus-specific *Cre* driver line (Korotkova et al., 2010). *Grin1*$^{\Delta PV}$ mice in this study showed normal locomotor activity, normal SRM and reversal learning assessed in the MWM, and no impairments in PPI (Carlén et al., 2012). Interestingly, *Grin1*$^{\Delta PV}$ mice in this study also displayed enhanced gamma oscillations under anaesthesia and a trend towards increased gamma oscillations in awake animals (Carlén et al., 2012). Taken together, these first three studies provide evidence that deletion of NMDARs from PV interneurons (Carlén et al., 2012; Korotkova et al., 2010), or a population of interneurons consisting largely of PV interneurons (Belforte et al., 2010), can induce SWM deficits, a possible endophenotype relevant to schizophrenia (Kellendonk et al., 2009) although the magnitude of these effects seemed extremely variable.

The picture becomes even less clear with subsequent studies which generated *Grin1*$^{\Delta PV}$ mice using the same combination of PV *Cre* driver line and “floxed” NR1 as Carlen *et al.*, which completely lacked SWM deficits assessed on the T-maze (Billingslea et al., 2014; Saunders et al., 2013). Both studies report social interaction deficits in *Grin1*$^{\Delta PV}$ animals (Billingslea et al., 2014; Saunders et al., 2013), and one reproduced the increase in baseline gamma power (Billingslea et al., 2014; gamma power not assessed by Saunders *et al.*).

Other genetic manipulations of interneuron populations can also lead to schizophrenia relevant phenotypes (del Pino et al., 2013; also see Cho et al., 2015). Deletion of the neuregulin receptor ErbB4 from the majority of PV and somatostatin (SOM) interneurons leads to a wide range of behavioural abnormalities, including hyperactivity and deficits in nest building, SWM and PPI (del Pino et al., 2013). Interestingly, similar to NR1 deletion, the interneuron KO of ErbB4 leads to enhanced baseline gamma oscillations (del Pino et al., 2013).

Overall, there is discrepancy in the literature regarding the precise phenotype of *Grin1* $^{\Delta PV}$ mice, particularly regarding cognitive deficits. These differences could be down to the use of different *Cre* driver and "floxed" NR1 mouse lines. However, the studies collectively show that manipulations to PV interneurons can alter baseline gamma power.

1.9 Tools for manipulating neuronal activity

To better understand neuronal circuit function, neuroscientists have sought to gain control over specific populations of neurons. Great advances have been made with regard to taking control over neuronal activity since the emergence of optogenetics and chemogentics.

Optogenetics involves the genetic delivery and expression of light sensitive "opsins" to populations of neurons which, when illuminated with light activate ion channels or pumps, that lead to depolarisation or hyperpolarisation of target cells (Boyden et al., 2005; Chow et al., 2010; Zemelman et al., 2002). These technologies have been used to study the role that defined populations of neurons play in behaviour (Claridge-Chang et al., 2009; Lima and Miesenböck, 2005).

Chemogenetics is similar, in principle, to optogenetics except that an inert ligand, rather than light, is used to activate modified receptors rather than light. Bryan Roth's lab created Designer Receptors Exclusively Activated by Designer Drugs (DREADDs) by cloning human muscarinic G-protein coupled receptors (GPCRs), expressing them in yeast cells, and then introducing random mutations to the receptor using mutagenic polymerase chain reaction (PCR) (Armbruster et al., 2007). These "mutant" clones were then screened and selected based on their affinity for an inert ligand Clozapine-N-oxide (CNO), and the lack of affinity for their endogenous ligand acetylcholine (in the case of muscarinic receptors) (Armbruster et al., 2007). Importantly, these mutant receptors, or DREADDs, were not activated when expressed in cells unless CNO was added, providing a "lock" (i.e. the DREADD receptor) and unique "key" (i.e. the CNO) mechanism for specific activation of the modified muscarinic receptors (Armbruster et al., 2007). As they are genetically encoded, DREADDs can be expressed in a cell type specific nature and can regulate the activity of neurons *in vivo*, inducing behavioural and physiological changes (Alexander et al., 2009). As CNO can cross the blood brain barrier, systemically administered CNO will reach the brain. This provides a non-invasive means of activating or inhibiting neuronal circuits *in vivo*. The time course of activation (or inhibition) is altogether different to optogenetics, where light pulses give millisecond control over neuronal activity, but this prolonged activation or inhibition with DREADDs is favourable under certain circumstances. The neuronal-silencing DREADD, hM4Di, is used in this thesis and is discussed in greater detail later (see **4.1.3)**.

1.10 Viral approaches to target neuronal circuits

As previously discussed, there are now a number of optogenetic and chemogenetic tools that can manipulate neuronal function. However, these tools still need to be

expressed in specific populations of neurons. Modified viruses are often used to express these tools in neurons.

1.10.1 Using adeno-associated viruses to target neurons

Adeno-associated viruses (AAVs) are routinely used to transfect neurons with genetic material (Betley and Sternson, 2011; McCown et al., 1996; Samulski et al., 1989). AAV is a good candidate for gene transfer because it is able to infect both dividing and post-mitotic cells (i.e. neurons), and because it only triggers a minor immune response (Miyake et al., 2015). In addition, *in vivo* application of AAV in the mouse brain has been shown to drive stable expression of transgenes such as green fluorescent protein (GFP) for over a year (Miyake et al., 2011). Use of promoter fragments, such as from the human synapsin (hSyn) gene, can efficiently drive transgene expression in a neuron selective manner (Kügler et al., 2003). Progress has been made to increase the stability of transgene expression which is discussed later (see **5.2.2**). The genome of AAV is single stranded and relatively small (~4.7 Kb) (Miyake et al., 2015), which limits the size of transgenes that can be transferred, but it is large enough for DREADD and optogenetic constructs.

Virally mediated gene transfer enables regional specificity in transgene expression when locally delivered via intracranial injection under stereotaxic control. This enables small populations of neurons in a given brain region to be manipulated which is often difficult with the alternative approaches of genomic (transgenic) delivery and *in utero* electroporation. In addition to regional specificity, cell-type specificity can be achieved by infusion of a modified virus into animals that express *Cre* recombinase in specific subtypes of neurons (Atasoy et al., 2008). To achieve this conditional expression the viral transgene is flipped into the incorrect orientation, flanked by pairs of inverted *LoxP* sites, which in the presence of *Cre* recombinase, flips the construct into the correct

orientation for transcription (Atasoy et al., 2008). In the absence of *Cre* recombinase the viral transgene remains in the incorrect orientation so that translation of the transgene is blocked, mainly by early occurrence of nonsense (STOP) mutations, i.e. absence of an open-reading frame (see **figure 4.1** for schematic explanation). Thus, regional and cell type specific manipulations can be made to neuronal circuits. This approach was used in this thesis to target the DREADD silencer hM4Di to PV neurons selectively (see **4.3.1**).

1.11 Aims of the thesis

This thesis aims to utilise a combination of genetic and chemogentic tools to study neuronal circuits that could be dysfunctional in schizophrenia. Chapters 2 to 4 focus on testing the Lisman/Grace model, in which NMDAR hypofunction on PV interneurons and the resulting decrease in PV interneuron-mediated inhibition is proposed to be a key starting point in the pathophysiology of schizophrenia (Lisman et al., 2008). This model is highly influential in the field and as such warrants further scrutiny. Chapter 5 takes a different genetic approach and explores a genetic model of glutamatergic dysfunction in mice lacking the GluA1 AMPAR subunit (*Gria1* KO). These animals have a well established behavioural phenotype thought to be relevant to the psychological processes disrupted in schizophrenia. The thesis aims to explore the neural circuit mechanism(s) that could underlie these psychological processes.

1.11.1 Chapter 2 aims

The second chapter uses a genetic approach to ablate NMDARs selectively from PV interneurons (*Grin1*$^{\Delta PV}$ mice) to test the Lisman/Grace model. *Grin1*$^{\Delta PV}$ animals were tested through a behavioural test battery chosen to assess phenotypes that could be relevant to schizophrenia. Although several studies have been published with similar

Grin1$^{\Delta PV}$ mice, the results are inconsistent between labs (Belforte et al., 2010; Billingslea et al., 2014; Carlén et al., 2012; Korotkova et al. 2010; Saunders et al., 2013). This could in part be due to the different PV *Cre* and "floxed" NR1 animals used in different studies in order to generate the different mutants. The behavioural screen tested here aimed to reconcile differences in the literature by assessing the phenotype of *Grin1*$^{\Delta PV}$ mice generated with the PV *Cre* line most widely used in the literature, in combination with the "floxed" NR1 mice predicted to give the strongest phenotype (Korotkova et al. 2010).

1.11.2 Chapter 3 aims

The third chapter re-investigates the interaction between PV interneuron NMDAR KO (*Grin1*$^{\Delta PV}$) mice and challenge with the NMDAR antagonist MK-801. NMDAR antagonists have for a long time been administered to rodents to model the glutamatergic hypofunction possibly relevant to schizophrenia. Recent studies have suggested that the effects of the NMDAR antagonist MK-801 could be via preferential action on NMDARs located on PV, and other corticolimbic, interneurons (Belforte et al., 2010; Carlén et al., 2012). These conclusions were made based on the fact that *Grin1*$^{\Delta PV}$ mice show an attenuated locomotor activity response when challenged with MK-801 compared to control animals. Thus, the drug effects were thought to be absent in *Grin1*$^{\Delta PV}$ mice, as their response is seemingly indistinguishable from that of vehicle-injected controls. This data chapter extends these studies and tests the effects of MK-801 in *Grin1*$^{\Delta PV}$ and control mice whilst they are assessed on a wider test battery including locomotor activity, motor coordination, sucrose preference and spatial working memory. In addition, electrophysiology recordings were made from the prefrontal cortex to record local field potential (LFP) signals whilst animals were

challenged with MK-801. NMDAR antagonists have been shown to induce slow (delta frequency) oscillations *in vitro* (Lisman, 2012), mimicking the enhanced delta oscillations seen in schizophrenics (Galderisi et al., 2009). To explore this further, the delta-inducing effects of MK-801 were assessed in awake, behaving *Grin1*$^{\Delta PV}$ and control animals.

1.11.3 Chapter 4 aims

The fourth chapter continues to test the Lisman/Grace model but by directly and acutely decreasing PV interneuron activity in the hippocampus with the DREADD silencer hM4Di. In the Lisman/Grace model reduced output from PV interneurons is proposed to lead to pathological network changes (Lisman et al., 2008). The Lisman/Grace model states that dysfunction of PV interneurons in the hippocampus could be particularly important as disinhibition of the hippocampus and increased hippocampal output can drive a hyperdopaminergic state (Floresco et al., 2001; Lisman et al., 2008). To directly address this, hM4Di was targeted to PV interneurons in the hippocampus. Specifically, area CA1 was targeted in either the dorsal or ventral hippocampus. The effect of hM4Di-mediated silencing of hippocampal PV interneurons on rodent behaviours relevant to schizophrenia was tested.

1.11.4 Chapter 5 aims

The manipulations assessed in chapters 2 - 4 (with the exception of additional NMDAR antagonist challenge) largely did not induce behavioural deficits relevant to schizophrenia. Therefore, for the final data chapter a different approach was taken. The behavioural phenotype of *Gria1* KO mice is well established and could result from a failure in short term habituation or even sensitisation (Barkus et al., 2014; Barkus et al., 2012; Sanderson et al., 2011b, 2009b). This could be relevant to the aberrant salience hypothesis of schizophrenia (Kapur, 2003). As such, these animals could

help us to understand how disruption of glutamatergic signalling and synaptic plasticity can impact on neural circuits and cellular mechanisms required for behavioural phenotypes possibly relevant to schizophrenia (Barkus et al., 2014).

One of the unanswered questions is precisely where in the brain GluA1 is required for normal behaviour. In the *Gria1* KO animals GluA1 is deleted in all neurons and throughout development (Zamanillo et al., 1999). In this thesis, a viral approach was used to reintroduce GluA1 selectively to the hippocampus of *Gria1* KO mice, to test if this was sufficient to rescue schizophrenia-relevant behavioural deficits. The hippocampus was chosen for a number of reasons. GluA1 is particularly enriched in the hippocampus (Zamanillo et al., 1999), and hippocampal expression of GluA1 appears to be reduced in schizophrenia (Eastwood et al., 1995, 1997). In addition, the hippocampus is known to be important for schizophrenia-relevant behaviours in rodents (Deacon et al., 2002; Sanderson et al., 2009a). Finally, there is evidence that hippocampal function is disrupted in schizophrenic patients (Harrison, 2004; Heckers et al., 2005; Schobel et al., 2013). Together, these data indicate that the hippocampus is a logical brain region to study with respect to where GluA1 is required for normal behaviour.

In addition, electrophysiological recordings of LFPs were made *in vivo* in an attempt to search for physiological correlates of the abnormal behaviour of *Gria1* KO mice. One such physiological “correlate” of schizophrenia is long range synchrony between neuronal circuits (Dickerson et al. 2010; Sigurdsson et al., 2010; Ford et al., 2002). Thus,

This thesis has therefore tested two circuit-specific genetic models of schizophrenia using *Grin1*$^{\Delta PV}$ mice, direct chemogenetic manipulations of PV interneurons with

hM4Di and general glutamatergic dysfunction in *Gria1* KO mice. By doing so, the aim was to explore neural circuits underlying psychological processes relevant to schizophrenia.

2 Behavioural phenotype of *Grin1*$^{\Delta PV}$ mice

2.1 Introduction

The neurobiology of schizophrenia is complex and a number of hypotheses have been proposed implicating the dopamine (Howes and Kapur, 2009), glutamate (Javitt and Zukin, 1991) and GABAergic neurotransmitter systems (Lewis et al., 2005). Rather than a dysfunction of one neurotransmitter system in isolation, it is highly likely that there is an interaction between multiple neurotransmitter systems in schizophrenia (Lisman et al., 2008).

2.1.1 The Lisman/Grace model

In 2008, Lisman, Grace and others proposed a model or "framework" to explain the interactions of multiple neurotransmitter systems in schizophrenia (Lisman et al., 2008). They proposed NMDAR hypofunction on parvalbumin (PV) interneurons as a starting point in schizophrenia, which could have important consequences on the network. PV interneurons provide fast perisomatic inhibition to pyramidal neurons (and other interneurons), efficiently controlling their output (Hu et al., 2014). As NMDARs provide excitatory drive to neurons, NMDAR hypofunction on PV interneurons will reduce their excitation and ability to provide effective feedback inhibition. This could lead to disinhibition of the network and an overall increase in pyramidal neuron firing. Separate to these immediate changes, there could also be secondary, slower, consequences of NMDAR hypofunction. If NMDARs on PV interneurons act as "activity sensors" to relay information about the activity levels of local excitatory circuits around them, then NMDAR hypofunction and the resulting reduction in excitatory drive to PV interneurons, will lead to a false "interpretation" of the activity levels of the local (Lisman et al., 2008). If the PV interneurons play a role in maintaining homeostatic

balance between excitation and inhibition, then the PV interneurons will undergo maladaptive compensatory changes by reducing their inhibitory output, leading to a disinhibition of the local circuit. Thus, the observed decrease in expression of glutamate decarboxylase isoform 67 (GAD67) (Lewis et al., 2005), an enzyme involved in the synthesis of GABA, could reflect compensatory changes to reduce GABAergic output again promoting disinhibition in the circuit (Lisman et al., 2008).

A delicate balance of excitation and inhibition is critical throughout the brain but could have particular significance in the hippocampus (Lisman et al., 2008). Increased output from the hippocampus, via the subiculum, can drive a hyperdopaminergic state via a tri-synaptic loop (Floresco et al., 2001; but see also Lou et al., 2011). Glutamatergic projections from the ventral subiculum excite the nucleus accumbens, a basal ganglia structure containing largely GABAergic neurons (Salgado and Kaplitt, 2015). The nucleus accumbens provides inhibition to the ventral pallidum, which in turn inhibits dopaminergic neurons of the ventral tegmental area (VTA). Stimulating the ventral hippocampus/subiculum can therefore release or reduce tonic inhibition of the VTA, increasing the number of dopamine neurons spontaneously firing (Floresco et al., 2001; but see also Lou et al., 2011).

This was experimentally shown by Floresco *et al.* who found that infusion of NMDA into the ventral hippocampus/subiculum dramatically increased the number of spontaneously active dopamine neurons in the VTA of anaesthetised rats (Floresco et al., 2001). In contrast, infusion of the Na^+ channel blocker TTX (used to locally block generation of action potentials) into the ventral hippocampus/subiculum, decreased (although not significantly) the number of spontaneously active dopamine neurons in the VTA, illustrating bidirectional control of the ventral hippocampus upon the activity of dopamine neurons in the VTA (Floresco et al., 2001).

One neurodevelopmental model of schizophrenia involves the challenge of pregnant rats (gestation day 17) with the DNA-alkylating compound methylazoxymethanol acetate (MAM) (Lodge and Grace, 2009). Resulting offspring from MAM treated rats exhibit a wide range of behavioral and physiological changes that could be relevant to schizophrenia (Lodge and Grace, 2009). For example, there is abnormal hippocampal regulation of dopamine neuron activity in MAM rats, seen by the increase in spontaneously active dopamine neurons in the VTA (Lodge and Grace, 2007). In MAM rats, the aberrant dopamine neuron activity is attributed to increased activity of the ventral hippocampus. Evidence for this comes from local infusions of tetrodotoxin (TTX) into the ventral hippocampus of MAM rats, which normalised dopamine neuron activity and amphetamine sensitivity when tested for psychostimulant induced hyperactivity (Lodge and Grace, 2007). It is possible that NMDAR hypofunction on PV interneurons can manifest in disinhibition of the hippocampus, boosting glutamatergic outputs, leading to the hyperdopaminergic phenotype strongly linked to schizophrenia and, in particular, positive symptoms of the disease (Howes and Kapur, 2009; Lisman et al., 2008).

In addition to explaining the hyperdopaminergic state, the Lisman/Grace model also seeks to explain cognitive symptoms associated with schizophrenia. Fast oscillations in the local field potential in the 30-100 Hz frequency range, known as gamma oscillations, are thought to be critical for a number of cognitive processes (Lisman and Jensen, 2013). In schizophrenia there are deficits in gamma oscillations (Howard et al., 2003), and changes in oscillatory activity have been proposed as an endophenotype of schizophrenia (Gandal et al., 2012; Uhlhaas and Singer, 2010). Abnormal gamma oscillations in schizophrenia could be responsible for cognitive deficits in the disease. As PV interneurons are thought to be critical for the generation

of gamma oscillations (Cardin et al., 2009; Mann et al., 2005; Sohal et al., 2009), the alterations in PV interneurons in schizophrenia could underlie changes in oscillations in the disease (Lisman et al., 2008).

2.1.2 Testing the Lisman/Grace model

The Lisman/Grace model (Lisman et al., 2008) is influential and has been widely cited (over 600 times at the time of writing). The model proposes a GABAergic origin of the pathophysiology of schizophrenia (Nakazawa et al., 2012), and accounts for the changes in multiple neurotransmitter systems seen in the disease (Lisman et al., 2008). Importantly, the model generates predictions that can be tested with animal models. The *Cre/LoxP* system has been used to generate PV NMDAR KO mice (hereafter referred to as *Grin1*$^{\Delta PV}$ mice; Billingslea et al., 2014; Carlén et al., 2012; Korotkova et al., 2010; Pozzi et al., 2014; Saunders et al., 2013). Another *Cre* line using the promoter for **p**rotein **p**hos**p**hatase **1**, **r**egulatory (inhibitor) subunit **2** (Ppp1r2^{cre}) that targets a population of forebrain interneurons, including a large population of PV positive interneurons, has also been used to generate Ppp1r2 NMDAR KO mice (hereafter referred to as *Grin1*$^{\Delta Ppp1r2}$ mice; Belforte et al., 2010; Jiang et al., 2013).

The behavioural phenotype of *Grin1*$^{\Delta PV}$ and *Grin1*$^{\Delta Ppp1r2}$ mice has been inconsistent between studies, particularly with respect to cognitive symptoms that are robust in some studies (Belforte et al., 2010; Korotkova et al., 2010) but completely absent in others (Billingslea et al., 2014; Saunders et al., 2013). This is likely because a combination of different *Cre* driver and floxed NR1 responder lines have been used in the different studies. The behavioural phenotypes of *Grin1*$^{\Delta PV}$ mice are summarised in **(table 2.1)** and were discussed above (see **1.8.4**).

Authors	Specificity	Positive	Negative	Cognitive	Physiology
Korotkova *et al.* 2010	PV (hippocampus specific)	Normal locomotor activity	Normal social interactions	Impaired spatial working memory (rewarded alternation on T-maze) Impaired novel object recognition	Increased baseline gamma power Decreased theta power
Belforte *et al.* 2010	PV + other interneuron types	Novelty induced hyperactivity Normal pre-pulse inhibition	Impaired nest building Impaired sucrose preference Impaired social interactions	Impaired spatial working memory (spontaneous alternation on Y-maze)	Increased firing of cortical pyramidal neurons
Carlen *et al.* 2011	PV	Normal locomotor activity Normal pre-pulse inhibition	Not tested	Impaired spatial working memory (rewarded alternation on T-maze) Normal spatial reference memory (Morris water maze) Impaired fear conditioning (contextual and cued)	Increased baseline gamma power Failure to induce further gamma with optogenetic drive of PV neurons
Saunders *et al*. 2013	PV	Not tested	Impaired social interactions	Normal spatial working memory (spontaneous alternation on T-maze)	Delayed N1 latency Reduced ultrasonic vocalisations
Billingslea *et al.* 2014	PV	Not tested	Impaired nest building Reduced social interactions	Normal/enhanced spatial working memory (spontaneous and continuous T-maze alternation)	Increased baseline gamma power No difference in auditory evoked gamma power
Pozzi *et al.* 2014	PV	Not tested	Normal sucrose preference	Not tested	Not tested

Table 2.1: Comparison of behavioural and physiological phenotypes of *Grin1*$^{\Delta PV}$ mice

2.1.3 Chapter 2 experimental aims

In an attempt to reconcile differences in the literature, the most commonly used PV^{cre} driver line (Hippenmeyer et al., 2005) was crossed with a floxed NR1 line (Korotkova et al., 2010) predicted to give the strongest phenotype based on the spacing between *LoxP* sites (a shorter distance between *loxP* sites should lead to faster recombination and hence faster ablation of NR1 from PV interneurons; see **1.8.4** and Belforte et al., 2010). The resulting $Grin1^{\Delta PV}$ and control mice were run through a test battery to look at rodent correlates of positive, negative and cognitive deficits of schizophrenia.

2.2 Methods

2.2.1 Breeding of animals

To gain genetic access to parvalbumin expressing neurons we utilised knockin mice containing a genomic insertion of *Cre* recombinase into the 3'-UTR of the parvalbumin-gene (PV^{cre}) (Hippenmeyer et al., 2005). PV^{cre} mice (background strain C57BL/6J) were crossed with *Grin1-2Lox* mice that contain *loxP* sites flanking exons 11-18 of *Grin1* (encoding NR1), the obligatory NMDAR subunit (Niewoehner et al., 2007) to generate cell type specific NR1 KO mice. In the absence of *Cre* recombinase, the *Grin1-2Lox* mice retain a functional *Grin1* gene, but expression of *Cre* recombinase will lead to the deletion of genomic DNA encoding exons 11-18, permanently blocking expression of *Grin1*, and accordingly the formation of any functional NMDARs in a cell type specific manner (Niewoehner et al., 2007).

The genotype of mice was determined with PCR from genomic DNA samples taken from ear clips using primers 5' – TGT GTC CCT GTC CAT ACT CAA – 3' and 5' – AAC ACT GTG GAC CAG GAC TTG – 3' giving a 325 bp product for the *Grin1* wildtype allele and a 375 bp product for the floxed allele. *Cre* recombinase was detected with primers 5'- CAC CCT GTT ACG TAT AGC CG – 3' and 5- GAG TCA TCC TTA GCG CCG TA – 3' resulting in a 330 bp product. Mice with two floxed *Grin1* and one *Cre* allele were used as $Grin1^{\Delta PV}$ knockouts, while *Cre* negative littermates homozygous (and rarely heterozygous) for the floxed *Grin1* allele(s) were used as controls (hereafter referred to as controls).

It is important to check the specificity and efficiency of *Cre* driver lines because promoters that are often assumed to be cell-type specific might actually be active in other neurons, confounding interpretation of results. For immunohistochemical validation of the PV^{cre} line used in this study PV^{cre} animals were crossed with Ai9 mice

that carry a *LoxP* flanked “Stop” cassette preventing transcription of the red fluorescent protein tdTomato (hereafter referred to as PV-Ai9 mice). In cells that express *Cre*, the “Stop” cassette will be removed and the targeted cell will express the fluorescent marker.

For *in vitro* electrophysiology experiments, PV-Ai9 mice were bred with *Grin1-2Lox* mice to generate triple transgenic animals, where PV cells with *Grin1* deletion will also express tdTomato. This enabled fluorescence guided patch-clamp recordings *in vitro*, to validate the functional loss of NMDARs.

All animals were bred and housed at the University of Oxford Biomedical Sciences Building in a temperature and humidity controlled vivarium with a 12-hour light/dark cycle with lights on at 07:00. Initially animals were raised in IVC cages, then transferred to open top cages by 6-12 weeks of age. Cages contained sawdust and enrichment in the form of sizzle nest and a cardboard house and tube. Mice were group housed at all times, except when short-term isolation was required for the experiment (e.g. sucrose preference testing). Experiments were conducted with the experimenter blind to genotype. All experiments conformed to the Animal (Scientific Procedures) Act 1986, UK, and the Local Ethical Review Committee at the University of Oxford.

2.2.2 Immunohistochemistry

To validate the PV^{cre} driver line, PV-Ai9 mice (10 weeks old) were transcardially perfused with PBS followed by 4% paraformaldehyde (PFA) and brains were post fixed for 24 hours in PFA. Coronal sections of 60 µm were cut on a vibratome in PBS and then washed 3 times in PBS. Sections were incubated in 0.15% TBS-Triton-X (TBST) for 20 minutes, then 20% horse serum/TBS-T for 1 hour, then slices were briefly washed in TBS-T and then incubated with the primary antibody (mouse anti-

parvalbumin, Swant, Switzerland) diluted 1:2000 in 2.5% horse serum-TBS-T for 48 hours. Following primary antibody incubation, the sections were washed 3 times in TBS-T and then incubated overnight with the fluorescent secondary antibody (Alexa488-coupled goat-anti-mouse, Molecular Probes, USA) diluted 1:500 in 2.5% horse serum-TBS-T. Sections were then washed 3 times with PBS, once in PB and mounted with Vectashield (Vector Labs, USA). All antibody incubations were done at 4°C and all other washes at room temperature.

To visualise fluorescent labelling with TdTomato (genetic) and Alexa488 (immunohistochemical), confocal stacks were acquired (Zeiss LSM510 confocal microscope) in the hippocampus and neocortex. The confocal stacks were imported into ImageJ (NIH, USA) and the cell counter plugin was used to quantify co-localisation of the fluorescent markers. A total of 11 stacks and 824 cells were counted for neocortex, 6 stacks and 95 cells for dHC, and 8 stacks and 154 cells for vHC.

2.2.3 *In vitro* patch clamp recordings[1]

Control (PV-Ai9, n = 2) and *Grin1*$^{\Delta PV}$ mice (PV-Ai9-Grin1-2Lox, n = 2) aged 2 months were transcardially perfused with a room-temperature solution containing (in mM): N-Methyl-D-glucamine, 92; KCl, 2.5; NaH_2PO_4, 1.25; Thiourea, 2; Ascorbic acid, 5; Na-Pyruvate, 3; $MgCl_2$, 10; D-Glucose, 25; $NaHCO_3$, 30; $CaCl_2$, 0.5; Sucrose, 1, and horizontal neocortical slices were prepared. The extracellular perfusion solution contained (in mM): NaCl, 119; KCl, 2.5; $CaCl_2$, 0.5; $MgSO_4$, 1.3; MgCl, 2; NaH_2PO_4, 1.25; $NaHCO_3$, 25; Glucose, 10. Picrotoxin (100 μM) was added to block $GABA_A$-receptors. PV-cells were identified according to red (tdTomato) fluorescence and recorded in voltage-clamp mode and whole-cell patch-clamp configuration. Pipette solution contained (in mM): CsGlu, 125; HEPES, 10; Na-Phosphocreatine, 10; NaCl, 8; Na-GTP, 0.33; EGTA, 0.2; TEA-Cl, 5; Mg-ATP, 4. A field extracellular stimulation (20-320 μA, 100 μs) was conducted at a distance of 200 – 500 μm from the recorded cells, every 40s. Stimulation-evoked AMPA-receptor-mediated currents were recorded as inward currents at a holding potential of -70 mV. Subsequently, 50 μM NBQX was added to the extracellular solution to block AMPA/Kainate-type glutamate receptors, and NMDA-receptor-mediated currents were recorded as outward currents at a constant holding potential of +40 mV. Neurons were held at +40 mV for at least 1 min before measuring the NMDA component to minimise contaminating outward current and ensure unblocking of the NMDA-receptor channel.

2.2.4 Behavioural studies

Behavioural studies were performed in the following order:

1. Novelty-induced locomotor activity

[1] Patch clamp recordings and data analysis were performed by Dr. Elizabeth Nicholson, UCL

2. Elevated plus maze
3. Spatial novelty preference
4. Rewarded alternation on the T-maze (subset of all animals)
5. Spatial reference memory and reversal learning (subset of all animals)
6. Social recognition memory (subset of all animals)
7. Novel object recognition (subset of all animals)
8. Sucrose preference
9. Nest building
10. Pre-pulse inhibition (subset of animals)

For some behaviours only a subset of animals was tested. Sucrose preference and nest building were assessed towards the end of the test battery because they required animals to be single housed and male animals can often not be re-housed together without fighting.

2.2.5 Novelty-induced locomotor activity

To assess novelty-induced hyperactivity mice were placed into novel clear plastic cages (length 43 cm, width 22 cm, height 20 cm) containing clean sawdust and locomotor activity was measured by infrared beam breaks (San Diego Instruments, San Diego, CA, US) for 2 hours in 5-minute time bins. Mixed sex cohorts were tested.

2.2.6 Pre-pulse inhibition[1]

Mice were placed into transparent plastic tubes inside startle-response test cabinets (San Diego Instruments, USA). After an adaptation/habituation period of 5 min with a background white noise of 65 dB, mice were subjected to a sequence of white-noise tones which started and ended with a series of five 120 dB startle-pulses, and

[1] PPI testing was done by Dr. Dennis Kätzel, data analysis by Alexei Bygrave.

contained 10 presentations each of startle-pulses (120 dB), pre-pulses at four levels (69 dB, 73 dB, 77 dB, 81 dB), and combinations of each pre-pulse with the startle-pulse (PPI-trials). Presentations were randomized for pre pulse intensity and occurred at random inter-trial-intervals of 10-20 s (average 15 s). Pre-pulses lasted 20 ms, startle-pulses 40 ms, and they were separated by a fixed 100 ms intra-trial interval in PPI-trials. Pre-pulse inhibition (PPI) was calculated for each PPI-intensity using the average startle-response from those ten 120 dB presentations interspersed with other trials (startle-response) as the baseline and the average response from the PPI-trial (PPI-response) according to the following formula:

PPI = 100 – (100 * PPI-response/startle-response)

The habituation to the startle pulse was calculated from the averages of the first five (startle(start)) and the last five (startle(end)) startle-responses. Only male mice were tested.

2.2.7 Elevated plus maze

An elevated plus maze (EPM) with two opposite grey closed arms (width 7 cm, length 38 cm, height 21 cm), and two open white arms (width 7cm, length 38 cm), elevated 72 cm above the ground, was used as a test of unconditioned anxiety. After a habituation period of 5 min in a novel cage in the test room, mice were placed in the centre of the maze facing an open arm and allowed to explore freely for 5 min. The position of the animal was tracked with EthoVisionXT (Noldus, Netherlands) and the preference for the open arms was calculated as the ratio of the total time in open arms and the time spent in open and closed arms combined (not including the centre). Transition between zones was determined by the position of the centre of the animal's body. Male and female mice were tested.

2.2.8 Sucrose preference

Mice were individually housed for this test and the test was conducted during the dark phase. Cages contained two water bottles, placed 20 cm apart on the same side of the cage. The test was conducted over three consecutive nights. During the first night, both bottles contained normal drinking water. The contents of one bottle was then replaced with 10 % sucrose (w/w; Sigma-Aldrich, Germany) in drinking water for the subsequent nights. During day time, the sucrose-containing bottle was removed and only the water bottle was left in the cage. The location of the sucrose-containing bottle was counterbalanced within each genotype, but not altered from one testing day to the next. Consumption between 7 pm and 10 am was measured for each bottle on each day and the preference for sucrose calculated as the ratio of consumption of sucrose-solution to total liquid consumption. Male and female mice were tested.

2.2.9 Nest building

Nest building was assessed as previously described (Deacon, 2006). Animals were single housed in cages containing clean sawdust and 3g of Nestlet™ bedding material 1 hour before the onset of the dark phase. Animals had *ad libitum* access to food and water. The following morning, nests were scored for quality, and unused bedding material was weighed. Nests were given a score between 1 and 5 based on the following scale:

1) Nestlet™ barely touched and more than 90% intact
2) Nestlet™ partially torn with 50-90% remaining intact
3) Nestlet™ mostly shredded but spread around the cage with no identifiable nest site

4) Nestlet™ shredded and formed into an identifiable but flat nest with the walls of the nest greater in height than a mouse lying down for less than 50% of the nests circumference
5) Nestlet™ shredded and formed into nest with walls higher than a mouse lying down for more than 50% of the nest's circumference

In some situations, the difference between nest scores were split and animals were assigned intermediate scores (i.e. a score of 4.5). Male and female mice were tested.

2.2.10 Social recognition memory

Testing was conducted in a 3-chamber apparatus as described previously (Moy et al., 2004), at low light levels (around 1 lux). CD1-mice of the same sex and roughly the same weight (± 10%) were used as stimulus mice and were repeatedly habituated to the small caged enclosures (square area with 7 cm side length) within the apparatus during the 3 days prior to testing. The test consisted of four phases, between which animals were enclosed in the central chamber but not removed from the apparatus. The phases were as follows; (1) habituation to the central chamber of the apparatus (5 min), (2) habituation to all three empty chambers (10 min), (3) social exposure (10 min) and (4) social memory (10 min). During the social exposure phase the test mouse was presented with two metal cage enclosures in the far corners of the peripheral chambers, one of which contained a CD1 stimulus mouse while the other was empty. For the social memory phase, the empty enclosure was replaced by an identical third enclosure containing a CD1 stimulus mouse from a different home cage. The location of the stimulus mouse was counterbalanced across genotypes in the sociability test (stimulus mouse in either left or right chamber) and the familiarity test (original stimulus mouse remaining in same location or swapping to other side of 3-chamber apparatus). The entries and time spent within a 2 cm interaction zone

surrounding the metal cages/enclosures were detected with automated tracking with AnyMaze (San Diego Instruments, USA). Entries into the interaction zone were registered if 30 % of the animal's body was present within the zone and exits were scored if less than 20 % was present in the zone. Animals were excluded from the analysis of the social memory experiment if they displayed an interaction time of < 180 s in the social exposure phase preceding the social memory test in order to ensure familiarity with the first stimulus mouse. Only male mice were tested.

2.2.11 Novel object recognition (object short-term memory)

Testing was conducted as previously described (Sanderson et al., 2011a). Mice were habituated to a dark grey open field (length 40 x width 40 cm, height 25 cm) for 5 minutes 3 times per day, for 2 days prior to testing. On the test day, mice were exposed to two identical copies of object X for 10 minutes. Mice were then removed from the open field for 2 minutes, during which the initial objects were replaced by an identical third copy of object X and a novel object Y. Mice were then returned to the open field and left to explore for 5 minutes. Videos were recorded using AnyMaze (San Diego Instruments, USA) and exploration of the objects was manually scored. Objects were cleaned with 70 % ethanol and water between animals. The identity of the first object and its position within the arena were counterbalanced for each genotype. The preference for the novel object was calculated as the ratio of the time spent with the novel object divided by the time spent with both objects combined. Only male mice were tested.

2.2.12 Spatial novelty preference

Spatial novelty preference was assessed using a clear Perspex Y-maze (each arm: width 8 cm, length 30 cm, height 20 cm) as previously described (Sanderson et al., 2009a). To promote exploratory behaviour, the maze was scattered with a mixture of

clean and dirty sawdust (mixed 3:1) from the cages of unfamiliar mice of the same sex. In the sample trial mice were placed in the start arm and allowed to explore the maze for 5 minutes with either the left or right arm blocked off (counterbalanced for genotype). Mice were then removed from the maze for an intra-trial interval (ITI) of 1 minute during which the sawdust was mixed and re-distributed around the maze and the divider (blocking off one arm) was removed. In the choice phase mice were given 2 minutes to explore the entire Y maze. The location of the mouse was tracked with EthoVisionXT (Noldus, Netherlands). The preference for the novel arm was calculated as the ratio of the time spent in the novel arm divided by the time spent in both familiar and novel arms combined. Male and female mice were tested.

2.2.13 Rewarded alternation on the T-maze

Rewarded alternation was tested in a wooden elevated T-maze painted grey (start arm: width 10 cm, length 47 cm; goal arms: width 10cm, length 35cm; wall-height 10 cm; elevated 100 cm above ground) with metal food wells fixed to the end of each goal arm. Prior to testing animals were put on a food-restricted diet to limit them to 85-90 % of their free-feeding weight. Mice were then habituated to the maze and to the condensed milk reward (mixed 50:50 with drinking water), initially in groups, and then individually.

During training and testing (when inter and intra-trial interval parameters were changed), each trial consisted of a sample and a choice run. In the sample run mice were placed in the start arm facing the experimenter and forced to run into one of the goal arms to gain a reward. The forced direction was pseudo-randomly assigned, with no more than three consecutive trials in the same direction, with overall equal numbers of left and right allocations. Mice were then removed from the maze for a defined intra-trial interval (1 s, 5 s or 15 s, as indicated), during which the door from the second goal

arm was removed. For the choice run mice were returned to the maze start arm facing the investigator and allowed to make a free choice between both goal arms, of which only the previously blocked (unvisited) one was rewarded. A decision was counted when the mouse had crossed the T-junction and all four paws were within a goal arm. Mice received 3 days of training with an inter-trial interval of 6-8 minutes (spaced trial regime) and an intra-trial interval of 5 seconds. After this initial training mice were tested with different intra- and inter-trial intervals to manipulate the difficulty of the task and to replicate conditions used in related previous studies (Carlén et al., 2012; Korotkova et al., 2010). Only male mice were tested. The cohort was initially tested at 2 months of age and re-tested again at 6 months of age.

2.2.14 Spatial reference memory and reversal learning[1]

Food deprivation, maze and reward habituation were as described for the rewarded alternation task above. An elevated grey wooden plus maze with 10 cm wall height and 10 cm inner arm width was used; arm-length was 35 and 40 cm for goal and start arms, respectively. For each mouse one goal arm location (as defined by allocentric extra-maze cues in the room consisting of posters on the walls and a Duplo™ tower positioned next to the maze in the north-east corner) was assigned to be rewarded (east or west arm). The arm allocation was counterbalanced for genotype. The maze was rotated by 180° once per day to prevent association of subtle intra-maze cues with the reward. On every trial the start arm was pseudo-randomly chosen from the two possible start arms (north or south arm) of the maze in order to reduce the possibility of mice using an egocentric strategy to solve the task (i.e. always turn left). Mice were trained to a criterion of 17/20 (85 %) correct choices across four consecutive blocks of 5 trials. Afterwards, the location-reward association was

[1] Testing was conducted by Michelle Berkemann under the supervision of Alexei Bygrave.

reversed (i.e. mice originally trained to go to the east arm reversed to the west arm) and training continued until mice reached the same criterion to assess reversal learning. One *Grin1*$^{\Delta PV}$ mouse was excluded from the analysis because it did not reach criterion for reversal learning even after >30 training blocks. Only male mice were tested.

2.2.15 Statistical analysis

Normality of data was assessed with the Shapiro-Wilk test and manual assessment of Q-Q plots. Where criteria for normality were met parametric analyses were performed (ANOVA and repeated measures ANOVA). Where data deviated from the normal distribution non-parametric tests were performed (Mann-Whitney U test, MWU). In some instances, non-normal data were Log_{10} transformed to normalise the data and allow parametric statistical testing (locomotor activity and social memory test). The exception to this is PPI, sucrose preference, and rewarded alternation on the T-maze where data met normality for some but not all of the repeating measures. As Log_{10} transformations did not normalise the data in these instances, data were analysed with a repeated measure ANOVA and one-way ANOVA despite this partial violation of normality. All statistical tests were performed using SPSS version 21 (IBM).

2.3 Results

2.3.1 Efficient and specific targeting of PV interneurons

To assess the extent of PV interneuron coverage with the PV^{cre} driver line PV-Ai9 mice were generated that express the red fluorescent protein tdTomato in a *Cre*-dependent manner. Successful *Cre*-mediated recombination will lead to expression of tdTomato, enabling visualisation of the cells targeted with the PV^{cre} knockin line. Expression of PV in PV-Ai9 mouse brain sections (2 mice aged 10 weeks) was probed with an anti-parvalbumin antibody and detected with a conjugated green fluorescent secondary antibody. Confocal stacks of the sections were acquired to enable co-localisation of green and red fluorescent markers **(figure 2.1a)**. PV (antibody labelled green) and tdTomato (genomically labelled) positive neurons were counted. The proportion/coverage of PV interneurons targeted (PV positive interneurons also tdTomato positive), as well as the specificity for PV interneurons (tdTomato positive and PV positive), was calculated in neocortex, dorsal and ventral hippocampus **(figure 2.1b)**.

In the neocortex there was near complete targeting of PV interneurons (95.6%± 3.9 %; mean ± S.D.). The targeting in the dorsal (84.5%± 10.7 % mean ± S.D.) and ventral (83.9%± 6.8 % mean ± S.D.) hippocampus was slightly lower. To check the specificity of recombination for PV interneurons, the reverse count was done; the percentage of TdTomato positive cells that were also PV positive was calculated **(figure 2.1c)**. The specificity was found to be very high in the neocortex (95.6% ± 4%; mean ± S.D.) and ventral hippocampus (94.6% ± 3.3%; mean ± S.D.) and slightly lower in the dorsal hippocampus (91.1% ± 6.6%; mean ± S.D.). The cells that were tdTomato-positive but were not PV-positive could be other cell types, or could indeed be PV neurons that just express PV at levels not detectable with immunohistochemistry (Sohal et al.,

2009). This is possible since the expression levels of PV are sensitive to the environment and can change dramatically (Donato et al., 2013). These data nevertheless confirm that the PV^{cre} driver line serves as a powerful tool for specifically targeting PV interneurons, in the neocortex and hippocampus.

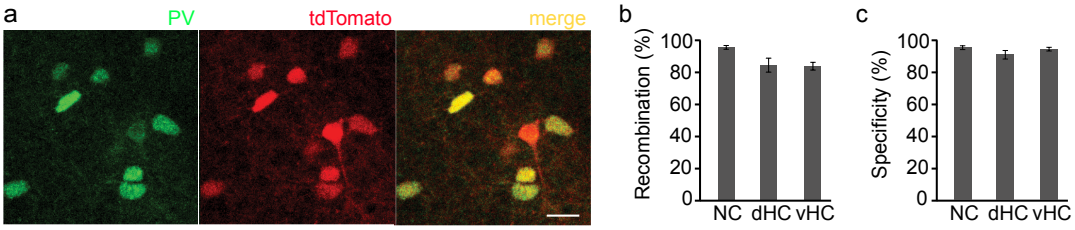

Figure 2.1: Specificity testing of PV^{cre} driver line
(a) Confocal projection of a neocortex section from a PV-Ai9 mouse immunostained for parvalbumin (PV). (b) Percentage of recombination (PV interneurons also tdTomato positive) and (c) specificity of recombination (tdTomato neurons also PV positive) in neocortex (NC), dorsal hippocampus (dHC) and ventral hippocampus (vHC). Scale bar represents 20μm. Counts from two male PV-Ai9 mice aged 10 weeks. A total of 11 stacks and 824 cells have been counted for neocortex, 6 stacks and 95 cells for dHC, and 8 stacks and 154 cells for vHC. Displayed are mean values ± SEM.

2.3.2 Validation of NMDAR ablation in *Grin1*$^{\Delta PV}$ knockouts

A lack of good antibodies prevented immunohistochemical validation of *Grin1* ablation from PV interneurons, so *in vitro* patch clamp recordings were made to probe the AMPAR and NMDAR currents in control and *Grin1*$^{\Delta PV}$ knockouts. For these experiments triple transgenic mice were used (PV-Ai9-Grin1-2Lox KOs or PV-Ai9 controls) to enable fluorescence-guided patch-clamp recordings of PV interneurons. Acute slices of neocortex were prepared and tdTomato positive cells were recorded in whole-cell configuration, voltage clamp mode. AMPAR and NMDAR currents were recorded at -70 mV and +40mV respectively **(figure 2.2a)**. The ratio of NMDAR to AMPAR currents was significantly lower in the *Grin1*$^{\Delta PV}$ knockouts compared to

controls indicating a functional loss of NMDAR currents **(figure 2.2b)** (MWU: P = 0.035).

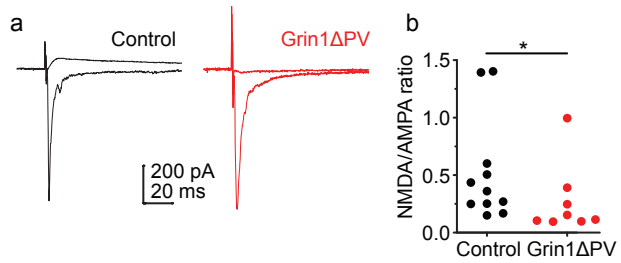

Figure 2.2: Confirmation of NMDAR ablation *in vitro*
Patch clamp recordings from PV interneurons in PV-Ai9 (control in this case) and PV-Ai9-Grin2-lox mice (shortened to *Grin1*$^{\Delta PV}$ in this case). (a) Example traces for the AMPA-receptor currents recorded at holding potentials of -70 mV indicated by a large downward slope in control (black) and *Grin1*$^{\Delta PV}$ (red) and the NMDAR-currents recorded at +40 mV holding potential indicated by a small upward slope in control and a flat line in *Grin1*$^{\Delta PV}$ mice. (b) NMDAR to AMPAR current ratio for control and *Grin1*$^{\Delta PV}$ mice. * indicates a significant effect of genotype ($P < 0.05$) on NMDA/AMPA ratio. Each dot indicates one cell.

2.3.3 Age-dependent novelty-induced hyperactivity in *Grin1*$^{\Delta PV}$ mice

Loss of NMDARs from PV interneurons could lead to disinhibition of neuronal circuits. In the hippocampus, this might lead to increased output from the subiculum driving a hyperdopaminergic state that could induce the positive symptoms seen in schizophrenia (Lisman et al., 2008). Locomotor activity is sensitive to levels of dopamine and, as such, hyperactivity is considered a readout of a hyperdopaminergic state in rodents (Pratt et al., 2012). To explore this possibility, two separate cohorts of control and *Grin1*$^{\Delta PV}$ mice were tested for novelty induced hyperactivity at different ages by exposing them to a novel environment and recording their locomotor activity via infrared beam breaks **(figure 2.3)**. The total number of beam breaks made over the course of 2 hours was calculated.

In two month old mice there was no significant difference in the number of beam breaks made by controls (N = 19) or *Grin1*$^{\Delta PV}$ (N = 25) mice, as revealed by a repeated measures ANOVA with genotype and sex as between subject factors and time bin as a within subject factor (effect of genotype: F(1,40) = 0.081, P = 0.778; effect of sex: F(1,40) = 3.266, P = 0.078; sex*genotype interaction: F(1,40) = 1.288, P = 0.263). The number of beam breaks significantly decreased over time, but this did not significantly differ between controls and *Grin1*$^{\Delta PV}$ mice (effect of time: F(23,920) = 154.744, P = 0.001; time*genotype interaction: F(23,920) = 1.051, P = 0.397).

However, in 5 month old mice, *Grin1*$^{\Delta PV}$ (N = 26) animals made significantly more beam breaks than controls (N = 21) indicating novelty induced hyperactivity, as revealed by the same analysis (effect of genotype: F(1,43) = 13.443, P = 0.001; effect of sex: F(1,43) = 0.216, P = 0.645; sex*genotype interaction: F(1,43)= 0.483, P= 0.491). The number of beam breaks significantly decreased over time, and the decrease was significantly different between genotypes (effect of time: F(23,989) = 76.756, P = 0.001; time*genotype interaction: F(23,989) = 1.883, P = 0.007).

Grin1$^{\Delta PV}$ animals therefore display a pronounced age-dependent hyperactivity phenotype, as revealed by a repeated measures ANOVA when the 2 and 5 month old cohorts were analysed together with age, sex and genotype as between subject factors and time as a within subject factor (effect of genotype: F(1,83) = 7.684, P = 0.007; age*genotype interaction: F(1,83) = 5.602, P= 0.020). There was no overall effect of sex or age on locomotor activity (effect of sex: F(1,83) = 2.601, P = 0.111; effect of age: F(1,83) = 1.555, P = 0.216).

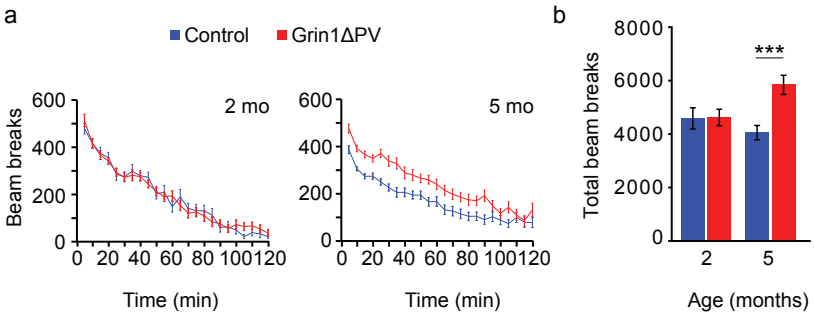

Figure 2.3: Age dependent novelty induced hyperactivity in *Grin1*$^{\Delta PV}$ mice
(a) 5-minute time bin and (b) total beam breaks for control (blue) and *Grin1*$^{\Delta PV}$ (red) mice aged 2 and 5 months. Error bars display SEM. *** indicates significant (P < 0.001) genotype difference in mice aged 5 months.

2.3.4 Normal pre pulse inhibition in *Grin1*$^{\Delta PV}$ mice

To assess sensorimotor gating (see **1.6.1**) male control (n = 12) and *Grin1*$^{\Delta PV}$ (N = 12) mice aged approximately 5 months were tested for pre-pulse inhibition (PPI) **(figure 2.4a)**. The percentage of PPI was calculated for the four pre-pulse intensities (69, 73, 77 and 81 dB) and analysed with a repeated measures ANOVA with pre-pulse intensity as a within subject factor and genotype as a between subject factor. There was no significant effect of genotype on PPI, indicating normal sensorimotor gating in control and *Grin1*$^{\Delta PV}$ mice (effect of genotype: $F(1,22) = 1.4$, $P = 0.249$). There was a significant effect of pre-pulse intensity on PPI, where greater intensity pre-pulses led to higher PPI, but this was not different between control and *Grin1*$^{\Delta PV}$ mice (effect of pre-pulse intensity: $F(3,66)= 114.392$, $P= 0.001$; genotype*pre-pulse intensity interaction: $F(3,66)= 2.535$, $P= 0.064$).

In addition to PPI, the average startle response to 120 dB pulses was measured at the start and end of the experiment to test for habituation of the startle response **(figure 2.4b)**. Normal habituation of the startle response was observed and this was not significantly different between genotypes as revealed by a repeated measures

ANOVA with test phase (start and end) as a within subject factor and genotype as a between subjects factor (effect of genotype; F(1,22) = 0.127, P = 0.725; effect of test phase: F(1,22)= 15.174; P= 0.001, test phase*genotype interaction: F(1,22)= 0.412, P= 0.527).

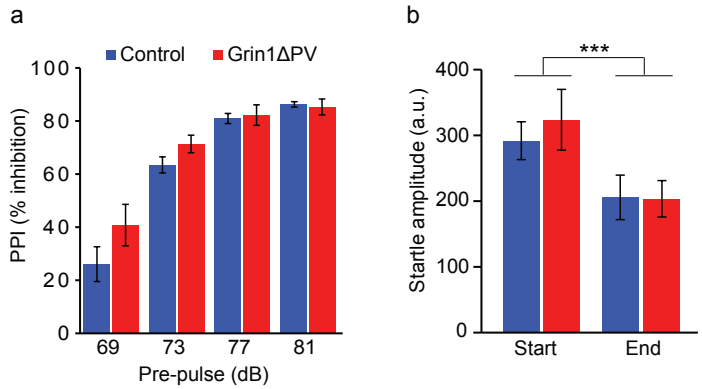

Figure 2.4: Normal pre pulse inhibition in *Grin1*$^{\Delta PV}$ mice
(a) PPI in control (blue) and *Grin1*$^{\Delta PV}$ (red) mice. (b) Startle response to the first (start) and last (end) five 120 dB pulses. Error bars display SEM. *** indicates significant (P < 0.001) effect of phase (start vs. end) on startle response. (a.u. = arbitrary units).

2.3.5 Normal sucrose preference in *Grin1*$^{\Delta PV}$ mice

To assess anhedonia (see **1.6.2**), male and female control (N = 20) and *Grin1*$^{\Delta PV}$ (N = 19) mice aged around 3 months were tested for sucrose preference. On day 1 mice were given two bottles both containing water. On day 2 and 3 animals were given the choice between water and 10% sucrose solution and the preferential consumption of sucrose was calculated (**figure 2.5**).

There was no significant overall effect of genotype on the sucrose preference of control and *Grin1*$^{\Delta PV}$ mice. However, there was a significant test day*genotype interaction, where the sucrose preference of *Grin1*$^{\Delta PV}$ increased on the second test day whilst the sucrose preference of controls decreased on the second day. This was revealed with a repeated measures ANOVA for sucrose preference with genotype and

sex as between subject factors and test day as a repeated measure (effect of genotype: F(1,35) = 0.002, P = 0.963; test day*genotype interaction: F(1,35) = 7.662, P = 0.009). The same analysis revealed that male mice in general showed higher levels of sucrose preference but this was the case in both control and *Grin1*$^{\Delta PV}$ mice (effect of sex: F(1,35)= 36.161, P= 0.001; sex*genotype interaction: F(1,35)= 3.230, P= 0.081).

Based on previous literature, *Grin1*$^{\Delta PV}$ mice were expected to show impaired sucrose preference (Belforte et al., 2010). The lack of a phenotype observed here cannot be explained by differences in the total amount of liquid consumed, as there was no significant effect of genotype or day*genotype interaction on the total liquid consumption across all three days. This was revealed with a repeated measures ANOVA for total liquid consumption with genotype and sex as between subject factors and day as a repeated measure (effect of genotype: F(1,33) = 1.989 P = 0.168; day*genotype interaction: F(2,66) = 0.700, P = 0.5; **figure 2.5).** In the above analysis one control and one *Grin1*$^{\Delta PV}$ animal had to be excluded because there was a slight leakage of the water bottle on day 1, preventing an accurate measurement of liquid consumption.

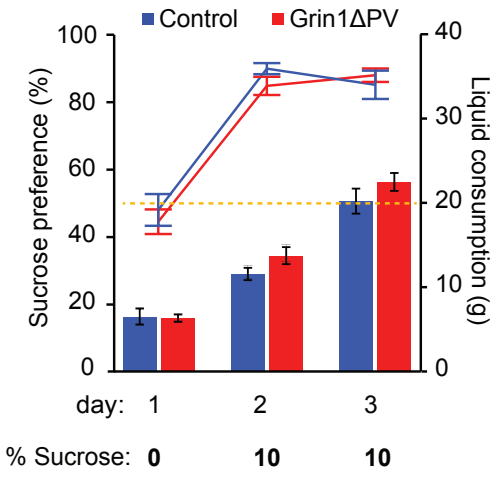

Figure 2.5: Normal sucrose preference in *Grin1*$^{\Delta PV}$ mice
Preference for sucrose (left axis and line graph) and the total liquid consumed (right axis and bars) in control (blue) and *Grin1*$^{\Delta PV}$ (red) mice. Yellow dashed line indicates chance preference for sucrose. Error bars display SEM.

2.3.6 Reduced anxiety in young *Grin1*$^{\Delta PV}$ mice

Unconditioned anxiety was assessed on the elevated plus maze in two distinct cohorts of control and *Grin1*$^{\Delta PV}$ mice aged 2 and 4 months **(figure 2.6)**. The conflict in whether to approach or avoid the open arms of the maze is anxiogenic, and assessing the time spent in the open versus the closed arms indicates the anxiety levels of the animal (anxious animals will stay in the closed arms).

In a cohort of animals aged 2 months (19 control and 25 *Grin1*$^{\Delta PV}$ mice) *Grin1*$^{\Delta PV}$ mice displayed a significantly higher preference for the open arms of the elevated plus maze, indicating reduced anxiety compared to controls (MWU: $U_{19,25}$ = 146, P = 0.03; median preference for open arm: 0.16 and 0.24 for control and *Grin1*$^{\Delta PV}$ mice respectively). The reduced anxiety observed in *Grin1*$^{\Delta PV}$ mice is unlikely to result from differences in locomotor activity, as the total number of closed arm entries (a pseudo-readout of overall activity) made by *Grin1*$^{\Delta PV}$ mice and controls was not significantly

different (MWU: $U_{19,25}$ = 282.5; P = 0.285; median number of closed arm entries: 27 and 25 for control and *Grin1*$^{\Delta PV}$ mice respectively; **data not shown**).

In a separate cohort aged 4 months (23 control and 32 *Grin1*$^{\Delta PV}$ mice) there was no significant difference in the preference for the open arms of the elevated plus maze indicating similar levels of anxiety in control and *Grin1*$^{\Delta PV}$ mice (MWU: $U_{23,32}$ = 294.5, P = 0.209; median time preference for open arm: 0.07 and 0.11 for control and *Grin1*$^{\Delta PV}$ mice respectively). However, aged 4 months, *Grin1*$^{\Delta PV}$ mice made significantly more closed arm entries when compared to controls, indicating *Grin1*$^{\Delta PV}$ mice were more active on the maze (MWU: $U_{23,32}$ = 240.5, P = 0.029; median number of closed arm entries: 12 and 19.5 for control and *Grin1*$^{\Delta PV}$ mice respectively; **data not shown**). This is in line with the age dependent novelty induced hyperactivity observed in *Grin1*$^{\Delta PV}$ mice (see **2.3.3**). It is worth noting that the 4 month old animals seemed to be more anxious compared with the 2 month old animals.

In the above analysis of the time preference for the open arm, one control (aged 4 months) and four *Grin1*$^{\Delta PV}$ mice (one at 2 months and three at 4 months) were identified as potential outliers (greater than 1.5 x the interquartile range), but these were not removed prior to statistical testing.

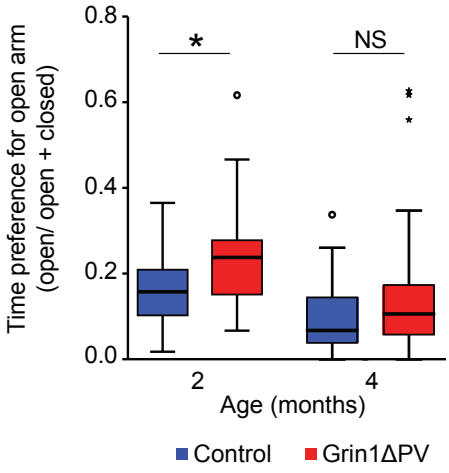

Figure 2.6: Reduced anxiety in young *Grin1*$^{\Delta PV}$ mice
Time preference for the open arms on the elevated plus maze in control (blue) and *Grin1*$^{\Delta PV}$ (red) mice. Boxplots display the median (thick black line) flanked by the 25th and 75th percentiles (bottom and top of box respectively) and whiskers display the maximum and minimum (excluding outliers). Data points that could reflect outliers are indicated by circles (if between 1.5 – 3x the interquartile range) or small stars (if greater than 3x the interquartile range). Outliers were not removed for statistical testing. * indicates significant ($P < 0.05$) effect of genotype. (NS, no significant difference).

2.3.7 Normal nest building in *Grin1*$^{\Delta PV}$ mice

To assess nest building, male and female control (N = 31) and *Grin1*$^{\Delta PV}$ (N = 33) mice aged 3-4 months were single housed in a clean cage containing 3g of Nestlet^{TM} material and left overnight (Deacon, 2006). The following morning the nests were scored for quality and unused bedding material was weighed **(figure 2.7)**.

There was no significant difference between genotypes in the nest scores (nest score: $U_{31,33} = 569.5$, $P = 0.424$; median nest score: 4.5 and 4 for control and *Grin1*$^{\Delta PV}$ mice respectively), or the weight of unused bedding material (unused bedding material: $U_{31,33} = 470.5$, $P = 0.567$; median unused bedding (g): 0.1 and 0.5 for control and *Grin1*$^{\Delta PV}$ mice respectively out of 3g of material provided), indicating normal nest building in *Grin1*$^{\Delta PV}$ mice.

Five controls (nest score) and one *Grin1*$^{\Delta PV}$ (unused bedding) were identified as potential outliers (greater than 1.5 x the interquartile range), but these were not removed prior to statistical testing.

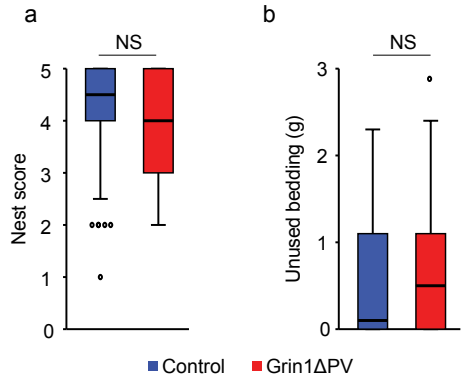

Figure 2.7: Normal nest building in *Grin1*$^{\Delta PV}$ mice
(a) Nest building score and (b) unused bedding material in control (blue) and *Grin1*$^{\Delta PV}$ (red) mice. Boxplots display the median (thick black line) flanked by the 25th and 75th percentiles (bottom and top of box respectively) and whiskers display the maximum and minimum (excluding outliers). Data points that could reflect outliers are indicated by circles (if between 1.5 – 3x the interquartile range). Outliers were not removed for statistical testing. (NS, no significant difference).

2.3.8 Normal social interaction and social memory in *Grin1*$^{\Delta PV}$ mice

A three chamber apparatus was used to assess social interaction and subsequently social memory. In the social interaction test, male control (N = 17) and *Grin1*$^{\Delta PV}$ (N = 23) mice aged 3 months were presented with two enclosures within the test apparatus, one containing a CD1 stimulus mouse and the other empty **(figure 2.8a)**.

There was no significant effect of genotype on the time control or *Grin1*$^{\Delta PV}$ mice spent investigating the stimulus mouse (vs. the empty enclosure) **(figure 2.8b)**, or the preference ratio that control and *Grin1*$^{\Delta PV}$ mice displayed for the stimulus mouse (vs. the empty enclosure) during the social interaction test phase **(figure 2.8c)** indicating normal social interactions in *Grin1*$^{\Delta PV}$ mice. This was revealed by an ANOVA with

genotype as a between subject factor (effect of genotype on investigation time: F(1,38) = 0.185, P = 0.670; effect of genotype on social preference as a ratio: F(1,38) = 0.050, P = 0.824). Both control and *Grin1*$^{\Delta PV}$ mice displayed a preference for the social chamber (vs. empty enclosure) during the social interaction test phase that was significantly above chance, as revealed by one-sample T-tests against chance (ratio of 0.5) preference (controls: t(1,16) = 6.616, P = 0.001; *Grin1*$^{\Delta P}$: t(1,22) = 7.487, P = 0.001).

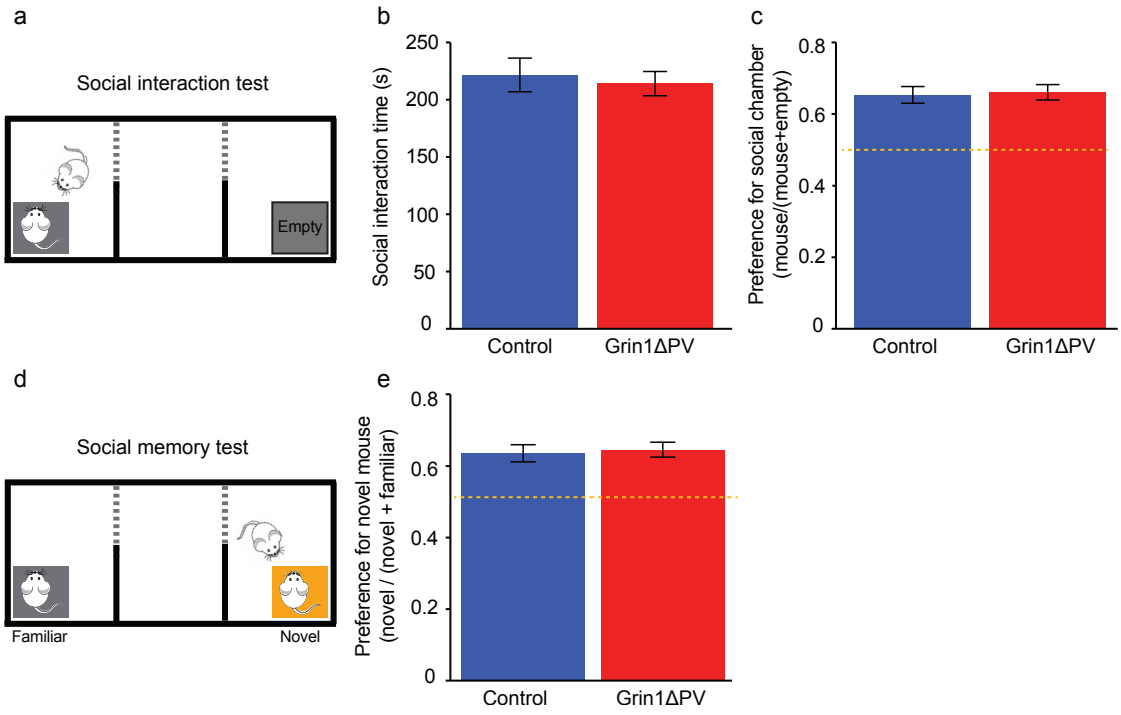

Figure 2.8: Normal social interaction and social memory in *Grin1*$^{\Delta PV}$ mice
(a) Apparatus for social interaction test. Grey dotted line illustrates sliding doors, and grey boxes represent enclosures (b) Total social investigation time of control (blue) and *Grin1*$^{\Delta PV}$ (red) mice during social interaction test. (c) Time preference for social versus empty enclosure in control and *Grin1*$^{\Delta PV}$ mice during social interaction test. (d) Apparatus for social memory test. Orange box illustrates enclosure with novel mouse. The location of the novel mouse was counterbalanced so 50% of the time the novel mouse is in the same position that the original (i.e. familiar) mouse was in during the social interaction test phase. (e) Time preference for novel versus familiar stimulus mouse in control and *Grin1*$^{\Delta PV}$ mice. Yellow dashed line indicates chance level preference. Error bars display SEM.

To assess social memory, the original mouse was kept in the apparatus (although the location i.e. left or right side of apparatus was counterbalanced) and the empty enclosure (used in the social interaction test phase) was swapped for an identical chamber containing a novel stimulus mouse (**figure 2.8d**). The preference for the novel stimulus mouse over the familiar mouse was then assessed. Because this depends on the test subject being familiar with the original stimulus mouse only animals that spent more than 180s investigating the stimulus mouse during the social interaction test phase were included in the analysis. This meant that 3 controls and 6 *Grin1*$^{\Delta PV}$ mice were excluded from the analysis. The time preference for the novel mouse was calculated, and Log_{10} transformed to normalise the data. Subsequent analyses were performed on the Log_{10} transformed data allowing parametric statistical analysis.

There was no significant effect of genotype on the social memory preference ratio, indicating normal social memory in control and *Grin1*$^{\Delta PV}$ mice. This was revealed by an ANOVA with genotype as a between subject factor (effect of genotype on social memory preference ratio: $F(1,29)= 0.115$, $P= 0.737$) (**figure 2.8e**). Both control and *Grin1*$^{\Delta PV}$ mice displayed a social memory preference ratio that was significantly above chance, as revealed by one-sample T-tests against chance (ratio of 0.5) preference (controls: $t(1,13) = 5.657$, $P = 0.001$; *Grin1*$^{\Delta PV}$: $t(1,16) = 7.022$, $P = 0.001$).

2.3.9 Intact novel object recognition in *Grin1*$^{\Delta PV}$ mice

Novel object recognition (NOR) was used as a non-spatial test of recognition memory. Male control (N = 8) and *Grin1*$^{\Delta PV}$ (N = 13) mice aged 5 months were familiarised to two identical objects and then, after a short delay, they were exposed to a third copy of the original object paired with a novel object (**figure 2.9a**).

For tests of recognition memory, it is important that animals show similar exploration of the objects during the exposure phase. There was no significant difference in the time control and *Grin1*$^{\Delta PV}$ mice spent investigating the novel objects in the exposure phase. This was revealed by an ANOVA with genotype as a between subject factor (effect of genotype on total exploration: $F(1,19) = 0.129$, $P = 0.723$; **figure 2.9b**). During the test phase the total exploration time of objects (time exploring novel and familiar objects) was also not significantly different between control and *Grin1*$^{\Delta PV}$ mice as revealed by an ANOVA with genotype as a between subject factor (effect of genotype on total exploration: $F(1,19) = 0.005$, $P = 0.946$; **data not shown**). Thus during both exposure and test phases there was similar total exploration of objects in control and *Grin1*$^{\Delta PV}$ mice.

The time spent exploring the novel object during the test phase was not significantly different between control and *Grin1*$^{\Delta PV}$ mice as revealed by an ANOVA with genotype as a between subject factor (effect of genotype on novel object exploration: $F(1,19) = 1.187$, $P = 0.290$; **figure 2.9c**). The novel object preference ratio (time investigating novel / time investigating novel + time investigating familiar) was also not significantly different between control and *Grin1*$^{\Delta PV}$ mice, although numerically *Grin1*$^{\Delta PV}$ mice showed a decreased preference for the novel object. This was revealed with an ANOVA with genotype as a between subject factor (effect of genotype on novel object preference as a ratio: $F(1,19) = 1.348$, $P = 0.260$; **figure 2.9d**). Both control and *Grin1*$^{\Delta PV}$ mice displayed a preference for the novel object during the test phase as both groups had novel object preference ratios significantly above chance. This was revealed with one-sample T-tests against chance (ratio of 0.5) preference (Controls:

t(1,7) = 4.508, P = 0.003; *Grin1*$^{\Delta PV}$: t(1,12) = 2.427, P = 0.032). Thus, *Grin1*$^{\Delta PV}$ mice display intact non-spatial recognition memory.

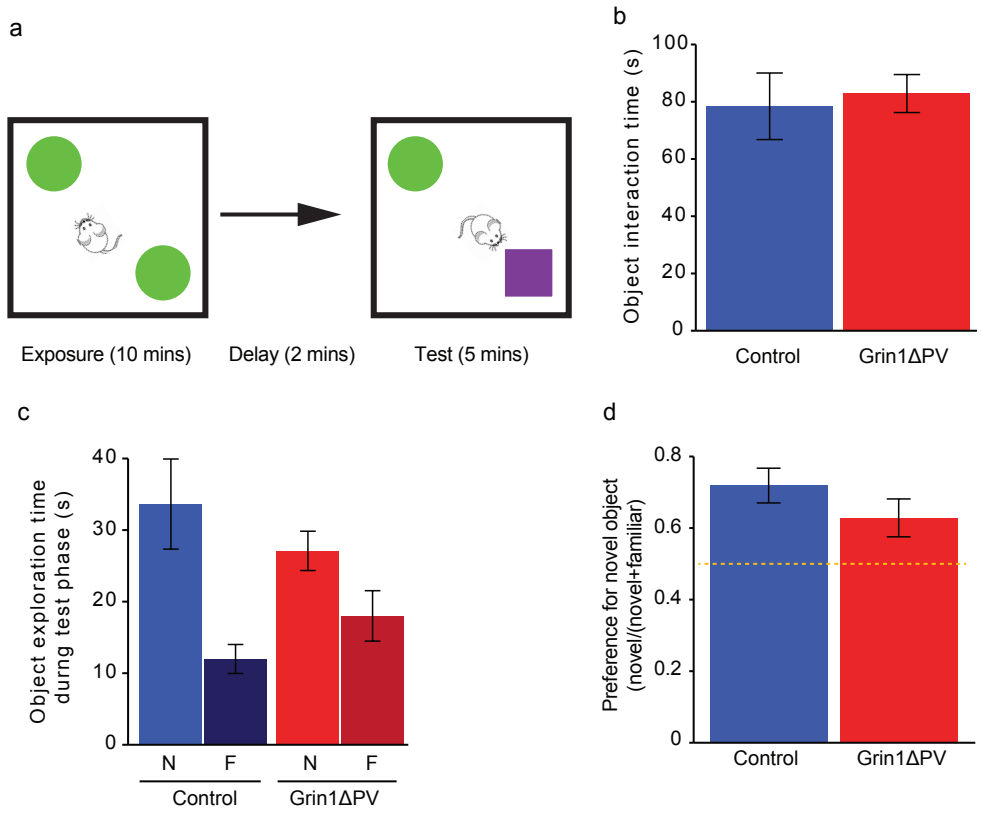

Figure 2.9: Intact novel object recognition in *Grin1*$^{\Delta PV}$ mice
(a) Experimental setup for novel object recognition test. (b) Total time spent exploring the novel object in control (blue) and *Grin1*$^{\Delta PV}$ (red) mice during the exposure phase. (c) Time spent exploring the novel (N; light blue and light red for control and *Grin1*$^{\Delta PV}$ mice respectively) and familiar (F; dark blue and dark red for control and *Grin1*$^{\Delta PV}$ mice respectively) objects during the test phase. (d) Time preference expressed as a ratio (novel/(novel + familiar)) in control and and *Grin1*$^{\Delta PV}$ mice during the test phase. Yellow dashed line indicates chance level preference. Bars display the mean and error bars display SEM.

2.3.10 Normal spatial novelty preference in *Grin1*$^{\Delta PV}$ mice

Spatial short-term memory was assessed with a novelty preference version of the Y-maze. Two cohorts of male and female control and *Grin1*$^{\Delta PV}$ mice aged 2 months (control: N = 19 ; *Grin1*$^{\Delta PV}$: N = 25) and 5 months (control: N = 19 ; *Grin1*$^{\Delta PV}$: N = 27)

were tested on the Y-maze. Animals were exposed to two arms of the Y-maze, then after a short delay (1 minute) they were given free access to the entire Y-maze, and the preference for the novel arm was assessed (**figure 2.10a**).

The amount of exploration during the exposure phase could influence task performance, so the total distance travelled during the exposure phase was calculated. *Grin1*$^{\Delta PV}$ mice showed significantly greater exploration during the sample phase. This was revealed when the distance travelled in the sample phase in the young and old cohorts was analysed with an ANOVA with genotype, age and sex as between subject factors (effect of genotype: $F(1,82) = 7.742$, $P = 0.007$; **figure 2.10b**). The greater exploration in *Grin1*$^{\Delta PV}$ mice looked to be driven by the 5 month old cohort but there was only a trend toward a genotype*age interaction to support this (genotype*age interaction: $F(1,82) = 2.936$, $P = 0.090$). In general the younger animals displayed greater exploration during the sample phase (effect of age: $F(1,82) = 68.364$, $P = 0.001$). Female mice generally explored less during the sample phase but this was not associated with interactions with genotype or age (effect of sex: $F(1,82) = 8.937$, $P = 0.004$; sex*genotype interaction: $(1,82) = 0.324$, $P = 0.571$, sex*age interaction: $F(1,82) = 0.187$, $P = 0.666$).

During the test phase wildtype animals should spend more time in the novel arm, compared to the “familiar” arm they have previously visited in the sample/exposure phase. The preference for time spent in the novel arm can be expressed as a ratio (time in novel / time in novel + time in familiar). There was no significant difference in the novel arm time preference ratio during the test phase between control and *Grin1*$^{\Delta PV}$ mice. This was revealed by an ANOVA with genotype, age and sex as between subject factors (effect of genotype: $F(1,82) = 0.012$, $P = 0.913$; **figure 2.10c**). The

novel arm time preference ratio was unaffected by age or sex (effect of age: F(1,82) = 2.453, P = 0.121; effect of sex: (1,82) = 0.032, P = 0.859).

Control and *Grin1*$^{\Delta PV}$ mice, in both young and old cohorts, displayed novel arm time preference ratios significantly above chance level performance as revealed by one-sample T-tests against chance (ratio of 0.5) preference (Controls at 2 months: t(1,18) = 7.375, P = 0.001; Controls at 5 months : t(1,18) = 3.761, P = 0.001; *Grin1*$^{\Delta PV}$ at 2 months: t(1,24) = 9.854, P = 0.001; *Grin1*$^{\Delta PV}$ at 5 months : t(1,26) = 7.226, P = 0.001). Thus, *Grin1*$^{\Delta PV}$ mice display intact spatial short-term memory.

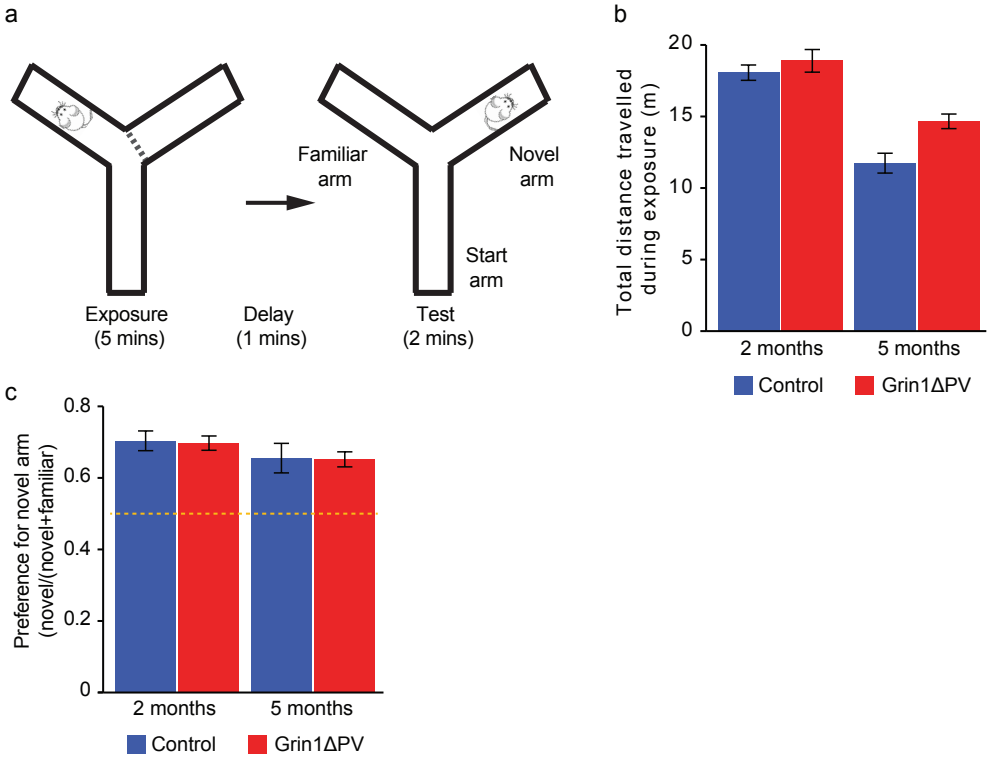

Figure 2.10: Normal spatial novelty preference in *Grin1*$^{\Delta PV}$ mice
(a) Y-maze setup for spatial novelty preference test. Grey dotted line illustrates a removable door. (b) Total distance travelled by control (blue) and *Grin1*$^{\Delta PV}$ (red) mice during the exposure phase in 2 and 5 month old cohorts (c) Time preference ratio (novel/(novel + familiar)) control and *Grin1*$^{\Delta PV}$ mice during the test phase in 2 and 5 month old cohorts. Yellow dashed line indicates chance level preference. Bars display the mean and error bars display SEM.

2.3.11 Normal spatial working memory in *Grin1*$^{\Delta PV}$ mice

SWM can be probed by testing rewarded alternation on the T-maze (Deacon and Rawlins, 2006). Rodents have a natural tendency for spontaneous alternation, aiding foraging behaviour where it is unfavourable to revisit a location once it has been depleted of food, water or explored more generally.

Reinforcing alternation behaviour by rewarding mice (rewarded alternation) enables more trials to be run each day per animal. Each trial consisted of a sample and choice run separated by an intra-trial interval, with individual trials separated by an inter-trial interval (**figure 2.11a**). A cohort of male control (N = 8) and *Grin1*$^{\Delta PV}$ (N = 12) mice were tested for rewarded alternation on the T-maze when aged 2 months, and the same cohort was retested when aged 6 months. Animals were first given three days of training (10 trials a day) with spaced trials (inter-trial interval 5-6 minutes) and an intra-trial interval of 5s. Then, during the test phase two different intra and inter-trial interval parameters were tested to manipulate the difficulty of the task and parallel previous studies utilising the same task. For example, Carlén *et al.* identified a selective impairment in *Grin1*$^{\Delta PV}$ mice specifically when a short (1s) intra-trial interval was used in combination with an inter-trial interval of 45s (massed trials), but not when the intra-trial interval was increased to 5 s and longer (Carlén et al., 2012). Another study (Korotkova et al., 2010) found *Grin1*$^{\Delta PV}$ mice to be impaired with an intra-trial interval of 15 s and an inter-trial interval of 5-6 minutes (spaced trials), although in that study they were the only test parameters used. In the present study **1 s-massed** (following Carlen *et al.*) and **15 s-spaced** (following Korotkova *et al.*) test parameters were used after initial training on the task (**figure 2.11b,c**).

At two months of age there was no significant difference in task performance of control and *Grin1*$^{\Delta PV}$ mice during the first three training blocks (see **figure 2.11b**). This was

revealed with a repeated measures ANOVA with genotype as a between subject factor and training day as a within subject factor (effect of genotype: $F(1,18) = 0.016$, $P = 0.9$). There was no significant effect of training day, or training day*genotype interaction (effect of training day: $F(2,36) = 0.916$, $P = 0.409$; training day*genotype interaction: $F(2,36) = 0.063$, $P = 0.939$).

The effect of changing the test parameters (**1 s-massed** and **15 s-spaced**) was then assessed. There was no significant effect of genotype or genotype*test parameter interaction on the task performance of control and *Grin1*$^{\Delta PV}$ mice (see **figure 2.11b**). This was revealed with a repeated measures ANOVA with genotype as a between subject factor and test parameter (**1 s-massed** and **15 s-spaced**) as a within subject factor (effect of genotype: $F(1,18) = 1.820$, $P = 0.194$; genotype*test parameter interaction: $F(1,18) = 2.111$, $P = 0.163$).

Based on *a priori* predictions from previous studies (Korotkova et al., 2010; Carlen et al., 2012), the task performance was analysed with each of the test parameters in isolation. With **1 s-massed** parameters (day 4) *Grin1*$^{\Delta PV}$ mice performed significantly worse than controls, thus replicating results in a previous study (Carlen et al., 2012). This was revealed by an ANOVA with genotype as a between subject factor (effect of genotype: $F(1,18) = 4.848$, $P = 0.041$). With **15 s-spaced** parameters (day 5) there was no significant difference in the performance of control and *Grin1*$^{\Delta PV}$ mice (effect of genotype: $F(1,18) = 0.152$, $P = 0.701$).

When the same cohort was retested aged six months there was again no significant overall difference in the task performance of control and *Grin1*$^{\Delta PV}$ mice during the three training blocks (see **figure 2.11c**). This was revealed with a repeated measures ANOVA with genotype as a between subject factor and training day as a within subject factor (effect of genotype: $F(1,18) = 0.128$, $P = 0.724$). There was no significant effect

of training day, or training day*genotype interaction (effect of training day: F(2,36) = 0.174, P = 0.841; training day*genotype interaction: F(2,36) = 0.542, P = 0.479).

The effect of changing the test parameters (**1 s-massed, 15 s-spaced, 1 s-massed repeat**) was then assessed (see **figure 2.11c**). One *Grin1*$^{\Delta PV}$ mouse was excluded from the analysis because it failed to run a full 10 trials on the **1 s-massed repeat** day. As in the young cohort, there was no significant effect of genotype or genotype*test parameter interaction on the task performance of control and *Grin1*$^{\Delta PV}$ mice as revealed by a repeated measures ANOVA with genotype as a between subject factor and test parameter (**1 s-massed**, **15 s-spaced,** and a **1 s-massed repeat**) as a within subject factor (effect of genotype: F(1,17) = 3.290, P = 0.087; genotype*test parameter interaction: F(2,34) = 1.373, P = 0.267).

As before, based on *a priori* predictions, the task performance was analysed with each of the test parameters in isolation. With **1 s-massed** parameters there was a non-significant trend towards *Grin1*$^{\Delta PV}$ mice performing worse than controls (day 4; effect of genotype: F(1,18) = 3.354, P = 0.084). Like in the younger cohort there was no significant difference in task performance in control and *Grin1*$^{\Delta PV}$ mice with **15 s-spaced** parameters (day 5; effect of genotype: F(1,18)= 2.962, P= 0.102). When the **1 s-massed** parameters were then tested again the test performance of control and *Grin1*$^{\Delta PV}$ mice was numerically identical and the trend towards an impairment in *Grin1*$^{\Delta PV}$ mice seen before was completely absent (day 6; effect of genotype: F(1,17)= 0.003, P= 0.959).

Together these data indicate that, when tested with **spaced-5 s** (during training) and **spaced-15 s** parameters, spatial working memory is normal in *Grin1*$^{\Delta PV}$ mice. Two month old *Grin1*$^{\Delta PV}$ mice showed significantly lower performance than controls when

tested with **massed-1 s** parameters. However, the lack of a significant genotype*test parameter interaction at age 2 or 6 months suggests this should be interpreted with caution. In addition, the trend towards reduced performance in *Grin1*$^{\Delta PV}$ mice with massed-1 s parameters at aged 6 months was transient as it was completely absent when repeated on day 6.

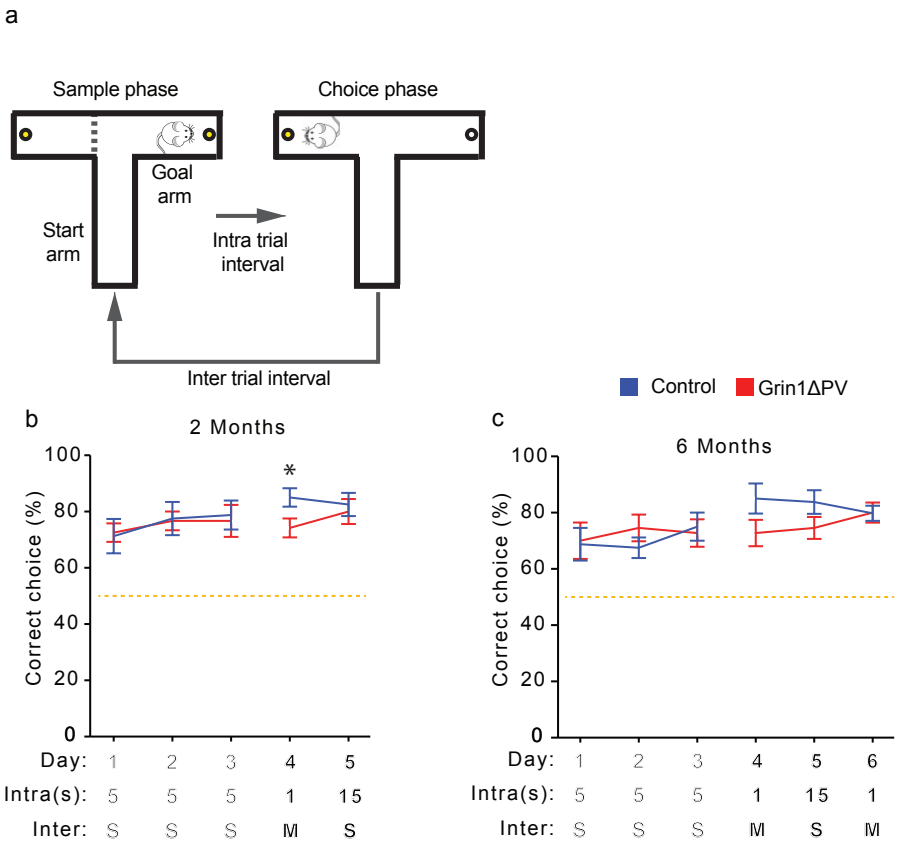

Figure 2.11: Largely normal spatial working memory in *Grin1*$^{\Delta PV}$ mice
(a) Rewarded alternation protocol using the T-maze. In this example the correct decision is to choose the left arm during the choice phase (b) Training (day 1-3) and task parameter tests (day 4-5) with 1s-massed (M) or 15s-spaced (S) parameters aged 2 months. (c) Training (day 1-3) and parameter tests (day 4-6) with 1s-massed (M) or 15s-spaced (S) parameters aged 6 months. Dashed line indicates chance level performance. Error bars display SEM. * indicates significant ($P < 0.05$) effect of genotype (ANOVA for Massed-1s test parameters based on *a priori* predictions).

2.3.12 Intact spatial reference memory and reversal learning in *Grin1*$^{\Delta PV}$ mice

The ability to form a consistent association with a particular spatial location is known as spatial reference memory (SRM) and can be tested with the appetitively motivated enclosed plus maze task (not to be confused with the elevated plus maze used as a test of anxiety). On each trial, a pseudo-randomly assigned start arm (north or south) is blocked off creating a T- shaped maze, but unlike rewarded alternation (tested in the T-maze), the animal has to learn to always choose a specific spatial location (e.g. the east arm) defined by the allocentric, distal extra-maze cues, rather than modifying its choice based on the previous experience in the sample run (**figure 2.12a**). Once animals acquire this association, the location of the reward can be changed and reversal learning can be assessed to test cognitive flexibility. A cohort of male control (N = 9) and *Grin1*$^{\Delta PV}$ (N = 12) mice aged 3-4 months were tested for acquisition and reversal learning on the plus maze (**figure 2.12b**).

There was no significant difference between control and *Grin1*$^{\Delta PV}$ mice during the acquisition phase as revealed by a repeated measures ANOVA with genotype as a between subject factor and training block (two training blocks of 5 trials combined to give blocks of 10 trials) as a repeated measure (effect of genotype: $F(1,19) = 0.047$, $P = 0.830$; genotype*training block interaction: $F(4,76) = 1.115$, $P = 0.356$). Significant acquisition of spatial reference memory was observed (effect of training block: $F(4,76) = 18.932$, $P = 0.001$).

To check that mice were not solving the task using olfactory cues (i.e. being able to smell the reward), each animal was given an additional 10 trials after acquisition of the original spatial reference memory task during which they received reward only after they had run to the correct arm (post-choice baiting). As performance remained high

during the 10 post-choice baiting trials it indicates that mice are not solving the task using olfactory cues from the reward.

When tested for reversal learning there was also no significant difference between control and *Grin1*$^{\Delta PV}$ mice. This was revealed by a repeated measures ANOVA with genotype as a between subject factor and training block as a repeated measure (effect of genotype: $F(1,19) = 0.073$, $P = 0.790$; genotype*training block interaction: $F(11,209) = 0.798$, $P = 0.554$). Significant acquisition of a reversed spatial reference memory was observed (effect of training block: $F(11,209) = 82.751$, $P = 0.001$).

There was no significant effect of genotype on the number of days it took for control or *Grin1*$^{\Delta PV}$ mice to reach criteria performance (85% correct in the last 20 trials) during acquisition or reversal of a spatial reference memory, as revealed by an ANOVA with genotype as a between subject factor (effect of genotype on acquisition: $F(1,19) = 0.177$, $P= 0.679$; effect of genotype on reversal: $F(1,18)= 0.045$, $P= 0.834$; **figure 2.12c**). In the analysis of reversal learning one *Grin1*$^{\Delta PV}$ animal was excluded because it failed to ever reach criteria performance even after >30 blocks of training (5 trials per block). Together, these data indicate normal spatial reference memory and cognitive flexibility in *Grin1*$^{\Delta PV}$ mice.

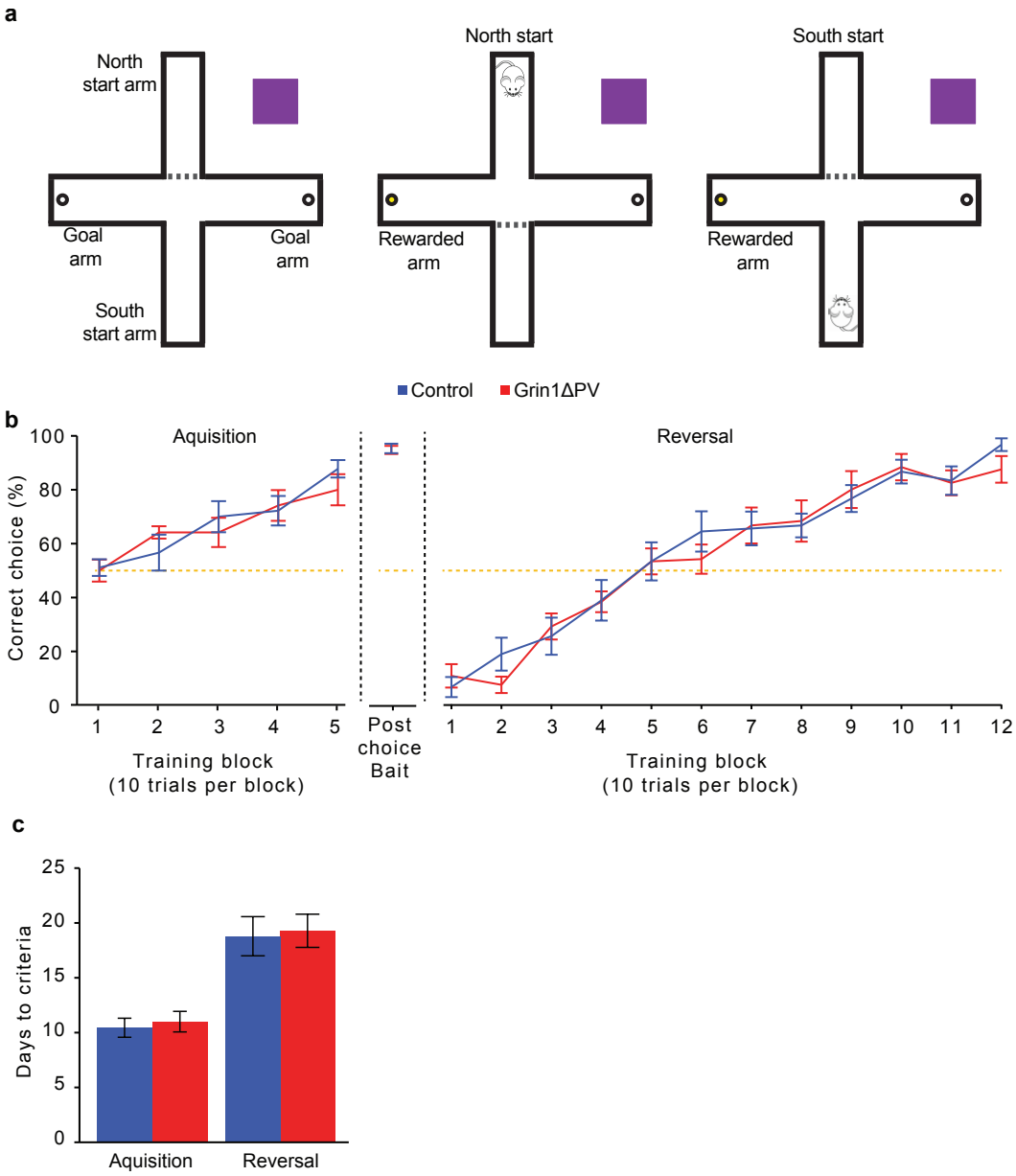

Figure 2.12: Normal spatial reference memory and reversal learning in *Grin1*$^{\Delta PV}$ mice
(a) Plus maze setup for spatial reference learning. Grey dashed line represents blockade of arm to allow allocation of the start arm to the north (centre graphic) or south (right graphic). The purple square indicates an extra-maze cue that remains in a constant location. The reward is always in the same spatial location (east goal arm in this example) regardless of start arm location. To test reversal learning the spatial location of the rewarded goal arm was switched. (b) Correct choices of control (blue) and *Grin1*$^{\Delta PV}$ (red) mice during acquisition (left) and reversal (right) learning. After successful acquisition of the spatial reference memory task, 10 trials of post choice baiting were given to test if animals were using olfactory cues from the reward to solve the task (centre). Data presented as blocks of 10 trials. Dashed line indicates chance level performance. (c) Average days taken for control (blue) and *Grin1*$^{\Delta PV}$ (red) mice to reach criteria during acquisition (left) and reversal (right) learning. Error bars display SEM.

2.4 Discussion

NMDAR hypofunction on PV interneurons has been proposed to be central to the pathophysiology of schizophrenia, upstream of changes in the dopamine system and hence possibly causative of a hyperdopaminergic state (Lisman et al., 2008). Genetically modified mice that lack NMDARs on PV interneurons (*Grin1*$^{\Delta PV}$ mice), have variably been reported to display schizophrenia-related behavioural deficits (Carlén et al., 2012; Korotkova et al., 2010), but there are important and substantial inconsistencies in the literature (see **table 2.1** and **1.8.4**). Surprisingly, *Grin1*$^{\Delta PV}$ mice tested in this study were found to be largely normal when compared to controls in a behavioural test battery of schizophrenia relevant tasks.

The PV^{cre} line used (Hippenmeyer et al., 2005) to generate the *Grin1*$^{\Delta PV}$ mice discussed here showed high specificity and coverage of PV interneurons (see **figure 2.1** and also Nassar *et al.*, 2015). So, it is unlikely that a lack of a behavioural phenotype is due to incomplete or unspecific targeting of PV interneurons. In addition, *in vitro* recordings from *Grin1*$^{\Delta PV}$ mice found significantly reduced NMDAR/AMPAR current ratios when compared to controls indicating successful ablation of NMDARs. There were some residual NMDAR currents in PV interneurons of *Grin1*$^{\Delta PV}$ mice (aged 2 months), with one cell displaying substantial currents. This probably reflects incomplete recombination of the *LoxP* sites flanking the critical NR1 exon and the delay in the clearance of remaining NMDARs in the postsynaptic densities. It is possible that a greater reduction in NMDAR/AMPAR current ratios would be seen in slightly older *Grin1*$^{\Delta PV}$ mice. However, aged 2 months there were already significant behavioural differences between control and *Grin1*$^{\Delta PV}$ mice on the elevated plus maze

test of anxiety, indicating that recombination had occurred enough to impact on behaviour.

2.4.1 *Grin1*$^{\Delta PV}$ mice and positive symptoms

To assess positive symptom correlates of schizophrenia, *Grin1*$^{\Delta PV}$ mice were tested for novelty induced hyperactivity and pre-pulse inhibition. When tested at 2 months there was normal locomotor activity, but aged 5 months the *Grin1*$^{\Delta PV}$ mice were hyperactive compared to controls. This hyperactivity is in line with the prediction from the Lisman/Grace model that PV-NMDAR hypofunction results in disinhibition of hippocampal circuits and over activity of glutamatergic hippocampal output that is capable of driving a hyperdopaminergic state (Floresco et al., 2001; Lisman et al., 2008). As yet, there is no direct evidence for physiological changes in the firing of VTA neurons in *Grin1*$^{\Delta PV}$ mice, but one prediction would be enhanced dopamine neuron activity in the VTA in these animals.

The Lisman/Grace model does not predict an age dependency on the effect of NMDAR deletion from PV interneurons. The age-dependency of hyperactivity seen here could result for a number of different reasons. It is possible that no phenotype was observed at two months because of incomplete recombination and ablation of NMDARs, since the PV^{cre} line used here only expresses *Cre* recombinase from the second postnatal week (Hippenmeyer et al., 2005). However this is unlikely because previous work with the same driver line crossed to a reporter has shown near complete recombination by 8 weeks (Carlén et al., 2012), and in our own immunohistochemical analysis we found close-to 100% recombination by 10 weeks of age. With aging, neurons (and indeed in cells within all tissues) are challenged with an increase in oxidative stress, an accumulation of damaged proteins and also a build up of DNA damage that could make the neuron more vulnerable (Mattson and Magnus, 2006).

Thus, an alternative explanation is that changes in *Grin1*$^{\Delta PV}$ mice can be accommodated for in a young network, and only manifest "pathologically" in a more susceptible older network. This is in line with findings from the group of Kazu Nakazawa (NIH) that observed an age-related increase of some deficits in *Grin1*$^{\Delta Ppp1r2}$ mice that lack NMDARs in a majority of PV interneurons (Belforte et al., 2010), and additionally showed, that NMDAR-ablation renders PV-interneurons more vulnerable to oxidative stress induced by social isolation (Jiang et al., 2013).

Sensorimotor gating impairments, assessed by testing PPI, are a commonly used measure of positive symptomatology in animal models of schizophrenia. However, no difference in pre pulse inhibition (PPI) was identified in *Grin1*$^{\Delta PV}$ mice tested here. This is in line with Carlen *et al.* who find no difference in PPI in *Grin1*$^{\Delta PV}$ mice generated using the same PV^{cre} driver line (Carlén et al., 2012). Belforte *et al.* found their knockouts to display impaired PPI, but these animals were generated with a different *Cre* driver line that targets a number of other interneuron subtypes, and also some excitatory cells, in addition to just PV interneurons (Belforte et al., 2010). So it is possible that NMDARs are not required on PV interneurons for normal PPI performance but instead are required on neuropeptide-Y or reelin expressing interneurons (or even the small population of excitatory neurons) also targeted with the other driver line (Belforte et al., 2010). Alternatively, the deficit seen by *Belforte et al.* could be due to a mass action effect, where there is a cumulative effect of several interneuron groups being targeted simultaneously.

2.4.2 *Grin1*$^{\Delta PV}$ mice and cognitive symptoms

Previous literature is probably most at odds when it comes to the cognitive symptoms of *Grin1*$^{\Delta PV}$ mice, with SWM deficits observed in some (Carlén et al., 2012; Korotkova

et al., 2010) but not other studies (Billingslea et al., 2014; Saunders et al., 2013). The only cognitive deficit found in *Grin1*$^{\Delta PV}$ mice tested here was a mild and transient impairment on the T-maze when the intra-trial interval was reduced to 1s with massed trials. This was exactly as reported by Carlen *et al.* who also observed normal performance when longer intra-trial interval delays were used (Carlén et al., 2012). Theoretically a shorter intra-trial interval delay will make the task easier. This is because animals are required to hold the information about the spatial location of the arm in the sample run in their working memory for a shorter amount of time.

When massed trials with an intra-trial interval of 1 s were tested, the performance of controls improved, possibly increasing the window of opportunity in which to detect a difference between the groups and thus exposing a mild spatial working memory deficit in *Grin1*$^{\Delta PV}$ mice. When the same cohort was retested aged 6 months with massed trials and a 1 s intra-trial interval there was only a non significant trend (P = 0.084) towards impaired performance in *Grin1*$^{\Delta PV}$ mice the first time they were tested, but performance between control and *Grin1*$^{\Delta PV}$ mice was identical following the second repeat of the short delay condition. As the effect was only significant in young animals and only after a protocol shift, it is unlikely that deletion of NMDARs from PV interneurons is directly influencing a mechanism that effects the encoding, stability, or the retrieval of a SWM trace. If this was the case, the impairment in *Grin1*$^{\Delta PV}$ mice with a 1s intra-trial interval should be consistent across time.

It is possible that the impairment seen in the *Grin1*$^{\Delta PV}$ mice is due to differences in arousal (or another mechanism) occurring when the mice are transferred rapidly from the goal arm to the start arm limiting the intra-trial interval delay to 1 s. With this short delay the mice have to be transferred rapidly from the goal arm back to the start arm, which is likely to be more arousing than when they are moved with a longer intra-trial

interval. This could lead to an increase in arousal, which will likely have an influence on task performance following a Yerkes-Dodson inverted U relationship, that could increase or decrease task performance depending upon the starting position on the curve. It is possible that controls are more sensitive to arousal changes following a shift in task parameters, so they could preferentially benefit from the shift in parameters if their starting position was to the left of the Yerkes-Dodson inverted U peak.

The most striking difference is with the study by Korotkova *et al.* who generated *Grin1*$^{\Delta PV}$ mice that had consistent chance level performance on the T-maze and novel object recognition (Korotkova et al., 2010). When tested with exactly the same test parameters on the T-maze, the *Grin1*$^{\Delta PV}$ mice generated in this study were completely normal and were performing consistently above chance. The PV^{cre} line used in the Korotkova *et al.* study is thought to be more hippocampus specific (Fuchs et al., 2007; Korotkova et al., 2010) but this has not been thoroughly tested, and the PV^{Cre} line has not been widely used. It is therefore possible that the differences between the current study and that of Korotkova *et al.* is due the hippocampus-preferring vs. whole brain targeting of PV interneurons. It could be that having disinhibition in just the hippocampus is worse than having disinhibition throughout the brain where the overall excitation is higher but there is not a large difference in the excitation/inhibition balance between the hippocampus and cortex. Alternatively, the differences could result from other differences related to the PV^{cre} driver line as its specificity targeting PV neurons only has not been as rigorously tested (Fuchs et al., 2007; Korotkova et al., 2010).

Belforte *et al.* identified impaired spatial working memory on a spontaneous alternation Y-maze task in *Grin1*$^{\Delta Ppp1r2}$ mice (Belforte et al., 2010). In this version of the task, mice are placed into the centre of a Y-maze and given free access to all arms of the

maze. Their location is tracked and they are considered to show alternation if they visit all three arms without re-entering the same or previously visited arm (i.e. arm A -> arm B -> arm C would be a successful alternation sequence but not A -> B -> A -> C). This task differs from the novelty preference version of the Y-maze used in this study with *Grin1*$^{\Delta PV}$ mice, and therefore makes a direct comparison difficult. For example, it is possible for mice to show perfect performance on the spontaneous Y-maze task by "wall hugging" and following a repeating A -> B -> C -> A -> B -> C arm entry pattern that does not require spatial working memory, since animals just need to follow the outer wall of the maze continuously. The "wall hugging" technique cannot be used to solve the Y-maze task used in this present study (see **figure 2.11**), as a high performance score is dependent on animals avoiding the familiar arm and spending time in the novel arm they had not previously explored. As Belforte *et al.* did not examine discrete trial-based rewarded or spontaneous alternation on the T-maze, it is hard to directly compare the behaviour of *Grin1*$^{\Delta Ppp1r2}$ mice to *Grin1*$^{\Delta PV}$ mice in other studies.

It is possible that the cognitive deficits Belforte *et al.* observe are due to NMDAR hypofunction on other interneurons targeted by their *Cre* driver line, either because these other interneurons are more important for cognitive function, or because of a summation effect of multiple interneuron groups being targeted simultaneously. There is also a suspicion that excitatory neurons are also targeted with the *Cre* driver line used by Belforte *et al.*, as a small number of CA1 pyramidal neurons were targeted in 8-12 week old mice, but this number increased dramatically in animals aged 20 weeks (Belforte et al., 2010). In fact the specificity of this line was tested in this thesis and considerable recombination was observed in hippocampal pyramidal neurons in *Grin1*$^{\Delta Ppp1r2}$ mice as young as 16 weeks (see **appendix 7.1.1**). NMDARs on pyramidal

neurons are known to be important for spatial working memory (see **1.8.2**), so off target recombination in pyramidal neurons could account for the observed cognitive deficits alone (Niewoehner et al., 2007; Tatard-Leitman et al., 2014; von Engelhardt et al., 2008). Thus, the potential for off target effects in *Grin1*$^{\Delta Ppp1r2}$ mice should be considered when interpreting the behavioural consequence of interneuron NR1 deletion.

2.4.3 *Grin1*$^{\Delta PV}$ mice and negative symptoms

Grin1$^{\Delta PV}$ mice tested in this study displayed normal nest building, sucrose preference and social interaction. In agreement with this, *Grin1*$^{\Delta PV}$ mice displayed normal sucrose preference in a study by Pozzi *et al.* who used the same PV^{cre} driver line as in this study (Pozzi et al., 2014). Belforte *et al.* found sucrose preference deficits in *Grin1*$^{\Delta Ppp1r2}$ mice but again this could be driven by ablation of NMDARs from other interneuron types or indeed off target recombination in pyramidal neurons (Belforte et al., 2010). The most striking difference between the present study and previously published work comes from the social interaction and nest building deficits repeatedly found to be impaired in *Grin1*$^{\Delta PV}$ (Billingslea et al., 2014; Saunders et al., 2013) and *Grin1*$^{\Delta Ppp1r2}$ mice (Belforte et al., 2010). These differences are hard to reconcile, since two of the three studies used an identical PV^{cre} driver line. It is possible that environmental factors interact with the genetic deletion of NMDAR from PV interneurons to manifest as deficits in nest building and social interaction. Belforte *et al.* showed that deficits in *Grin1*$^{\Delta Ppp1r2}$ mice were exacerbated by social isolation stress (Belforte et al., 2010), which could be mediated via oxidative stress mechanisms (Jiang et al., 2013). The fact that mice were housed in groups and highly

environmentally enriched cages in the present study could have prevented exacerbation of symptoms.

2.4.4 Conclusions

In the present study *Grin1*$^{\Delta PV}$ mice were found to be largely normal across a battery of tests thought to measure correlates of positive, cognitive and negative symptoms. It is possible that this mild phenotype is due to compensatory mechanisms elsewhere in the circuit overcoming the lack of NMDARs on PV interneurons. To address this issue it would be possible to generate inducible *Grin1*$^{\Delta PV}$ mice where *Cre* mediated recombination can be switched on only in adulthood. The Sternson lab recently developed a tool to probe NMDAR function with unprecedented precision. The technology utilises “masked-MK-801” and cell type specific expression of an “unmasking” esterase to enable rapid blockade of NMDARs only in a genetically defined population of neurons (Yang et al., 2015). If this technology were used in PV interneurons, the role that NMDA receptors have on behaviour and circuit function could be probed acutely, ruling out the possibility of compensatory changes.

Alternatively, it could be that NMDAR ablation does not happen early enough in development in the present study. The PV^{cre} driver line used in this study (recapitulating the temporal expression profile of parvalbumin itself) does not become active until the second postnatal week, so if NMDARs are required during development for proper circuit wiring then the critical window for causing a disruption could be missed. The correct formation of inhibitory synapses on pyramidal neurons is dependent on NMDARs during development (Gu et al., 2015), and this could also be the case with PV interneurons. This problem is harder to address without new genetic markers for PV neurons that switch on expression earlier in development.

There is some debate about the contribution of NMDAR currents (compared to AMPAR currents) to PV interneuron excitation at different points during development. Wang and Gao made patch clamp recordings *in vitro* to show that PV interneurons in the prefrontal cortex of juvenile rats do have NMDAR currents, but they found NMDAR currents were largely absent in slices taken from adult rats (Wang and Gao, 2010). In contrast NMDAR currents remained largely stable in pyramidal neurons into adulthood (Wang and Gao, 2010). In addition, Rotaru *et al.* found that PV interneurons in the adult prefrontal cortex had excitatory post synaptic potentials (EPSPs) with little NMDAR contribution, indicating that NMDAR currents on PV interneurons (in adulthood) could be minimal (Rotaru et al., 2011). Interestingly, Belforte *et al.* only found behavioural deficits when a Floxed NR1 mouse with a short distance between the two *LoxP* sites was used to generate *Grin1*$^{\Delta Ppp1r2}$ mice (Belforte et al., 2010). The distance of the *LoxP* sites should impact on the time taken for successful recombination, and subsequent ablation of NMDARs. When the Ppp1r2^{cre} line was crossed with a floxed NR1 mouse with greater spacing between the *LoxP* sites recombination started at 8 weeks and was complete by 20 weeks, and remarkably these animals did not show behavioural abnormalities (although only a few behavioural tests are reported; Belforte et al., 2010). It is therefore possible that there is a critical period during development when NMDARs on PV interneurons are essential for the correct circuit development, during which deletion of NMDARs from PV interneurons has long lasting effects. Whereas, after this period deletion of NMDARs from PV interneurons might have little consequence.

It is also possible that genetic and environmental factors converge (Jiang et al., 2013) to exacerbate behavioural deficits in *Grin1*$^{\Delta PV}$ mice. In the present study mice were group housed in an enriched environment with sizzle nest and a cardboard house and

tube. Donato *et al.* recently showed that PV interneurons are particularly sensitive to environmental enrichment, which can change the circuit in a manner that promotes performance on cognitive tasks such as novel object recognition (Donato et al., 2013). It is possible that *Grin1*$^{\Delta PV}$ mice housed individually in less enriched cages might display behavioural deficits missed in the current study. *Grin1*$^{\Delta Ppp1r2}$ mice display exacerbated phenotypes when subject to social isolation stress, highlighting the sensitivity of behavioural testing to environmental factors (Belforte et al., 2010; Jiang et al., 2013).

Chapter 3 will explore the interaction between ablation of NMDARs from PV interneurons and the acute challenge of NMDAR antagonists, which are commonly used to model psychosis in rodents and human volunteers.

3 NMDAR antagonist studies in *Grin1*$^{\Delta PV}$ mice

3.1 Introduction

The glutamate hypothesis of schizophrenia emerged as a result of landmark studies, linking symptoms of schizophrenia induced by drugs of abuse with antagonism of NMDARs (Javitt and Zukin, 1991). This led to the NMDAR hypofunction hypothesis of schizophrenia, with changes in the glutamate system upstream of the dopaminergic system, which has long been associated with schizophrenia. Subsequently, challenge with NMDAR antagonists has been used to model elements of schizophrenia in rodents (see **1.8.3**)

3.1.1 Disinhibition following NMDAR challenge

As NMDARs provide excitatory glutamatergic drive to neurons, antagonism of NMDARs would logically lead to a decrease in neuronal activity. At the circuit level, however, NMDAR antagonists lead to a paradoxical increase in neuronal activity *in vivo*. In 2004, Jackson *et al.* investigated the consequences of NMDAR antagonism (with MK-801) on neuronal activity in the prefrontal cortex of freely moving rats (Jackson et al., 2004). They observed that doses of MK-801, capable of impairing working memory, resulted in an increase in the firing rate of putative excitatory neurons in freely moving, awake rats (Jackson et al., 2004). Interestingly, this increase in firing rate occurred as a result of an increase in the frequency of random spikes, and not an increase in the number of spikes during periods of burst firing (Jackson et al., 2004). In fact, the number of spikes per burst and the total number of bursts were decreased in a dose dependent manner with MK-801 challenge (Jackson et al., 2004). Together a reduction of burst firing and an increase in random spikes could reduce efficiency of

neurotransmitter release and increase “noise” in the signal respectively, impairing prefrontal cortex function (Jackson et al., 2004).

In the medial prefrontal cortex of awake rats, Homayoun and Moghaddam found that MK-801 increased the firing of putative excitatory neurons whilst reducing the firing rate of putative inhibitory GABAergic neurons (Homayoun and Moghaddam, 2007). These data indicated that fast spiking, putative interneurons could be more sensitive to NMDAR antagonists such as MK-801 and consequently, reduced excitation of these inhibitory interneurons might drive the increase in putative excitatory neuron activity via disinhibition. Homayoun and Moghaddam were unable to identify the subtypes of inhibitory interneurons they recorded from, but they speculate that the majority were PV-positive interneurons. These PV positive interneurons are well suited to initiate the disinhibition of excitatory neurons that was observed (Homayoun and Moghaddam, 2007).

The possibility that it is PV interneurons that show this reduction in firing rate is poignant because NMDAR hypofunction on PV positive interneurons has been proposed to be central to the pathophysiology of schizophrenia in the Lisman/Grace model (Lisman et al., 2008; see **2.1.1**). Indeed, the concept that NMDAR antagonist challenge disproportionally affects NMDARs on PV interneurons has experimental support (Belforte et al., 2010; Carlén et al., 2012).

3.1.2 PV NMDAR KO protects from MK-801-induced hyperactivity

In wildtype rodents, acute challenge with NMDAR antagonists robustly induces hyperactivity, a possible correlate of a positive symptom of schizophrenia. The importance of NMDARs on interneurons for the induction of NMDAR antagonist induced hyperactivity was assessed by Belforte *et al.,* who generated *Grin1*$^{\Delta Ppp1r2}$ mice that lack NMDARs from 40-50 % of forebrain interneurons, including a large

population of PV positive interneurons. *Grin1*$^{\Delta Ppp1r2}$ mice showed a vastly attenuated locomotor response to acute MK-801 (0.2 mg/kg) challenge (Belforte et al., 2010). Belforte *et al.* concluded that the knockout animals were already in a "brain state similar to that of the MK-801-sensitised mice" and thus further actions of MK-801 were occluded (Belforte et al., 2010). In a later study, Carlen *et al.* generated *Grin1*$^{\Delta PV}$ mice (that lacked NMDARs selectively from PV interneurons) and showed that these mice also lack MK-801-induced hyperlocomotion (Carlén et al., 2012). In addition, they found that MK-801-induced increases in gamma oscillation power in the somatosensory cortex were absent in *Grin1*$^{\Delta PV}$ mice (Carlén et al., 2012). They concluded that PV interneurons represent "an important target for the non-competitive NMDAR antagonists" for both the induction of gamma oscillations and, behaviourally, for the expression of hyperactivity (Carlén et al., 2012). Taken together, these studies appeared to indicate that NMDAR antagonists, such as MK-801, induce hyperlocomotion primarily via NMDARs on PV interneurons. However, these conclusions are at odds with the findings that most PV neurons in the prefrontal cortex of adult rats do not have detectable NMDAR currents (Wang and Gao, 2010), and that the excitatory post synaptic potentials (EPSPs) in adult mouse prefrontal cortex appear to have limited NMDAR contribution (Rotaru et al., 2011). Although it is important to note that the above electrophysiology experiments were made in the prefrontal cortex, and might not be representative of PV interneurons in other brain regions that could be responsible for the hyperactivity phenotype (e.g. the hippocampus).

3.1.3 Chapter 3 experimental aims

NMDAR antagonists can induce deficits in the positive, negative and cognitive domains (Javitt and Zukin, 1991; Krystal et al.,1994). The studies by Carlen *et al.* and

Belforte *et al.* suggest that NMDARs on PV interneurons could be critical for the induction of positive symptoms of schizophrenia, but it remains unknown if NMDARs on PV interneurons are also required for the induction of cognitive and negative symptoms following NMDAR antagonist challenge. The following experiments attempt to explore these questions by testing the ability of MK-801 to induce positive, negative and cognitive symptoms in control and *Grin1*$^{\Delta PV}$ mice. If NMDARs on PV interneurons are, as previously suggested, the most crucial target of NMDAR antagonists, then *Grin1*$^{\Delta PV}$ mice should be protected from deficits induced by acute challenge with MK-801.

3 Methods

3.2.1 Breeding of animals

Grin1$^{\Delta PV}$ mice were generated and housed as described previously (see **2.2.1**).

3.2.2 Drugs

MK-801 ((+)-MK-801 maleate, Tocris, Bristol, UK) was administered via intraperitoneal (i.p.) injection as a solution of 0.025 mg/ml (for doses 0.1 and 0.15 mg/kg) or 0.05 mg/ml (for doses 0.2, 0.4 and 0.5 mg/kg), dissolved in sterile saline. Doses of MK-801 were administered based on the salt weight of MK-801 maleate. Sterile saline injections of corresponding volumes served as vehicle controls. MK-801-injections were distributed across cohorts, so that mice had received either vehicle or only one (low-dose) injection of MK-801 before each experiment (i.e. animals that had been given a high dose of MK-801 were not used for other tests), then sequential drug doses were counterbalanced for genotype.

3.2.3 Locomotor activity: MK-801 challenge

Locomotor activity was assessed with infrared beam breaks as previously described (see **2.2.5**) with a slightly modified protocol. Mice were placed in clean locomotor cages and activity was recorded for 30 minutes. Then mice were removed from the locomotor boxes and injected with either MK-801 (0.1, 0.2 or 0.5 mg/kg) or vehicle, and then returned to the same locomotor cage. Locomotor activity was assessed for 90 minutes following injection. In addition to the automated beam break detection the behaviour of the mice was scored visually online by experimenters blind for genotype. The time spent in stereotypies (mostly circling) or in a flat-state was scored. Behavioural states were characterised as follows:

Flat-state: epochs of complete immobility, with a flat stretched posture with head and/or body on the floor with legs stretched out. This was clearly distinguishable from the rounded posture of normal mice sleeping.

Stereotypies: mostly repetitive circling behaviour but also repetitive head-shaking, face washing, excessive grooming and jumping.

3.2.4 Motor coordination: MK-801 challenge

The accelerating rotarod was used as a test of motor coordination. Mice were transferred onto a rotarod (Ugo Basile, Gemonio, IT), rotating at 4 rpm, using a wooden dowel, 30 and 60 minutes following injection of MK-801 (0.15 mg/kg in females and 0.2 mg/kg in males) or vehicle. After an acclimatisation period of 10 seconds with the rotarod at 4 rpm the speed of rotation was linearly accelerated until 20 rpm. The time taken to fall from the rotarod was recorded. If the mouse fell during the 10 second acclimatisation period, the trial was considered a failure. In these instances, the mouse was immediately placed back onto the rotarod and given up to two more chances to stay on the rotating rod. Animals that failed all three trials were given a time score of 0 seconds. Male and female mice were tested. Drug effects were tested following a between subject design.

3.2.5 Spatial working memory: MK-801 challenge

Spatial working memory was assessed by testing rewarded alternation on the T-maze as previously described (see **2.2.13**). Mice were trained on the T-maze until reaching a criterion of 80% correct performance for two consecutive days (or for at least 3 training days if performance was high from the onset of training). During initial training mice were given massed trials (inter- trial interval of 45 seconds) with an intra-trial interval of 5 seconds. Once criteria level performance was reached, mice were injected with escalating doses of MK-801 (0.1, 0.15, 0.2 and 0.4 mg/kg) or vehicle, and after

30 minutes given 10 trials of rewarded alternation with the same massed trial protocol and 5 second intra-trial interval parameters. Each dose of MK-801 was accompanied with its own within subject vehicle injection condition (counterbalanced for order of drug vs. vehicle). The dose of MK-801 was escalated over time and not counterbalanced for order (i.e. 0.1, 0.15, 0.2, and then 0.4 mg/kg) Only male mice were tested.

3.2.6 Sucrose preference: MK-801 challenge

To assess anhedonia, mice were tested for sucrose preference. The task was as previously described (see **2.2.8**) with a few modifications. Mice were given two nights of habituation to the apparatus (before drug testing commenced), with a choice between normal drinking water or sucrose solution (1% and not 10% as used before). On test days, MK-801 (0.1 and 0.15 mg/kg) or vehicle injections (order of MK-801 or vehicle was counterbalanced) preceded the onset of the dark phase. Measurements were taken 2.5 hours after injections to assess how much water and sucrose solution had been consumed. Drug effects were tested following a within subject design with each dose of MK-801 having its own within subject vehicle control.

3.2.7 Surgery for electrode implantation

Mice were anaesthetized with Isoflurane, injected subcutaneously (s.c.) with Metacam (5 mg/kg), Vetergesic (0.08 mg/kg), Marcaine (2 mg/kg, injected under the shaved skin above the skull) and 0.5 mL of sterile saline and placed into a stereotaxic frame (David Kopf instruments). A heating blanket, under a feedback control loop, was placed under the mouse. A surgical depth of anaesthesia was maintained with Isoflurane (typically 1-2 %) and confirmed with the absence of a hind-paw pedal reflex. Craniotomies were made above the recording and reference electrode sites, and for ground and anchor screws. The dura was removed to expose the brain surface, and straightened

polyimide-insulated tungsten wires of 50 µm inner diameter (Wiretronic, CA, USA) were inserted into the medial prefrontal cortex (AP +1.7 mm, ML +0.25-0.35 mm, 1.7-1.9 mm below pia), dorsal hippocampus (AP -2 mm, ML + 1.5 mm, -1.4-1.3 mm below pia) and ventral hippocampus (AP -3.2 mm, ML -3 mm, -3.4-3.3 mm below pia) of the right hemisphere. A 125 µm stainless steel (Advent Research Materials, UK) reference electrode was placed touching the brain surface in the posterior part of the frontal cortex (AP -0.5mm, ML -1 mm) and a ground screw was inserted above the cerebellum. Both were contralateral with respect to the recording electrodes. Light curable dental cement (Pentron, USA) was used to fix the electrodes in position. The electrodes, ground and reference wires were connected to an adaptor (Millmax). Mice were injected s.c. with 500 µL glucose saline at the end of the surgery and Metacam (5 mg/kg) was given 24 hrs later (either s.c. or orally by feeding palatable strawberry jelly containing the drug).

3.2.8 Electrophysiology: MK-801 challenge

To assess the influence of MK-801 on local field potentials *in vivo*, MK-801 challenge was combined with electrophysiology recordings. Mice were tethered to a recording cable via the adaptor on the headcap, and placed into a novel clear plastic cage (l 43 cm, w 22 cm, h 20 cm) containing clean sawdust. Baseline signals were recorded for 10 minutes as the animal explored the environment. Mice were then challenged with injection of MK-801 (0.2 mg/kg or 0.5 mg/kg) or vehicle and recordings made for 40 minutes in 10-minute time bins blocks. Only male mice were tested.

3.2.9 Electrophysiology recordings

Mice were given at least 1-week recovery before recordings commenced. Data were acquired at a sampling rate of 15 kHz with a 0.1-300 Hz bandpass filter using an RHD2132 amplifier board (Intan Technologies, CA, USA), an Open E-Phys USB

interface board and the Open E-Phys acquisition software (Open E-Phys, MA, USA). Raw data were exported into MatLab (Mathworks, MA, USA) and down sampled to 1 kHz. Further analysis was done using IgorPro (Wavemetrics, OR, USA) using custom written scripts. The IgorPro procedure “PowerSpectralDensity.ipf” was used to calculate power-spectra using Hann-windowing and a segment length of 8192 points. Time by frequency power spectrographs (for visualisation of power changes) were generated in IgorPro using Morlet wavelets (custom script from Dr. Edward Mann).

3.2.10 Histology

Mice were euthanized (Euthatal) and miniature lesions were made by electrical stimulation of recording electrodes, immediately before transcardial perfusion with PBS followed by 4% paraformaldehyde (PFA). Brains were post-fixed for 24 hours in PFA. Coronal sections of 60 µm were cut on a Vibratome in PBS, and then washed 3 times in PBS with the last wash containing DAPI (1:1000, Invitrogen). Sections were washed once more in PB and then mounted with Vectashield (Vector Labs, USA). Slices were scanned with a fluorescent microscope (Axio Zoom, Carl Zeiss) to detect DAPI staining and reveal electrode lesion sites. Locations of lesion sites were estimated based on the mouse brain atlas (Paxinos).

3.2.11 Statistical analysis

As described previously (see **2.2.15**), normality of data was tested with the Shapiro-Wilks test and assessment of Q-Q plots. Where data followed the normal distribution, parametric statistical tests were used. If data could not be normalised with transformations, then non-parametric statistical tests were used. All statistical tests were performed using SPSS version 21 (IBM).

3.3 Results

NMDARs on PV interneurons could be particularly important targets of NMDAR antagonists, and it is possible that NMDARs on PV interneurons are required for the behavioural deficits induced by MK-801. To explore this hypothesis, the ability of the NMDAR antagonist MK-801 to induce schizophrenia-like behavioural deficits was assessed in mice lacking NMDARs on PV interneurons (*Grin1*$^{\Delta PV}$ mice).

3.3.1 *Grin1*$^{\Delta PV}$ mice show an attenuated locomotor response to acute MK-801 challenge

Locomotor activity was tested in control and *Grin1*$^{\Delta PV}$ mice following challenge with the NMDAR antagonist MK-801. After a baseline period of 30 minutes animals were injected with either vehicle or MK-801, and locomotor activity was recorded for a further 90 minutes **(figure 3.1a,d,g)**. Three doses of MK-801 were tested (0.1, 0.2 and 0.5 mg/kg) in male and female, control and *Grin1*$^{\Delta PV}$ mice, with each dose having its own between subjects, vehicle control group. Previous studies have reported that *Grin1*$^{\Delta PV}$ mice display an attenuated locomotor response in the 60 minute time period following injection of MK-801. Therefore the total beam breaks between 0-60 minutes following MK-801/vehicle injection was calculated (**figure 3.1b,e,h**).

At doses of 0.1 and 0.2 mg/kg, data were not normally distributed so non-parametric (Kruskal-Wallis) statistical tests were utilised. At a dose of 0.5 mg/kg the data were normally distributed, so parametric (two-way ANOVA) statistical tests were used (but data are still presented as boxplots for consistency).

When challenged with 0.1 mg/kg of MK-801 (control: 11 vehicle, 12 MK-801; *Grin1*$^{\Delta PV}$: 12 vehicle, 13 MK-801), there was no significant difference between groups

in the first 60 minutes post injection as revealed by a Kruskal-Wallis test (H(3) = 4.019, P = 0.259; **figure 3.1a,b**).

However, when the dose was increased to 0.2 mg/kg (control: 11 vehicle, 13 MK-801; *Grin1*$^{\Delta PV}$: 16 vehicle, 15 MK-801) the same analysis revealed a significant group difference (H(3) = 21.963, P = 0.001). Control, but not *Grin1*$^{\Delta PV}$ mice injected with 0.2 mg/kg MK-801 made significantly more beam breaks when compared to vehicle injected animals. This was revealed with pairwise comparisons with significance value corrected for multiple comparisons (control MK-801 vs. control Vehicle: H(3) = 29.587, P = 0.001; *Grin1*$^{\Delta PV}$ MK-801 vs. *Grin1*$^{\Delta PV}$ vehicle (H(3) = 5.250, P = 1). There was no significant difference in the number of beam breaks made by control or *Grin1*$^{\Delta PV}$ mice injected with MK-801 (control MK-801 vs. *Grin1*$^{\Delta PV}$ MK-801: H(3) = 14.796, P = 0.090; **figure 3.1d,e**). There was also no significant difference in the number of beam breaks made by control or *Grin1*$^{\Delta PV}$ mice injected with vehicle (control vehicle vs. *Grin1*$^{\Delta PV}$ vehicle: H(3) = 9.568, P = 0.764; **figure 3.1d,e**).

At a dose of 0.5 mg/kg MK-801 (control: 11 vehicle, 11 MK-801; *Grin1*$^{\Delta PV}$: 11 vehicle, 12 MK-801), there was a significant overall effect of genotype and drug on the total number of beam breaks in the first 60 minutes post injection, with MK-801 inducing hyperactivity to a greater extent in control animals, as revealed by an ANOVA with genotype, drug and sex as between subject factors (effect of genotype: F(1,37) = 16.045, P = 0.001; effect of drug: F(1,37) = 52.144, P = 0.001; drug*genotype interaction: F(1,37) = 34.705, P = 0.001). There was no significant effect of sex on the response to MK-801 (effect of sex: F(1,37) = 0.248, P = 0.621). There was a significant effect of drug in control but not in *Grin1*$^{\Delta PV}$ mice when scrutinised further with simple main effects analysis (effect of drug in controls: F(1,37) = 84.012, P = 0.001; effect of

drug in *Grin1*$^{\Delta PV}$ mice: F(1,37) = 0.905, P = 0.347). In addition, control mice made significantly more beam breaks than *Grin1*$^{\Delta PV}$ animals following MK-801, but not vehicle injection (effect of genotype after MK-801 injection: F(1,37) = 50.138, P = 0.001, effect of genotype after vehicle injection: F(1,37) = 1.737, P = 0.196; **figure 3.1g,h**). These data replicate the findings by Carlen *et al.*, in which *Grin1*$^{\Delta PV}$ mice display an attenuated locomotor response to MK-801 challenge (Carlén et al., 2012).

A qualitative inspection of the locomotor data over time indicated that activity might increase in *Grin1*$^{\Delta PV}$ mice following MK-801 challenge at later time periods (i.e. after 60 minutes; **figure 3.1a,d,g)**. To investigate this further the total beam breaks were also calculated for the 61-90 minute time period **(figure 3.1c,f,i)**. Data from the 0.5 mg/kg MK-801 experiment were normally distributed but data for 0.1 and 0.2 mg/kg experiments were not, so the same combination of non-parametric (Kruskal-Wallis) and parametric (ANOVA) analyses were performed as for the analysis of the first 60 minutes of locomotor activity.

At a dose of 0.1 mg/kg MK-801 there was an overall significant difference between groups (H(3) = 11.911, P = 0.008) during the 61-90 minute period. Controls, but not *Grin1*$^{\Delta PV}$ mice, injected with 0.1 mg/kg MK-801, made significantly more beam breaks when compared to their respective vehicle injected animals, as revealed by pairwise comparisons with significance values corrected for multiple comparisons (control MK-801 vs. control vehicle: H(3) = 17.720, P = 0.015; *Grin1*$^{\Delta PV}$ MK-801 vs. *Grin1*$^{\Delta PV}$ vehicle: H(3) = 5.115, P = 1). There was no significant difference in the number of beam breaks made by control or *Grin1*$^{\Delta PV}$ mice injected with MK-801 (control MK-801 vs. *Grin1*$^{\Delta PV}$ MK-801: H(3) = 0.468, P = 1; **figure 3.1c**). In addition, there was no significant difference in the number of beam breaks made by control or *Grin1*$^{\Delta PV}$ mice

injected with vehicle (control vehicle vs. *Grin1*$^{\Delta PV}$ vehicle: H(3) = 12.136, P = 0.227; **figure 3.1c**).

Similarly, at a dose of 0.2 mg/kg of MK-801 there was an overall significant difference between groups (H(3) = 34.278, P = 0.001) during the 61-90 minute period. However, at this dose both control and *Grin1*$^{\Delta PV}$ mice injected with 0.2 mg/kg MK-801 made significantly more beam breaks when compared to their respective vehicle injected animals, as revealed by pairwise comparisons with significance value corrected for multiple comparisons (control MK-801 vs. control vehicle: H(3) = 32.591, P = 0.001; *Grin1*$^{\Delta PV}$ MK-801 vs. *Grin1*$^{\Delta PV}$ vehicle: H(3) = 16.348, P = 0.027). There was no significant difference in the number of beam breaks made by control or *Grin1*$^{\Delta PV}$ mice injected with MK-801 or vehicle (control MK-801 vs. *Grin1*$^{\Delta PV}$ MK-801: H(3) = 11.933, P = 0.296; control vehicle vs. *Grin1*$^{\Delta PV}$ vehicle: H(3) = -4.310, P = 0.1; **figure 3.1f**).

With a dose of 0.5 mg/kg MK-801 (control: 11 vehicle, 11 MK-801; *Grin1*$^{\Delta PV}$: 11 vehicle, 12 MK-801), there was a significant overall effect of genotype and drug on the total number of beam breaks in the 61-90 minute period post-injection, with MK-801 inducing hyperactivity to a greater extent in control animals. This was revealed by an ANOVA with genotype, drug and sex as between subject factors (effect of genotype: F(1,37) = 27.209, P = 0.001; effect of drug: F(1,37) = 101.730, P = 0.001; drug*genotype interaction: F(1,37) = 29.217, P = 0.001). There was no significant effect of sex on the response to MK-801 (effect of sex: F(1,37) = 0.293, P = 0.592). MK-801 significantly increased locomotor activity in both control and *Grin1*$^{\Delta PV}$ mice relative to vehicle injections, when scrutinised further with simple main effects analysis (effect in controls: F(1,37) = 117.265, P = 0.001; effect in *Grin1*$^{\Delta PV}$: F(1,37) = 11.216, P = 0.002). Control mice made significantly more beam breaks than *Grin1*$^{\Delta PV}$ animals

following MK-801, but not vehicle injection (effect of genotype after MK-801 injection: $F(1,37) = 57.752$, $P = 0.001$, effect of genotype after vehicle injection: $F(1,37) = 0.017$, $P = 0.896$; **figure 3.1i**).

Together these data replicate the finding that *Grin1*$^{\Delta PV}$ mice show an attenuated locomotor response to MK-801, but only when looking at the first 60 minutes following drug injection following the analysis of Carlen *et al.* (Carlén et al., 2012). When locomotor activity is assessed in the 61-90 minute post drug period, a previously unrecognised MK-801-induced increase in locomotor activity in *Grin1*$^{\Delta PV}$ mice was identified.

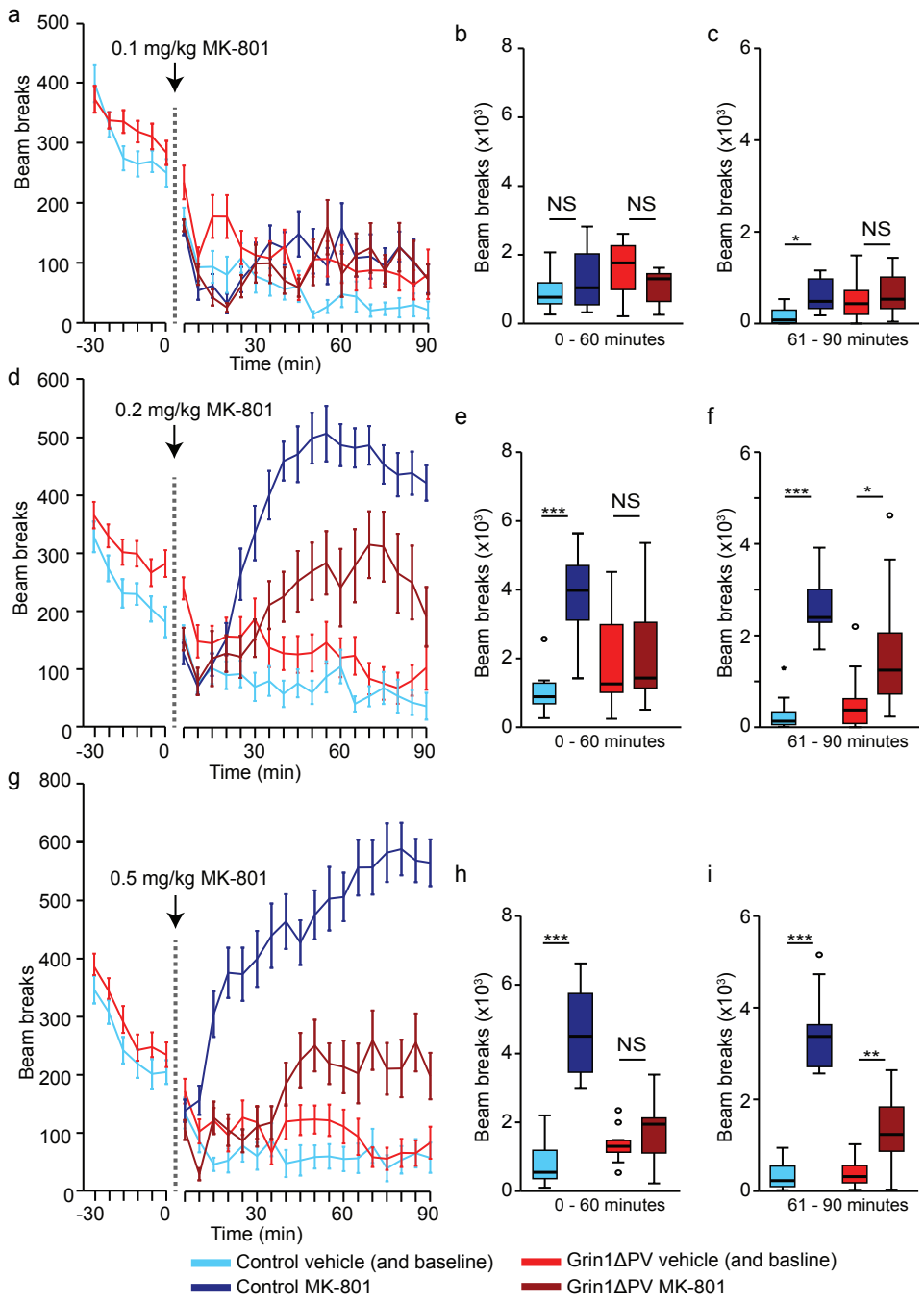

Figure 3.1: Attenuated locomotor response in Grin1$^{\Delta PV}$ mice following MK-801 challenge

Locomotor activity in control and *Grin1*$^{\Delta PV}$ mice following challenge with MK-801. Activity is plotted over time for doses of (a) 0.1mg/kg, (d) 0.2mg/kg and (g) 0.5mg/kg. Activity plots over time show the mean and error bars display SEM. Boxplots illustrate total beam breaks in (b,e,h) 0-60 and (c,f,i) 61-90 minute post injection period. Boxplots display the median (thick black line) flanked by the 25 and 75 percentiles (bottom and top of box respectively) and whiskers display the maximum and minimum (excluding outliers). Data points that could reflect outliers are indicated by circles (1-3 x the interquartile range) or small stars (>3 x the interquartile range). Outliers were not removed for statistical testing. Light blue represents control animals in baseline or saline conditions and dark blue represents

controls with MK-801 challenge. Light red represents *Grin1*$^{\Delta PV}$ mice in baseline or saline conditions and dark red represents *Grin1*$^{\Delta PV}$ mice with MK-801 challenge. * indicates significant difference between groups (* P < 0.05, ** P < 0.01, *** P < 0.001).

3.3.2 *Grin1*$^{\Delta PV}$ mice display a pronounced flat-posture and stereotypies following MK-801 challenge

Assessment of beam breaks (and distance travelled) in locomotor assays provides a useful measure but can be confounded by behavioural states induced with psychostimulants such as NMDAR antagonists. For example, in addition to hyper-locomotor activity, MK-801 is known to induce stereotypical behaviours in rodents (Wu et al., 2005). Stereotypies can be classified as repetitive movements, commonly manifesting as circling or repetitive movements (including head shaking) in rodents.

In a pilot study with control and *Grin1*$^{\Delta PV}$ mice, MK-801 induced stereotypies as expected but, surprisingly, a subset of animals also entered a flat-state clearly dissociable from normal sleep (data not shown). In the flat-state mice adopted a stretched out posture lying flat on their stomachs, with their tails straight and sometimes erect. This prompted manual scoring of stereotypies and flat-state behaviour in control and *Grin1*$^{\Delta PV}$ mice challenged with MK-801 in all subsequent locomotor activity studies. Stereotypies were not observed with MK-801 challenge at 0.1 mg/kg (**data not shown**). At a dose of 0.2 mg/kg, MK-801 induced a flat-state in *Grin1*$^{\Delta PV}$ mice but not in controls **(figure 3.2a,b)**. The total percentage of time spent in a flat-state was significantly greater in *Grin1*$^{\Delta PV}$ mice in the total 90 minutes post-drug period than for the control mice as revealed by a Mann-Whitney U test (effect of genotype: $U_{13,15} = 2$, P = 0.001; median % of time in a flat-state: 0 and 27.4 for control and *Grin1*$^{\Delta PV}$ mice respectively) **(figure 3.2a,b)**. Notably, there was also a significant

effect of genotype on the percentage of time spent in stereotypy with *Grin1*$^{\Delta PV}$ mice spending more time displaying stereotypies than controls (effect of genotype: $U_{13,15}$ = 149.5, P = 0.015, median % time in stereotypy: 7.1 and 19.2 for control and *Grin1*$^{\Delta PV}$ mice respectively) **(figure 3.2c,d)**.

With a dose of 0.5 mg/kg MK-801, the flat-state was again selectively observed in *Grin1*$^{\Delta PV}$ mice (effect of genotype: $U_{11,12}$ = 0, P = 0.001, median % time in a flat-state: 0 and 28.7 for control and *Grin1*$^{\Delta PV}$ mice respectively) **(figure 3.2e,f)**. At a dose of 0.5mg/kg MK-801, there was no effect of genotype on the time spent in stereotypy (effect of genotype: $U_{11,12}$ = 57, P = 0.608; median % time in stereotypy: 19.6 and 25.1 for control and *Grin1*$^{\Delta PV}$ mice respectively) **(figure 3.2g,h)**.

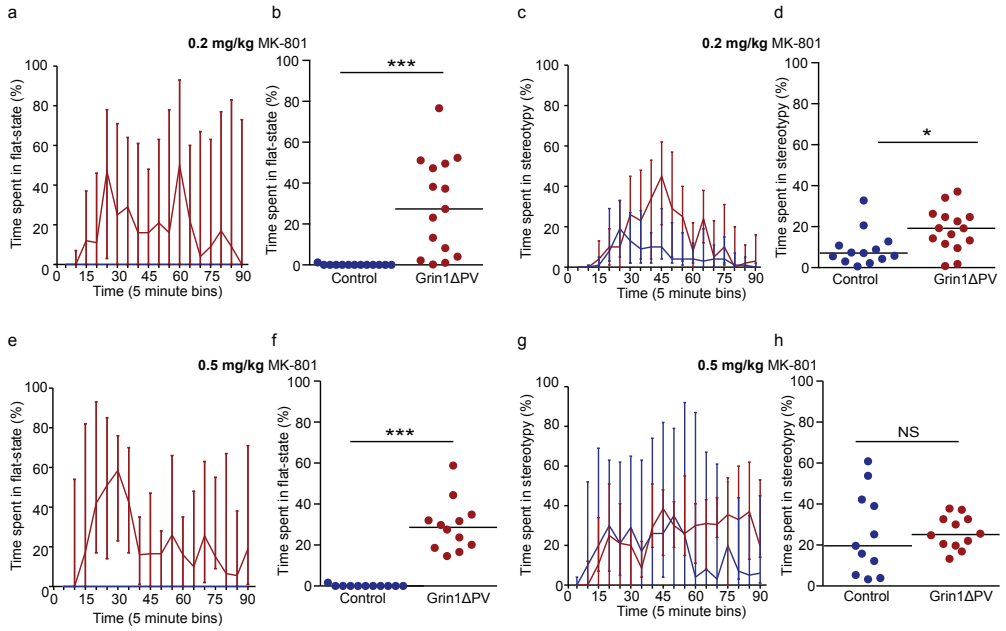

Figure 3.2: Induction of stereotypies and a flat-state in *Grin1*$^{\Delta PV}$ mice following MK-801 challenge

Induction of a flat-state and stereotypy in control and *Grin1*$^{\Delta PV}$ mice following MK-801 challenge. Time plots (a,c,e,g) display the percentage of time spent in a flat-state in 5 minute time bins following MK-801 challenge at 0.2mg/kg (top panel) and 0.5mg/kg (lower panel). Line graphs display the median and error bars display 95% confidence intervals. Dark blue and red shows control and *Grin1*$^{\Delta PV}$ mice respectively. Dot plots (b,d,f,h) show the percentage of time spent in each behavioural state in the entire 90-minute post drug period. Each dot indicates an animal. Black horizontal lines

display the group median. * indicates significant difference between genotypes (* P < 0.05, *** P < 0.001).

The pronounced flat-state observed in the *Grin1*$^{\Delta PV}$ mice was surprising and can account for their lack of an MK-801-induced increase in locomotor activity in terms of total beam breaks. Coupled with the fact *Grin1*$^{\Delta PV}$ mice also displayed similar (i.e. at 0.5mg/kg MK-801) or even enhanced (i.e. at 0.2 mg/kg MK-801) stereotypies, these data provide the first indication that *Grin1*$^{\Delta PV}$ mice are not protected from the effects of MK-801.

The flat-state could be on the same symptom scale as MK-801-induced hyperactivity (with a flat-state being the most severe behavioural response observed), and the fact that *Grin1*$^{\Delta PV}$ mice enter a flat-state could be a result of them being sensitised to the drug. However, it is possible that the flat-state and hyperactivity could be completely separate processes that are mutually exclusive of each other. In this situation, *Grin1*$^{\Delta PV}$ mice could appear “protected” from the hyperactivity-inducing effects of MK-801, because the provoked flat-state dominates their behaviour by rendering them immobile. To follow this up, control and *Grin1*$^{\Delta PV}$ mice were challenged with MK-801, whilst being tested for other behaviours.

3.3.3 *Grin1*$^{\Delta PV}$ mice are sensitised to MK-801 induced motor coordination impairments

Locomotor testing following MK-801 challenge revealed striking differences between control and *Grin1*$^{\Delta PV}$ mice. In order to see if these differences existed in other domains, and if *Grin1*$^{\Delta PV}$ mice are sensitised to the effects of MK-801, motor coordination was assessed following MK-801 challenge. The accelerating rotarod is commonly used to assess motor coordination in mice (Deacon, 2013). A cohort of control and *Grin1*$^{\Delta PV}$ mice were tested on the rotarod following MK-801 or vehicle injection. Male control (5 vehicle and 6 MK-801) and *Grin1*$^{\Delta PV}$ mice (6 vehicle and 7 MK-801) were tested with

0.2 mg/kg of MK-801. Female control (6 vehicle and 7 MK-801) and *Grin1*$^{\Delta PV}$ mice (9 vehicle and 9 control) were tested with 0.15mg/kg of MK-801. The time animals maintained themselves on the rotarod was measured at both 30 and 60 minutes after vehicle or MK-801 challenge. Before acceleration of the rotarod, mice had to successfully stay on the slowly rotating rod for a baseline period of 10s. Some animals failed to stay on the rotarod for this period, and in these cases the trial was considered a failure. The number of failures was recorded (maximum of 3 before the animal was given a score of 0 s). As data did not follow the normal distribution, non-parametric statistical tests were used to compare the different drug/genotype groups (Kruskal-Wallis test with subsequent pairwise comparisons) for the time on the accelerating rotarod and the number of failures recorded.

Time spent accelerating in male mice

In male animals assessed 30 minutes post injection there was an overall significant difference between groups in the time spent on the accelerating rotarod (H(3) = 11.359, P = 0.01). *Grin1*$^{\Delta PV}$ mice injected with MK-801 stayed on the accelerating rotarod for significantly less time than control mice injected with MK-801 (control MK-801 vs. *Grin1*$^{\Delta PV}$ MK-801: H(3) = 12.296, P = 0.01; **figure 3.3a**).

When re-tested at 60 minutes post injection (estimated to be the time of maximal drug effect based on locomotor activity data after MK-801 challenge) there was an overall significant difference between groups on the time spent on the accelerating rotarod (H(3) = 15.107, P = 0.002). Pairwise comparisons, with significance values corrected for multiple comparisons, revealed a significant reduction in the time spent on the accelerating rotarod in *Grin1*$^{\Delta PV}$ mice challenged with MK-801 compared to *Grin1*$^{\Delta PV}$ mice injected with vehicle (*Grin1*$^{\Delta PV}$ MK-801 vs. *Grin1*$^{\Delta PV}$ vehicle: H(3) = 10.667, P = 0.036). There was no difference in the time spent accelerating in control mice injected

with MK-801 or vehicle (control MK-801 vs control vehicle: H(3) = 2.667, P = 1). *Grin1*$^{\Delta PV}$ mice injected with MK-801 stayed on the accelerating rotarod for significantly less time than control mice injected with MK-801 (control MK-801 vs. *Grin1*$^{\Delta PV}$ MK-801: H(3) = 12.083, P = 0.011; **figure 3.3b**).

Number of failures in male mice

In male mice 30 minutes post injection there was no significant difference between control or *Grin1*$^{\Delta PV}$ mice injected with either drug or vehicle on the number of failures (control vehicle vs. control MK-801, *Grin1*$^{\Delta PV}$ vehicle vs. *Grin1*$^{\Delta PV}$ MK-801 for time accelerating and total number of failures: all P > 0.667; **figure 3.3a,c**).

In male mice 60-minutes post injection there was an overall significant difference between groups on the number of failures (H(3) = 18.870, P = 0.001). There was a significant increase in the number of failures made by drug treated *Grin1*$^{\Delta PV}$ mice but not drug treated controls (control MK-801 vs control vehicle: H(3) = 2.667, P = 1; *Grin1*$^{\Delta PV}$ MK-801 vs. *Grin1*$^{\Delta PV}$ vehicle: H(3) = 11.917, P = 0.004). *Grin1*$^{\Delta PV}$ mice injected with MK-801 had significantly more failed trials than control mice injected with MK-801 (control MK-801 vs. *Grin1*$^{\Delta PV}$ MK-801: H(3) = 10.883, P = 0.011; **figure 3.3d**).

Time spent accelerating in female mice

In female animals assessed 30 minutes post injection there was an overall significant difference between groups on the time spent on the accelerating rotarod (H(3) = 14.097, P = 0.003). MK-801 significantly reduced the amount of time *Grin1*$^{\Delta PV}$ mice, but not control mice, spent on the accelerating rotarod 30 minutes post injection (control MK-801 vs control vehicle: H(3) = 5.524, P = 1; *Grin1*$^{\Delta PV}$ MK-801 vs. *Grin1*$^{\Delta PV}$ vehicle: H(3) = 14.111, P = 0.006). There was no significant difference in the time

female control and *Grin1*$^{\Delta PV}$ mice injected with MK-801 stayed on the accelerating rotarod (control MK-801 vs. *Grin1*$^{\Delta PV}$ MK-801: H(3) = 9.143, P = 0.271; **figure 3.3e**).

In female animals assessed 60 minutes post injection there was also an overall significant difference between groups in the time spent on the accelerating rotarod (H(3) = 16.596, P = 0.001). There was a significant decrease in time spent on the accelerating rotarod in drug treated *Grin1*$^{\Delta PV}$ mice but not in drug treated controls (control MK-801 vs control vehicle: H(3) = 1.429, P = 1; *Grin1*$^{\Delta PV}$ MK-801 vs. *Grin1*$^{\Delta PV}$ vehicle: H(3) = 17.333, P = 0.001). There was no significant difference in the time drug treated control and drug treated *Grin1*$^{\Delta PV}$ mice stayed on the accelerating rotarod (control MK-801 vs. *Grin1*$^{\Delta PV}$ MK-801: H(3) = 8.405, P = 0.394; **figure 3.3f**).

Number of failures in female mice

In female mice 30-minutes post injection there was an overall significant group difference in the number of failures (H(3) = 19.196, P = 0.001). MK-801 significantly increased the number of failures in drug treated *Grin1*$^{\Delta PV}$ mice but not by drug treated controls (control MK-801 vs control vehicle: H(3) = 6.571, P = 0.868; *Grin1*$^{\Delta PV}$ MK-801 vs. *Grin1*$^{\Delta PV}$ vehicle: H(3) = 17.278, P = 0.001). There was a non-significant trend towards a greater number of failures in drug treated *Grin1*$^{\Delta PV}$ mice compared to drug treated controls (control MK-801 vs. *Grin1*$^{\Delta PV}$ MK-801: H(3) = 10.706, P = 0.052; **figure 3.3g**).

In female mice 60-minutes post injection there was also an overall significant difference between groups in the number of failures made (H(3) = 19.168, P = 0.001). There was a significant increase in the number of failures made by drug treated *Grin1*$^{\Delta PV}$ mice, but not by drug treated controls (control MK-801 vs control vehicle: H(3) = H(3) = 4.357, P = 1; *Grin1*$^{\Delta PV}$ MK-801 vs. *Grin1*$^{\Delta PV}$ vehicle: H(3) = 11.917, P = 0.004). There was also a non-significant trend towards a greater number of failures in drug

treated *Grin1*$^{\Delta PV}$ mice compared to drug treated controls (control MK-801 vs. *Grin1*$^{\Delta PV}$ MK-801: H(3) = 9.476, P = 0.073; **figure 3.3h**).

Together these data show that MK-801 can significantly impair motor coordination in *Grin1*$^{\Delta PV}$ mice but not in controls, as seen by a reduction in time spent on the accelerating rotarod and by the number of failures during the 10s baseline period. As controls were not significantly impaired by MK-801 it raises the possibility that *Grin1*$^{\Delta PV}$ mice are actually sensitised to the effects of MK-801.

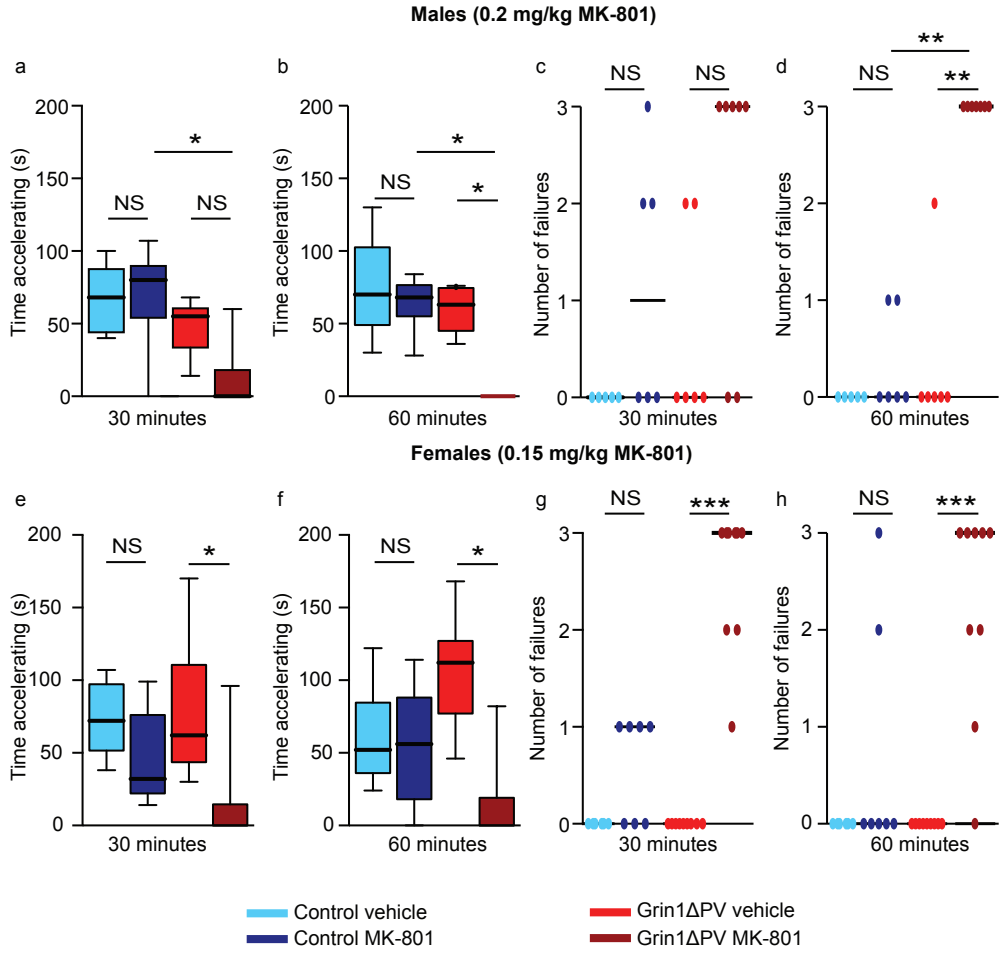

Figure 3.3: MK-801 impairs motor coordination in Grin1$^{\Delta PV}$ mice
Motor coordination was tested on the accelerating rotarod in male (top panel) and female (bottom panel) control and *Grin1*$^{\Delta PV}$ mice. Boxplots display the time until falling on the accelerating rod 30 minutes (a,e) and 60 minutes (b,f) after vehicle or MK-801. Boxplots display the median (thick black line) flanked by the 25 and 75 percentiles (bottom and top of box respectively) and whiskers display the maximum and minimum values. Dot

plots show the number of failures 30 minutes (c,g) and 60 minutes (d,h) following vehicle or MK-801 challenge. Each dot indicates an animal. Black horizontal lines display the group median. Light and dark blue represent control mice with vehicle and MK-801 respectively and light and dark red represent *Grin1*$^{\Delta PV}$ mice with vehicle and MK-801 respectively. * indicates significant difference between groups (* P < 0.05, ** P<0.01, *** P<0.001).

3.3.4 *Grin1*$^{\Delta PV}$ mice are sensitised to anhedonia induced by MK-801

Acute administration of MK-801 has been shown to impair sucrose preference in rats, indicating that NMDAR antagonists can induce anhedonia in rodents (Vardigan et al., 2010). Under baseline conditions *Grin1*$^{\Delta PV}$ mice displayed normal sucrose preference (see **figure 2.5**). It is possible that drugs such as MK-801 induce anhedonia via action on NMDARs on PV interneurons. The ability of MK-801 to induce impairments in sucrose preference, a possible negative symptom correlate, was therefore assessed in control and *Grin1*$^{\Delta PV}$ mice to test if NMDARs on PV interneurons are required for the expression of anhedonia with NMDAR antagonists. A cohort of male control (n = 10) and *Grin1*$^{\Delta PV}$ mice (n = 9) were given two days of sucrose preference testing to familiarise them with the testing apparatus (**figure 3.5**). One control animal was excluded because a water bottle leaked during testing so an accurate preference for sucrose could not be calculated.

As expected, there was no significant difference in the preference for sucrose over normal drinking water in control and *Grin1*$^{\Delta PV}$ mice, as revealed by a repeated measures ANOVA with genotype as a between subject factor and habituation day (before drug challenge) as a within subject factor (effect of genotype: $F(1,16)= 0.098$, $P = 0.758$). Animals were then challenged with MK-801 (0.1 and 0.15 mg/kg), with each drug dose having its own within subject vehicle injection control condition (drug

order counterbalanced), and sucrose preference assessed during the subsequent 2.5-hour period (**figure 3.5**). Unfortunately, in some instances water or sucrose bottles leaked, so some animals had to be excluded as sucrose preference values could not be accurately calculated (Total N number included for 0.1 mg/kg: 7 control and 7 *Grin1*$^{\Delta PV}$ mice; 0.15 mg/kg: 10 control and 9 *Grin1*$^{\Delta PV}$ mice).

At a dose of 0.1 mg/kg MK-801, there was no overall effect of drug or genotype on sucrose preference as revealed by a repeated measures ANOVA with genotype as a between subject factor and drug condition (MK-801 vs. vehicle) as a repeated measure (effect of drug: $F(1,12) = 0.002$, $P = 0.965$; effect of genotype: $F(1,12)= 0.003$, $P = 0.960$). However, there was a significant drug*genotype interaction, with MK-801 leading to a qualitative decrease in sucrose preference in *Grin1*$^{\Delta PV}$ mice and a qualitative increase in sucrose preference in controls (drug*genotype interaction: $F(1,12)= 8.779$, $P = 0.012$). The drug*genotype interaction was scrutinised with simple main effects analysis and revealed a trend towards increased and decreased sucrose preference in control and *Grin1*$^{\Delta PV}$ mice respectively (sucrose preference in control vehicle vs. control MK-801: $F(1,12) = 4.258$, $P = 0.055$; sucrose preference in *Grin1*$^{\Delta PV}$ vehicle vs. *Grin1*$^{\Delta PV}$ MK-801: $F(1,12) = 4.524$, $P = 0.061$). Following vehicle injection, *Grin1*$^{\Delta PV}$ mice showed significantly enhanced sucrose preference compared to controls (control vehicle vs. *Grin1*$^{\Delta PV}$ vehicle: $F(1,12) = 5.524$, $P = 0.036$). Following MK-801 injection there was a trend towards a decrease in sucrose preference in *Grin1*$^{\Delta PV}$ mice (control MK-801 vs. *Grin1*$^{\Delta PV}$ MK-801: $F(1,12) = 4.518$, $P = 0.055$).

When the dose of MK-801 was increased to 0.15mg/kg the sucrose preference of both control and *Grin1*$^{\Delta PV}$ mice was significantly decreased as revealed by an overall effect of drug (effect of drug: $F(1,17) = 7.661$, $P = 0.013$). At a dose of 0.15mg/kg there was

no overall effect of genotype and there was no significant drug*genotype interaction (effect of genotype: F(1,17)= 2.417, P = 0.161; drug*genotype interaction: F(1,17) = 0.595, P = 0.451).

These data suggest that MK-801, at a dose of 0.15 mg/kg, can induce a state of anhedonia in control and *Grin1*$^{\Delta PV}$ mice. The drug*genotype interaction, at a dose of 0.1 mg/kg MK-801, was driven by a non-significant increase in sucrose preference in control animals and a non-significant decrease in sucrose preference in *Grin1*$^{\Delta PV}$ mice resembling the effects seen with the higher dose of MK-801. This tentatively suggests that *Grin1*$^{\Delta PV}$ mice could be sensitised to the anhedonia-inducing effects of MK-801 when compared to control animals. Together with the rotarod and locomotor activity data, these results indicate that *Grin1*$^{\Delta PV}$ mice could be sensitised to the effects of MK-801.

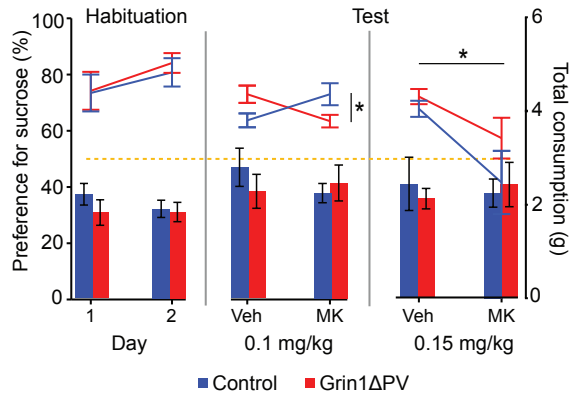

Figure 3.4: *Grin1*$^{\Delta PV}$ mice are sensitised to anhedonia inducing effects of MK-801
Anhedonia was assessed with the sucrose preference test in control and *Grin1*$^{\Delta PV}$ mice. Average preference for sucrose is plotted for the two days of habituation and following challenge with vehicle or MK-801 (0.1 and 0.15 mg/kg). Preferences are displayed (left axis and line graph) as the mean and error bars show the SEM. The yellow dashed line indicates equal preference for water and sucrose. Total liquid consumption is shown (right axis and bars) as the mean and error bars display SEM.* in 0.1mg/kg panel indicates significant drug*genotype interaction. * in 0.15mg/kg panel indicates overall significant effect of drug (P < 0.05).

3.3.5 *Grin1*$^{\Delta PV}$ mice are sensitised to MK-801 induced SWM deficits

Both genetic (Niewoehner et al., 2007; von Engelhardt et al., 2008) and pharmacological studies (McHugh et al., 2008) have highlighted the importance of hippocampal NMDARs for win-shift spatial working memory tasks such as rewarded alternation. Under baseline conditions *Grin1*$^{\Delta PV}$ mice displayed essentially normal spatial working memory with intra-trial intervals >1s (see **figure 2.11**). To test if NMDAR antagonists such as MK-801 induce cognitive impairments via blockade of NMDARs specifically on PV interneurons, or if *Grin1*$^{\Delta PV}$ mice are sensitised to the cognitive impairing effects of MK-801 compared to control mice, a cohort of male control (n = 8) and *Grin1*$^{\Delta PV}$ mice (n = 6) aged 6-7 months were trained on the rewarded alternation T-maze task. Animals were trained until they reached a criterion of 80% correct for two consecutive training blocks (10 trials per block), and then they were challenged with escalating doses of MK-801 or vehicle following a within subject design, where each dose of MK-801 had its own within subject vehicle injection condition (counterbalanced for drug order).

There was no significant difference in the number of days taken for control and *Grin1*$^{\Delta PV}$ mice to reach criteria level performance, in agreement with previous data (see **2.3.11**) (effect of genotype: $U_{8,6} = 33$, $P = 0.282$, median days to criteria: 7 and 4 for control and *Grin1*$^{\Delta PV}$ mice respectively; **figure 3.5a**). Animals were then injected with MK-801 or vehicle and performance was tested 30 minutes later (**figure 3.5b**). Performance after drug challenge (at each of the doses) was analysed with a repeated measures ANOVA with genotype as a between subject factor and drug condition (vehicle vs. MK-801) as a repeated measure.

At a dose of 0.1 mg/kg MK-801 there was no effect of either drug, genotype or drug*genotype interaction on task performance (effect of genotype: F(1,10) = 0.288, P = 0.603; effect of drug: F(1,10) = 0.388, P = 0.547; drug*genotype interaction: F(1,10) = 2.427 , P = 0.15).

When the dose was increased to 0.15 mg/kg MK-801, there was no overall effect of drug or genotype on task performance (effect of genotype: F(1,12) = 0.443, P = 0.518; effect of drug: F(1,12) = 0.4, P = 0.539). However, there was a significant drug*genotype interaction with MK-801 seeming to reduce task performance in *Grin1*$^{\Delta PV}$ mice (drug*genotype interaction: F(1,12) = 10.614, P = 0.007). This interaction was scrutinised with simple main effects analysis which revealed a trend towards increased task performance in drug treated control mice and a significant decrease in task performance in *Grin1*$^{\Delta PV}$ mice (task performance in control vehicle vs. control MK-801: F(1,12) = 4.022, P = 0.068; task performance in *Grin1*$^{\Delta PV}$ vehicle vs. *Grin1*$^{\Delta PV}$ MK-801: F(1,12) = 6.621, P = 0.024). Following vehicle injection, there was no significant difference in task performance in control and *Grin1*$^{\Delta PV}$ mice (control vehicle vs. *Grin1*$^{\Delta PV}$ vehicle: F(1,12) = 1.582, P = 0.232). Following MK-801 injection there was significant decrease in task performance in *Grin1*$^{\Delta PV}$ mice (control MK-801 vs. *Grin1*$^{\Delta PV}$ MK-801: F(1,12) = 7.235, P = 0.02).

Results with 0.2 mg/kg MK-801 were similar as there was a reduction in task performance selectively in *Grin1*$^{\Delta PV}$ mice, with a significant overall effect of genotype, no overall effect of drug but a significant drug*genotype interaction (effect of genotype: F(1,12) = 5.413, P = 0.043; effect of drug: F(1,12) = 2.338, P = 0.152; drug*genotype interaction: F(1,12) = 11.314, P = 0.006). This interaction was scrutinised with simple main effects analysis which revealed no significant change in task performance in drug

treated control mice and a significant decrease in task performance in *Grin1*$^{\Delta PV}$ mice (task performance in control vehicle vs. control MK-801: F(1,12) = 1.964, P = 0.186; task performance in *Grin1*$^{\Delta PV}$ vehicle vs. *Grin1*$^{\Delta PV}$ MK-801: F(1,12) = 10.743, P = 0.007). The overall significant effect of genotype on task performance at 0.2 mg/kg MK-801 is driven by the drop in performance of *Grin1*$^{\Delta PV}$ mice following MK-801 challenge, as the groups are almost identical under vehicle conditions (mean performance +/- SE: 90 +/- 5.1% and 89 +/- 3.5% for control and *Grin1*$^{\Delta PV}$ mice respectively), and not significantly different (control vehicle vs. *Grin1*$^{\Delta PV}$ vehicle: F(1,12) = 0.043, P = 0.839). Following MK-801 injection there was a significant decrease in task performance in *Grin1*$^{\Delta PV}$ mice compared to controls (control MK-801 vs. *Grin1*$^{\Delta PV}$ MK-801: F(1,12) = 11.874, P = 0.005; **figure 3.5b**).

When the dose was increased to 0.4 mg/kg MK-801 the performance of both control and *Grin1*$^{\Delta PV}$ mice decreased, as indicated by an overall significant effect of drug (effect of drug: F(1,12) = 22.313, P = 0.001). However, there was no drug*genotype interaction (drug*genotype interaction: F(1,12) = 1.004, P = 0.336), in contrast to MK-801 at doses of 0.15 and 0.2 mg/kg. At 0.4 mg/kg MK-801 there was also a significant overall effect of genotype (effect of genotype: F(1,12) = 6.767, P = 0.023) but simple main effects analysis revealed no significant difference between control and *Grin1*$^{\Delta PV}$ mice injected with vehicle or MK-801 (control vehicle vs. *Grin1*$^{\Delta PV}$ vehicle: F(1,12) = 1.714, P = 0.215, control MK-801 vs. *Grin1*$^{\Delta PV}$ MK-801: F(1,12) = 3.818, P = 0.074; **figure 3.5b**).

Importantly there were no signs of flat-state or circling behaviour whilst animals were being tested. Choice trial latencies largely remained under 10s (**figure 3.5c**) and there were no signs of stereotypical circling or flat-state behaviour whilst animals were on

the maze. However, statistically significant increases in choice latencies were observed with 0.2 and 0.4 mg/kg doses of MK-801, particularly in *Grin1*$^{\Delta PV}$ mice (see **appendix 7.2.1** and **appendix figure 7.2**).

Together these data suggest that *Grin1*$^{\Delta PV}$ mice are actually sensitised to the SWM impairing effects of MK-801. This indicates that NMDAR antagonists such as MK-801 are unlikely to exert their cognitive impairing effects primarily via NMDARs on PV interneurons.

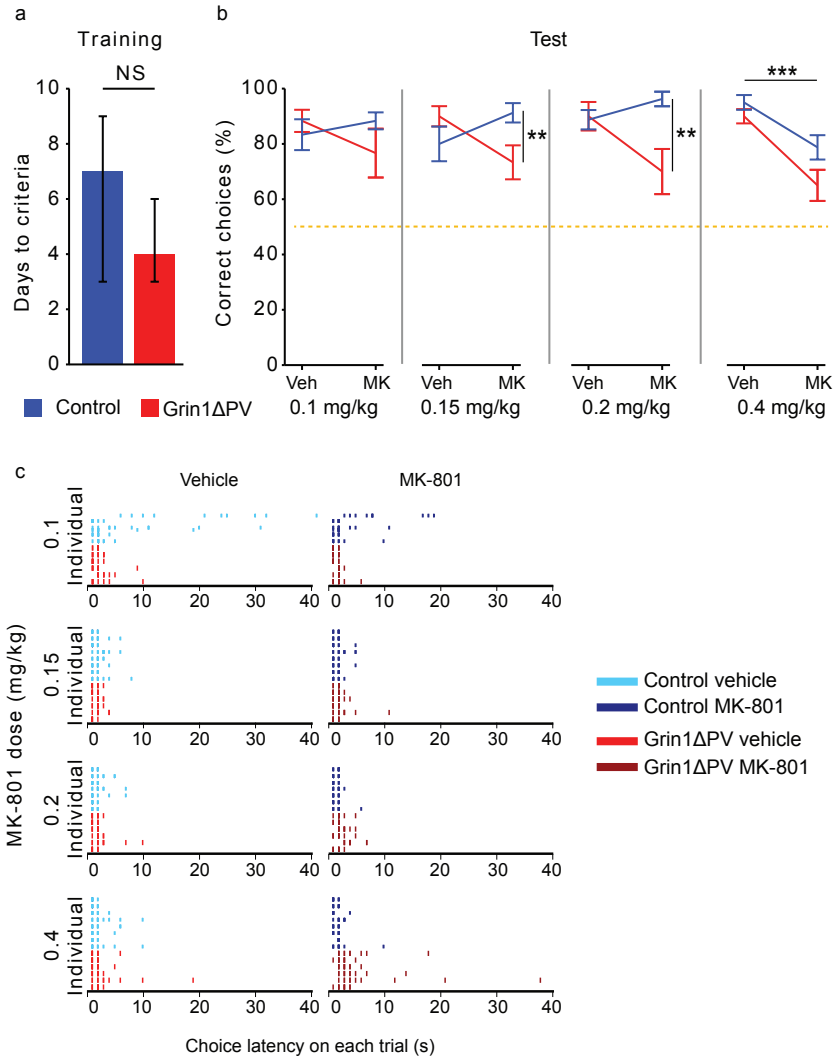

Figure 3.5: *Grin1*$^{\Delta PV}$ mice are sensitised to the cognitive impairing effects of MK-801
Rewarded alternation was tested on the T-maze to assess spatial working memory. (a) Days taken to reach training criteria in control (blue) and *Grin1*$^{\Delta PV}$ mice (red). Bar chart displays the median and error bars show 95%

confidence intervals. (b) Performance of control (blue) and *Grin1*$^{\Delta PV}$ mice (red) after challenge with escalating doses of MK-801. Lines display mean and error bars show the SEM. The dotted yellow line indicates chance level performance. (c) Individual choice trial latencies on the choice trial of control (light blue = vehicle and dark blue = MK-801) and *Grin1*$^{\Delta PV}$ mice (light red = vehicle and dark red = MK-801). Latencies were rounded to the nearest 1s. Each row represents the data from one animal. **P < 0.01, *** P < 0.001.

3.3.6 Induction of prominent 3-5 Hz oscillations in *Grin1*$^{\Delta PV}$ mice following MK-801 challenge

The pronounced flat-state observed in *Grin1*$^{\Delta PV}$ mice but not control animals represents a clear behavioural divergence in response to MK-801 challenge. In an attempt to understand the physiological changes associated with MK-801 challenge, male control (n = 6) and *Grin1*$^{\Delta PV}$ mice (n = 7) were implanted with electrodes in the prefrontal cortex and hippocampus (**data not shown for hippocampus**), and local field potentials (LFPs) were recorded in awake animals under baseline conditions, and after MK-801 challenge (0.2 mg/kg) or vehicle injections. Electrodes placements in the mPFC were either in prelimbic cortex, infralimbic cortex or medial orbital cortex, and in one case the anterior cingulate cortex (see **appendix 7.2.2** and **figure 7.3** for reconstructions of electrode placements).

Under baseline conditions the prefrontal LFP spectra were similar between control and *Grin1*$^{\Delta PV}$ mice (**figure 3.6d**). However, following MK-801 challenge there was a divergence in the LFPs recorded in the prefrontal cortex, with slow oscillations emerging in *Grin1*$^{\Delta PV}$ but not in control mice (example traces in **figure 3.6a,b**). To visualise changes in prefrontal LFPs, a power spectrograph was generated for a *Grin1*$^{\Delta PV}$ animal during 1 minute of baseline and then for 1-minute during the post MK-801 period. Post MK-801 challenge there was a qualitative increase in 3-5 Hz oscillatory power in the prefrontal cortex compared with a pre-drug baseline period **(figure 3.6c)**. To assess power changes in the 3-5 Hz range quantitatively, power spectral density (PSD) plots were generated for each animal during the baseline (-10 to 0 minute) and post injection (30 - 40 minute) period. The PSD plots were normalised to total power and averaged across groups. In the 10-minute baseline period (before

vehicle or MK-801 injection) there was no difference in the PSD of control and *Grin1*$^{\Delta PV}$ mice **(figure 3.6d)**. However, following MK-801 challenge at a dose of 0.2 mg/kg, a peak in the PSD around 4 Hz emerged in *Grin1*$^{\Delta PV}$ animals that was lacking in controls **(figure 3.6e)**. The 3 - 5 Hz power (area under the PSD plot between 3 - 5 Hz) was normalised to the total power (total area under the PSD plot between 0-500 Hz) and the relative change in 3 - 5 Hz power was assessed by calculating the post drug/baseline ratio for control and *Grin1*$^{\Delta PV}$ mice.

MK-801 at a dose of 0.2 mg/kg led to a significant overall increase in the post-drug/baseline ratio of 3-5 Hz power which was greater in *Grin1*$^{\Delta PV}$ mice than in controls (**figure 3.6f**). This was revealed by a repeated measures ANOVA with genotype as a between subject factor and drug (vehicle or MK-801) as a within subject factor that found no overall effect of genotype but an overall significant effect of drug, and a significant drug*genotype interaction (effect of genotype: $F(1,11) = 4.058$, $P = 0.069$; effect of drug: $F(1,11) = 6.310$, $P = 0.029$; drug*genotype interaction: $F(1,11) = 7.169$, $P = 0.022$).

Simple main effects analysis revealed that MK-801 significantly increased the drug/baseline ratio of 3-5 Hz power in *Grin1*$^{\Delta PV}$ mice but not in controls (drug/baseline ratio in control vehicle vs. control MK-801: $F(1,11) = 0.013$, $P = 0.912$; drug/baseline ratio in *Grin1*$^{\Delta PV}$ vehicle vs. *Grin1*$^{\Delta PV}$ MK-801: $F(1,11) = 14.587$, $P = 0.003$). Under vehicle conditions there was no significant difference between control and *Grin1*$^{\Delta PV}$ mice (drug/baseline ratio in control vehicle vs. *Grin1*$^{\Delta PV}$ vehicle: $F(1,11) = 0.256$, $P = 0.623$). However, there was a significantly greater drug/baseline ratio of 3-5 Hz power in MK-801 treated *Grin1*$^{\Delta PV}$ mice compared to MK-801 treated controls (drug/baseline ratio in control MK-801 vs. *Grin1*$^{\Delta PV}$ MK-801: $F(1,11) = 8.299$, $P = 0.01$).

Slow oscillations in the delta range (generally classified as 1-4 Hz) are normally observed during slow wave sleep. During these recordings *Grin1*$^{\Delta PV}$ mice did enter a flat-state as observed in the first locomotor experiment in this chapter (see **figure 3.2**). As NMDAR antagonists have been shown to induce delta oscillations in other studies (Zang et al., 2009), it is possible that the selective increase in 3-5 Hz oscillations observed in *Grin1*$^{\Delta PV}$ mice reflects further evidence of their sensitisation to NMDAR antagonism.

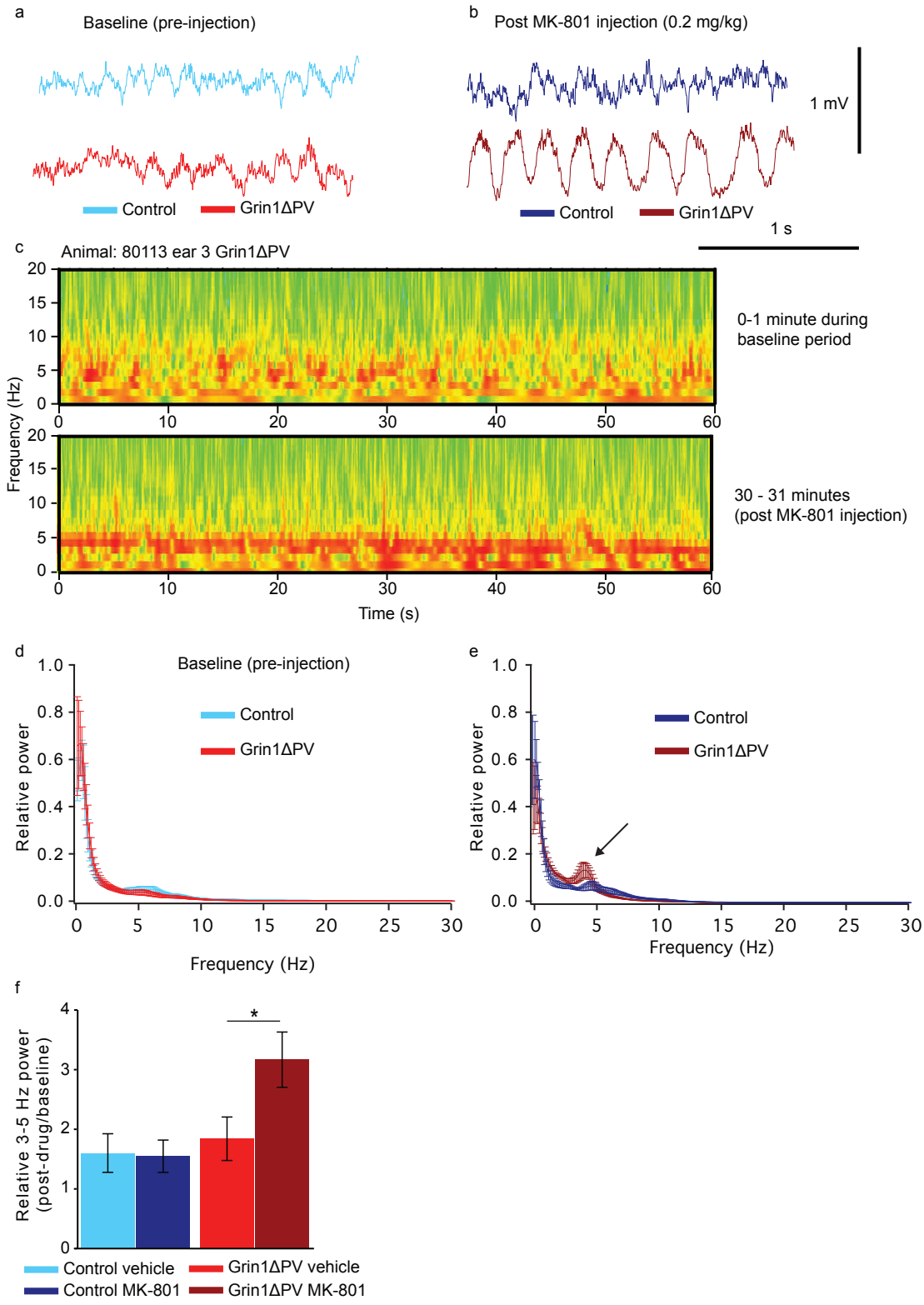

Figure 3.6: Induction of slow oscillations in *Grin1*$^{\Delta PV}$ mice following MK-801 challenge
LFPs were recorded from the prefrontal cortex of control and *Grin1*$^{\Delta PV}$ mice. Example traces from (a) baseline period (light blue and light red represent control and *Grin1*$^{\Delta PV}$ mice respectively) and (b) post-MK-801 (dark blue and dark red represent control and *Grin1*$^{\Delta PV}$ mice respectively). (c) Visualisation

of power changes in one *Grin1*$^{\Delta PV}$ animal during baseline (top panel) and after MK-801 (bottom panel). Power is indicated via a heat map with red indicating greatest power. Power spectrum density (PSD) plots for control and *Grin1*$^{\Delta PV}$ mice during (d) baseline and (e) post MK-801 (0.2 mg/kg) time periods. The PSD for each animal was normalised to the total power. Lines show group averages and error bars display SEM. (f) Bar chart displaying the relative change in 3-5 Hz power (pre-drug/baseline) following vehicle (light blue and light red for control and *Grin1*$^{\Delta PV}$ mice respectively) and MK-801 (dark blue and dark red for control and *Grin1*$^{\Delta PV}$ mice respectively). Error bars display SEM. * indicates a significant drug*genotype interaction ($P<0.05$).

3.4 Discussion

These experiments tested the hypothesis that NMDARs on PV interneurons are required for not only the induction of positive symptoms following the administration of NMDAR antagonists (as previously suggested by Carlen *et al.,* 2012 and Belforte *et al.,* 2010), but also for the induction of negative and cognitive symptoms post-drug.

3.4.1 MK-801-induced hyperlocomotion in control and *Grin1*$^{\Delta PV}$ mice

The locomotor-inducing effects of three doses of MK-801 (0.1, 0.2 and 0.5 mg/kg) were tested and, as expected, induced hyperactivity in control mice (Belforte et al., 2010; Carlén et al., 2012; Wu et al., 2005). In *Grin1*$^{\Delta PV}$ mice the situation is more complicated. In the first 60 minutes following MK-801 challenge (analogous to the analysis done by Carlen *et al.,* 2012), there was no increase in locomotor activity in *Grin1*$^{\Delta PV}$ mice. However, when looking at the 61-90-minute post-injection period there was an increase in locomotor activity in *Grin1*$^{\Delta PV}$ mice at doses of 0.2 and 0.5 mg/kg. This shows that *Grin1*$^{\Delta PV}$ mice do show MK-801-induced hyperactivity compared to vehicle-injected *Grin1*$^{\Delta PV}$ animals, it is just delayed and weaker in comparison to control animals. Thus, induction of hyperactivity following MK-801 challenge is not solely dependent on NMDARs on PV neurons.

3.4.2 MK-801-induced flat-state and stereotypies in *Grin1*$^{\Delta PV}$ mice

In addition to the automated beam breaks, the behaviour of animals was manually scored “online” to test for stereotypical behaviours that could be missed by assessing beam breaks alone. Strikingly, *Grin1*$^{\Delta PV}$ mice entered a flat-like state (hereafter referred to as flat-state) following MK-801 challenge (0.2 and 0.5 mg/kg). This flat-

state was absent in control mice but observed in every *Grin1*$^{\Delta PV}$ animal challenged with 0.5mg/kg of MK-801. This was surprising given that previous studies have not reported such a flat-state in *Grin1*$^{\Delta PV}$ mice or other interneuron specific NR1 knockouts (Belforte et al., 2010; Carlén et al., 2012). This highlights a limitation of using distance travelled or number of beam breaks alone in locomotor activity studies, in the absence of visual inspection of the animals. The attenuation of MK-801-induced beam breaks in the first 60 minutes following injection in *Grin1*$^{\Delta PV}$ mice likely results because they enter a flat-state which obviously could prevent the expression of hyperlocomotion.

It is possible that the flat-state and hyperactivity result from different, competing processes. It could be argued that the flat-state is only observed because MK-801 is not able to induce hyperactivity in *Grin1*$^{\Delta PV}$ mice. Thus, *Grin1*$^{\Delta PV}$ mice could indeed be "protected" from the locomotor inducing effects of MK-801 as previously reported (Carlén et al., 2012). However, as *Grin1*$^{\Delta PV}$ mice appear to be sensitised to MK-801 in other domains (stereotypies in the very same locomotor assessments but also motor coordination, sucrose preference and working memory in separate tests), and show MK-801 induced hyperactivity at later time points, this is unlikely to be the case. Therefore, caution should be taken when interpreting the lack of an MK-801-induced rise in beam breaks in *Grin1*$^{\Delta PV}$ mice as ineffectiveness of the drug because MK-801 is just affecting *Grin1*$^{\Delta PV}$ mice in a different and seemingly in a more profound way.

Carlen *et al.* reported that MK-801 induced stereotypies in control but not *Grin1*$^{\Delta PV}$ mice (Carlén et al., 2012). It was therefore surprising to observe robust stereotypies in *Grin1*$^{\Delta PV}$ mice in this study. In fact, at a dose of 0.2 mg/kg *Grin1*$^{\Delta PV}$ mice displayed significantly more stereotypies than control animals. This shows that *Grin1*$^{\Delta PV}$ mice are not protected from MK-801-induced stereotypies as previously reported (Carlén et

al., 2012). These differences could arise because automated detection of stereotypies was used by Carlen *at al.* compared to manual online scoring in this study.

3.4.3 Impaired motor coordination in MK-801-challenged *Grin1*$^{\Delta PV}$ mice

MK-801 has previously been shown to impair motor performance on the rotarod in mice (O'Neill and Bolger, 1989). As *Grin1*$^{\Delta PV}$ mice were not fully protected from the hyperlocomotor- or stereotypy-inducing effects of MK-801 it is possible that MK-801 differentially effects motor function in control and *Grin1*$^{\Delta PV}$ mice.

Grin1$^{\Delta PV}$ mice and control mice were tested for motor coordination on the rotarod to explore if *Grin1*$^{\Delta PV}$ mice were protected, or indeed sensitised to MK-801 induced deficits. There were no significant effects of MK-801 challenge on motor coordination in control animals. In contrast, MK-801 significantly impaired the ability for *Grin1*$^{\Delta PV}$ mice to perform the rotarod task, as seen by a reduction in the time spent on the accelerating rod, and an increase in the number of failures when animals were initially placed on the rotarod. These data indicate that *Grin1*$^{\Delta PV}$ mice are actually sensitised to motor impairments induced by MK-801. This strongly argues against the hypothesis that NMDAR antagonists such as MK-801 are acting preferentially through NMDARs on PV interneurons.

3.4.4 *Grin1*$^{\Delta PV}$ mice are sensitised to MK-801 induced anhedonia

The mechanism by which NMDAR antagonists such as MK-801 induce negative symptoms of schizophrenia (i.e. anhedonia) is not known. It is possible that NMDARs on PV interneurons are required for the induction anhedonia by MK-801. However, *Grin1*$^{\Delta PV}$ mice, if anything, showed increased sensitivity to MK-801-induced sucrose

preference deficits when challenged with 0.1 mg/kg of MK-801. Future studies to assess sucrose preference following MK-801 challenge could be more refined by utilising an automated lickometer (Tye et al., 2012), rather than relying on the aggregate readout of total sucrose or water consumed 2.5 hours after injection. However, these results indicate that NMDARs on PV interneurons are not the main target of MK-801 required for the induction of anhedonia.

3.4.5 *Grin1*$^{\Delta PV}$ mice are sensitised to cognitive impairing effects of MK-801

If MK-801 induces spatial working memory impairments preferentially via blocking NMDARs on PV interneurons, then it is logical that *Grin1*$^{\Delta PV}$ mice (which under baseline conditions show normal spatial working memory; see **figure 2.11**) should not be impaired by low doses of MK-801. In fact, the opposite was observed and *Grin1*$^{\Delta PV}$ mice showed impaired spatial working memory performance on the T-maze at doses of MK-801 that did not impair performance in controls. It is possible that, indirectly, motor coordination is responsible for this drop in performance, as *Grin1*$^{\Delta PV}$ mice were previously shown to be more sensitive to MK-801-induced deficits in motor coordination on the accelerating rotarod. Does the observed decrease in T-maze performance actually reflect a true cognitive deficit? It is unlikely that non-specific motor effects account entirely for the observed effects because at a dose of 0.15 mg/kg there was no difference in choice trial latencies (that might indicate motor impairments; see **appendix 7.2.1** and **figure 7.2**) in *Grin1*$^{\Delta PV}$ mice, yet their performance was still significantly impaired. However, non-cognitive side effects cannot be ruled out, so future control behavioural experiments would be useful to show that *Grin1*$^{\Delta PV}$ mice challenged with low doses of MK-801 can still perform similar tasks.

For example, animals could be trained on a visual discrimination T-maze task, where animals learn to associate a visual cue on the arm with a food reward (Morris et al., 1986). Then the effects of MK-801 could be assessed on task performance (although it is possible that MK-801 could impair the cognitive processes required for this task as well, but see Morris et al., 1986). It is also possible that motivation is reduced following MK-801 challenge, which could indirectly lead to impaired task performance. To test if MK-801 influences motivation, a progressive ratio task could be used with and without MK-801 injection. In this task animals are required to lever press for a food reward. Then the number of lever presses required for reward delivery is increased and the motivation animals have to continue to press the lever is assessed. Issues with assessing the cognitive impairments of NMDAR antagonists in rodents have been discussed by Gilmour *et al.*, who highlight that cognitive tasks commonly used in humans usually require little motor action compared to rodent based tasks that often require considerable motor action (Gilmour et al., 2012). Thus, sensorimotor side effects should always be considered when assessing cognitive ability in drug-treated rodents.

3.5.6 Induction of slow oscillations in *Grin1*$^{\Delta PV}$ mice

Recording local field potentials in the prefrontal cortex of mice challenged with MK-801 revealed the selective emergence of slow 3 - 5 Hz oscillations in *Grin1*$^{\Delta PV}$ mice. Slow “delta” oscillations are usually observed during slow wave sleep, so it is possible that *Grin1*$^{\Delta PV}$ mice enter a brain state usually associated with sleep whilst they are still awake (Lisman, 2012). It is possible that periods of slow oscillations correlated with episodes of flat-state behaviour in *Grin1*$^{\Delta PV}$ mice. However, it is unclear whether this shift in local field potential is causative of the flat-state or a result of this behavioural state. Unfortunately, it is exceptionally difficult to test causality when it comes to linking

neuronal oscillations to behaviour. In relation to schizophrenia this finding is very interesting because elevated delta oscillations have emerged as a clear biomarker of the disease (Boutros et al., 2008). As NMDAR antagonists have been shown to induce delta oscillations in rodents (Zang et al., 2009), it is tempting to speculate that *Grin1*$^{\Delta PV}$ mice have increased sensitivity to the delta-inducing effects of NMDAR antagonists.

3.5.7 Conclusions

Previous studies have concluded that NMDARs on PV interneurons represent a key target of NMDAR antagonists such as MK-801 for induction of schizophrenia like behaviours (Belforte et al., 2010; Carlén et al., 2012). Results presented here strongly argue against this conclusion and show that not only are *Grin1*$^{\Delta PV}$ mice not protected, but actually seem to be sensitised to the effects of MK-801. Thus, ablation of NMDARs from PV interneurons has acted as a risk factor to NMDAR hypofunction elsewhere in the circuit. One possibility is that the excitation/inhibition balance is being more strongly disrupted in *Grin1*$^{\Delta PV}$ mice compared to controls. MK-801 will reduce excitatory drive to both excitatory and inhibitory neuron populations. In control mice this will be somewhat balanced, but could lead to an overall disinhibition of excitatory neurons as observed experimentally (Homayoun and Moghaddam, 2007; Jackson et al., 2004). In *Grin1*$^{\Delta PV}$ mice around 20 -30 % of the inhibitory interneuron population (i.e. the share of PV interneurons; Hu et al., 2014) lack NMDARs, so when challenged with MK-801 there is the same number of excitatory neurons that will receive reduced excitation, but there will be fewer inhibitory neurons whose excitation will be reduced. This could occlude the disinhibition seen in control animals and lead to an overall decrease in activity accounting for the increased sensitivity of *Grin1*$^{\Delta PV}$ mice to MK-801.

However, this requires there to be functional NMDARs on PV interneurons to block, which might not be the case based on *in vitro* recordings made from adult rat and mouse prefrontal cortex (Rotaru et al., 2011; Wang and Gao, 2010). However, these *in vitro* studies have focussed on slices taken from the prefontal cortex, so the contribution of NMDARs on PV interneurons in other brain regions is less known. Rotaru *et al.* have argued that NMDAR hypofunction at synapses other than those onto PV neurons are likely to be responsible for the disinhibition and molecular changes associated with acute NMDAR challenge (Rotaru et al., 2013).

It would be very interesting to record single units from the prefrontal cortex of control and *Grin1*$^{\Delta PV}$ mice (as in (Homayoun and Moghaddam, 2007)) to see if MK-801 still leads to an increase in putative excitatory neuron firing in *Grin1*$^{\Delta PV}$ mice. It would be better still to make juxtacellular recordings from head fixed animals so the firing rate could be combined with post-hoc immunohistochemical identification of cell type.

It is perhaps not surprising that NMDAR antagonists do not seem to exert their effects exclusively or preferentially via NMDARs on PV interneurons. A recent study generated mice with NR1 ablated from excitatory neurons in the forebrain (Tatard-Leitman et al., 2014). These animals displayed hyperactivity, reduced social interactions and cognitive impairments as well as electrophysiological abnormalities such as enhanced baseline gamma oscillation and reduced evoked gamma oscillation power (Tatard-Leitman et al., 2014). In addition, selective deletion of NR1 from the dentate gyrus (Niewoehner et al., 2007), or NR2B from the hippocampus or forebrain (von Engelhardt et al., 2008) leads to selective deficits in spatial working memory. Therefore, it is likely that MK-801-induced behavioural deficits are mediated, at least in part, through targeting NMDARs directly on excitatory neurons in the hippocampus

and forebrain in general (Niewoehner et al., 2007; Tatard-Leitman et al., 2014; von Engelhardt et al., 2008).

It would be interesting to search for electrophysiological correlates of the spatial working memory deficits seen on the T-maze in *Grin1*$^{\Delta PV}$ mice at doses of MK-801 that do not impair controls. Theta oscillations in the medial prefrontal cortex and hippocampus become coordinated whilst mice perform spatial working memory tasks (Jones and Wilson, 2005), and this has been observed to be reduced in rodent models of schizophrenia (Sigurdsson et al., 2010b). Future experiments simultaneously recording oscillations from medial prefrontal cortex and hippocampus in *Grin1*$^{\Delta PV}$ mice on the T-maze, with and without MK-801 challenge, will be interesting in this regard. It is possible that hippocampal-prefrontal coherence is more sensitive to NMDAR antagonism in *Grin1*$^{\Delta PV}$ mice compared to controls, and this could underlie their increased sensitivity to cognitive impairing effects of MK-801 on the T-maze.

In summary, MK-801 does not seem to exert its effects preferentially via PV interneurons, as was expected based on previous studies (Belforte et al., 2010; Carlén et al., 2012). As *Grin1*$^{\Delta PV}$ mice appear sensitised to the effects of MK-801, it is possible that NMDAR hypofunction on these interneurons acts as a risk factor exacerbating NMDAR hypofunction elsewhere in the circuit. Chapter 4 will explore the effects of acutely silencing PV neurons in the hippocampus on behaviours relevant to schizophrenia.

4 Chemogenetic silencing of parvalbumin positive interneurons

4.1 Introduction

4.1.1 GABAergic dysfunction in schizophrenia

There is an abundance of evidence that GABAergic deficits exist in schizophrenia (Lewis et al., 2012; Lisman et al., 2008). Inhibitory interneurons form an extremely heterogeneous population, classified by unique molecular expression profiles, electrophysiological characteristics and by their morphology (Klausberger and Somogyi, 2008). Inhibitory interneurons seem to be affected in schizophrenia, as mRNA levels of interneuron markers such as parvalbumin and somatostatin are significantly reduced in post mortem tissue from schizophrenia patients (Fung et al., 2010; Hashimoto et al., 2008). Parvalbumin positive interneurons consist of morphologically distinct subtypes, including PV positive basket cells (PVBC) and PV positive chandelier cells (PVChC) that innervate the soma and axon initial segment (AIS) of target neurons respectively (Lewis et al., 2012). The molecular profile of PVBCs and PVChCs is changed in schizophrenia, along with the expression of GABA receptors on pyramidal neurons at PV interneuron synapses (Lewis et al., 2005, 2012). In particular there is loss of GAD67 and GAT1 immunoreactivity within PV interneurons, and postsynaptic to PVChCs there is upregulation of the $\alpha 2$ $GABA_A$ receptor subunit in pyramidal neurons (see **1.2.3**).

Post mortem studies have found reduced expression of GAD-67 in schizophrenia, particularly in PV positive interneurons (Curley et al., 2011). In the dorsolateral prefrontal cortex (DLPFC) the absolute number of PV interneurons does not appear to be changed but expression of GAD-67 mRNA is only detectable in around 50% of

PV positive interneurons (Hashimoto et al., 2003). It is possible that these molecular changes are part of a homeostatic mechanism in response to reduced excitation of layer 3 pyramidal neurons on the DLPFC, aimed at decreasing inhibitory output of PV interneurons to increase the overall excitation in the network (Lewis et al., 2012).

4.1.2 Circuit based models of GABAergic dysfunction

The Lisman/Grace model similarly accounts for changes in levels of GAD-67 as a compensatory mechanism following NMDAR hypofunction, specifically on PV interneurons (Lisman et al., 2008). In this model NMDAR hypofunction on PV interneurons is the starting point of the pathophysiology in schizophrenia, with reduced excitation of PV interneurons thought to be responsible for causing disinhibition within the hippocampus, as well as impaired generation of gamma oscillations (Lisman et al., 2008). In contrast, Lewis *et al.* propose that the molecular changes seen in PV interneurons are a result of an upstream decrease in the excitability of layer 3 pyramidal neurons in the DLPFC (Lewis et al., 2012), rather than being a primary step in the pathophysiology of schizophrenia. Interestingly, however, both models involve a reduction of output from PV interneurons as a homeostatic mechanism to reset the excitation/inhibition balance in schizophrenia (Lewis et al., 2012; Lisman et al., 2008). Evidence of PV interneuron dysfunction in schizophrenia is also supported directly and indirectly from studies in animal models. Direct evidence comes from “circuit-based” models of schizophrenia that find behavioural deficits in mice harbouring genetic deletions specifically in PV interneurons (i.e. *Grin1*$^{\Delta PV}$ mice, but see data in **chapter 2**). In addition, selective mutants where the neuregulin receptor ErbB4 is conditionally deleted from a population of interneurons (most PV and somatostatin positive interneurons) derived from the medial ganglionic eminence display schizophrenia-like

behavioural deficits, as well as associated decreases in GAD-67 and PV expression (del Pino et al., 2013).

Indirect evidence comes from the maternal immune activation (MIA) model of schizophrenia. In this model, pregnant rodents are challenged with polyriboinosinic-polyribocytidilic acid to induce cytokine production mimicking a prenatal infection (Meyer et al., 2005). In MIA rats, there is evidence of reduced expression of GAD-67 in PV positive interneurons of the dorsal hippocampus, as well as behavioural deficits relevant to schizophrenia (Dickerson et al., 2014; Wolff et al., 2011). This indicates that maternal immune challenge, a risk factor for schizophrenia, can induce changes in PV interneurons, similar to those seen in post mortem tissue from schizophrenia patients.

Specific genetic mutants, including cell type specific KOs (such as *Grin1*$^{\Delta PV}$ mice, and ErbB4 conditional KOs), provide a useful means of testing the function of different receptors on a particular cell type. However, having direct control over the activity of a specific cell type is critical when trying to determine the role which that cell type plays in controlling behaviour. There is a clear prediction that reducing PV interneuron output from specific brain regions (i.e. hippocampus and/or DLPFC) will lead to schizophrenia-like behaviours. There are a number of ways in which the importance of PV interneuron function for behaviours relevant to schizophrenia can be, and indeed have been, tested (Cho et al., 2015; Kim et al., 2016; Murray et al., 2011, 2015; Nguyen et al., 2014; Yizhar et al., 2011).

4.1.3 Tools to study neuronal circuits

In recent years, optogenetics has emerged as a powerful technique for enabling direct control over the activity of populations of neurons, via expression of light sensitive opsins and delivery of light to the brain with fibre optic cannula (Bernstein and Boyden,

2011; Boyden et al., 2005). However, the technique does have its limitations, especially when coupling manipulations with behavioural testing. Firstly, delivery of light requires previous surgery and the implantation of a fibre optic cannula (except in cases where neurons in superficial layers of the cortex are being targeted) which is invasive and inevitably leads to tissue damage. In addition, light delivery requires animals to be tethered to a fibre optic cable which can influence behaviours that are sensitive to free movement.

Chemical-genetic tools, such as DREADDS (Armbruster et al., 2007; Rogan and Roth, 2011), also enable specific control over neuronal activity, and have some benefits when compared to optogenetics (see **1.9**). DREADD tools can be used to target a greater number of neurons than is possible with optogenetics. This is because light delivery is not a limiting factor, as systemic injection of CNO will lead to activation of DREADDs throughout the brain. This is particularly useful when trying to target large brain structures such as the hippocampus that would be very difficult to completely target with light. In addition, there is no need for animals to be tethered during behavioural testing, so behaviour will not be influenced/confounded by tethering of animals to optical fibres. Finally, DREADD tools can be useful when prolonged activation or silencing of neurons is desired. The effects of CNO are long lasting (several hours), which is desirable when combined with long-lasting behavioural tests (Alexander et al., 2009). Achieving prolonged activation or inhibition with optogenetics, in contrast, could risk brain warming due to continual light delivery (Stujenske et al., 2015).

When activated by CNO, the DREADD silencer hM4Di leads to cell hyperpolarisation due to the activation of inward rectifying potassium channels, reducing neuronal excitability (Rogan and Roth, 2011). There could also be secondary effects that reduce

neurotransmitter release due to inhibition of Ca^{2+} channels at the synapse (Kätzel et al., 2014; Stachniak et al., 2014). The DREADD silencer hM4Di should therefore be well suited to test the specific hypothesis that reduced output from PV interneurons can induce schizophrenia-like behavioural deficits.

4.1.4 Chapter 4 experimental aims

Chronically blocking the output from PV interneurons, via expression of tetanus light chain toxin, in area CA1 of the dorsal hippocampus induced deficits in SWM (Murray et al., 2011). This highlights the importance of PV interneuron function for SWM performance and would be predicted based on the Lisman/Grace model. However, this technique chronically blocks neurotransmitter release from PV interneurons (Murray et al., 2011). At the time the thesis project started, it was not known if transient inhibition of PV interneurons would produce similar effects (but see discussion regarding Nguyen *et al.*, 2014, published later). In this chapter, hM4Di was used to acutely reduce the excitability of PV interneurons in the dorsal or ventral hippocampus, whilst animals were tested for behaviours relevant to schizophrenia. This enabled direct testing of the Lisman/Grace model in a manner that is likely to be more physiologically relevant than chronically blocking PV interneuron output.

4.2 Methods

4.2.1 Breeding of animals

PV^{cre} mice (as described in **2.2.1** and by Hippenmeyer *et al.*, 2005) were bred and maintained homozygous for *Cre*. All animals were bred and housed at the University of Oxford Biomedical Sciences Building in a temperature and humidity controlled vivarium, with a 12-hour light/dark cycle and with lights on at 07:00. Initially animals were raised in IVC cages, then transferred to open-top cages by 6-12 weeks of age. Cages contained sawdust and enrichment in the form of sizzle nest and a cardboard house and tube. Mice were group housed at all times and only male mice were tested.

4.2.2 Virus constructs

Viruses were all obtained from the Viral Vector Core at the University of North Carolina (UNC-VC) (NC, USA) having been initially created by Bryan Roth. To selectively target PV interneurons, the *Cre*-dependent AAV8-hSyn-DIO-hM4D(Gi)-mCherry and AAV8-hSyn-DIO-mCherry viruses were used, for the experimental and control group respectively. Viruses were injected as delivered from UNC-VC without dilution.

4.2.3 Surgery

The equipment used and initial stage of surgery were as previously described (see **3.2.7**). Craniotomies were made over the injection sites (see **table 4.1** for coordinates), and constructs were injected with a Hamilton syringe (34g needle) held by a digital injector (WPI Instruments, USA) at a rate of 100 nl/min. After injection, the needle was kept in place for 5-10 minutes and then slowly withdrawn to minimise backflow of virus, thereby promoting virus spread through the tissue.

Mice were injected (s.c.) with 0.5 ml sterile saline at the end of the surgery and Metacam (5 mg/kg) was given 24 hrs later (either s.c. or orally by feeding palatable strawberry jelly containing the drug).

Target	AP coordinate(s):	ML coordinate(s):	Z coordinates: (from brain surface)	Injection volume (nL)
Dorsal CA1	-1.7	+/- 1.5	-1.1, -1	200, 200
Ventral CA1	-3.1	+/- 3.5	-3 , -2.7	100, 200
Complete hippocampus	-2.1 -2.8 -3.2	+/- 1.8 +/- 3 +/- 3	-1.3 -2.5, -1.5 -3.5, -2.5	1000 500, 500 500, 500

Table 4.1: Stereotaxic coordinates for virus injection
Stereotaxic coordinates used to target the dorsal CA1, ventral CA1 and complete hippocampus (including CA1, CA3 and DG). All coordinates are relative to bregma. Where there are multiple injection volumes it refers to injections at the first and second Z coordinate respectively.

4.2.4 Immunohistochemistry

To validate expression of hM4Di-mCherry in PV interneurons, PV^{cre} mice injected with DIO-hM4Di-mCherry into dorsal hippocampus were transcardially perfused with PBS followed by 4% paraformaldehyde (PFA) and post fixed for 24 hours in PFA. Immunohistochemistry, probing for PV expression, was then performed as previously described (see **2.2.2**) on sections estimated to be at the virus injection site. PV expression was detected with a fluorescent secondary antibody (Alexa488-coupled goat-anti-mouse, Molecular Probes, USA). Sections were mounted (as previously described) and confocal microscopy (Leica, Germany) was used to determine co-localisation of hM4Di-mCherry (red channel) and PV expression (green channel).

To estimate the number of PV interneurons targeted with hM4Di-mCherry, a subset of slices from dorsal (n = 6) and ventral (n = 5) animals injected with hM4Di-mCherry were processed for immunohistochemistry. Sections estimated to be around the virus

injection site (based on mouse brain atlas coordinates) were stained for PV expression (as previously described) with a DAPI counterstain to label nuclei. After mounting of sections, epi-fluorescent stacks were acquired (Carl Zeiss Zoom Microscope, Germany), centred on the CA1 pyramidal layer in either dorsal or ventral hippocampus. Stacks were imported into ImageJ (NIH) and PV (green channel) and hM4Di-mCherry (red channel) expressing cells were counted using the in-built cell counting software. Cells were counted in all layers of area CA1. The percentage of PV interneurons that were also hM4Di-mCherry-positive was calculated to estimate the efficiency of PV interneuron targeting. Stacks (1 - 6 stacks per animal) were counted from both hemispheres and the average co-expression was calculated per animal. The mean co-expression per animal was then averaged across animals to give an overall group average, estimating the number of PV interneurons targeted with hM4Di-mCherry in the dorsal and ventral CA1. The same count was also performed to calculate the percentage of hM4Di positive neurons that were also PV positive, thus giving an indication of the specificity of the virus transfection.

4.2.5 *In vitro* patch clamp recordings[1]

PV^{cre} mice injected with hM4Di-mCherry (n = 4) or mCherry control virus (n = 2) were deeply anaesthetised with isoflurane and decapitated. The brain was extracted in cutting solution (in mM: Sucrose, 150; Glucose, 15; NaCl, 40; $NaHCO_3$, 25; KCL, 3; NaH_2PO_4, 1.25; $CaCl_2$, 1; $MgSO_4$, 10, with osmolarity between 310.5-315.5 mOsmol/kg) at 30-35^oC and glued to a base plate to enable slicing on a vibratome. Coronal slices (350 μm) were cut and sections containing the hippocampus were transferred to an interface storing chamber containing artificial cerebrospinal fluid

[1] Patch clamp recordings made in collaboration with Pantelis Antonoudiou in animals provided by Alexei Bygrave

(aCSF) (in mM: $CaCl_2.6H_2O$, 2; glucose, 10; $MgS0_4.7H_2O$, 1; KCl, 3.5; NaCl, 126; $NaH_2PO_4.H_2O$; 1.25, with osmolarity between 280-300 mOsmol/kg) at 30-35^oC where they were kept for 1 hour in order to equilibrate or until recordings were made. All solutions were continuously bubbled with carbogen gas (95% O_2 and 5% CO_2) starting 30 minutes before the initiation of the experiment. Whole cell recordings were made from CA1 PV interneurons in current clamp mode (internal solution, in mM: Potassium D-gluconate, 110; HEPES, 40; ATP-Mg, 2; GTP-NaCl, 0.3, NaCl, 4, with osmolality between 270-290 mOsmol/kg). PV interneurons expressing hM4Di-mCherry or mCherry were targeted for recordings guided by red fluorescence (Filtercube, Thor labs, USA). A step protocol with current injections of increasing magnitude was given to assess the electrophysiological properties of the cell before drug application. After completion of the step protocol, CNO (10 μM) was applied and the step protocol was repeated. Data were low-pass filtered at 3 kHz, digitized using the HEKA InstruTECH ITC-18 (Digitimer) and acquired with a 10 kHz sampling rate. All data were acquired and analyzed using the Igor Pro software (Wavemetrics, USA).

4.2.6 Drugs

Clozapine-N-oxide (CNO) was purchased from Tocris (UK) and dissolved in sterile saline at a concentration of 0.5 mg/ml. Aliquots of CNO were stored at -20^oC. For all *in vivo* experiments CNO was given at a dose of 0.5 mg/kg.

4.2.7 Behavioural testing

After surgery animals were given at least 2 weeks to recover and to provide time for expression of hM4Di in PV interneurons. Behavioural testing was performed as described previously (see **2.2**) with the following modifications:

Locomotor testing

Animals were injected (i.p.) with CNO immediately before being transferred to locomotor boxes for 90 minutes of locomotor activity monitoring.

Spatial novelty preference Y-maze

Animals were injected (i.p.) with CNO 30 minutes before the start of testing and kept in separate cages until the test commenced.

Rewarded alternation testing (T-maze)

After habituation of the animals to the maze they were injected (i.p.) with CNO and transferred to an empty cage 30 minutes before the start of each test block. Each block consisted of 10 trials of rewarded alternation with massed trials (inter-trial interval of 45s) and an intra-trial interval of 5s. Thus, all trials of rewarded alternation tested were conducted under the influence of CNO.

The duration of CNO action is estimated to be at around 1 hour (although effects could persist up to 8 hours) and thus all behavioural testing was conducted whilst CNO was still active and whilst the activity of hM4Di-positive neurons should be suppressed (Alexander et al., 2009). All experiments were designed in a between-subjects manner, with animals injected with hM4Di-mCherry or mCherry viruses serving as experimental and control groups respectively. This approach was chosen so that all mice could be injected with CNO. Although CNO is reported to be inert (Alexander et al., 2009), there is always a possibility that it has, as yet unidentified endogenous targets. By having the mCherry control group, any effect of CNO injection alone was taken into account. All virus-injected animals were tested for each of the behavioural tasks above, in the order listed.

4.3 Results

Dysfunction of PV positive interneurons has been proposed to be central to the pathophysiology of schizophrenia. In order to test a causal role of PV interneuron

function in behaviours relevant to schizophrenia, the chemogenetic DREADD silencer hM4Di was expressed selectively in PV interneurons of the dorsal and ventral hippocampus.

4.3.1 Successful targeting of PV neurons with hM4Di

DREADD tools are powerful because they facilitate cell type specific manipulation of neuronal activity. In order to selectively target PV interneurons, the PV^{cre} driver line (see **2.3.1**) was used in combination with an adenovirus carrying the hM4Di-mCherry construct flipped into the incorrect orientation and flanked by two pairs of *loxP* sites (DIO-hM4Di-mCherry). The virus will target all neurons but only in *Cre* positive neurons (i.e. PV interneurons) will the hM4Di-mCherry construct be flipped into the correct, open-reading frame orientation to enable translation of the transgene (**figure 4.1a**).

To validate the targeting of PV interneurons, a PV^{cre} mouse was injected with the DIO-hM4Di-mCherry construct into the dorsal hippocampus. After 2 weeks, to give time for expression of hM4Di-mCherry, the animal was perfused and the brain removed and sliced. Sections were probed for PV expression with an anti-parvalbumin antibody and a green fluorescent conjugated secondary antibody. Confocal microscopy revealed that hM4Di-mCherry expression co-localised with expression of PV at the site of injection (**figure 4.1b**). Thus, adenovirus delivery of the DIO-hM4Di-mCherry construct into PV^{cre} mice can successfully target PV interneurons.

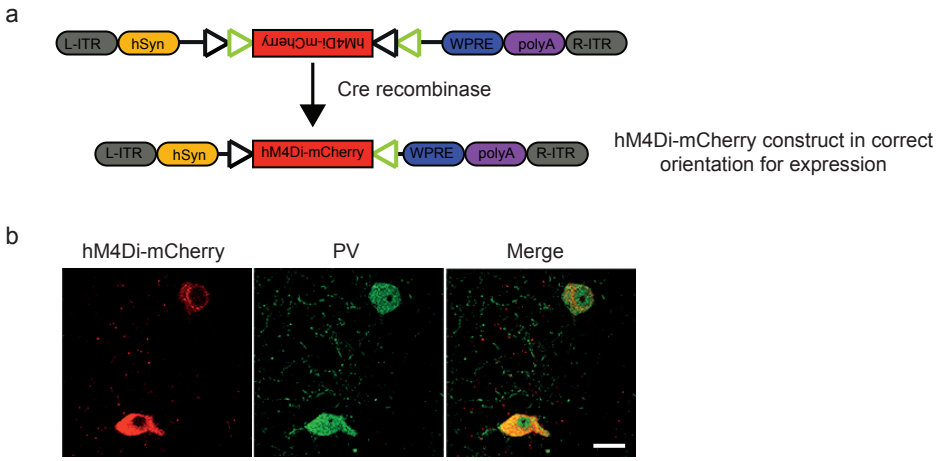

Figure 4.1: Successful targeting of PV neurons with hM4Di
(a) Schematic of the DIO-hM4Di-mCherry construct packaged into the AAV8 viral vector. hSyn indicates the human synapsin promoter fragment, pairs of LoxP sites are illustrated by black and green triangles, WPRE indicates Woodchuck Hepititis Virus Posttranscriptional Regulatory Element, L-ITR and R-ITR indicates left and right inverted terminal repeats respectively. Cre recombinase expression is required to flip the hM4Di-mCherry into the correct orientation for cellular transcription, translation and protein synthesis of hM4Di-mCherry. (b) Confocal image of a PV^{cre} mouse injected with the DIO-hM4Di-mCherry construct. hM4Di-mCherry (red) co-localised with PV expression (green). Scale bar indicates 20 μm.

4.3.2 Expression of hM4Di in dorsal or ventral CA1

PV interneurons in area CA1 of the hippocampus have been shown to be important for SWM in mice (Murray et al., 2011). Murray *et al.* selectively blocked output from PV interneurons of the dorsal CA1, via expression of tetanus toxin light chain, and found impairments on a SWM task but normal performance on a SRM task. To assess the effect of acute silencing of PV interneurons on behaviours relevant to schizophrenia, PV interneurons were targeted with hM4Di in area CA1 of the dorsal or ventral hippocampus. Different stereotaxic injection coordinates were tested in order to preferentially target area CA1 in the dorsal or ventral hippocampus (**optimisation data not shown**).

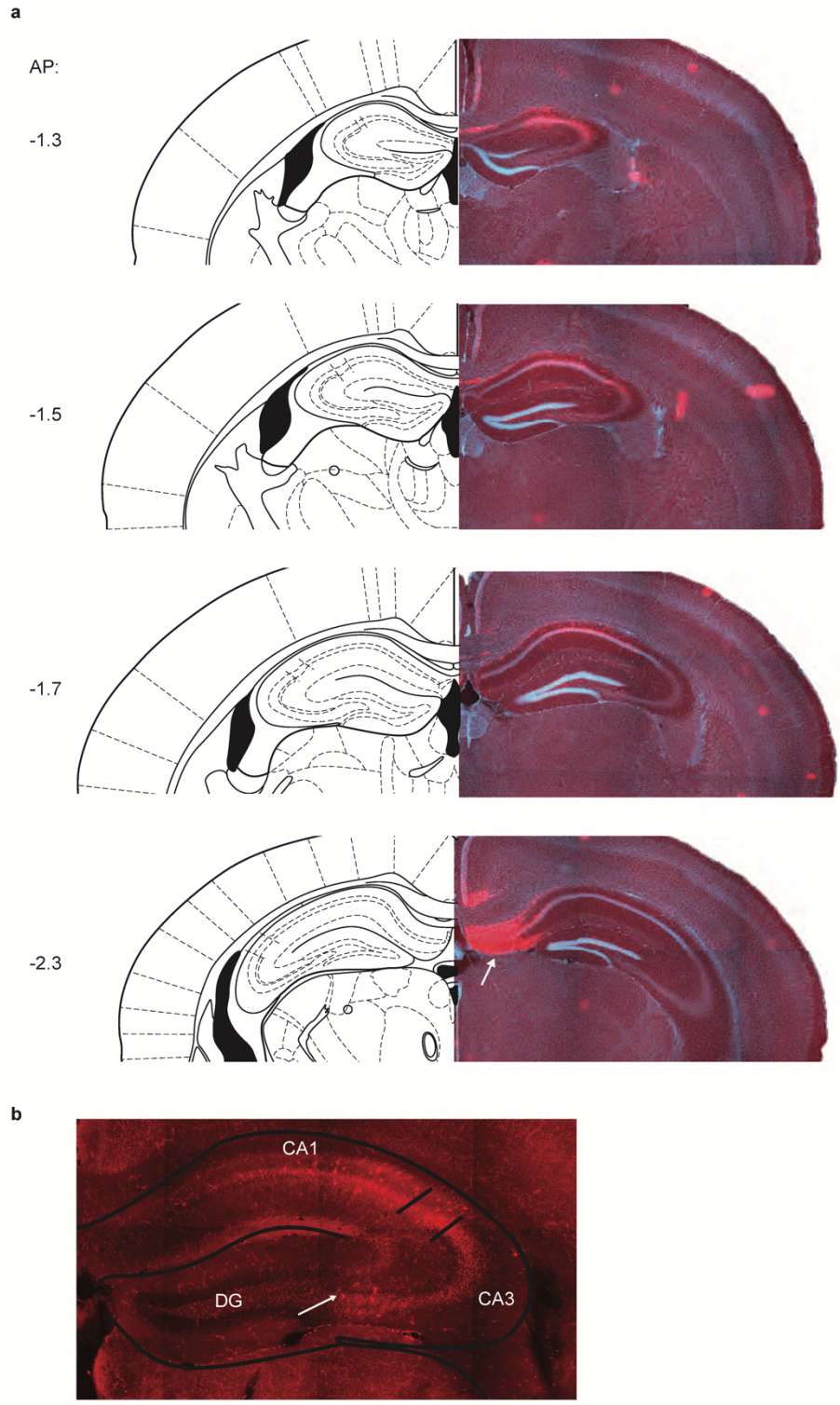

Figure 4.2: Targeting of dorsal hippocampus with hM4Di-mCherry
(a) Coronal sections through the dorsal hippocampus showing expression of hM4Di-mCherry (red) and DAPI nucleus stain (blue) with corresponding reference atlas images (Paxinos, 2001). White arrow indicates expression in the dorsal subiculum. (b) Slice at the site of stereotaxic virus injection with hippocampal subfields indicated. Qualitatively the expression of hM4Di-mCherry (red) was most prominent in area CA1, with some cells labelled in area CA3 (white arrow).

In dorsal hippocampus injected mice, area CA1 was transfected well but there was also some expression of hM4Di-mCherry in area CA3, dorsal subiculum and occasionally the DG (**figure 4.2b**). Interestingly, virus expression was more robust in sections anterior to the injection site (AP – 1.7), compared to posterior sections. Most animals showed expression from AP -1.4 to -2, with expression becoming very weak beyond AP -2 as in the representative example (**figure 4.2a**). Beyond AP -2 there was some expression of hM4Di-mCherry in the dorsal subiculum (**figure 4.2a**, bottom image).

In the ventral hippocampus injected animals, expression of hM4Di-mCherry was largely limited to ventral area CA1, with some sparse expression in area CA3 and DG (**figure 4.3b**). CA1 expression was most prominent between AP -2.8 and -3.6 as in the representative example (**figure 4.3a**).

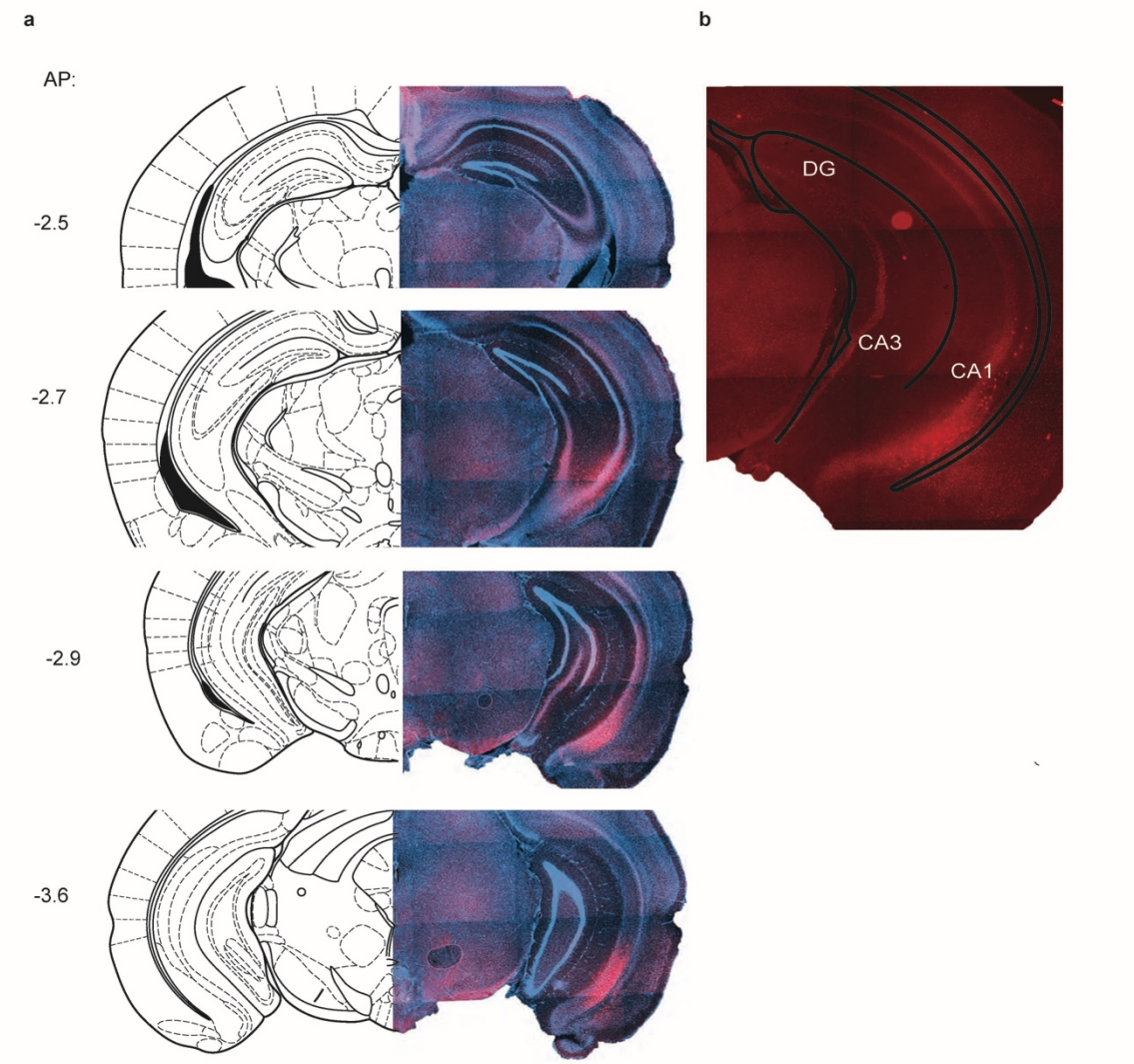

Figure 4.3: Targeting of ventral hippocampus with hM4Di-mCherry
(a) Coronal sections through the ventral hippocampus showing expression of hM4Di-mCherry (red) and DAPI nucleus stain (blue) with corresponding reference atlas images (Paxinos, 2001). (b) Slice at the site of stereotaxic virus injection (AP: -3.1) with hippocampal subfields indicated. Qualitatively the expression of hM4Di-mCherry (red) was most prominent in area CA1 subfield.

4.3.3 Efficient targeting of PV interneurons at the virus injection site

To estimate the efficiency of PV interneuron targeting with the DIO-hM4Di-mCherry construct at the site of injection, dorsal (n = 6) and ventral (n = 5) hippocampus injected mice were perfused and brains removed and sliced. Sections estimated to be at the injection site (AP -1.7 for dorsal and -3 for ventral) were probed for PV expression with

an anti-parvalbumin antibody and a green fluorescent conjugated secondary antibody. Epi-florescence stacks were acquired to detect hM4Di-mCherry (red channel), PV (green channel) and DAPI (blue channel) (**figure 4.4a**). The percentage of PV positive interneurons that were also hM4Di-mCherry positive was calculated in area CA1.

At the injection site in dorsal CA1, 78% (+/- 12%, SD) of PV neurons were also hM4Di-mCherry positive (**figure 4.4b**). At the injection site in ventral CA1 68% (+/- 9%, SD) of PV neurons were also hM4Di-mCherry positive (**figure 4.4b**). Thus, at the injection site a large proportion of PV interneurons are being successfully targeted with hM4Di-mCherry.

The specificity of hM4Di-mCherry expression for PV interneurons was also assessed. At the injection site in dorsal CA1 68% (+/- 8%, SD) of hM4Di-mCherry neurons were also PV positive (**data not shown**). In the ventral CA1 injection site, 65% (+/- 4%, SD) of hM4Di-mCherry positive neurons were also PV positive (**data not shown**). This specificity is lower than expected but likely reflects a failure of the PV immunoreactivity rather than low specificity for PV interneurons using the *Cre* and DIO-*loxP* method. In fact, it is known that levels of PV can fall below levels detectable with immunohistochemistry (Sohal et al., 2009).

It is important to note that expression of hM4Di-mCherry did vary along the AP axis relative to the injection sites (see **figure 4.2** and **figure 4.3** for representative examples) but these changes in expression were not quantitatively assessed. Nevertheless, it is very clear that expression was not complete throughout area CA1 of either the dorsal or ventral hippocampus (see **figure 4.2a** and **figure 4.3a** bottom images).

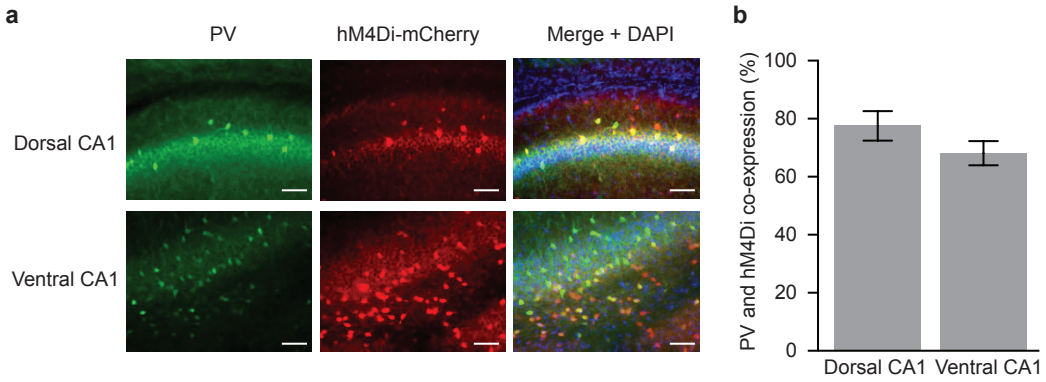

Figure 4.4: Efficient transfection of PV interneurons at the virus injection site
(a) Epi-fluorescence stacks showing expression of PV (green), hM4Di-mCherry (red) and a merged image with DAPI (blue). Scale bar indicates 100μm. (b) Percentage of PV interneurons co-expressing hM4Di-mCherry at the injection site. Bars display the mean. Error bars display S.E.M.

4.3.4 *In vitro* validation of DREADD mediated PV interneuron silencing

Although there is expression of hM4Di-mCherry in PV interneurons, it remains to be seen if the construct can reduce the activity of this cell type in the presence of CNO. To test if the hM4Di-mCherry construct can reduce PV interneuron activity, patch clamp recordings were made *in vitro*. Acute brain slices were taken from PV^{cre} mice injected with DIO-hM4Di-mCherry or a DIO-mCherry control virus. Cells expressing the fluorescent reporter (8 hM4Di-mCherry positive cells from 4 mice, 6 mCherry positive cells from 2 mice) were patched and held in current clamp mode (**figure 4.5a**). A step protocol was then initiated where current steps of increasing magnitude were injected into the cells to induce spiking. Then CNO (10 μM) was applied to the bath solution being perfused over the slices and the step protocol was repeated (see **figure 4.5b** for example current step). The number of spikes initiated by the largest current step was calculated under baseline conditions and again after CNO application. Activation of hM4Di with CNO is expected to lead to hyperpolarisation and would

therefore be expected to reduce the excitability of the neuron. Under control conditions (expression of mCherry alone), CNO is not expected to modulate excitability as the drug is reported to be inert (Armbruster et al., 2007).

The percentage of baseline (pre-CNO) firing was calculated for hM4Di-mCherry and mCherry positive cells with the largest current step (same size current step for pre- and post-CNO) following CNO addition to the bath solution (**figure 4.5c**). An ANOVA of this percentage change with virus as a between subject factor (hM4Di-mCherry or mCherry) revealed that the firing rate of hM4Di-mCherry positive neurons was significantly reduced after CNO addition (effect of virus: $F(1,12) = 14.523$, $P = 0.002$; statistics calculated on cells not animals). Thus, hM4Di-mCherry is able to significantly reduce the excitability of PV interneurons in the hippocampus.

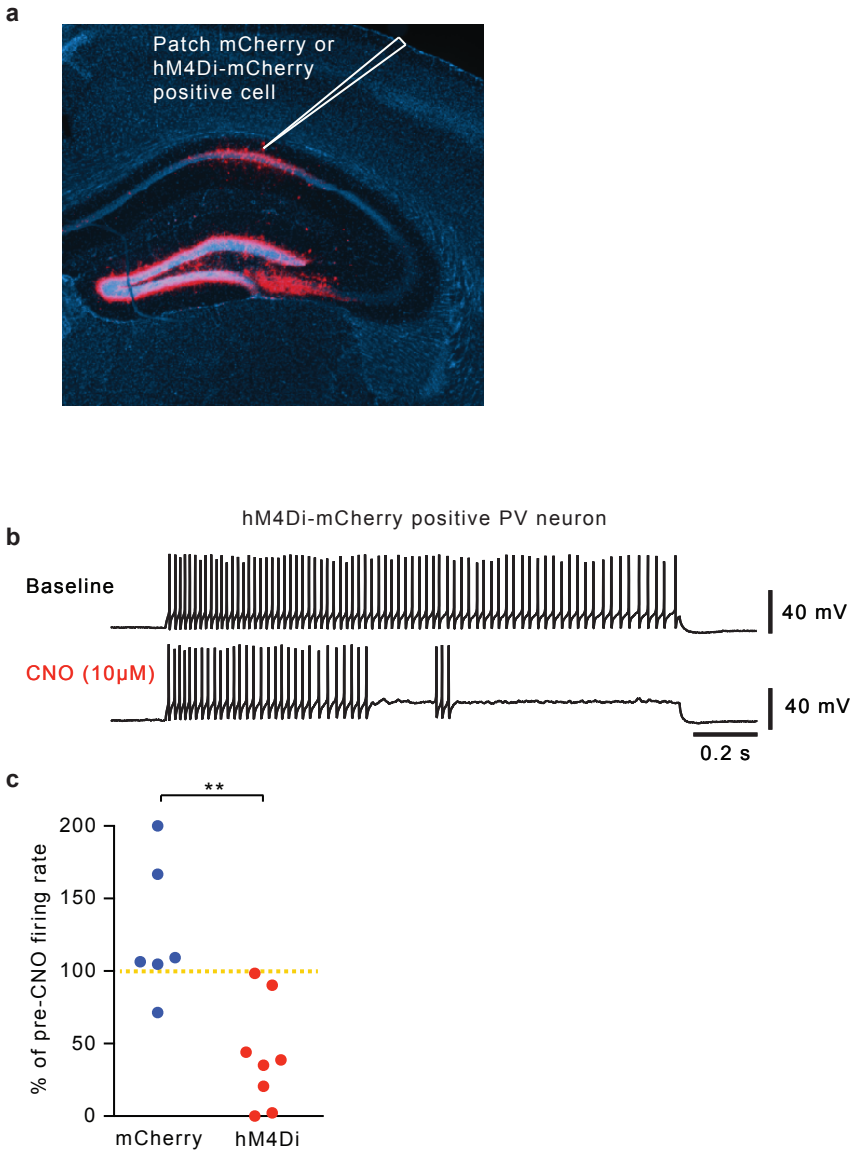

Figure 4.5: hM4Di can reduce excitability of PV interneurons *in vitro*
(a) hM4Di-mCherry and mCherry positive PV interneurons were patched in acute hippocampal slices and held in current clamp mode. (b) Example trace of a hM4Di-mCherry positive PV interneuron with the same current injection under baseline conditions and following application of CNO (10μM). (c) The percentage of baseline (pre-CNO) firing rate was calculated following addition of CNO. Each dot represents one cell recorded from mCherry (blue) or hM4Di-mCherry (red) positive PV interneurons. Yellow dashed line indicates 100% of baseline (i.e. no change). ** indicates a significant effect of virus ($P < 0.01$).

4.3.5 Silencing of PV interneurons in dorsal and ventral hippocampus does not induce hyperactivity

PV interneurons are thought to be involved in the pathophysiology of schizophrenia, with reduced PV interneuron output central to the Lisman/Grace model (Lisman et al., 2008). As PV interneurons provide powerful perisomatic inhibition to pyramidal neurons they are well placed to regulate output from pyramidal neurons. Therefore, a state of disinhibition could be initiated following PV silencing with hM4Di. Disinhibition within the hippocampus could lead to enhanced glutamatergic output from the subiculum, driving a hyperdopaminergic state via a tri-synaptic loop (Floresco et al., 2001; but see also Lou et al., 2011) that could promote hyperactivity.

To test this hypothesis, two cohorts of PV^{cre} mice were injected with hM4Di-mCherry or mCherry control virus into dorsal (12 hM4Di-mCherry, and 9 mCherry) or ventral (9 hM4Di-mCherry, and 6 mCherry) hippocampus (preferentially targeting area CA1). Animals were then tested for locomotor activity in a novel environment following CNO injection (**figure 4.6a,b**). As the dorsal and ventral cohorts were run at different times, data were analysed separately for each cohort.

In the 90 minutes following CNO injection, a repeated measures ANOVA with virus as a between subject factor and time bin as a repeated measure (5 minute bins) revealed no effect of virus on the number of beam breaks in either the dorsal or ventral cohorts (effect of virus; dorsal: $F(1,19) = 0.230$, $P = 0.637$; ventral: $F(1,13)= 0.490$, $P = 0.496$). In both the dorsal and ventral hippocampus cohorts the locomotor activity decreased over time (effect of time bin; dorsal: $F(17,323) = 81.450$, $P = 0.001$; ventral: $F(17,221) = 27.506$, $P = 0.001$). In addition, there was no virus*time bin interaction in either group, indicating the decrease in locomotor activity was the same over time with PV interneuron silencing in both cohorts (effect of virus*time bin interaction; dorsal: F(17,

323) = 0.796, P = 0.697; ventral F(17,221) = 0.951, P = 0.515). These data show that reducing excitability of a population of PV interneurons in the dorsal and ventral hippocampus does not increase novelty-induced hyperactivity.

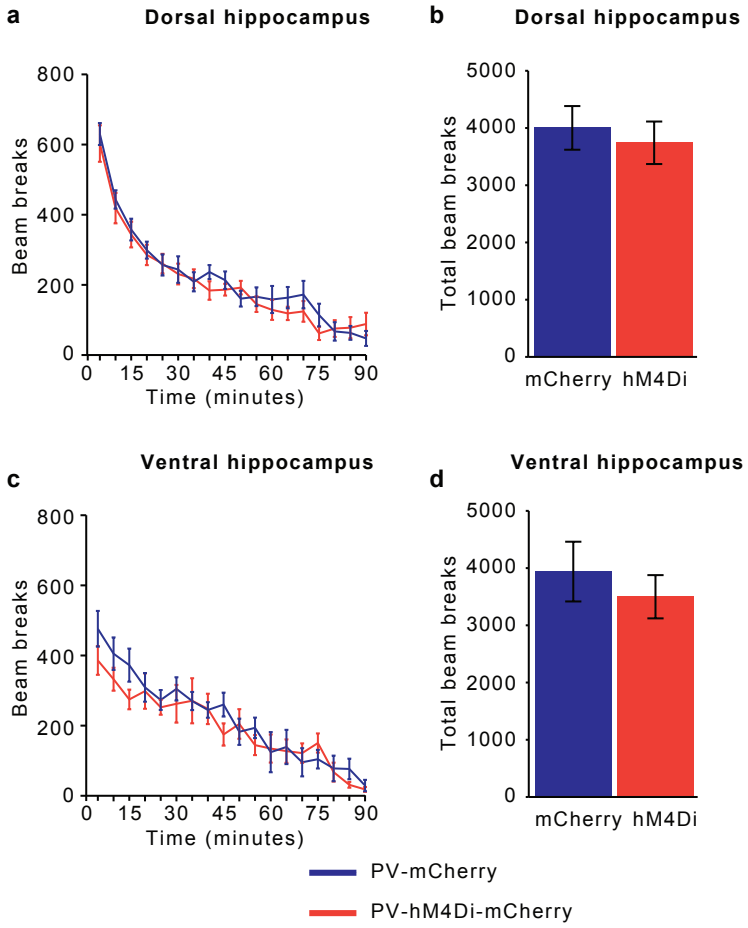

Figure 4.6: Silencing of PV interneurons in dorsal and ventral hippocampus does not induce hyperactivity
PV^{cre} mice expressing mCherry (blue) or mM4Di-mCherry (red) in the dorsal (a,b) or ventral (c,d) hippocampus were injected with CNO (5mg/kg) and locomotor activity in a novel environment was measured for 90 minutes. (a,c) Beam breaks displayed in 5 minute time bins. Lines display the mean and error bars show S.E.M. (b,d) Total beam breaks in the 90 minutes post CNO injection. Bars display the mean and error bars show S.E.M.

4.3.6 Silencing of PV interneurons in dorsal and ventral hippocampus does not impair spatial novelty preference

Manipulations of PV interneurons have been shown to induce short term spatial memory impairments that could reflect deficits in spatial working memory (Fuchs et al., 2007; Korotkova et al., 2010; Murray et al., 2011). To test short term spatial memory, spatial novelty preference was assessed in mice expressing hM4Di-mCherry or mCherry in PV positive interneurons in the dorsal (12 hM4Di-mCherry, and 14 mCherry) or ventral (9 hM4Di-mCherry, and 6 mCherry) hippocampus (preferentially targeting area CA1) 30 minutes after injection of CNO.

During the sample phase, animals were given 5 minutes to explore two of the three Y-maze arms (start and familiar arm). After an intra-trial interval of 1 minute, animals were then given a free choice of all three Y-maze arms (start, familiar and novel) and tested for spatial novelty preference.

Similar levels of exploration were observed in hM4Di-mCherry and mCherry injected animals during the sample phase, as measured by the time spent within the familiar arm and by the total distance travelled in the familiar and start arm in the sample phase. During the sample phase, an ANOVA with virus as a between subject factor revealed no difference in the time hM4Di-mCherry and mCherry injected mice spent exploring the familiar arm in dorsal and ventral cohorts (effect of virus; dorsal: $F(1,24) = 2.223$, $P = 0.149$; ventral: $F(1,13)= 0.097$, $P = 0.760$; **figure 4.7a,d**). Analysis also revealed no difference in the total distance travelled by hM4Di-mCherry and mCherry injected mice during the sample phase, indicating similar levels of exploration between groups (effect of virus; dorsal: $F(1,24) = 0.168$, $P = 0.685$; ventral: $F(1,13)= 0.847$, $P = 0.374$; **figure 4.7b,e**).

Silencing of PV interneurons in the dorsal or ventral hippocampus did not impair the expression of short term spatial memory as all groups showed a preference for the novel vs. familiar arm in the test phase. During the test phase, an ANOVA with virus as a between subject factor revealed that there was no significant difference between the preference of hM4Di-mCherry or mCherry-injected mice for the novel arm on the Y-maze (effect of virus; dorsal: $F(1,24) = 0.100$, $P = 0.755$; ventral: $F(1,13)= 1.103$, $P = 0.313$; **figure 4.7c,f**). One-sample T-tests against chance performance (novelty preference ratio of 0.5) revealed that both hM4Di-mCherry and mCherry-injected controls displayed novelty preference ratios significantly above chance level performance in dorsal (mCherry: $t(1,13) = 2.895$, $P = 0.013$; hM4Di-mCherry: $t(1,11) = 2.402$, $P = 0.035$) and ventral (mCherry: $t(1,5) = 2.787$, $P = 0.039$; hM4Di-mCherry: $t(1,8) = 3.993$, $P = 0.004$) hippocampus cohorts. These data indicate that short term spatial novelty preference is not impaired with hM4Di-mediated silencing of a population of PV interneurons in dorsal or ventral hippocampus.

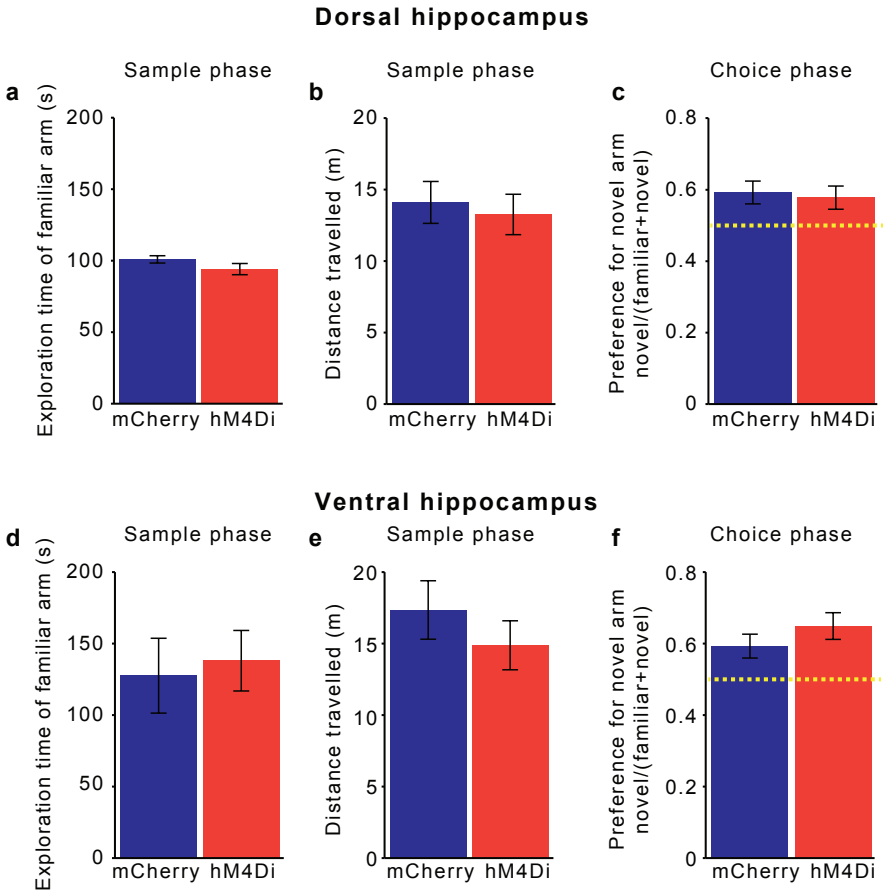

Figure 4.7: Silencing of PV interneurons in dorsal or ventral hippocampus does not impair spatial novelty preference
PV^{cre} mice injected with mCherry (blue) or hM4Di-mCherry (red) into dorsal (a-c) or ventral (d-f) hippocampus were tested for spatial novelty preference on the Y-maze following injection of CNO (5 mg/kg). Time spent investigating the familiar arm (a,d) and the total distance travelled (b,e) during the sample phase. In the choice phase mice were given access to all arms of the Y-maze and the preference ratio for the novel arm was calculated (novel arm time / (novel arm time + familiar arm time)) (c,f). All bars display the mean and error bars display S.E.M. The yellow dashed lines in (c,f) indicate chance level performance.

4.3.7 Silencing of PV interneurons in dorsal or ventral hippocampus does not impair spatial working memory

SWM is thought to require PV interneurons, as manipulations to reduce glutamatergic input to PV interneurons lead to impaired rewarded alternation performance (Fuchs et

al., 2007; Korotkova et al., 2010). In addition, manipulations that chronically block neurotransmitter release from PV interneurons in dorsal CA1 also lead to deficits in SWM tasks (Murray et al., 2011).

PV^{cre} mice were injected with hM4Di-mCherry or mCherry control virus to test if silencing of PV interneurons in the dorsal (12 hM4Di-mCherry, and 9 mCherry) or ventral (9 hM4Di-mCherry, and 6 mCherry) hippocampus (preferentially targeting area CA1) impairs rewarded alternation on the T-maze to assess SWM. CNO was injected 30 minutes before the start of each 10 trial training block to test if hM4Di-mediated PV interneuron silencing impaired rewarded alternation performance. The dorsal hippocampus cohort was given 4 blocks of 10 trials and the ventral hippocampus cohort 6 blocks of 10 trials.

Silencing of PV interneurons in the dorsal or the ventral hippocampus did not impair spatial working memory performance (**figure 4.8a,b**). In the dorsal hippocampus cohort, a repeated measures ANOVA with virus as a between subject factor and training block as a within subject repeated measure revealed no significant effect of virus on task performance ($F(1,19) = 0.297$, $P = 0.592$). There was significant learning over the 4 training blocks and this did not differ between hM4Di-mCherry and mCherry injected animals (effect of training block: $F(3,57) = 5.211$, $P = 0.003$; virus*training block interaction: $F(3,57) = 0.450$, $P = 0.718$).

In the ventral hippocampus cohort, similar analysis revealed no significant effect of virus on task performance (effect of virus: $F(1,13) = 0.235$, $P = 0.636$). There was significant learning over the 6 training blocks (effect of training block: $F(5,65) = 7.818$, $P = 0.001$). The analysis also revealed a significant virus*training block interaction (virus*training block interaction: $F(5,65) = 2.558$, $P = 0.036$), where it appears that mCherry injected animals displayed poorer performance on block 3 and 4 compared

to hM4Di-mCherry injected animals. Although pairwise comparisons (LSD) revealed there was no significant difference between hM4Di-mCherry and mCherry injected animals on either day 3 or 4 (day 3 hM4Di-mCherry vs. mCherry: $F(1,13) = 2.310$, $P = 0.152$; day 4 hM4Di-mCherry vs. mCherry: $F(1,13) = 3.628$, $P = 0.079$). It seems unlikely that silencing of PV interneurons in the ventral hippocampus is facilitating the rate of learning, as on the 5th training day the performance of mCherry injected animals is above that of the hM4Di-mCherry group (pairwise comparisons (LSD) on day 5 hM4Di-mCherry vs. mCherry: $F(1,13) = 4.895$, $P = 0.045$) and on the 6th training day performance of both groups was equivalent. Therefore, the significant virus*genotype interaction observed likely reflects random fluctuations in behavioural performance with controls performing slightly worse on training blocks 3 and 4 and slightly better on training day 5.

One-sample T-tests of average performance (collapsed across all training blocks) against chance performance of 50% revealed that both hM4Di-mCherry and mCherry injected controls performed significantly above chance in both dorsal (mCherry: $t(1,8) = 5.091$, $P = 0.001$; hM4Di-mCherry: $t(1,11) = 4.959$, $P = 0.001$) and ventral (mCherry: $t(1,5) = 7.334$, $P = 0.001$; hM4Di-mCherry: $t(1,8) = 6.156$, $P = 0.001$) hippocampus cohorts. Together, these data show that hM4Di-mediated silencing of a population of PV neurons in the dorsal or ventral hippocampus (largely CA1 subfield specific) does not impair spatial working memory.

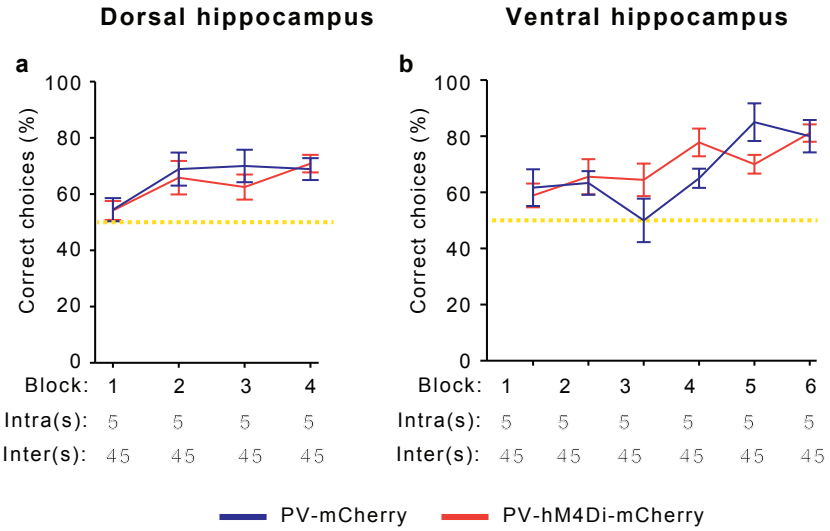

Figure 4.8: Silencing of PV interneurons in the dorsal or ventral hippocampus does not impair spatial working memory
PV^{cre} mice injected with mCherry (blue) or hM4Di-mCherry (red) into dorsal (a) or ventral (b) hippocampus were tested for spatial working memory on the T-maze following injection of CNO (5mg/kg). For each training block mice received 10 trials of rewarded alternation and the % of correct choices were calculated. Lines display mean performance and error bars show S.E.M.

4.3.8 Silencing PV interneurons throughout the hippocampus can induce seizures

The results above indicate that hM4Di-mediated PV interneuron silencing in either dorsal or ventral hippocampus alone does not induce hyperactivity or impair short-term spatial memory. It is possible that too few PV interneurons were successfully targeted with hM4Di to induce behavioural deficits on the tasks used. Alternatively, hM4Di might not work *in vivo* despite reducing excitability of PV interneurons *in vitro* (see **figure 4.5**). To address the former possibility, two PV^{cre} mice were injected with larger volumes of virus (DIO-hM4Di-mCherry) at multiple injection sites in both dorsal and ventral subregions to target the entire hippocampus (as part of a pilot study). Expression of hM4Di was no longer limited to area CA1 and was present throughout the hippocampus (**figure 4.9**).

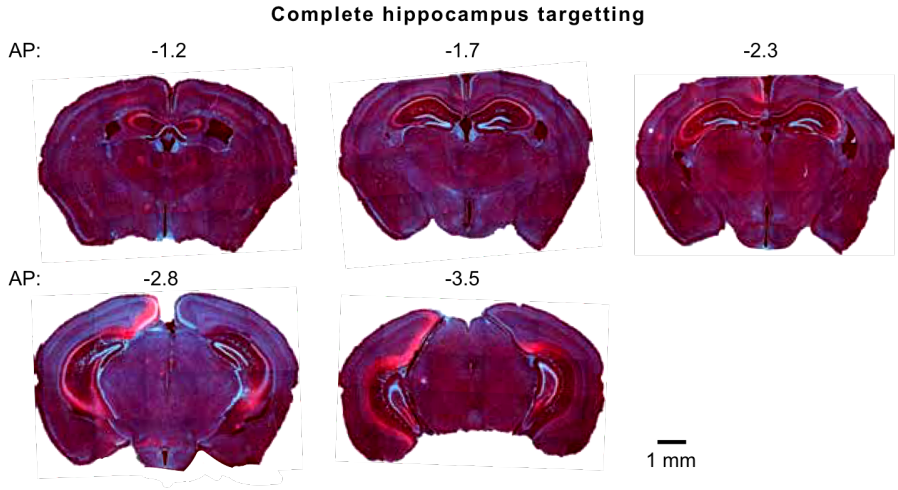

Figure 4.9: Expression of hM4Di-mCherry in PV interneurons throughout the hippocampus
Example epifluorescence scans of a PV^{cre} animal expressing hM4Di (red) throughout the hippocampus and stained for DAPI (blue). Estimates of the anterior/posterior (AP) position are shown (relative to bregma). Scale bar indicates 1mm.

Before perfusion and histological validation of expression of hM4Di-mCherry, the two animals were injected with CNO (5 mg/kg) in their home cage. After 20 minutes one animal displayed seizure like behaviour with head weaving and jumping in the cage. This required immediate termination of the experiment and euthanasia of the animal to comply with Home Office regulations stipulated by the project license. Observation of this chemogenetic-induced seizure prevented follow up studies for ethical reasons. However, this clearly demonstrates that hM4Di is functional *in vivo*.

4.4 Discussion

In this study two populations of PV interneurons, largely restricted to either the dorsal or ventral CA1 respectively, were acutely silenced *in vivo*, whilst mice were behaviourally tested. Validation of the DREADD tools used and the effect (or lack thereof) on behaviour will be discussed. Whilst experiments in this chapter were being conducted, a study was published that also expressed hM4Di in PV interneurons of the ventral hippocampus, although not preferentially in area CA1 (Nguyen et al., 2014). They found that hM4Di-mediated silencing of the ventral hippocampus did indeed cause behavioural deficits relevant to schizophrenia (Nguyen et al., 2014). Results from this paper will be discussed and compared to the results presented in this chapter. Area CA1 was targeted based on evidence that PV interneurons in this region are required for SWM (Murray et al., 2011) and because hyper metabolism in area CA1 is observed in at-risk patients of schizophrenia (Schobel et al., 2013). Following ischemia, area CA1 is more vulnerable to damage compared to other hippocampal subfields (Schmidt-Kastner, 2015). It is possible that changes in area CA1 in schizophrenia (i.e. hyper metabolism) result from “hypoxia-like metabolic stress” since a number of schizophrenia-risk genes appear to be associated with the ischemia-hypoxia response (Schmidt-Kastner, 2015).

4.4.1 hM4Di is able to reduce the excitability of PV interneurons *in vitro*

DREADD mediated neuronal manipulations differ from optogenetic techniques because they require expression of endogenous ion channels (i.e. inward rectifying K^+ channels) to exert their effect. For example, hM4Di activation initiates a G-protein coupled receptor signalling cascade that causes neuronal hyperpolarisation as a result of activation of inward rectifying potassium channels (Rogan and Roth, 2011). But this

requires the endogenous expression of inward rectifying potassium channels in the target neuron for the effects of hM4Di activation to be initiated. Because levels of these endogenous channels will undoubtedly vary between different neuron cell types, it is essential that the effectiveness of hM4Di is assessed in each neuronal cell type being targeted.

In the present study, patch clamp recordings from mice expressing hM4Di in PV interneurons revealed that hM4Di could significantly reduce the excitability of PV interneurons *in vitro*, in agreement with two previous studies that show hM4Di can effectively be used in PV interneurons to alter behaviour (Nguyen et al., 2014; Perova et al., 2015). These effects were seen when CNO was applied to the bath at a concentration of 10 μM, based on the study by Perova *et al.*, but it should be noted that this is a dose 10 fold higher than used by Nguyen *et al.* (Nguyen et al., 2014; Perova et al., 2015). It remains possible that less robust effects would have been seen in this study if a lower dose of CNO was used for the patch clamp recordings. It is also difficult to extrapolate the dose of drug applied *in vitro* to the amount of drug that will end up in the brain after systemic injection *in vivo*.

The effects of DREADD mediated neuronal “silencing” are largely attributed to hyperpolarisation of the neurons following activation of inward rectifying potassium channels. But another mechanism may exist whereby neurotransmitter release is blocked via inhibition of Ca^{2+} channels at the synapse (Kätzel et al., 2014; Stachniak et al., 2014). This secondary effect would not have been detectable in the present *in vitro* experiments, as only the direct excitability of the PV interneuron was assessed. Stachniak *et al.* clearly demonstrate that the mild hyperpolarising effects of hM4Di were unable to block action potential generation but that the synaptic silencing by hM4Di could block neurotransmitter release in hM4Di-expressing pyramidal neurons

(Stachniak et al., 2014). To test the effects of hM4Di on PV interneurons more thoroughly it would be interesting to patch neighbouring pyramidal neurons and measure mini inhibitory post synaptic potentials (mIPSPs) under baseline conditions and after the application of CNO. If there is a reduction in neurotransmitter release from PV interneurons after CNO application, then there should correspondingly be fewer mIPSPs in neighbouring pyramidal neurons.

Thus, the precise effects of hM4Di expression in PV interneurons *in vivo* are still unknown and could easily be overestimated (if the effective CNO dose used in the behavioural studies is not comparable to that used *in vitro*), or underestimated (if the effect on neurotransmitter release is as robust in PV interneurons as it is in pyramidal neurons). *In vivo* electrophysiological recordings are required to fully understand the effects of hM4Di on PV interneurons and the surrounding network.

4.4.2 hM4Di-mediated PV interneuron silencing in dorsal or ventral CA1 does not induce hyperactivity

Reduction of PV interneuron output could lead to disinhibition of the hippocampus, and therefore increased glutamatergic output from the subiculum. This could drive a hyper-dopaminergic state via a tri-synaptic loop (Floresco et al., 2001; but see also Lou et al., 2011). However, in this study there was no effect on novelty-induced hyperactivity following CNO injection in mice expressing hM4Di in PV interneurons in the dorsal or ventral hippocampus (preferentially targeting area CA1). This is in line with observations by Nguyen *et al.*, who found no effect of PV interneuron inhibition in the ventral hippocampus alone (Nguyen et al., 2014). Interestingly, Nguyen *et al.*, did induce hyperactivity when targeting all inhibitory interneurons that express GAD-65, suggesting that inhibition of a larger population of interneurons can induce a state of hippocampal disinhibition that can drive hyperlocomotor activity (Nguyen et al., 2014).

It is perhaps surprising that silencing of such a large population of inhibitory neurons does not induce seizures given the results of the pilot study reported in this chapter but none are reported by Nguyen *et al*. (Nguyen et al., 2014).

It is possible that hyperactivity was not observed as the test environment was novel and potentially promotes locomotor activity to such an extent that there is a ceiling effect capable of obscuring subtle hM4Di-induced enhancement of locomotor activity. However, this seems unlikely as the activity decreases during the 90 minutes in which animals were tested (hM4Di silencing should persist for at least 2 hours post CNO injection), providing a large window in which to observe effects on hyperactivity.

4.4.3 hM4Di-mediated PV interneuron silencing in dorsal or ventral CA1 does not induce cognitive deficits

In this study, spatial short term memory was tested with the Y-maze spatial novelty preference task and SWM was tested with rewarded alternation on the T-maze. Normal performance was observed in animals expressing hM4Di in PV interneurons in either the dorsal and ventral hippocampus (preferentially targeted to area CA1) in both tests. Unimpaired SWM memory following PV interneuron silencing is at odds with previous studies that found deficits in spatial working memory following PV interneuron manipulations (Murray et al., 2011; Nguyen et al., 2014). There are a number of possible explanations for these discrepancies.

The behavioural paradigms used to assess SWM were different between studies. In the present study, rewarded alternation was used as a test of SWM. This task is very well established and is known to be acutely sensitive to hippocampal lesions in rodents (Deacon and Rawlins, 2006). Nguyen *et al.* also assessed SWM on the T-maze but with a continuous variation of the task (Gerlai, 1998). In the continuous T-maze task mice are not rewarded on the maze, so the natural tendency to alternate is assessed.

Initially, animals are forced into one of the goal arms. Then, after the animal returns to the start arm it is given free choice of both the arms. After the choice is made the animal is guided back to the start arm and then given another free choice of both goal arms. The process is then repeated, with alternation between consecutive choices considered to be correct. This version has also been shown to be sensitive to hippocampal damage (Gerlai, 1998), and it is possible that continuous alternation is more sensitive to hippocampal dysfunction than rewarded alternation. Thus, it is possible that PV interneuron manipulations in the present study would have been uncovered if tested on the continuous alternation version of the T-maze. Nevertheless, this seems unlikely.

Murray *et al.* tested SWM with a water Y-maze test where animals needed to "match to place" in order to find a hidden escape platform (Murray et al., 2011). Firstly, animals were given a "free swim/extinction" trial where they were exposed to the start arm and one of the goal arms that did not contain the escape platform. Then after a brief intra-trial interval, animals were returned to the maze for a "sample trial" where they were given access to the start arm and one of the goal arms this time containing an escape platform. Finally, after another brief intra-trial interval, animals were returned to the start arm for the "match trial" where they had to return to the same goal arm position as in the "sample" trial to find the escape platform. This task is very different to rewarded alternation on the T-maze as it is aversive and based on an animals drive to escape from an unpleasant/distressing environment. In addition, with rewarded alternation, animals are trained to "not match to place" (win-shift) which could involve different psychological processes and neuronal circuits than those required to solve "match to place"(win-stay) tasks (Sanderson and Bannerman, 2012). It is therefore hard to compare results in the present study with the those by Murray *et al.* It is

possible that the manipulation used by Murray *et al.*, would not impair SWM if assessed in an appetitive task such as rewarded alternation on the T-maze.

Furthermore, Murray *et al.*, they also used a different PV^{cre} line (Fuchs et al., 2007), that has been less widely used than the PV^{cre} line used here (Hippenmeyer et al., 2005), and also seems to target a small population of somatostatin and parvalbumin double-positive interneurons (Murray et al., 2011; Nassar et al., 2015). Differences could therefore arise from subtly different neuronal populations being targeted with the two different PV^{cre} driver lines. Korotkova *et al.,* used the same PV^{cre} line as Murray *et al.* to generate *Grin1*$^{\Delta PV}$ mice, which have a vastly different behavioural phenotype to *Grin1*$^{\Delta PV}$ mice when the same Grin1-2lox mice were crossed with a different PV^{cre} line (see **2.3.11**). This indicates that there could be important differences between the *Cre* lines used in those studies (Korotkova et al., 2010; Murray et al., 2015) and the one used here. However, this does not explain the discrepancies with the study by Nguyen *et al.*, who used the same PV^{cre} driver line (Hippenmeyer et al., 2005) as used in the present study.

Murray *et al.* used expression of tetanus toxin light chain to completely and chronically block output from PV interneurons, permanently removing PV interneurons from the circuit (Murray et al., 2011). This manipulation will likely have a much greater effect than the transient, and probably weaker, effects of hM4Di in PV interneurons. Although, again this does not account for the differences with the study by Nguyen *et al.*, who also used hM4Di to inhibit PV interneurons. Finally, the absolute number of PV interneurons targeted could explain the lack of a behavioural phenotype in the present study (see below for comparison).

4.4.4 Targeting of PV interneurons in the dorsal and ventral hippocampus cohorts

In this study hM4Di was expressed selectively in PV interneurons in the dorsal or ventral hippocampus. In addition to the cell type specificity, the aim was to selectively target the CA1 hippocampal subfield. At the injection site in area CA1 around 78 and 68% of PV interneurons were targeted with hM4Di in the dorsal and ventral hippocampus respectively. The spread around the injection site in the anterior/posterior axis, or to the other hippocampal subfields was not quantitatively assessed, but, as expected, qualitatively expression of hM4Di-mCherry looked to decrease with distance from the injection site. The percentage of PV interneurons targeted is therefore likely to be less than the numbers reported by Nguyen *et al.*, who transfected 80% of PV interneurons in the ventral CA1 with hM4Di (Nguyen et al., 2014) and Murray *et al.*, who targeted, on average, 84% of PV interneurons in the dorsal CA1, and excluded behavioural data from mice that expressed tetanus toxin light chain in less than 75% of PV interneurons in the dorsal CA1 (Murray et al., 2011). Nguyen *et al.* also did not restrict expression of hM4Di to the CA1 subfield, and also targeted CA3. It therefore remains possible that the lack of behavioural deficits seen here arises as a result of incomplete targeting of PV interneurons within the hippocampus.

When PV interneurons were silenced throughout the hippocampus, in an attempt to target a greater proportion of hippocampal PV interneurons, a seizure in one (of two CNO injected mice) animals was induced. This showed that hM4Di mediated PV interneuron silencing can induce profound effects but posed ethical and scientific constraints on future work. It might be possible to titrate a level of transfection of PV interneurons in the hippocampus that leads to behavioural deficits without causing

seizures. Nevertheless, the ability of hM4Di to induce a seizure when expressed in PV interneurons throughout the hippocampus helps when interpreting the negative behavioural results with more limited targeting of PV interneurons largely restricted to the dorsal or ventral CA1. The induction of a seizure provides direct evidence that hM4Di is functional *in vivo* at the doses used here.

4.4.5 Do PV interneurons outside of the hippocampus contribute to schizophrenia like behavioural deficits?

Manipulations of PV interneurons in the medial prefrontal cortex were recently found to impair SWM (Murray et al., 2015). By expressing tetanus toxin light chain in PV interneurons, Murray *et al.* found that blocking PV interneuron output in the medial prefrontal cortex induced deficits in working memory and reversal learning (Murray et al., 2015). In another study, PV interneurons in the medial prefrontal cortex have been reported to play an important role in the control of attention (Kim et al., 2016). Kim *et al.* used the three-choice serial reaction time task (a variation of the five choice serial reaction time task) to test attentional processing in mice. In this task mice have to attend to a set of nose poke holes that contain lights. On each trial a light will come on in one of the nose poke holes and the mouse has to respond by nose-poking into that same hole to obtain a food reward. Kim *et al.* found that optogenetic silencing of PV interneurons could dramatically increase the number of errors made during the three choice task (Kim et al., 2016). Although, it is worth pointing out that the study did lack controls to account for the effect of light delivery alone, which could distract animals and account for some of the observed effects (Kim et al., 2016). In future studies it would therefore be interesting to assess the effects of hM4Di-silencing of PV interneurons in the mPFC, as regions other than the hippocampus are also likely to

be important in generating schizophrenia symptoms, particularly as there is evidence of PV interneuron dysfunction in the DLPFC in schizophrenia (Lewis et al., 2005).

4.4.6 Conclusions

These results confirm that hM4Di can be used to manipulate the activity of PV interneurons. However, PV silencing in a subpopulation of area CA1 PV interneurons in this study did not induce deficits in SWM as might have been expected. Because of differences in the number of PV interneurons targeted, the subfield specificity, and the behavioural tasks used to assess spatial working memory, it is hard to reconcile the results in this study with those in previously published studies (Murray et al., 2011; Nguyen et al., 2014).

It remains possible that PV interneurons in area CA1 are required for spatial working memory. For example, PV interneurons that were not transfected with hM4Di might be able to effectively compensate for the silenced PV neurons. In the future it would be interesting to test if more extensive area CA1 targeting along the AP axis of the hippocampus is able to produce deficits in SWM or induce novelty induced hyperactivity provided this increased expression did not result in an increased propensity for seizures.

5 Rescue of behavioural and physiological abnormalities in *Gria1* KO mice with GluA1 re-introduction to area CA3

5.1 Introduction

5.1.1 Role of *Gria1* for plasticity

AMPARs mediate the majority of excitatory neurotransmission in the brain. The dynamic trafficking of AMPARs can modulate synaptic transmission and is required for processes such as long term potentiation (LTP), which is thought to be a molecular correlate of memory (Huganir and Nicoll, 2013). The role of the GluA1 subunit, encoded by the *GRIA1* gene, for the induction of LTP has been particularly well studied (see **1.5.10**).

5.1.2 *Gria1* and schizophrenia

The GluA1 AMPAR subunit has been linked to schizophrenia in the largest GWAS study to date that compared control and schizophrenia patients (Ripke et al., 2013, 2014). As yet, it is not known if this single nucleotide polymorphism (SNP) upstream of the *GRIA1* gene locus leads to biologically meaningful changes in *GRIA1* expression. However, the GWAS by Ripke *et al.* complements previous research in which post- mortem decreases in GluA1 mRNA (Eastwood et al., 1995), and GluA1 protein (Eastwood et al., 1997), have been observed in the hippocampus of schizophrenia patients. Thus, there are indications that GluA1 levels (along with a number of other plasticity related genes) could be altered in schizophrenia (Barkus et al., 2012, 2014; Fitzgerald et al., 2010; Wiedholz et al., 2008).

5.1.3 Synaptic plasticity and behaviour of *Gria1* KO mice

Subunit selective drugs are not currently available for AMPARs, so to study the role that specific subunits play in physiology and behaviour, genetically modified mice have been utilised that harbour deletions or knockin mutations. In 1999, Zamanillo *et al.* generated *Gria1* KO mice to study the effect of GluA1 deletion on synaptic plasticity and spatial reference memory (Zamanillo et al., 1999). *Gria1* KO mice lack GluA1 globally in the brain and throughout all of development. Zamanillo *et al.* found that LTP was absent in the CA1 of *Gria1* mice when using a tetanic stimulation protocol that induced LTP in hippocampal slices from control animals. Initial studies indicated that baseline synaptic transmission was normal in *Gria1* KO mice (Zamanillo et al., 1999), although subsequent studies report that CA3 to CA1 synaptic transmission is reduced in *Gria1* KO animals (Hoffman et al., 2002; Romberg et al., 2009).

At the behavioural level, Zamanillo *et al.* only used the Morris Water Maze (MWM) test, a task where animals are placed into a circular tank of water and are required to swim and find a sunken (and not visible) platform, onto which they can climb and escape from the water (Zamanillo et al., 1999). The location of the sunken platform remains constant but the starting position of the animal in the water maze is changed. Animals are given multiple trials and the latency to find the escape platform or the total path length to the escape platform, is measured. Spatial learning is reflected by a decrease in the latency and path length to reach the escape platform. Surprisingly, *Gria1* KO mice show normal spatial reference learning on the water maze, despite LTP being absent (Zamanillo et al., 1999). However, it was later found that LTP could, in fact, be induced in the CA1 of *Gria1* KO mice by following a paired theta burst stimulation protocol where the Schaffer collateral pathway was stimulated with a theta burst, whilst, after a slight temporal offset, the identical stimulation protocol was

applied to the alveus of the CA1(Romberg et al., 2009 and also Hoffman et al., 2002). This protocol aimed to induce synaptic events that also coincided with back propagating action potentials in the postsynaptic neuron in CA1. Romberg *et al.* observed that, whilst long lasting potentiation was induced in *Gria1* KO mice to the same extent as controls, the rapidly decaying, immediate (or short term potentiation (STP)) potentiation observed in controls was absent in *Gria1* KO mice (Romberg et al., 2009). Moreover, the induction of STP was studied directly by Erickson *et al.*, who found that STP induced in control animals, following a weak stimulation protocol, was completely absent in *Gria1* KO mice (Erickson et al., 2010). Thus, it appears to be short term potentiation (STP) that is particularly lacking in *Gria1* KO mice.

5.1.4 *Gria1* KO as a mouse model of psychological processes relevant to schizophrenia

Despite exhibiting normal hippocampus-dependent SRM, mice lacking the *Gria1* subunit show a range of behavioural deficits that could be relevant to schizophrenia (Barkus et al., 2012, 2014) . Initial studies found that SWM assessed on the T-maze (Reisel et al., 2002) and radial maze (Schmitt et al., 2003) was abolished in *Gria1* KO animals, whilst SRM was left intact (Reisel et al., 2002; Schmitt et al., 2003; Zamanillo et al., 1999). This apparent short term memory impairment of *Gria1* KO animals was assessed further on a spatial novelty preference version of the Y-maze. *Gria1* KO mice show chance level spatial novelty preference performance (Sanderson et al., 2007, 2009b).

It has been argued that the phenotype of *Gria1* KO mice results from a failure in stimulus-specific short-term habituation (Sanderson et al., 2009b; Sanderson and Bannerman, 2012; and see **1.6.3**). Rewarded alternation on the T-maze is widely regarded as testing SWM but deficits in *Gria1* KO mice can also be thought of as a

failure of short-term habituation, where mice fail to habituate to the goal arm they are forced into during the sample run (Sanderson and Bannerman, 2012). Thus, upon reaching the decision point during the choice run, mice are unable to assess which goal arm is less familiar to them (i.e. the more novel arm) and display poor levels of alternation performance (Sanderson and Bannerman, 2012). Similarly, spatial novelty preference assessed on the Y-maze and also novelty-induced hyperactivity could result from a failure in short-term habituation (Sanderson and Bannerman, 2012).

The failure of short term habituation in *Gria1* KO mice can, under certain conditions, lead to sensitisation to stimuli (Sanderson et al., 2011b). Sanderson *et al.* measured (albeit indirectly) the orienting response of *Gria1* KO and WT mice to pairs of visual stimuli (Sanderson et al., 2011b). The pairs of stimuli were presented with a 30 s delay between stimuli and such that the second stimulus was either the same as the first or different (Sanderson et al., 2011b). When the second stimulus was different to the first then the orientation of *Gria1* WT and *Gria1* KO mice was identical. However, when the second stimulus of the pairing was the same as the first, WT animals showed decreased orientation (i.e. habituation), whilst *Gria1* KO mice showed a greater degree of orientation (i.e. sensitisation) (Sanderson et al., 2011b). This stimulus specific sensitisation observed by Sanderson *et al.* is particularly noteworthy since it could reflect aberrant salience being attributed to a stimulus (Barkus et al., 2014; Sanderson et al., 2011b). Kapur has proposed that aberrant attribution of salience to stimuli is central to psychosis in schizophrenia (see **1.2.1**) (Kapur, 2003). Therefore, studying the mechanisms underlying aberrant salience in *Gria1* KO mice could aid our understanding of how changes in the glutamatergic system can lead to schizophrenia relevant behavioural phenotypes.

5.1.5 Where in the brain is GluA1 needed for short term memory?

The striking behavioural phenotype of *Gria1* KO mice has prompted investigation into where in the brain GluA1 is required for different behaviours. In 2001, Mack *et al.*, re-introduced GFP-tagged-GluA1 in a forebrain specific manner in *Gria1* KO mice (Mack et al., 2001). Using this approach, Mack *et al.* were able to rescue deficits in CA3 to CA1 LTP in *Gria1* KO mice (Mack et al., 2001). In the hippocampus GluA1-GFP was re-introduced in the majority of CA1 neurons (~70%), whilst expression was almost completely absent in the CA3 (Schmitt et al., 2005). At the behavioural level, this rescue approach was sufficient to partially restore spatial working/short term memory in *Gria1* KO mice (Schmitt et al., 2005). However, other behavioural deficits of *Gria1* KO mice, such as the profound novelty induced hyperactivity, were not significantly rescued with this forebrain specific approach (Schmitt et al., 2005).

The above rescue approach limits re-introduction of GluA1 to excitatory neurons in the forebrain. GluA1 (along with GluA4) is also expressed in inhibitory neurons, including PV interneurons (Geiger et al., 1995). To explore the function of GluA1 specifically in PV interneurons, Fuchs *et al.* generated mice that specifically lacked GluA1 on PV positive interneurons (hereafter referred to as *Gria1*$^{\Delta PV}$ mice; Fuchs et al., 2007). *Gria1*$^{\Delta PV}$ mice displayed impaired spatial working/short term memory but had intact SRM memory, which mirrors the phenotype of global deletion of GluA1 in *Gria1* KO mice (Fuchs et al., 2007). Thus, it is possible that deletion of GluA1 from PV neurons is driving in part the behavioural changes in *Gria1* KO mice, explaining the only partial (but still significant) rescue of spatial working memory when GluA1-GFP was reintroduced to forebrain excitatory neurons (Fuchs et al., 2007; Schmitt et al., 2005). To investigate this further a viral-rescue approach was used in this chapter, aiming to reintroduce GluA1 specifically into the hippocampus of *Gria1* KO mice. This was

followed by behavioural testing to assess of short-term memory performance. Because of the clear contribution of GluA1 in both excitatory and inhibitory neurons to short-term memory processes a virus promoter that drives expression in both inhibitory and excitatory neurons was utilised.

5.1.6 *In vivo* electrophysiology in *Gria1* KO animals

A remarkable feature of pyramidal neurons in area CA1 is their spatially selective responsiveness which renders them “place cells”, that only fire when an animal is in a specific spatial location (see **1.4.3**). Place cells were recorded in area CA1 of *Gria1* KO mice which, in comparison to WT controls, showed decreased spatial selectivity in their firing rates (Resnik et al., 2012). The impaired place cell activity is interesting, and could perhaps underlie the spatial working/short term memory deficits observed in *Gria1* KO mice (Resnik et al., 2012). However, this is at odds with the normal SRM performance of *Gria1* KO mice.

Disconnection studies utilising local infusions of the $GABA_A$ agonist muscimol (to silence the brain region locally) into the mPFC and ventral hippocampus, have indicted that intact connectivity between mPFC and ventral hippocampus circuits is critical for SWM performance of rats (Floresco et al., 1997; Wang and Cai, 2006). Performance of SWM tasks has also been linked to changes in prefrontal-hippocampal theta oscillations (see **1.3.3**). Theta frequency coherence between the prefrontal cortex and hippocampus is observed on the T-maze when animals prepare to make a choice (Jones and Wilson, 2005; O’Neill et al., 2013; Sigurdsson et al., 2010). As yet, prefrontal-hippocampal coherence has not been measured in *Gria1* KO mice. Considering the behavioural phenotype of these animals, it would be interesting to see if prefrontal-hippocampal coherence is disrupted in *Gria1* KO mice and if so, whether abnormalities are rescued with viral re-introduction of GluA1 into the hippocampus.

5.1.7 Chapter 5 experimental aims

To investigate where in the brain GluA1 is required, a viral rescue approach was taken to re-introduce GluA1 into the hippocampus of *Gria1* KO mice. SWM, spatial novelty preference and novelty induced hyperactivity were then tested. In addition, LFP oscillations were recorded from the dorsal hippocampus, prefrontal cortex and ventral hippocampus of *Gria1* WT, *Gria1* KO and *Gria1* KO rescue animals to assess long range synchrony in awake, behaving animals.

5.2 Methods

5.2.1 Generation of *Gria1* KO mice

Gria1 KO mice were generated by Zamanillo *et al.* as previously described (Zamanillo et al., 1999). Briefly, a targeting vector was designed that flanked exon 11 (encoding critical transmembrane segments of GluA1 encoded by exon 11 and portions of intron 10 and 11 immediately bordering the exon) and contained the neomycin (*neo*) antibiotic resistance gene, and two *loxP* sites located upstream of exon 11 and immediately downstream of the *neo* antibiotic resistance gene. Embryonic stem (ES) cells were electroporated with the targeting construct and grown in media containing *neo*, and positive clones were identified with polymerase chain reaction (PCR). ES cells were then transfected with a virus that expressed *Cre* recombinase, triggering deletion of exon 11 (flanked by *LoxP* sites). The ES cells were then injected into a C57Bl/6 mouse blastocyst creating chimeric animals that were selected for germline transmission and then backcrossed for at least 10 generations into a C57BL/6 background. Animals that were heterozygous for *Gria1* ($Gria1^{+/-}$) were bred together, giving 25% of offspring that are *Gria1* KOs ($Gria1^{-/-}$), 25% that are WT controls ($Gria1^{+/+}$) and 50% heterozygous ($Gria1^{+/-}$). In this study only *Gria1* KO and WT controls were used. Where possible littermate controls were used. Animals were housed as previously described (see **1.2.1**).

5.2.2 Design and synthesis of *Gria1* rescue virus

An adeno-associated virus (AAV) was used to reintroduce GluA1 into *Gria1* KO mice. GluA1 receptors can be alternatively spliced into Flip and Flop isoforms (see **1.5.7**). The mouse Flip isoform of GluA1 was used in this study. The DNA sequence of the GluA1 (Flip) transcript was obtained from GenBank (NCBI) and modified to contain

Not1 and Sal1 restriction enzyme sites upstream and downstream of the GluA1 construct respectively. To enable antibody-mediated identification of recombinant GluA1 expression, an AU1 tag was added after the first 54 bp of the N-terminus of the GluA1 sequence that encode the signal peptide for transmembrane localisation. DNA was synthesised *de novo* by GenScript to give AU1-GluA1(Flip). The plasmid AAV-hSyn-NPAS4-2pA-AU1-WPRE-pA (provided by Dennis Kätzel) served as plasmid and AAV-backbone into which the AU1-GluA1(Flip) transgene was inserted via *Not1/Sal1* digestion of both constructs and religation yielding AAV-hSyn-AU1-GluA1(Flip)-WPRE-pA (using services from GenScript). Plasmid DNA was amplified using an Endotoxin-free Maxi-prep kit (Qiagen), and DNA was sent to the University of North Carolina Vector Core where it was packaged into an AAV5 capsid. Upon arrival the virus was aliquoted and stored at -80°C.

5.2.3 Surgery (virus injection and electrode implantation)

The equipment used and initial stage of surgery were as described above (see **3.2.7**). Craniotomies were made over the injection and electrode sites, and virus was injected with a Hamilton syringe (34g bevelled needle) controlled by a digital injector pump (WPI Instruments, USA) at a rate of 100 nl/minute. Each animal received 3 injections of virus per hemisphere in an attempt to target the majority of the hippocampus along the AP axis (see **table 5.1** for coordinates). After injection of the virus the needle was kept in place for 5-10 minutes before slow withdrawal to minimise backflow of virus and promote virus spread through the tissue.

AP coordinate:	ML coordinate:	Z coordinates: (from brain surface)	Injection volumes (nL)
-2.2	+/- 1.8	-1.5, -1.1	400 and 600
-2.8	+/- 3	-2, -1.5	500 (at each)
-3.3	+/- 3	-2.5, -3.5	500 (at each)

Table 5.1: Stereotaxic coordinates for virus injection
Stereotaxic coordinates used for injection of GluA1 rescue virus. Three injection sites along the AP axis were used to target as much of the hippocampus as possible. All coordinates are relative to bregma. Where there are multiple injection volumes it refers to injections at the first and second Z coordinate respectively.

After virus injection electrodes were implanted into the brain. The dura was removed to expose the brain surface and straightened polyimide-insulated tungsten wires of 50 µm inner diameter (Wiretronic, CA, USA) were inserted into the medial prefrontal cortex (AP +1.7mm, ML +0.25-0.35, 1.7-1.9 mm below pia), dorsal hippocampus (AP -2 mm, ML + 1.5 mm, -1.3 mm below pia) and ventral hippocampus (AP -3.3 mm, ML -2.9 mm, -3.3 mm below pia) of the right hemisphere. A 125 µm stainless steel (Advent Research Materials, UK) reference electrode was placed touching the brain surface in the posterior part of the frontal cortex (AP -0.5mm, ML -1 mm) and a ground screw was inserted into the cerebellum, both contralateral with respect to the recording electrodes. Light curable dental cement (Pentron, USA) was used to fix the electrodes in position. The electrodes, ground and reference wires were connected to a plastic adaptor (Millmax) with gold pins via press-fit.

Mice were injected (s.c.) with 500 µL saline at the end of the surgery and Metacam (5 mg/kg) was given 24 hrs later (either s.c. or orally by feeding palatable strawberry jelly containing the drug). Mice were given 4 weeks to recover from the surgery and for viral expression of GluA1 to occur (in *Gria1* KO mice injected with the rescue virus).

A total of 10 WT and 9 Gria1 KO mice were implanted with electrodes. A further 8 *Gria1* KO mice were injected with the GluA1 rescue virus and implanted with electrodes. Both male and female mice were tested. The same cohort was tested in each of the behaviours but numbers included in each group for the different behavioural tests varied slightly due to exclusion of some animals with noisy electrophysiology signals. N numbers are given for each of the behaviours tested.

5.2.4 Immunohistochemistry

To assess viral expression of GluA1 in *Gria1* KO mice and electrode positions, mice were euthanized (Euthatal) and miniature lesions were made by electrical stimulation of recording electrodes. Animals were transcardially perfused with PBS followed by 4% paraformaldehyde (PFA) and post fixed for 24 hours in PFA. Coronal sections 60 μm thick were cut on a vibratome and collected around the electrode recording sites and throughout the entire hippocampus in *Gria1* KO mice injected with the GluA1 rescue virus.

Immunohistochemistry was performed as previously described (see **2.2.2**) on sections throughout the hippocampus. GluA1 expression was detected in two ways, firstly with a rabbit anti-GluA1 antibody (Chemicon, used at 1:500) and also with a mouse anti-AU1 antibody (Covance, used at 1:500) to detect the AU1 tag on the N-terminus of virally introduced GluA1. GluA1 and AU1 antibodies were detected with fluorescent secondary antibodies (Alexa488-coupled goat-anti-rabbit and Alexa546-coupled goat-anti-mouse for GluA1 and AU1 respectively, both from Molecular Probes and used at 1:1000). Sections were mounted as previously described (see **2.2.2**) and scanned on an epifluorescent microscope (Axio Zoom, Carl Zeiss) to visualise GluA1 (green channel), AU1 expression (red channel) and the nuclear stain DAPI (blue channel). Electrolytic lesions were detected as previously described (see **3.2.10**).

5.2.5 Locomotor activity testing

To test locomotor activity and simultaneously record LFPs, mice were tethered and placed into a novel cage (length 43 cm, width 22 cm, height 20 cm; distinct from their home cage) containing clean sawdust and allowed to explore for 5 minutes. Testing occurred in a different part of the same room in which animals were previously tested for rewarded alternation (see below). During the 5-minute exploration, the animals' position was tracked using AnyMaze (Stoelting, USA). The distance travelled (path length) was calculated every 5 seconds. From this, the total distance, as well as the distance travelled in 1-minute time bins was calculated for the full 5 minutes. The average running speed was also calculated for the full 5 minutes.

5.2.6 Electrophysiology recordings

Electrophysiological data were acquired at a sampling rate of 15 kHz and subsequently filtered with a 0.1-300 Hz bandpass filter using an RHD2132 amplifier board (Intan Technologies, CA, USA), an Open E-Phys USB interface board and the Open E-Phys acquisition software (Open E-Phys, MA, USA). Raw data were exported into MatLab (Mathworks, MA, USA) and down sampled to 1 kHz. Further spectral analysis was all performed in Matlab, using the Chronux toolbox (http://chronux.org/). All recordings were referenced to the ground screw above the cerebellum and not to the cortical reference electrode. Electrophysiology data from all 9 WTs and 8 *Gria1* KO mice were analysed. Data from one *Gria1* KO rescue mouse was excluded due to exceptionally poor signals (presumably due to a fault in the electrode).

LFPs were recorded to assess long range coherence in awake, behaving mice. The placements of electrodes in the prefrontal cortex and ventral hippocampus were more variable than in the dorsal hippocampus (see **figure 5.4** and **appendix 7.3.1**). For this

reason, initial analyses focussed on assessing theta oscillations in the dorsal hippocampus. Only these initial analyses have been included here in the thesis.

5.2.7 Calculation of theta power

Power spectrum density plots for the frequency range 4 - 40 Hz were estimated using a multi-taper approach using the mtspectrumc function (Chronux toolbox) for the entire 5-minute exploratory period (using a total of 119 tapers). Between 5 - 12 Hz (theta range), the area under the curve (between 5 - 12 Hz) was calculated from the power spectral density plots from each animal to assess overall theta power. In addition, the frequency of the peak theta power in the 5-12 Hz range was calculated for each animal. To generate group average data power spectra were averaged across animals and plotted with jack-knife error bars (again using the mtspectrumc function).

5.2.8 T-maze rewarded alternation test

Spatial working/short term memory was tested on the T-maze as before (see **2.2.13**), but with some modifications. LFP data were recorded during testing, although electrophysiology data are not presented here. Thus, all mice were tethered during behavioural testing and the protocol was necessarily modified so animals did not have to be picked up in between trials (which could introduce noise to the electrophysiology data). To achieve this, sliding doors were added to the maze on the goal arms and also onto the start arm to create a “start box” where animals could be held between trials. Food wells were placed at the end of each goal arm, and an additional food well was placed in the start box, so animals could be trained to return to the start arm.

Animals were placed on a food-restricted diet to limit their body weight to 85-90% of their free fed weight, and habituated to the condensed milk reward (mixed 50:50 with drinking water) both in their home cage and on the T-maze. Once animals were consuming the condensed milk reward without hesitation on the T-maze, testing

commenced. Animals were given 7 blocks of T-maze testing, with 10 trials per animal per day (i.e. per training block). Animals were tethered and placed into the start arm of the maze (goal arms closed off) for 60s to get re-accustomed to being tethered. Then animals were directed into the "start box" at the end of the start arm so testing could commence. During the sample run animals were released from the "start box" and forced into one of the goal arms to collect a condensed milk food reward. Animals then returned to the "start box" of their own volition (where they could collect another food reward) and then were transiently enclosed in the "start box" by sliding the door closed. Then, after a delay of 5s, the door to the "start box" was opened and animals could make a free choice between either of the goal arms in the choice run. As before, animals were able to gain a reward by choosing the arm they did not enter during the sample run (i.e. by alternating). After making a choice (correct or incorrect) mice returned to the "start box" to consume a further reward. There was then an inter-trial interval of 30s before the next trial was initiated. As before, animals were forced into the left or right goal arm during the sample run following a pseudorandom sequence (with the same arm not being used as the sample goal arm for more than 3 times consecutively). The number of correct choices were recorded for each block of 10 trials.

5.2.9 Y-maze novelty preference test[1]

Spatial novelty preference was tested with apparatus and a protocol previously described (see **2.2.12**), with the only difference being that the location of mice was manually scored from videos after testing using an event timer. The number of arm entries into, and the time spent in, each arm was calculated. Importantly, the test was

[1] Test and manual scoring from videos was conducted by Dr. Thomas Jahans-Price under supervision of Alexei Bygrave. All data analysed by Alexei Bygrave.

conducted in a novel room so animals were not already familiar with extramaze cues that could reduce exploratory drive or reduce the novelty of spatial locations within the arms of the maze. There was no recording of electrophysiology data during this task.

5.3 Results

5.3.1 Viral re-introduction of GluA1 was limited to area CA3 of the hippocampus

A rescue virus was designed to reintroduce GluA1 into *Gria1* KO mice (**figure 5.1a**). The human synapsin 1 (hSyn) promoter was used to drive expression in a neuron-specific manner (Kügler et al., 2003), targeting both excitatory and inhibitory neurons (Nathanson et al., 2009). The woodchuck hepatitis virus post-transcriptional regulatory element (WPRE) was included in the virus design to enhance viral expression (Glover, 2002).

To test the AAV5-hSyn-GluA1 rescue virus (hereafter GluA1 virus), stereotaxic surgery was performed on two *Gria1* KO mice and GluA1 virus was injected into the dorsal hippocampus. After 4 weeks, to give time for virus expression, the animals were sacrificed and perfused along with *Gria1* WT (n = 2) and un-injected *Gria1* KO controls (n = 2). Immunohistochemistry was performed on hippocampal sections to detect GluA1 (endogenous and virally expressed) and AU1 (only present on the virally expressed GluA1). Viral expression was observed in both animals injected with the GluA1 virus but only data from one animal is shown (**figure 5.1b-h**).

In WT mice, GluA1 expression (determined with the anti-GluA1 antibody) was particularly prominent in the hippocampus (**figure 5.1b and c**). As expected, GluA1 was not detected in *Gria1* KO mice, except for some weak background signal observed in area CA3, and to a lesser extent area CA1, presumably due to the

antibody binding to other AMPAR subunits or other targets (**figure 5.1d and e**). In *Gria1* KO mice injected with the GluA1 virus, GluA1 was detected in the hippocampus, although surprisingly, the expression appeared preferentially in area CA3 (**figure 5.1f and g**). The area CA3 specificity was unexpected as stereotaxic injection coordinates were not intended to be CA3 specific.

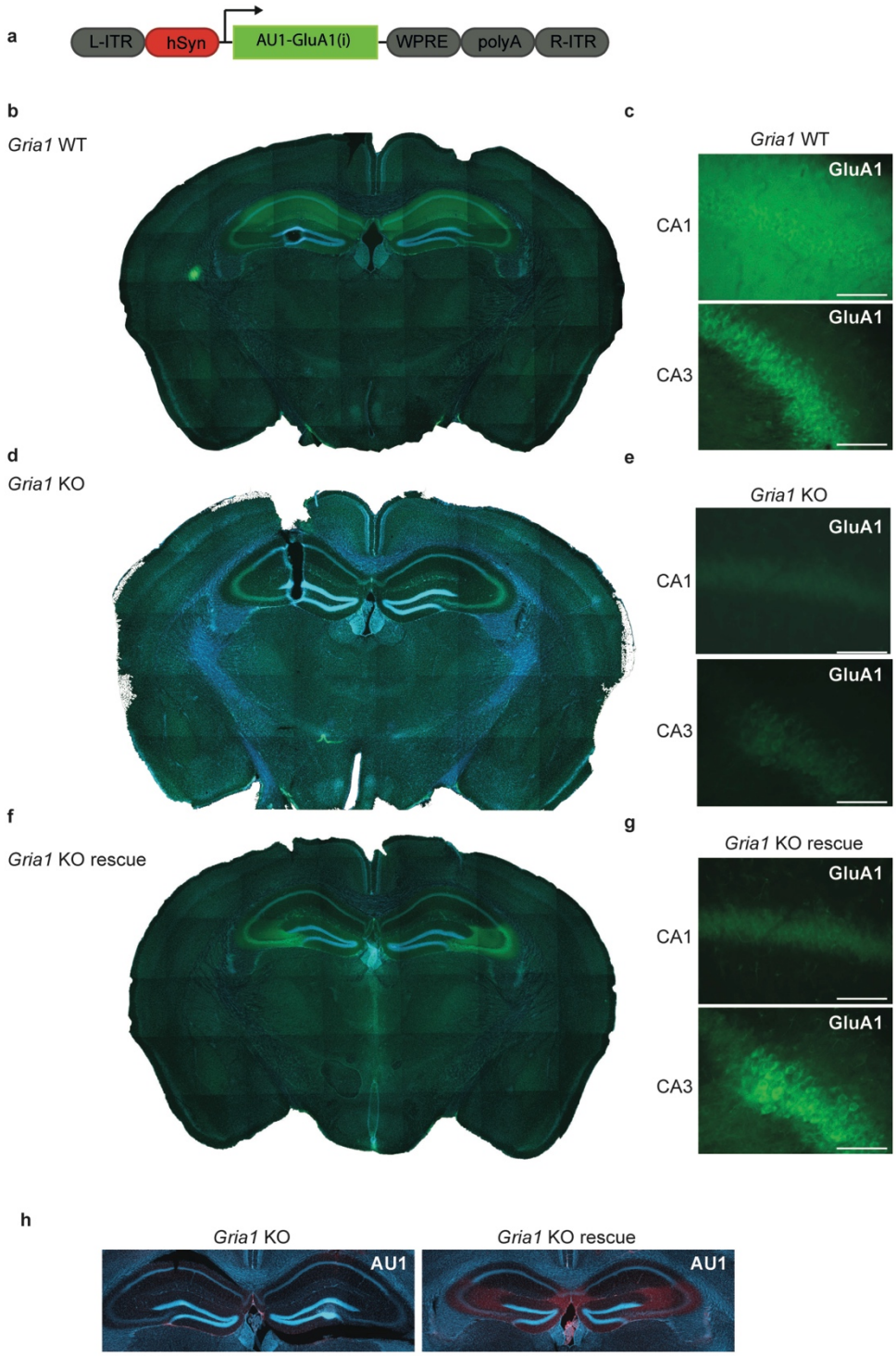

Figure 5.1: GluA1 virus can reintroduce GluA1 in an area CA3 specific manner in *Gria1* KO mice

(a) Schematic of GluA1 rescue virus. Epifluorescent images taken from coronal slices of (b) *Gria1* WT, (d) *Gria1* KO and (f) *Gria1* KO + GluA1 virus (*Gria1* KO rescue) mice stained with an anti-GluA1 antibody. GluA1 (green) was enriched in WT hippocampus, absent in KO and restricted to area CA3 in KO mice injected with the GluA1 virus. Nuclei were stained with DAPI (blue). High magnification images (c, e and g) were taken centred on the

pyramidal cell layer in area CA1 (top images) and area CA3 (bottom images). In high magnification images the scale bar indicates 100μm. Virally-expressed GluA1 (containing an AU1 tag) was also detected with an anti-AU1 antibody (red) (h), confirming the area CA3 specific expression in *Grin1* KO rescue animals but not KO animals. Note that lesions in the left hemisphere of the *Gria1* WT and *Gria1* KO were from electrode sites.

In addition, detection of GluA1 with the AU1 antibody indicated area CA3 specific expression patterns in *Gria1* KO mice injected with the GluA1 virus but not in un-injected *Gria1* KO controls (**figure 5.1h**). The neuronal subtypes in which GluA1 was expressed following virus injection into *Gria1* KO mice was not assessed.

5.3.2 Viral re-introduction of GluA1 to area CA3 throughout the hippocampus

To estimate the extent of GluA1 expression in the hippocampus of *Gria1* KO mice, coronal sections were taken from *Gria1* KO rescue animals along the AP axis of the hippocampus. Sections were then stained for GluA1 and epifluorescent images acquired. Sections throughout a representative *Gria1* KO rescue animal, with corresponding mouse brain atlas schematics, are shown (**figure 5.2**). Expression of GluA1 was strong in the dorsal hippocampus and became weaker in more ventral sections (more posterior than AP: -3, relative to bregma). Again, the expression pattern of GluA1 appeared to be area CA3 specific along the entire AP axis. This indicated that the virus injection coordinates were sufficient to target a large portion of the hippocampus, preferentially targeting area CA3.

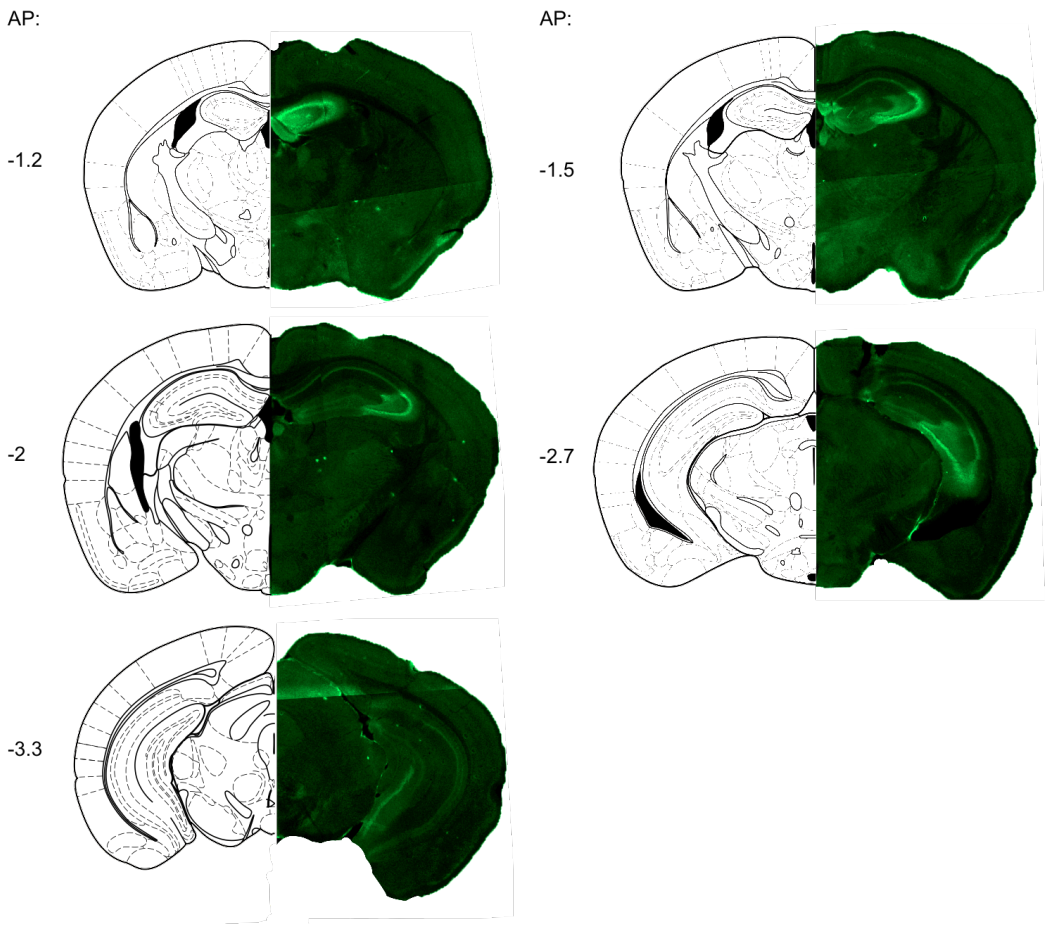

Figure 5.2: Viral expression of GluA1 throughout the hippocampus of a *Gria1* KO mouse Representative example of viral-GluA1 expression (green) in the hippocampus of a *Gria1* KO mouse injected with the GluA1 rescue virus. Estimates of AP position of sections are indicated based on the mouse brain atlas (Paxinos).

5.3.3 Hyperactivity is rescued in *Gria1* KO rescue mice

Gria1 KO mice have previously been found to be hyperactive when exposed to a novel environment (Bannerman et al., 2004; Barkus et al., 2010; Fitzgerald et al., 2010; Procaccini et al., 2011, 2013; Wiedholz et al., 2008), but importantly, not in their home cage (Fitzgerald et al., 2010). It is possible that this hyperactivity is linked to over-activation of the hippocampus upon exposure to a novel environment, as Procaccini *et al.* found greater induction of the activity dependent immediate early gene cFos in *Gria1* KO mice compared to controls (Procaccini et al., 2011). If hyperactivity is due to

hippocampal dysfunction, then it is possible that reintroducing GluA1 into the hippocampus could rescue novelty induced hyperactivity in *Gria1* KO mice.

To investigate if re-introduction of GluA1 to area CA3 is sufficient to rescue the hyperactivity of *Gria1* KO mice, a cohort of 8 *Gria1* KO animals (4 males, 4 females) were injected with GluA1 rescue virus and tested, along with 9 un-injected *Gria1* WT (6 males, 3 females) and 8 *Gria1* KO mice (5 males, 3 females). All of the animals were implanted with tungsten electrodes in the hippocampus and prefrontal cortex enabling LFP recordings.

Locomotor activity was assessed as animals explored a novel environment for 5 minutes. The distance travelled was calculated over the course of 5 minutes in 1-minute time bins, along with the total distance travelled (**figure 5.3a,b**).

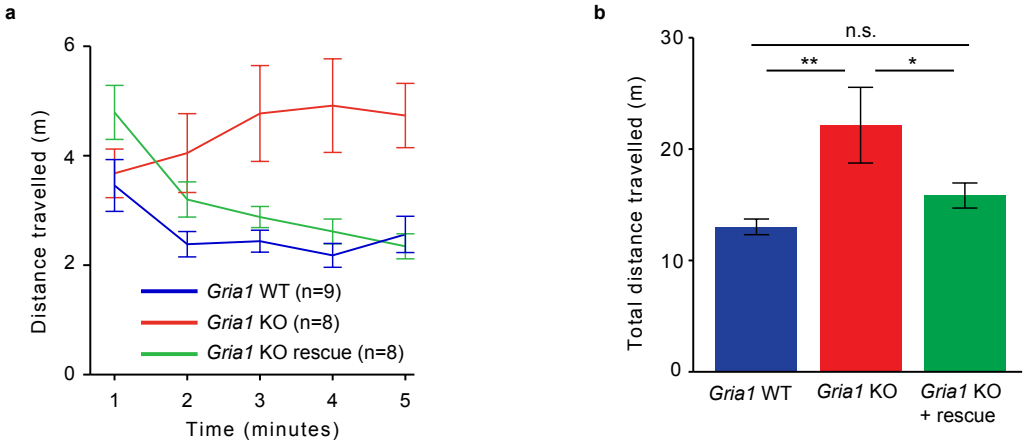

Figure 5.3: Viral expression of GluA1 preferentially into area CA3 of *Gria1* KO mice rescues novelty induced hyperactivity
Gria1 KO (red), *Gria1* WT (blue) and *Gria1* KO with GluA1 rescue virus (green) mice were tested for novelty induced hyperactivity during 5-minutes of exploration of a novel environment. (a) Distance travelled in 1-minute time bins and (b) total distance travelled. Error bars display S.E.M. Significance stars indicate post hoc comparisons (LSD). * represents $P<0.05$, ** represents $P<0.01$.

Gria1 KO mice displayed novelty-induced hyperactivity compared to WT controls. Interestingly, hyperactivity was rescued in *Gria1* KO mice injected with the GluA1

virus. A repeated measures ANOVA with sex and group (*Gria1* WT, *Gria1* KO and *Gria1* KO rescue) as between subject factors, and time bin as a repeated measure revealed a significant overall effect of group but not sex, and no group*sex interaction on the distance travelled (effect of group: $F(2,19) = 3.866$, $P = 0.039$; effect of sex: $F(1,19) = 1.836$, $P = 0.191$; group*sex interaction: $F(2,19) = 2.372$, $P = 0.125$). There was an overall significant effect of time bin and also a significant group*time bin interaction for the distance travelled (effect of time bin: $F(4,76) = 4.799$, $P = 0.002$; group*time bin interaction: $F(8,76) = 6.400$, $P = 0.001$). There was no significant triple group*sex*time bin interaction for the distance travelled by each group.

Post hoc comparisons (LSD) revealed that *Gria1* KO mice travelled significantly further than both *Gria1* WT and *Gria1* KO with GluA1 rescue mice (*Gria1* KO vs. *Gria1* WT: $F(1,19) = 11.861$, $P = 0.003$; *Gria1* KO vs. *Gria1* KO rescue: $F(1,19) = 5.361$, $P = 0.032$). There was no significant difference in the distance travelled by *Gria1* WT or Gria1 KO rescue mice (*Gria1* WT vs. *Gria1* KO rescue: $F(1,19) = 1.127$ $P = 0.302$). These data show that re-introduction of GluA1 to area CA3 throughout the hippocampus is sufficient to rescue novelty induced hyperactivity seen in *Gria1* KO mice.

5.3.4 Enhanced theta power in the dorsal hippocampus of *Gria1* KO mice is rescued with re-introduction of GluA1 to area CA3

Previous *in vivo* electrophysiology studies in *Gria1* KO animals have not assessed LFP oscillations in the hippocampus (or other structures). Theta oscillations, and their coordination between brain structures, have been proposed to be important for SWM performance (Jones and Wilson, 2005; O'Neill et al., 2013; Sigurdsson et al., 2010; Tamura et al., 2016). It is possible that theta oscillations are different in WT and *Gria1* KO mice. To investigate this, LFPs were recorded in *Gria1* WT, *Gria1* KO and *Gria1*

KO with GluA1 rescue virus mice, whilst animals were exploring a novel environment. During the 5-minutes of exploration in the novel environment local field potentials (LFPs) were recorded from the dorsal hippocampus, ventral hippocampus and prefrontal cortex. Initially, only LFP data from the dorsal hippocampus were analysed, because electrode placements in the ventral hippocampus and prefrontal cortex were more variable (see **appendix 7.3.1** for discussion). Unfortunately, this prevented analysis of long range neuronal synchrony between prefrontal cortex and hippocampus, as at the time of writing, it is not known how variations in placement in the ventral hippocampus and prefrontal cortex could influence coherence.

Electrode placements in the dorsal hippocampus were generally at the fissure between area CA3 and the DG, which is known to show the highest amplitude theta oscillations (Buzsáki, 2002). The estimated location of electrode recording sites are shown superimposed over mouse brain atlas diagrams (**figure 5.4a**). In one *Gria1* KO mouse the electrode recording site could not be found, presumably due to a failure in electrolytic lesioning. Data from this animal was included in the analysis because the electrophysiology signals were indistinguishable from other *Gria1* KO animals.

The theta range (5 - 12 Hz) power and peak theta frequency were calculated for each animal during the 5 minutes of novel environment exploration. Theta power has previously been correlated with running speed, with faster running speeds associated with enhanced theta power (McFarland et al., 1975). As *Gria1* KO animals are known to be hyperactive (see **figure 5.3**) this could drive observations of enhanced theta oscillation power in *Gria1* KO animals. Therefore, average running speed was included as a covariate in analysis relating to theta power.

Theta power in *Gria1* KO mice was enhanced compared to *Gria1* WT animals and re-introduction of GluA1 to area CA3 of *Gria1* KO animals normalised theta power to

levels of *Gria1* WTs (**figure 5.4b,c**). ANOVA with sex and group (*Gria1* WT, *Gria1* KO and *Gria1* KO + rescue) as between subject factors, and average running speed as a covariate, revealed an overall effect of group, but not sex, and no sex*group interaction (effect of group: $F(2,17) = 6.846$, $P = 0.007$; effect of sex: $F(1,17) = 0.815$, $P = 0.379$; sex*group interaction: $F(2,17) = 0.497$, $P = 0.617$).

Post Hoc comparisons (LSD) revealed that theta power in *Gria1* KO mice was significantly greater than in both *Gria1* WT and *Gria1* KO rescue animals (theta power in *Gria1* KO vs. *Gria1* WT: $F(1,17) = 11.603$, $P = 0.003$; and *Gria1* KO vs. *Gria1* KO rescue: $F(1,17) = 9.985$, $P = 0.006$). There was no significant difference in the theta power in *Gria1* WT and *Gria1* KO rescue animals (theta power in *Gria1* WT vs. *Gria1* KO rescue: $F(1,17) = 0.234$ $P = 0.634$). These data suggest that global deletion of *Gria1*, and hence GluA1, results in elevated hippocampal theta. Surprisingly, re-introduction of GluA1 preferentially to area CA3 in *Gria1* KO mice normalises the aberrant theta oscillation power seen in the dorsal hippocampus of *Gria1* KO mice.

The frequency of peak theta power has also been shown to be sensitive to running speed, with faster running speeds being correlated with faster theta oscillations (Bender et al., 2015). As *Gria1* KO mice are hyperactive in a novel environment it was surprising that the peak theta frequency in *Gria1* KO animals appeared actually to be lower than in *Gria1* WTs (**figure 5.4d**).

ANOVA with sex and group (*Gria1* WT, *Gria1* KO and *Gria1* KO + rescue) as between subject factors, and average running speed as a covariate, revealed no overall effect of group, sex and no sex*group interaction on the peak theta frequency (effect of group: $F(2,17) = 0.793$, $P = 0.468$; effect of sex: $F(1,17) = 0.365$, $P = 0.554$; sex*group interaction: $F(2,17) = 0.025$, $P = 0.976$).

However, because of *a priori* predictions that faster running speed should correlate with faster (not slower) theta rhythms, an additional analysis was performed where the average running speed was **not** included as a covariate in the analysis of peak theta frequency. ANOVA with sex and group (*Gria1* WT, *Gria1* KO and *Gria1* KO + rescue) as between subject factors revealed no overall effect of group or sex, and no overall sex*group interaction (effect of group on peak theta frequency: $F(2,18) = 3.005$, $P = 0.075$; effect of sex: $F(1,18) = 0.007$, $P = 0.932$; sex*group interaction: $F(2,18) = 0.306$, $P = 0.740$). Although not strictly appropriate, post hoc comparisons (LSD) revealed that *Gria1* KO animals had a peak theta frequency that was significantly lower than *Gria1* WT mice (peak theta frequency in *Gria1* KO vs. *Gria1* WT: $F(1,18) = 5.975$, $P = 0.025$). There was no significant difference in the peak theta frequency of *Gria1* KO rescue animals with either *Gria1* WT or *Gria1* KO animals (peak theta frequency in *Gria1* KO rescue vs. *Gria1* WT: $F(1,18) = 1.660$, $P = 0.293$; *Gria1* KO rescue vs. *Gria1* KO: $F(1,18) = 1.174$, $P = 0.214$).

Together these analyses suggest that variations in running speed migth account for the different peak theta frequencies. However, it is interesting that the increased running speed of *Gria1* KO mice seems to lead to decreased (rather than increased) peak theta frequency. The effect of area CA3 GluA1 re-introduction in *Gria1* KO mice on short term spatial memory tasks was then subsequently investigated.

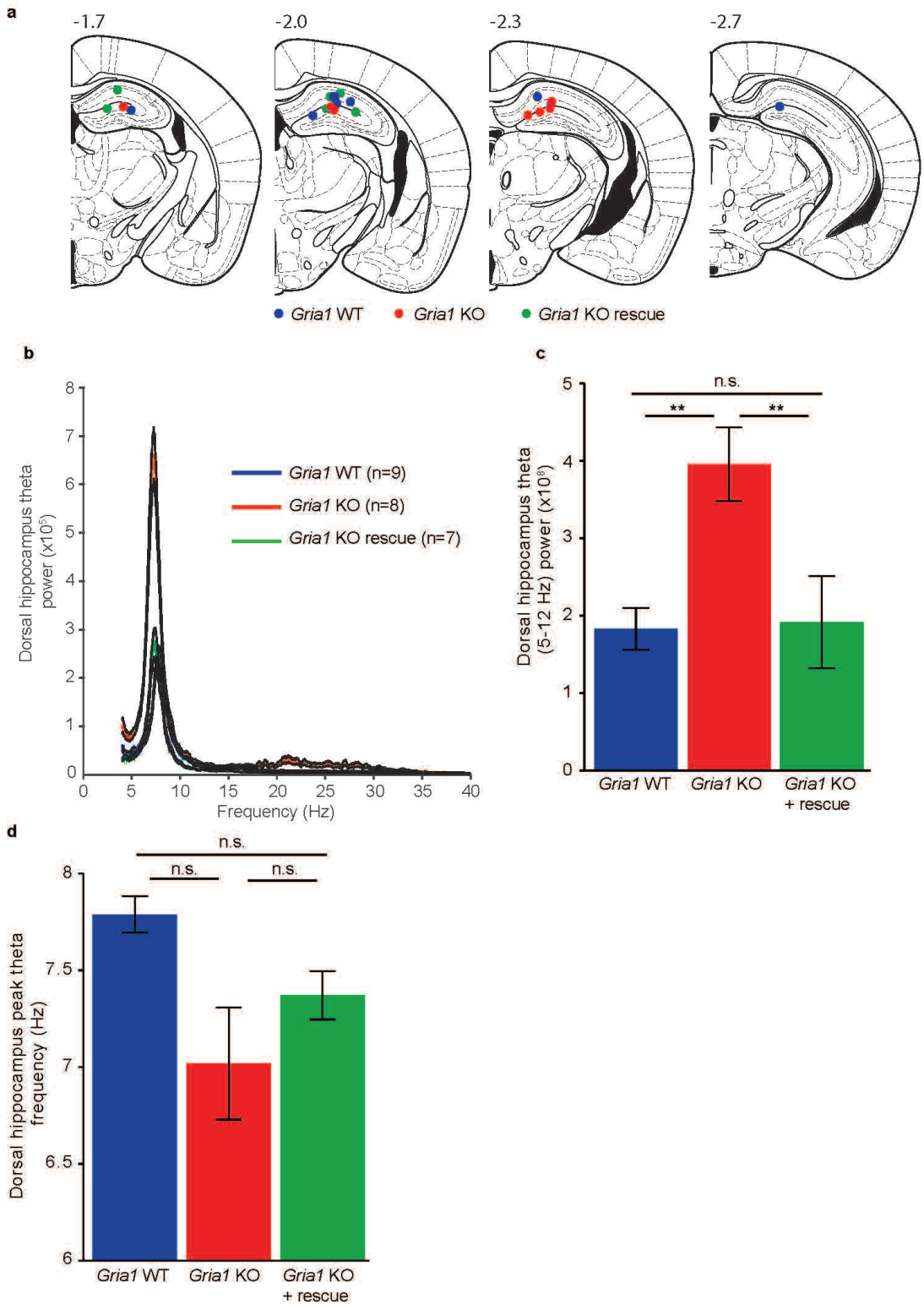

Figure 5.4: Elevated theta power in dorsal hippocampus of *Gria1* KO mice is rescued with area CA3 re-introduction of GluA1

(a) Estimated electrode recording sites in dorsal hippocampus superimposed onto corresponding mouse brain atlas images (Paxinos and Franklin, 2001) in *Gria1* WT (blue dots), *Gria1* KO (red dots) and *Gria1* KO with GluA1 rescue (green dots). (b) Average power spectrum density plots between the power of 4-40 Hz frequency oscillations in the dorsal

hippocampus. Prominent theta oscillations are indicated by the large peak in power in the 5 – 12 Hz range. Jack-knife error bars are shown. (c) Theta power (5-12 Hz) was elevated in *Gria1* KO mice and normalised to WT levels in *Gria1* KO with rescue virus. (d) Frequency of peak theta power. Bars display the group mean. Error bars display the S.E.M. Significant stars indicate significant post hoc comparisons (LSD) with analyses that include running speed as a covariate. ** represents $P < 0.01$. There was no obvious systematic difference in electrode placement across groups.

5.3.5 Re-introduction of GluA1 to area CA3 in *Gria1* KO mice does not rescue SWM on the T-maze

In addition to novelty-induced hyperactivity, *Gria1* KO mice display chance level performance when tested for SWM on the T-maze (Reisel et al., 2002; Schmitt et al., 2005). This phenotype was partially rescued when GluA1 was reintroduced to forebrain excitatory neurons using a genetic strategy (Schmitt et al., 2005).

To test if GluA1 re-introduction in area CA3 is sufficient to rescue SWM performance in *Gria1 KO* mice a subset of *Gria1* WT (4 males and 2 females) and *Gria1* KO (3 males and 3 females) and all *Gria1* KO rescue (4 males and 4 females) animals were tested for SWM performance on the elevated T-maze. Only a subset of mice were tested as some of the mice did not run well on the maze during habituation sessions. Electrophysiology data were recorded simultaneously (data not shown), requiring animals to be tethered during testing, and slight protocol modifications were introduced so animals did not have to be handled between trials (see **5.2.9** and **figure 5.5a**).

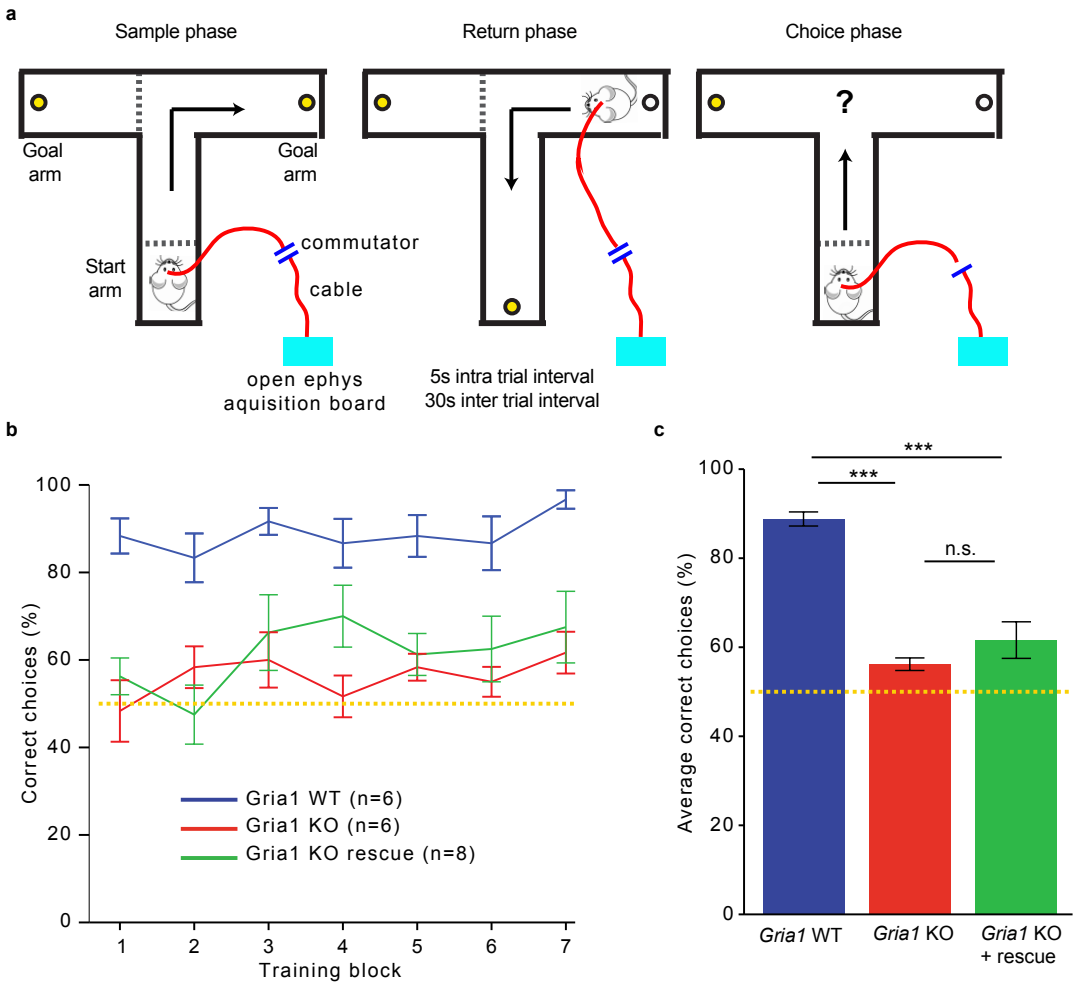

Figure 5.5: Re-introduction of GluA1 to area CA3 of *Gria1* KO mice does not rescue SWM on the T-maze

(a) Schematic representation of the test protocol. In the sample phase animals are forced into one of the goal arms to collect a food reward. Animals were trained to return to the start arm (return phase) where they collected another food reward and were transiently (5s delay) enclosed in the "start box" indicated by the dashed line at the end of the start arm. Then animals were given a free choice of both goal arms in the choice phase, and were rewarded for alternating into the previously non-visited goal arm. After a choice was made animals returned to the start arm and were enclosed in the "start box" for an inter-trial interval period of 30s. Animals were tethered during testing so electrophysiology data could be recorded (red line in (a)) but electrophysiology data are not shown. (b) % of correct choices in *Gria1* WT (blue line), *Gria1* KO (red line) and *Gria1* KO rescue (green line) animals over 7 blocks of SWM testing (10 trials per block). Yellow dashed line indicates chance level performance. (c) % of correct choices for each group, collapsed over the 7 blocks tested. Error bars display S.E.M. Significant stars indicate significant post hoc comparisons (LSD). *** represents P<0.001.

Gria1 WT mice showed high levels of alternation behaviour across training blocks, whereas, as expected, *Gria1* KO mice performed at around chance levels throughout testing (**figure 5.5b,c**). Re-introduction of GluA1 to area CA3 in *Gria1* KO mice did not rescue SWM performance (**figure 5.5b,c**).

A repeated measures ANOVA with sex and group (*Gria1* WT, *Gria1* KO and *Gria1* KO + rescue) as between subject factors and training block as a repeated measure revealed a significant overall effect of group but no effect of sex, and no sex*group interaction on the % of correct choices (effect of group on correct choices: $F(2,14) = 30.621$, $P = 0.001$; effect of sex: $F(1,14)= 1.888$, $P = 0.191$; sex*group interaction: $F(2,14) = 1.198$, $P = 0.331$). There was no significant effect of training block, training block*sex, training block*group, or triple training block*sex*group interaction on the % of correct choices (all F values < 1.848).

Post hoc comparisons (LSD) revealed a significant difference in the % of correct choices made by *Gria1* WT animals compared to *Gria1* KO and *Gria1* rescue mice (% correct choices in *Gria1* WT vs. *Gria1* KO: $F(1,14) = 56.606$, $P = 0.001$; *Gria1* WT vs. *Gria1* KO rescue: $F(1,14) = 44.990$, $P = 0.001$). There was no significant difference in the % of correct choices made by *Gria1* KO mice compared to *Gria1* KO rescue animals (% correct choices in *Gria1* KO vs. *Gria1* KO rescue: $F(1,14) = 1.784$, $P = 0.203$). These data confirm that *Gria1* KO mice are impaired in this slightly modified variation of the T-maze spatial working/short term memory task, and that re-introduction of GluA1 preferentially to area CA3 only does not rescue this deficit.

5.3.6 Re-introduction of GluA1 to area CA3 rescues spatial novelty preference in *Gria1* KO mice

Spatial novelty preference can be tested using a Y-maze and assesses the preference mice exhibit for a previously unvisited, and therefore novel, arm of the maze. This provides a measure of how much animals have habituated to the previously visited/familiar arm. Previous work found that *Gria1* KO mice show chance level performance when spatial novelty preference is tested in this way (Sanderson et al., 2007, 2009b). In the present study, *Gria1* WT (7 males and 3 females), *Gria1* KO (6 males and 3 females) and *Gria1* KO rescue (4 males and 4 females) animals were tested for spatial novelty preference on the Y maze, to investigate whether area CA3 re-introduction of GluA1 into the hippocampus of *Gria1* KO mice is sufficient for task performance. Animals were not tethered whilst being tested as electrophysiology recordings were not made.

Sample phase exploration

Exploration of the familiar arm during the exposure phase (see **figure 5.6a**) could influence task performance, since adequate exploration of this arm is important if animals are to perceive the novel arm as novel during the test phase. Thus, animals that show greater levels of exploration of the would-be familiar arm could be biased towards increased task performance.

Notably, both *Gria1* KO and *Gria1* KO rescue animals showed significantly greater exploration of the to-be familiar arm, as measured by the time spent in this arm during the exposure phase (**figure 5.6b**). ANOVA with sex and group (*Gria1* WT, *Gria1* KO and *Gria1* KO rescue) as between subject factors revealed an overall significant effect of group, but no effect of sex and no sex*group interaction on time spent in the to-be familiar arm during the exposure phase (effect of group on exploration time: $F(2,21) =$

6.161, P = 0.008; effect of sex: F(1,21) = 0.967, P = 0.337; effect of sex*group interaction: F(2,21) = 0.776, P = 0.473).

Post hoc comparisons (LSD) revealed that *Gria1* WT animals spent significantly less time exploring the to-be familiar arm in the exposure phase compared to *Gria1* KO and *Gria1* KO rescue animals (time exploring in *Gria1* WT vs. *Gria1* KO: F(1,21) = 14.712, P = 0.001; *Gria1* WT vs. *Gria1* KO rescue: F(1,21) = 7.450, P = 0.013). There was no difference in the time spent exploring the to-be familiar arm between *Gria1* KO and *Gria1* KO rescue animals during the exposure phase (time exploring in *Gria1* KO vs. *Gria1* KO rescue: F(1,21) = 0.926, P = 0.347). Thus, *Gria1* KO and *Gria1* KO rescue animals have, on average, experienced the familiar arm to a greater extent than *Gria1* WT animals, but to a similar extent as each other.

In addition, during the sample phase *Gria1* KO mice made more entries into the to-be familiar arm than *Gria1* WT and *Gria1* KO rescue animals. *Gria1* KO rescue animals made more entries into the to-be familiar arm than *Gria1* WT mice, but fewer entries compared to *Gria1* KO mice (see **figure 5.6c**). ANOVA with sex and group (*Gria1* WT, *Gria1* KO and *Gria1* KO rescue) as between subject factors revealed an overall significant effect of group, a significant sex*group interaction, but no overall effect of sex on the number of entries into the to-be familiar arm during the exposure phase (effect of group on exploration time: F(2,21) = 7.823, P = 0.003; effect of sex: F(1,21) = 0.215, P = 0.648; effect of sex*group interaction: F(2,21) = 3.693, P = 0.042).

Post hoc comparisons (LSD) revealed that *Gria1* WT animals made significantly fewer entries into the to-be familiar arm in the exposure phase compared to *Gria1* KO and *Gria1* KO rescue animals (number of entries in *Gria1* WT vs. *Gria1* KO: F(1,21) = 24.424, P = 0.001; *Gria1* WT vs. *Gria1* KO rescue: F(1,21) = 5.648, P = 0.027). However, *Gria1* KO rescue animals made significantly fewer entries into the to-be

familiar arm compared to *Gria1* KO animals (number of entries in *Gria1* KO vs. *Gria1* KO rescue: F(1,21) = 5.538, P = 0.028). Together these data show that *Gria1* KO animals have, on average, made more entries into the to-be familiar arm compared to *Gria1* WT and *Gria1* KO rescue mice. Interestingly, the increase in entries observed in *Gria1* KO mice is partially rescued in *Gria1* KO rescue animals.

Test phase

During the test phase *Gria1* KO mice displayed impaired spatial novelty preference when compared to *Gria1* WT animals. The deficit in *Gria1* KO animals was rescued (borderline significant for novel arm time preference ratio, and significantly for novel arm entries preference ratio) in Gria1 KO rescue animals (**figure 5.6d,e**).

The preference animals show for the novel arm can be expressed as a novel arm time preference ratio. ANOVA with sex and group (*Gria1* WT, *Gria1* KO and *Gria1* KO rescue) as between subject factors revealed an overall significant effect of group, but not sex, and no sex*group interaction on the novel arm time preference ratio (effect of group on novel arm time preference ratio: F(2,21) = 3.909, P = 0.036; effect of sex: F(1,21) = 0.756, P = 0.394; sex*group interaction: F(2,21) = 1.524, P = 0.241).

Post hoc comparisons (LSD) revealed that *Gria1* WT animals displayed significantly greater time preference ratios compared to *Gria1* KO mice (time preference ratio in *Gria1* WT vs. *Gria1* KO: F(1,21) = 8.490, P = 0.008). The time preference ratio was not significantly different in *Gria1* WT and *Gria1* KO rescue animals (time preference ratio in *Gria1* WT vs. *Gria1* KO rescue: F(1,21) = 0.572, P = 0.458). There was a strong trend towards an increased time preference ratio in *Gria1* KO rescue animals compared to *Gria1* KO mice (time preference ratio in *Gria1* KO rescue vs. *Gria1* KO: F(1,21) = 4.063, P = 0.057). In addition, one sample T-tests found that *Gria1* WT and *Gria1* KO rescue, but not *Gria1* KO mice, displayed novel arm time preference ratios

that were significantly above chance (i.e. above 0.5) (*Gria1* WT: t(1,9) = 4.525, P = 0.001; *Gria1* KO rescue: t(1,7) = 3.104, P = 0.017; *Gria1* KO: t(1,8) = 1.543, P = 0.161).

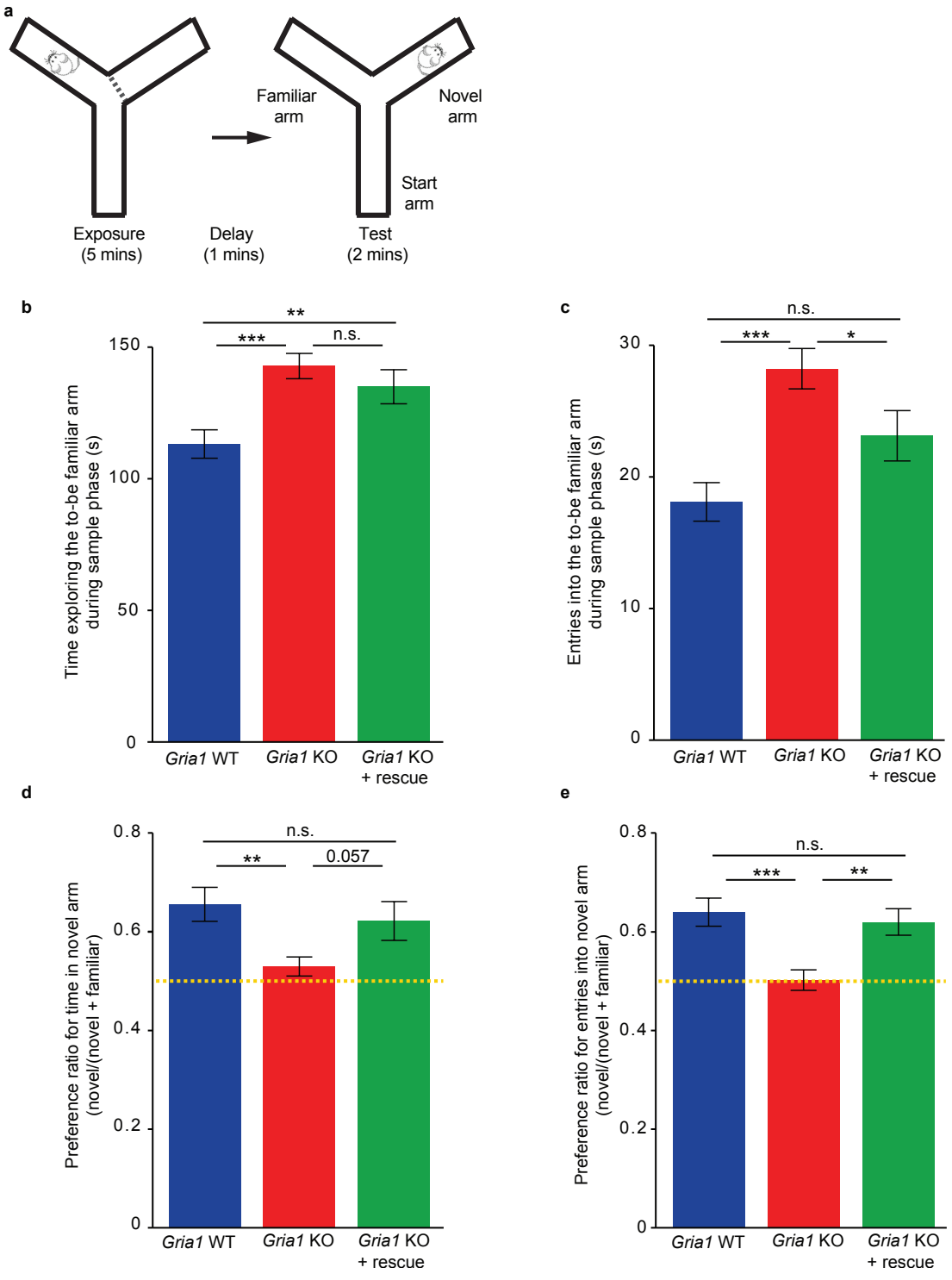

Figure 5.6: Area CA3 re-introduction of GluA1 in *Gria1* KO mice restores short term spatial novelty preference

(a) Schematic representation of the Y-maze novelty preference task. (b) Time spent exploring the to-be familiar arm during the 5-minute exposure phase in *Gria1* WT (blue), *Gria1* KO (red) and *Gria1* KO rescue (green)

animals. (c) Number of entries into the to-be familiar arm during the sample phase. (d) Time preference ratio and (e) entries preference ratio during the test phase. Error bars display S.E.M. Significant stars indicate significant post hoc comparisons (LSD). * $P < 0.05$, ** $P < 0.01$ and *** $P < 0.001$.

Spatial novelty preference can also be assessed by calculating the novel arm entries preference ratio. ANOVA with sex and group (*Gria1* WT, *Gria1* KO and *Gria1* KO rescue) as between subject factors revealed an overall significant effect of group, but not sex, and no sex*group interaction on the novel arm entries preference ratio (effect of group on novel arm entries preference ratio: $F(2,21) = 7.260$, $P = 0.004$; effect of sex: $F(1,21) = 0.782$, $P = 0.386$; sex*group interaction: $F(2,21) = 0.098$, $P = 0.907$). Post hoc comparisons (LSD) revealed that *Gria1* KO mice displayed a reduced novel arm entries preference ratio compared to both *Gria1* WT and *Gria1* KO rescue animals (novel arm entries preference ratio in *Gria1* KO vs. *Gria1* WT: $F(1,21) = 13.670$, $P = 0.001$; *Gria1* KO vs. *Gria1* KO rescue: $F(1,21) = 8.945$, $P = 0.007$). There was no significant difference in the novel arm entries preference ratio in *Gria1* KO rescue and *Gria1* WT animals (novel arm entries preference ratio in *Gria1* KO rescue vs. *Gria1* WT: $F(1,21) = 0.267$, $P = 0.611$). In addition, one sample T-tests found that *Gria1* WT and *Gria1* KO rescue, but not *Gria1* KO mice, displayed novel arm entries preference ratios that were significantly above chance (i.e. above 0.5) (*Gria1* WT: $t(1,9) = 4.915$, $P = 0.001$; *Gria1* KO rescue: $t(1,7) = 4.468$, $P = 0.003$; *Gria1* KO: $t(1,8) = 0.111$, $P = 0.915$).

Together these data suggest that re-introduction of GluA1 preferentially into area CA3 of *Gria1* KO mice is sufficient to rescue short term spatial novelty preference. The rescue is unlikely to be simply due to the increased time *Gria1* KO rescue animals spend exploring during the exposure phase (**figure 5.6b**), since *Gria1* KO mice also

show this increased level of exposure phase exploration of the to-be familiar arm and their performance is not above chance in the test phase.

5.4 Discussion

The present study replicated behavioural deficits in SWM on the T-maze, spatial novelty preference on the Y-maze, and novelty induced hyperactivity, that have been previously reported in *Gria1* KO mice (Bannerman et al., 2004; Procaccini et al., 2013, 2011; Reisel et al., 2002; Sanderson et al., 2009a; Schmitt et al., 2003; Wiedholz et al., 2008). This study sought to determine where in the (mouse) brain GluA1 is required for the expression of normal SWM, spatial novelty preference and novelty induced hyperactivity (or, perhaps, collectively a deficit in short term habituation; see **1.6**). To do this a rescue approach was taken in which GluA1 was re-introduced into *Gria1* KO animals, to test if normal behavioural performance was restored. GluA1 was preferentially reintroduced to area CA3 throughout the hippocampus of *Gria1* KO mice. Despite the subfield specific re-introduction of GluA1 into *Gria1* KO animals, both novelty induced hyperactivity and spatial novelty preference were normalised to levels close to those observed in WT animals. Strikingly, there was no rescue of SWM on the T-maze.

In addition, LFP recordings were made and theta oscillations were assessed in the dorsal hippocampus of *Gria1* KO, *Gria1* WT and *Gria1* KO rescue animas. Recordings were also made from the prefrontal cortex and ventral hippocampus, so prefrontal cortex-hippocampal coherence could be investigated in *Gria1* KO, *Gria1* WT and *Gria1* KO rescue animals. As mentioned, there was variation in electrode placements in the prefrontal cortex and ventral hippocampus. This has prevented prefrontal-hippocampal coherence analysis at this stage. Theta power was elevated in *Gria1* KO animals and was normalised by viral re-introduction of GluA1 to area CA3. This study

reports a hitherto unidentified role of area CA3 GluA1 in regulating the power of dorsal hippocampal theta oscillation, that could not be simply explained by differences in running speed.

5.4.1 Preference of AAV5-hSyn-GluA1 virus for area CA3

The AAV5-hSyn-GluA1 rescue virus was able to reintroduce GluA1 in *Gria1* KO mice but expression of GluA1 was preferentially in area CA3. This subfield specific rescue was unexpected and the mechanism for this specificity is not known. For example, it is not known if the virus is only able to transfect area CA3 neurons, or whether the virus does indeed transfect all subfields of the hippocampus, with transcription and/or translation being suppressed in areas other than CA3.

The expression levels of GluA1 in rescue animals were not quantitatively assessed, so it is not known to what extent the levels of GluA1 in *Gria1* KO rescue animals compare to that of *Gria1* WT mice. It remains possible that GluA1 is even being over-expressed in CA3 to levels greater than in *Gria1* WT mice in CA3. In the future, fresh tissue could be dissected from *Gria1* KO rescue and *Gria1* WT control animals, and different hippocampal subfields dissected. Then SDS-PAGE and western blot analysis could then be used to measure levels of GluA1 following viral rescue.

Furthermore, although the hSyn promoter is predicted to drive expression in both excitatory and inhibitory neurons (Nathanson et al., 2009), this has not been assessed. Immunohistochemistry and confocal microscopy could be used to investigate whether virally reintroduced GluA1 co-localises with markers of specific neuronal types. It would be particularly interesting to assess if GluA1 is reintroduced to PV positive interneurons, since Fuchs *et al.* showed that GluA1 KO from PV interneurons is sufficient to induce robust deficits in SWM (assessed on the T-maze) and novel object recognition (Fuchs et al., 2007).

Re-introduction of GluA1 to the CA3 subfield extended throughout the dorsal and ventral hippocampus (see **figure 5.2**). However, levels of expression have not been quantified. Although immunohistochemistry is considered only semi-quantitative at best, it would be possible to compare the "fluorescence intensity" of GluA1 observed in *Gria1* KO rescue compared to *Gria1* WT control animals. This would give a rough guide to the extent of the GluA1 rescue along the anterior/posterior (AP) axis of the hippocampus, and would complement a more quantitative assessment of protein levels with SDS-PAGE and western blots (**see above**).

5.4.2 Viral re-introduction of GluA1 to area CA3 of *Gria1* KO mice rescues novelty induced hyperactivity

Novelty induced hyperactivity is a robust phenotype of Gria1 KO mice (Barkus et al., 2012; Procaccini et al., 2011, 2013; Wiedholz et al., 2008). It is possible that a failure of short term habituation underlies the novelty induced hyperactivity in *Gria1* KO mice, as failure to habituate to an environment will result in environmental cues staying apparently "novel" for longer, driving exploratory behaviour. *Gria1* KO hyperactivity could be linked to abnormal activation of the hippocampus, as levels of the immediate early gene, cFos, are elevated in the hippocampus of *Gria1* KO animals to a greater extent than in WT controls upon exposure to a novel environment (Procaccini et al., 2011, 2013). Here, it is shown that re-introduction of GluA1 preferentially to area CA3 of *Gria1* KO mice is sufficient to rescue novelty induced hyperactivity.

Two studies are of particular interest when assessing where in the brain GluA1 is required for normal novelty induced hyperactivity. Firstly, Freudenberg *et al.* recently (un-published at time of initiating experiments in this thesis) showed that viral re-introduction of GluA1 throughout all subfields of the hippocampus in *Gria1* KO mice was sufficient to rescue novelty induced hyperactivity (Freudenberg et al., 2016). This

strongly implicates GluA1 in the hippocampus as being, at least partially, responsible for the novelty induced hyperactivity seen in *Gria1* KO mice. Using a different approach, Schmitt *et al.* had previously reintroduced GluA1 into the forebrain of *Gria1* KO mice using a genetic strategy that targeted excitatory neurons throughout the cortex and the hippocampus (Schmitt et al., 2005). In the hippocampus, GluA1 rescue was present in around 69% of the dorsal and 40% of the ventral CA1, with expression almost completely absent in the CA3 (there was also expression of GluA1 in the DG but this was not assessed; Schmitt et al., 2005). In these mice there was no significant rescue of novelty induced hyperactivity (although there was a slight numerical trend towards decreased activity in the rescue animals compared to the complete KO animals), despite a partial rescue of SWM on the T-maze and radial maze (Schmitt et al., 2005). This suggests that alone, re-introduction of GluA1 to the CA1 and DG (and forebrain excitatory cortical neurons), is not sufficient to rescue novelty induced hyperactivity to the levels of WT animals. Collectively, these studies suggest that GluA1 in area CA3 could be particularly important for normal novelty induced activity levels in rodents.

5.4.3 Viral re-introduction of GluA1 to area CA3 of *Gria1* KO mice fails to rescue SWM on the T-maze

In this study a modified version of the T-maze was used, such that electrophysiological recordings could be made without the animals being picked up between trials. To this end, animals were trained to run back to the start arm following both the sample and choice runs. It is possible that this could change the psychological processes required for the task. Nevertheless, despite the protocol modifications, there was still a pronounced deficit in *Gria1* KO animals compared to WT controls (KOs exhibited essentially chance levels of performance), replicating a large body of literature

showing *Gria1* KO mice display impaired SWM (Reisel et al., 2002; Schmitt et al., 2003, 2005).

Notably, SWM performance was not restored in *Gria1* KO rescue animals, suggesting that GluA1 in the CA3 subfield is not sufficient to rescue SWM on the T-maze (however see **appendix 7.3.2**). This is in line with the recent study by Freudenberg *et al.*, who find GluA1 rescue in all subfields of the hippocampus fails to rescue T-maze performance (Freudenberg et al., 2016). In addition, the same group previously used a viral-*Cre* approach in mice harbouring *LoxP* sites flanking a critical exon of the *Gria1* gene ($Gria1^{fl/fl}$) to delete GluA1 selectively from the dorsal or ventral hippocampus (Freudenberg et al., 2013). Conditional deletion of GluA1 from the dorsal or ventral hippocampus only mildly impaired SWM performance on the T-maze, leading to the conclusion that GluA1 was likely also required in brain structures outside of the hippocampus (Freudenberg et al., 2013). In contrast, Schmitt *et al.* found that forebrain re-introduction of GluA1 in *Gria1* KO animals led to a partial, but significant, rescue of SWM on the T-maze (Schmitt et al., 2005). Thus, it could be GluA1 in forebrain cortical excitatory neurons that is indispensable for SWM performance on the T-maze.

5.4.4 Viral re-introduction of GluA1 to area CA3 of *Gria1* KO mice rescues spatial novelty preference

Short term spatial novelty preference was impaired in *Gria1* KO mice, in line with previous studies (Sanderson et al., 2007, 2009a). Remarkably, the performance of *Gria1* KO rescue animals was comparable to controls, indicating that GluA1 re-introduction to area CA3 is sufficient to support intact short term spatial novelty preference. Statistically, the rescue in this study was only significant when looking at the novel arm entries preference ratio but there was a strong trend towards rescued performance when looking at the novel arm time preference ratio as well. These

results are in line with the recent study of Freudenberg *et al.*, that reintroduced GluA1 into the entire hippocampus and found a partial (although not strictly statistically significant) rescue of spatial novelty preference assessed with an identical behavioural protocol (Freudenberg et al., 2016; un-published when experiments in this thesis were conducted).

It has been suggested that both spatial novelty preference and SWM on the T-maze require GluA1-dependent short term habituation for task performance (Sanderson and Bannerman, 2012). It is interesting that T-maze performance is not rescued, whilst spatial novelty preference is restored, when GluA1 is reintroduced preferentially to area CA3 in *Gria1* KO animals. It is possible that performance on the two tasks require different psychological processes, that required GluA1 in area CA3 to different extents. For example, it is possible that rewarded alternation on the T-maze is more difficult for animals than spatial novelty preference because of proactive interference due to memories from previous trials (Deacon and Rawlins, 2006). Novelty preference tested on the Y-maze is a single trial test and thus not influenced by proactive interference from previous trials. It would be interesting to test the *Gria1* WT, *Gria1* KO and *Gria1* KO rescue animals for spontaneous alternation on the T-maze (Deacon and Rawlins, 2006). Typically, animals are given one trial each morning and afternoon for several days, thereby decreasing proactive interference. *Gria1* KO mice are also impaired on this version of the task (Bannerman et al., 2004), so it would be interesting to see if *Gria1* KO rescue can normalise spontaneous alternation on the T-maze.

Another difference between the two tasks is the degree of ambiguity which they elicit. In the T-maze animals need to make a decision as to which of the two identical grey arms they should run down to collect a food reward. This is expected to generate high levels of ambiguity, as both arms are identical, and both are associated with a food

reward. Whilst the Y-maze is similar in this respect, the Y-maze arms are arguably less ambiguous because the arms have not previously been associated with a food reward and therefore will not elicit a conditioned response like the goal arms of the T-maze. Therefore, it is possible that *Gria1* KO rescue animals struggle with the highly ambiguous nature of the two goal arms of the T-maze and thus show poor level of alternation. In the Y-maze the ambiguity is possibly lower, potentially explaining why *Gria1* KO rescue animals are able to perform the task normally.

One interesting phenotype of *Gria1* KO mice is the enhanced long term spatial novelty preference (or long term habituation), observed under certain testing conditions with multiple sample trials (Sanderson et al., 2009a). Whilst not strictly a deficit, *Gria1* KO mice under these conditions display memory that is not present in WT mice, thus the memory could be considered abnormal. The neuronal circuitry underlying enhanced long term habituation performance in *Gria1* KO mice is not known. It would be interesting to see if GluA1 re-introduction preferentially in area CA3 of the hippocampus can normalise long term spatial novelty preference in *Gria1* KO mice.

5.4.5 Viral re-introduction of GluA1 to area CA3 of *Gria1* KO mice normalises theta power

In this study, theta oscillations were measured in the dorsal hippocampus whilst animals explored a novel environment. Theta power in *Gria1* KO mice was elevated compared to *Gria1* WT controls. In addition, the peak theta frequency was decreased numerically in *Gria1* KO mice, although this was not statistically significant when running speed was included as a covariate in the analysis but notably this is in the opposite direction to what is expected based on previous studies (Bender et al., 2015). Interestingly, viral re-introduction of GluA1 preferentially in area CA3 normalised theta power to levels observed in *Gria1* WT controls. Output from CA3 pyramidal neurons

to CA1 pyramidal neurons (Shaffer collaterals) is known to contribute to CA1 theta (Buzsáki, 2002), providing a means by which manipulation of area CA3 could influence the theta oscillations recorded in the present study. These data suggest a role for GluA1 in regulating theta power, either at the molecular level influencing oscillation generation and/or by altering the expression of a psychological process that can regulate and/or influence theta power.

The peak theta frequency was slower in *Gria1* KO mice. As the reduced theta speed was not rescued when GluA1 was reintroduced into area CA3 of *Gria1* KO mice, it suggests a role of GluA1 in other brain regions (or other hippocampal subfields) in regulating hippocampal theta speed. One candidate brain structure is the medial septum (MS) that sends inhibitory projections to the hippocampus, which have been identified as being key in the regulation of hippocampal theta oscillations (Bender et al., 2015; Buzsáki, 2002).

It is important to consider that the elevated theta power in *Gria1* KO mice could result from their pronounced novelty-induced hyperactivity, since theta power and peak theta frequency have been shown to be sensitive to running speed (Bender et al., 2015; McFarland et al., 1975). In an attempt to control for this, the average running speed was included as a covariate when analysing theta power. Thus, it appears that the elevated theta power in *Gria1* KO animals is not due to their hyperactivity alone. Re-introduction of GluA1 preferentially in area CA3 in *Gria1* KO mice normalised both the elevated theta power and novelty induced hyperactivity.

It is hard to determine causality in these experiments. For example, is the reduction of theta power a result of behavioural rescue of novelty induced hyperactivity? Or, is novelty induced hyperactivity rescued as a result of the reduced theta power? To address these questions, recordings could be made from animals that are

behaviourally matched for locomotor activity. This could be achieved with electrophysiology recordings in the home cage, where *Gria1* KO animals do not show hyperactivity (Fitzgerald et al., 2010). If theta power is equivalent in *Gria1* WT, *Gria1* KO and *Gria1* KO rescue animals whilst in the home cage, it would suggest that theta oscillations could be influenced by the novelty of the environment and the effects of GluA1 ablation on habituation. In contrast, if the group differences remain (i.e. greater theta power in *Gria1* KO mice) it would possibly suggest that theta power is being driven by inherent circuit differences in *Gria1* KO animals, irrespective of behavioural state. It is perhaps unlikely that increased theta power is directly driving hyperlocomotion in *Gria1* KO animals, as artificially induced theta oscillations in CA1, via optogenetic activation of MS-CA1 inhibitory interneuron projections, did not cause stationary animals to initiate movement (Bender et al., 2015).

5.4.6 Conclusions

In summary, data in this chapter indicate that expression of GluA1 preferentially in area CA3 could be particularly important for the expression of normal spatial novelty preference, normal locomotor activity levels upon exposure to a novel environment, and normal power of dorsal hippocampus theta oscillations. Post mortem data have indicated that there is reduced expression of GluA1 in schizophrenia, and it is interesting to note that at the level of mRNA, area CA3 (along with DG) seems to be preferentially affected (Eastwood et al., 1995). *Gria1* KO mice could be useful as a tool for studying the biology underlying psychological processes (habituation and sensitisation) related to schizophrenia (Barkus et al., 2012, 2014; Fitzgerald et al., 2010). It would therefore be interesting to investigate the extent to which area CA3 GluA1 is required for behaviours such as habituation and sensitisation that could be

relevant to the aberrant salience theory of schizophrenia (Barkus et al., 2014; Kapur, 2003).

6 General Discussion

An overarching theme of the thesis was to explore if manipulation of glutamate receptors can result in schizophrenia relevant behavioural deficits in mice. Another major and overlapping focus of the thesis was experimental testing of the Lisman/Grace model of the pathophysiology of schizophrenia. Initially, the behavioural phenotype of mice lacking NMDARs selectively from PV neurons was scrutinised, with and without pharmacological challenge. Secondly, a chemogenetic approach was taken to acutely manipulate the activity of PV interneurons *in vivo*, whilst animals were tested for schizophrenia-relevant behaviours. Finally, working backwards from an established behavioural phenotype, a rescue approach was utilised and GluA1 was reintroduced into *Gria1* KO mice, to test where in the brain GluA1 is required for schizophrenia-relevant behaviours. Electrophysiology recordings were made from these animals with the intention to assess long range synchrony between prefrontal cortex and the hippocampus. However, variability in the electrode recordings sites in the prefrontal cortex and ventral hippocampus has, at this stage, limited analysis to oscillatory activity in the dorsal hippocampus.

Results from each chapter will be summarised and, where possible, considered within the framework of the Lisman/Grace model, which this thesis set out to test. Limitations of the techniques used have been mentioned throughout the thesis but will be revisited with suggestions for future experiments to address unanswered questions.

6.1 Chapter 2 summary: “Normal” phenotype of *Grin1*$^{\Delta PV}$ mice

Experiments in chapter 2 explored the behavioural phenotype of mice lacking NMDARs specifically on PV interneurons. Based on predictions from the Lisman/Grace model, such animals should display a wide range of schizophrenia-relevant behavioural deficits. However, *Grin1*$^{\Delta PV}$ mice appeared largely normal,

displaying only mild phenotypes. These “mild” phenotypes of *Grin1*$^{\Delta PV}$ mice consisted of age-dependent novelty induced hyperactivity, reduced anxiety in young animals and a transient, and subtle, decrease in SWM performance on the T-maze, again in young animals. The SWM effect was not consistent with a SWM impairment *per se*, and instead likely reflects changes in the task parameters that could influence the arousal level of the animal.

These results were surprising given the strong cognitive deficits reported in the first two publications with similar animals (Belforte et al., 2010; Korotkova et al., 2010). Differences in the *Cre* lines used have been extensively discussed (see **1.8.4** and **2.4**), but warrant further discussion as they could explain behavioural differences between not only *Grin1*$^{\Delta PV}$ mice but also the results of Murray *et al.* with the data presented in chapter 4 (Murray et al., 2011). The PV^{cre} line used in this thesis had both high coverage of PV interneurons (i.e. it targeted the vast majority of PV interneurons) and a high level of specificity (i.e. the vast majority of *Cre* positive cells were also PV positive). This is in agreement with previous studies that also validated the same *Cre* line (Carlén et al., 2012; Nassar et al., 2015; Sohal et al., 2009). The PV^{cre} line used to generate the first PV specific NR1 KOs is different to the *Cre* line used in this thesis (Fuchs et al., 2007; Korotkova et al., 2010). This line has not been as rigorously tested for specificity and the importance of hippocampus selectivity of PV neuron targeting is also not clear. The phenotype of *Grin1*$^{\Delta PV}$ mice generated using this *Cre* line shows strong deficits compared to two other recent publications (Billingslea et al., 2014; Saunders et al., 2013), and also to the data presented in this thesis (see **chapter 2**). It is therefore plausible that results from the original study are driven by the PV^{Cre} line used, either as a consequence of NR1 deletions selectively from PV neurons in the

hippocampus, or due to a lack of specificity in the targeting of PV interneurons (which is not as well characterised) resulting in the ablation of NMDARs from other neurons. It is also possible that behavioural deficits in *Grin1*$^{\Delta Ppp1r2}$ mice (the first such interneuron specific NR1 KO animals generated) are being driven, at least in part, by expression of *Cre* in excitatory pyramidal neurons or other interneurons. A qualitative assessment of this line was made in this thesis (results presented in appendix, see **7.1**), which indicated extensive expression of *Cre* in pyramidal neurons in area CA1 as early as 16 weeks of age. Thus, the wide range of "schizophrenia-related" behavioural deficits that *Grin1*$^{\Delta Ppp1r2}$ mice show might not be due to NR1 ablation from interneurons only. Taken together, these results highlight that *Cre* lines **must** be thoroughly validated for specificity and coverage of the expected target neuron population.

Nevertheless, robust novelty-induced hyperactivity was observed in older *Grin1*$^{\Delta PV}$ mice. This phenotype is interesting and does potentially support the Lisman/Grace model where disinhibition of the hippocampus can drive a hyperdopaminergic state promoting enhanced locomotor activity (Floresco et al., 2001; Lisman et al., 2008).

6.1.2 Chapter 2 unanswered questions

Results from this chapter indicated a largely normal phenotype of *Grin1*$^{\Delta PV}$ animals. Why is the phenotype so mild? It is possible that gene*environmental risk factors could interact with the genetic manipulation to uncover behavioural deficits in *Grin1*$^{\Delta PV}$ animals (see **2.4.4**). For example, social isolation stress has been shown to exacerbate symptoms of *Grin1*$^{\Delta Ppp1r2}$ mice (Jiang et al., 2013). Therefore, it remains possible that raising *Grin1*$^{\Delta PV}$ animals in social isolation (Jiang et al., 2013), or with reduced environmental enrichment (Donato et al., 2013), could reveal behavioural

deficits. Differences in housing and environmental enrichment could also contribute to the different outcomes (behavioural) in different studies with *Grin1*$^{\Delta PV}$ and *Grin1*$^{\Delta Ppp1r2}$ mice. Therefore the phenotype of *Grin1*$^{\Delta PV}$ animals could be assessed following exposure to such environmental stressors.

Despite the overall mild phenotype of *Grin1*$^{\Delta PV}$ animals, novelty induced hyperactivity was observed in older animals. The Lisman/Grace model could explain this phenotype via disinhibition of glutamatergic output from the hippocampus and subsequently increased activity of dopamine neurons in the VTA (Floresco et al., 2001; Lisman et al., 2008). It would be interesting to record the electrical activity of dopamine neurons in the VTA of *Grin1*$^{\Delta PV}$ animals to see if there are more spontaneously active dopamine neurons as the Lisman/Grace model would predict.

6.2 Chapter 3 summary: *Grin1*$^{\Delta PV}$ mice appear sensitised to the effects of MK-801

Chapter 3 explored the idea that NMDAR antagonists, such as MK-801, preferentially exert their effects via NMDARs located on PV interneurons. PV interneurons are well placed in the circuit to regulate the excitation/inhibition balance of neuronal circuits. It has been suggested that the overall disinhibition that follows NMDAR antagonist challenge is a result of inhibitory interneurons being more sensitive to blockade of NMDARs than excitatory pyramidal neurons (Homayoun and Moghaddam, 2007). Experimental evidence that PV interneurons were the “preferential” target of MK-801 came from two studies that found that *Grin1*$^{\Delta PV}$ and *Grin1*$^{\Delta Ppp1r2}$ animals displayed a reduced locomotor response to MK-801 challenge (Belforte et al., 2010; Carlén et al., 2012).

Data in this thesis clearly reproduce an attenuated locomotor response following MK-801 challenge in *Grin1*$^{\Delta PV}$ mice. However, closer inspection of the animals indicated that this might not be via a "protection" mechanism as previously thought. In fact, all the data in chapter 3 indicated that *Grin1*$^{\Delta PV}$ animals are actually sensitised to the effects of MK-801. The attenuated locomotor response is easily explained since *Grin1*$^{\Delta PV}$ animals enter a flat-state following MK-801 challenge (which was never observed in controls). In subsequent experiments assessing motor coordination (rotarod), anhedonia (sucrose preference) and SWM (T-maze alternation), *Grin1*$^{\Delta PV}$ animals were clearly more susceptible to MK-801-induced impairments.

Interestingly, *Grin1*$^{\Delta PV}$ animals were also sensitised to MK-801-induced increases in delta oscillation power recorded in the prefrontal cortex. There is evidence that NMDAR antagonists can induce delta oscillations *in vitro* (Zang et al., 2009). In addition, schizophrenic patients appear to have elevated delta oscillation power (Boutros et al., 2008; Galderisi et al., 2009). *In vivo*, MK-801 induced greater increases in delta oscillation power in *Grin1*$^{\Delta PV}$ animals compared to controls (see **3.3.6**). Taken together, results in chapter 3 provide evidence that the effects of MK-801 are **not** mediated preferentially via NMDARs on PV interneurons. Instead, genetic ablation of NMDARs from PV interneurons sensitised mice to the effects of MK-801, indicating that loss of NMDARs from PV interneurons could serve as a risk factor that exacerbates the effects of NMDAR antagonists in other parts of the circuit or on other cell types.

6.2.1 Chapter 3 unanswered questions

It would be interesting to test whether the sensitisation to MK-801 observed in this study is specific to MK-801, or a feature of all NMDAR antagonists. It would therefore be valuable to repeat these experiments with a battery of other NMDAR antagonists.

It is possible that other NMDAR antagonists will have different effects, especially considering that rats challenged with different NMDAR antagonists showed highly variable behavioural effects (Gilmour et al., 2009).

It would also be interesting to explore potential mechanisms underlying the decrease in SWM performance in *Grin1*$^{\Delta PV}$ mice following challenge with intermediate (0.15 and 0.2 mg/kg) doses of MK-801. Long range theta frequency coherence between medial prefrontal cortex and the hippocampus is thought to be important for SWM performance. It is possible that there is selective breakdown in prefrontal - hippocampal coherence in *Grin1*$^{\Delta PV}$ animals following MK-801 challenge. In the future, electrophysiology recordings could be made as *Grin1*$^{\Delta PV}$ animals perform a SWM task on the T-maze, with and without MK-801 challenge.

In addition, it would be important to explore whether MK-801-induced cognitive impairments in *Grin1*$^{\Delta PV}$ animals extend to deficits in SRM or even to tasks that are not dependent on the hippocampus. To assess this, animals could be tested on a visual discrimination task in the T-maze known to be hippocampus-independent (von Engelhardt et al., 2008). This would help to identify the psychological process being affected in *Grin1*$^{\Delta PV}$ mice following MK-801 challenge. If the underlying psychological process can be identified, then it will help narrow the search for the neural mechanism(s) involved. In addition, when considering the translational link of research in rodents through to humans, it is important to establish that the psychological processes that are being studied in rodent models are indeed the same as those in humans.

6.3 Chapter 4 summary: Acute silencing of PV interneurons does not induce schizophrenia-relevant behavioural deficits

Driven by the subtle phenotypes identified in *Grin1*$^{\Delta PV}$ mice in chapter 2, a more direct approach was taken in chapter 4 to acutely silence PV interneurons using the DREADD tool hM4Di. In particular, PV interneurons in area CA1 were targeted (although there was not complete subfield specificity), based on previous studies that found an important role of PV interneurons in the dorsal CA1 for SWM performance (Murray et al., 2011; but see **6.1** for potential caveats with this *Cre* line). *In vitro* electrophysiology experiments confirmed that hM4Di was capable of decreasing the activity of PV interneurons following the addition of CNO. However, in contrast to expectations, silencing of PV interneurons in either the dorsal or ventral CA1 did not induce novelty-induced hyperactivity or deficits in Y-maze novelty preference or SWM (T-maze alternation). It is unlikely that these negative results reflect the inability of hM4Di to silence PV interneurons *in vivo*, since targeting PV interneurons throughout the entire hippocampus with hM4Di induced a seizure in one animal, demonstrating a likely effect of hM4Di-mediated PV interneuron silencing on network activity.

It is of course possible that activity of PV interneurons in area CA1 is not required for the behaviours tested in this study. However, there is a large caveat to this conclusion, as not all CA1 PV interneurons were targeted with hM4Di at the injection site and even less so further away from this site. In fact, the efficiency of PV interneuron targeting in this study appears to be lower than in two previous studies (Murray et al., 2011; Nguyen et al., 2014; and discussed extensively in **4.4**). Therefore, it remains possible that more complete targeting of CA1 PV interneurons would induce behavioural deficits on the tasks employed in this thesis. In addition, it is also possible that the

behavioural tasks used in this study were not sensitive enough to detect the effect of hM4Di-mediated PV interneuron silencing although this seems unlikely.

Taken together results from this chapter suggest that silencing (or reducing the activity of) a population of PV interneurons, preferentially in area CA1 of the dorsal or ventral hippocampus, is unable to induce schizophrenia-like behavioural deficits. This observation is particularly interesting since a previous study suggests that hM4Di-mediated silencing of PV interneurons in the ventral hippocampus (including area CA1 and CA3) is able to induce schizophrenia-relevant behavioural deficits (Nguyen et al., 2014). These results suggest, albeit tentatively, that PV interneurons in area CA3 could be particularly important for inducing schizophrenia-like behavioural deficits. However, it is also possible that there is a mass-action effect, where Nguyen *et al.* simply targeted more hippocampal PV interneurons than in the present study (Nguyen et al., 2014). The area CA1 vs. CA3 function of PV interneurons will be discussed again with respect to the generation of gamma oscillations (see **6.7**). Overall, the data from chapter 2 and chapter 4 suggest that two different manipulations of PV interneurons are largely unable to induce schizophrenia-related behavioural deficits. This questions the key role that PV interneurons play in the pathophysiology of schizophrenia although important caveats remain as described above.

6.3.1 Chapter 4 unanswered questions

It would be interesting to explore the effect of more extensive PV interneuron silencing in area CA1 throughout the entire hippocampus. This would enable firmer conclusions to be made about the contribution of area CA1 PV interneurons to behaviours relevant to schizophrenia. Likewise, it would also be interesting to test the effect of CA3-specific PV interneuron silencing. However, both of the above experiments are technically challenging, as it is very difficult to specifically target subfields of the hippocampus

with stereotaxic viral injections, especially since the shape of the hippocampus changes so dramatically along the anterior/posterior axis.

It would be informative to record local field potentials in the hippocampus whilst PV interneurons are acutely silenced with hM4Di in awake, behaving animals. This would enable the effect on the network to be monitored following PV neuron silencing. In particular, it would be interesting to investigate if gamma oscillations are modulated following PV interneuron silencing, in both area CA1 and area CA3 (see **6.7**).

6.4 Chapter 5 summary: re-introduction of GluA1 to area CA3 of *Gria1* KO mice rescues some schizophrenia-relevant behaviours

Chapter 5 had two main aims. The first was to establish where in the brain GluA1 is required in order to rescue schizophrenia-related behaviours. The second aim was to measure long range coherence between the prefrontal cortex and hippocampus in awake, behaving animals. With respect to the latter, less progress was made as variability in electrode recording sites in the prefrontal cortex and ventral hippocampus limited the initial analysis to recordings made from the dorsal hippocampus. Substantially greater progress was made in trying to address where in the brain GluA1 was required to rescue schizophrenia-related behavioural deficits in *Gria1* KO animals.

Using a viral rescue approach, GluA1 was introduced to the hippocampus of *Gria1* KO animals. Surprisingly, this approach led to preferential expression of GluA1 in area CA3. Remarkably, re-introduction of GluA1 preferentially into area CA3 was able to rescue novelty induced hyperactivity and Y-maze spatial novelty preference. SWM assessed on the T-maze was not rescued, and possibilities for the selective rescue of spatial novelty preference and hyperactivity have been discussed above (see **5.4.4**).

These results build upon the finding that re-introduction of GluA1 into all subfields of the hippocampus can rescue novelty-induced hyperactivity, and at least numerically, rescue spatial novelty preference (Freudenberg et al., 2016), by highlighting a key role of GluA1 in area CA3.

Electrophysiology recordings in dorsal hippocampus revealed that *Gria1* KO animals have elevated theta oscillation power when exploring a novel environment. Remarkably, this elevated theta power was normalised to wildtype levels in *Gria1* KO animals with GluA1 reintroduced preferentially in area CA3. These changes could not simply be attributed to differences in animal running speed, and indicate a previously unknown role of GluA1, particularly in area CA3, in the regulation of theta oscillation power either directly or indirectly. How elevated theta power in *Gria1* KO mice relates to their behavioural abnormality is less clear. Nevertheless, it is tempting to speculate that the elevated theta power in *Gria1* KO animals reflects their failure to habituate to the environment which they are exploring. Theta power in the hippocampus measured whilst rats run on a linear track has been shown to decrease after animals have run many trials, potentially linking the process of habituation to a decrease in theta power although there are other possible explanations (Hinman et al., 2011).

6.4.1 Chapter 5 unanswered questions

A number of unanswered questions arise from this study. Firstly, it is very important to establish the specificity of GluA1 rescue for area CA3 to establish whether GluA1 re-introduction to other subfields is contributing to the phenotype. Methods to assess this have been proposed (see **5.4.1**). It will be interesting to test if the rescue approach used in this study is able to rescue other behavioural deficits in *Gria1* KO animals. Arguably one of the most schizophrenia-relevant behavioural phenotypes of *Gria1* KO animals is stimulus-specific short term sensitisation (Sanderson et al., 2011; also see

5.1.4). It would be interesting to test if viral re-introduction of GluA1 preferentially to area CA3 could rescue the sensitisation seen in *Gria1* KO animals. It would also be informative to generate CA3 specific *Gria1* KO animals, by crossing a CA3 specific *Cre* driver line (Nakazawa et al., 2002) and "floxed" *Gria1* (Fuchs et al., 2007) animals together. This will enable testing of whether GluA1 in area CA3 is necessary for behaviours such as novelty-induced hyperactivity and spatial novelty preference.

In addition, these experiments provide a unique opportunity to test how subtle manipulations to the GluA1 subunit can influence novelty induced hyperactivity. The GluA1 subunit can be phosphorylated at two sites on its intracellular cytoplasmic C-terminus (Shepherd and Huganir, 2007). It would be interesting to re-design a GluA1 rescue virus with these phosphorylation sites mutated such that they can no longer be phosphorylated. Then the necessity of these phosphorylation sites for behaviours such as novelty induced hyperactivity and spatial novelty preference could be tested by reintroducing this modified GluA1 into *Gria1* KO animals.

With respect to electrophysiology there are important unanswered questions. It remains unknown if long range prefrontal-hippocampal synchrony/coherence is disrupted in *Gria1* KO animals. It would be particularly interesting to assess this whilst animals are performing a SWM task on the T-maze.

6.5 How do experiments in this thesis fit within the Lisman/Grace framework?

The novelty induced hyperactivity of *Grin1*$^{\Delta PV}$ animals supports the Lisman/Grace model. However, as yet one can only speculate that this phenotype arises due to dysfunction of hippocampal circuits. Novel tools from the Sternson lab provide a means of selectively and acutely blocking NMDARs in a cell-type specific manner (Yang et al., 2015; see **2.4.4**). This means it would now be possible to acutely block

NMDARs on PV interneurons in the hippocampus. If selectively blocking NMDARs on PV interneurons in the hippocampus was able to generate novelty-induced hyperactivity, as observed in *Grin1*$^{\Delta PV}$ animals, then it would provide strong evidence that it is indeed dysregulation of hippocampal circuits that leads to this phenotype.

The observation that *Grin1*$^{\Delta PV}$ animals are sensitised to challenge with MK-801 argues that PV interneurons are not the only targets of NMDAR antagonists. This is at odds with the Lisman/Grace model, and suggests that NMDARs on other interneurons could mediate the disinhibition observed following NMDAR challenge. Behavioural deficits observed following MK-801 challenge are also compatible with blockade of NMDARs on excitatory neurons (Bannerman et al., 2012; Tatard-Leitman et al., 2014; von Engelhardt et al., 2008). However, at the physiological level, blockade of NMDARs on excitatory neurons would require a circuit level explanation of the overall increase in activity seen in the network following NMDAR antagonist challenge (Homayoun and Moghaddam, 2007).

As the Lisman/Grace model predicts that reduced output of PV interneurons in the hippocampus is central to the pathophysiology of schizophrenia, it was surprising that hM4Di-mediated silencing of PV interneurons did not induce schizophrenia-relevant behavioural deficits including locomotor hyperactivity. Therefore, the results in this thesis argue, albeit with caveats, against the Lisman/Grace model. Caution must be taken when interpreting the negative results presented here, since only a sub-population of PV interneurons were targeted within area CA1. As discussed, more extensive PV interneuron silencing could well induce schizophrenia-relevant deficits, like those reported with greater targeting of PV interneurons in the ventral hippocampus (Nguyen et al., 2014).

Hyperactivity in *Gria1* KO animals could result from over activity of hippocampal circuits, possibly reflected in the elevated theta power observed in the dorsal hippocampus of *Gria1* KO animals. Evidence for this also comes from elevated levels of cFos expression in the hippocampus of *Gria1* KO animals following exposure to a novel environment (Procaccini et al., 2011, 2013). Experiments in this thesis indicate that re-introduction of GluA1 preferentially to area CA3 can rescue novelty-induced hyperactivity. It is therefore tempting to speculate that the rescue of hyperactivity in this study could be a result of reducing hippocampal over-activation. Consistent with this possibility is the rescue of elevated theta power in the dorsal hippocampus when GluA1 was re-introduced preferentially to area CA3 of *Gria1* KO animals. This could also be tested by assessing cFos activation levels in *Gria1* KO rescue animals, following exposure to a novel environment. In addition, if there is an overactive hippocampus in *Gria1* KO mice then, based on the Lisman/Grace model, predictions can be made about the activity of dopamine neurons in the VTA in *Gria1* KO animals.

6.6 General considerations for the role of NMDARs on PV interneurons for gamma oscillation generation

The Lisman/Grace model links NMDAR hypofunction on PV interneurons to reduced gamma oscillations, that could underlie cognitive deficits in schizophrenia (Lisman et al., 2008). However, there are potential problems with this interpretation, as the role of NMDAR currents in the excitation of PV interneurons in adulthood has possibly been overstated (Wang and Gao, 2010). Gamma oscillations require fast feedback inhibition from PV interneurons onto pyramidal neurons, and this in turn is dependent on fast and reliable excitation of PV interneurons through glutamatergic input from pyramidal neurons (Mann et al., 2005). Computational modelling studies have identified that AMPAR currents are better suited to the fast excitation required for

gamma oscillation generation because they have shorter post synaptic currents compared with NMDAR currents (Rotaru et al., 2013, 2011). There is experimental evidence for this as ablation of the GluA1 AMPAR receptor subunit from PV interneurons (*Gria1*$^{\Delta PV}$ mice) reduces the power of gamma oscillations recorded from the hippocampus *in vitro* (Fuchs et al., 2007). In line with predictions from computational models (Rotaru et al., 2011), *Grin1*$^{\Delta PV}$ mice actually show enhanced gamma oscillation power *in vivo* under baseline conditions (Carlén et al., 2012; Korotkova et al., 2010). These data question the Lisman/Grace model in which reduced NMDAR currents on PV interneurons contribute to reduced gamma oscillation power (Lisman et al., 2008).

6.7 Do PV interneurons contribute to gamma oscillations in area CA1?

Silencing of PV interneurons in CA1 was expected to induce cognitive deficits based on previous studies (Murray et al., 2011; Nguyen et al., 2014), and also because PV interneurons have been proposed to be critical for the induction of gamma oscillations (Sohal et al., 2009). Mechanisms regulating the generation and control of gamma oscillations are commonly studied *in vitro*. Gamma oscillations can be induced in acute hippocampal slices following bath application of the muscarinic agonist carbachol (Fisahn et al., 1998), or local pressure application of kainate (Gloveli et al., 2005). Computational models predict that at least two mechanisms can support gamma oscillations. In the interneuron network gamma (ING) model, a network of reciprocally connected interneurons is sufficient for gamma oscillation generation. In contrast, in the pyramidal interneuron network gamma (PING) model, excitatory pyramidal neurons excite inhibitory neurons that provide fast perisomatic inhibition back onto the

pyramidal neurons. In this model the coordinated activity of excitatory and inhibitory neurons facilitates gamma oscillation generation.

Gamma oscillations in CA1 vary in speed from around 25 Hz up to 150 Hz, and can be split into a fast and slow component, driven by input from medial entorhinal cortex and CA3 respectively (Colgin et al., 2009). A recent *in vitro* study by Craig and McBain identified CA1 as an independent gamma generator (Craig and McBain, 2015). Interestingly, gamma oscillations generated in CA1 (in contrast to CA3) appeared not to require involvement of either pyramidal neurons or fast spiking basket cells (i.e. PV positive interneurons; Craig and McBain, 2015). They concluded that in CA1 a pure ING mechanism likely underlies gamma oscillation generation (Craig and McBain, 2015). If this holds true *in vivo*, then it remains possible that selective targeting of PV interneurons with hM4Di in CA1 (as in this thesis) will have little effect on gamma oscillation generation in the hippocampus. If gamma oscillations are left intact then it could explain the lack of cognitive deficits observed with PV neuron silencing in the CA1 reported here.

In this thesis LFPs were not recorded whilst PV interneurons were silenced with hM4Di, so the consequences of this manipulation on oscillatory activity *in vivo* remains unknown. In future studies it would be highly interesting to see if manipulation of PV interneurons in the CA1 subfield does influence gamma oscillations *in vivo*. In addition, it would be interesting to compare the effects of PV interneuron silencing in CA3 vs. CA1, as fast perisomatic inhibition from PV positive interneurons in CA3 does seem to be critical for the gamma oscillations in that subfield (Craig and McBain, 2015; Mann et al., 2005).

6.8 Conclusions

As is natural in science, this thesis opened up more questions than it has answered. The greatest contribution of this study to the field is arguably the finding that the NMDAR antagonist MK-801 appears **not to** preferentially act via NMDARs expressed on PV interneurons. This challenges previous reports and will hopefully prompt renewed effort in the search for the neuronal subtype(s) that NMDAR antagonists might target in order to induce disinhibition within the network, that could be an important mechanism through which NMDAR antagonists can produce schizophrenia like symptoms in humans and rodents. In addition, results in this thesis highlight the potential importance of GluA1 expression in area CA3, for normal Y-maze novelty preference and for normal locomotor activity in response to a novel environment.

7 Appendix

7.1 Specificity testing of Ppp1r2^{cre} driver line

7.1.1 Ppp1r2^{cre} line targets pyramidal neurons as early as 16 weeks of age

Belforte *et al.* generated the Ppp1r2^{cre} driver line to target a population of forebrain interneurons (Belforte et al., 2010). They then crossed the Ppp1r2^{cre} line with Floxed NR1 mice to generate *Grin1*$^{\Delta Ppp1r2}$ mice, which are reported to have behavioural deficits relevant to schizophrenia. Some recombination was reported in pyramidal neurons but this was thought to only occur beyond 20 weeks of age (Belforte et al., 2010).

To test the specificity of the Ppp1r2^{cre} driver line, we crossed the mice with floxed Ai9 mice to produce Ppp1r2-Ai9 mice (see **2.2.1**). At different ages Ppp1r2-Ai9 mice were perfused and the brains sliced, mounted and scanned on an epifluorescence microscope (same as with PV-Ai9 mice except without immunohistochemistry to probe for PV- see **2.2.2**). At 16 weeks of age there was already clear expression of TdTomato (red fluorescence) in pyramidal neurons in the CA1 of the hippocampus (the dendritic arbors are a hallmark of pyramidal neurons) (see **figure 7.1**).

The number of pyramidal neurons was not quantitatively assessed but it was very clear that by 16 weeks of age many pyramidal neurons were being targeted with the Ppp1r2^{cre} driver line. This was surprising considering the reports from Belforte *et al.*, and is a serious issue if trying to assess the role of NMDARs on interneurons for behaviours related to schizophrenia, because NMDARs on pyramidal neurons are known to be important for a number of behavioural tasks that are relevant to

schizophrenia and thus this off target expression represents a serious confound (Niewoehner et al., 2007; Tatard-Leitman et al., 2014; von Engelhardt et al., 2008).

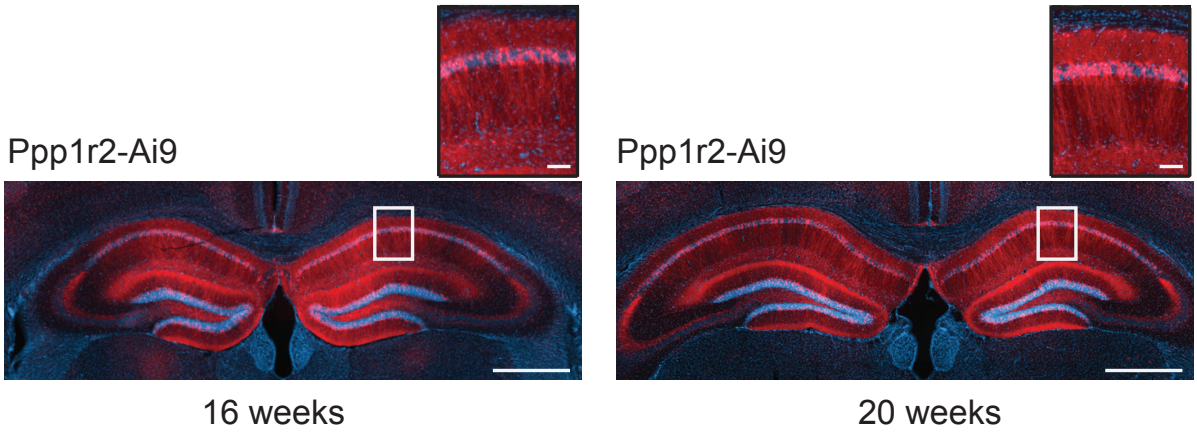

Figure 7.1: Recombination in pyramidal neurons in 16 weeks old Ppp1r2-Ai9 mice
Epifluorescence images of slices from Ppp1r2-Ai9 mice aged 16 weeks (left) and 20 weeks (right). TdTomato expression (red) indicates successful recombination and shows the neurons targeted with the Ppp1r2^{cre} driver line. White boxes over a region of dorsal CA1 pyramidal layer indicate the region that has been enlarged in the zoomed images (above main images). Scale bars indicate 1mm and 100μm in main and zoomed images respectively.

7.2 NMDAR antagonist studies in *Grin1*$^{\Delta PV}$ mice

7.2.1 MK-801 influence on choice latency on the T-maze in control and *Grin1*$^{\Delta PV}$ mice

Rewarded alternation performance could be influenced by the latency during the sample and choice runs. The choice latency could be of particular importance because a slower animal would be required to hold information about the location of the goal arm from the sample run in their "working memory" for longer- theoretically making the task more difficult. In addition, increased latencies could indicate motoric impairments or reduced motivation.

Each dose of MK-801 had its own within subject vehicle control condition and for each of the 10 trials the average sample and choice latency was calculated. The sample latency was defined as the time taken to run from the start arm to the food well in the goal arm. The choice trial latency was the time taken to run from the start arm to a decision point (i.e. when all four paws were in one of the goal arms). The average choice latency was calculated for each animal at each dose tested (see **figure 7.2**). At a dose of 0.1 mg/kg a repeated measures ANOVA with drug as a repeated measure and genotype as a between subject factor revealed no significant effect of genotype or drug and no drug*genotype interaction on the average choice latency in control and *Grin1*$^{\Delta PV}$ mice (effect of genotype: $F(1,10) = 2.096$, $P = 0.178$; effect of drug: $F(1,10) = 4.021$, $P = 0.073$; drug*genotype interaction: $F(1,10) = 2.494$, $p = 0.145$).

Similarly, at a dose of 0.15 mg/kg the same analysis revealed no significant effect of genotype or drug and no drug*genotype interaction on choice latency (effect of genotype: $F(1,12) = 0.001$, $P = 0.994$; effect of drug: $F(1,12) = 0.011$, $P = 0.916$; drug*genotype interaction: $F(1,12) = 3.314$, $P = 0.094$).

At a dose of 0.2 mg/kg the same analysis revealed no significant effect of genotype or drug, but a significant drug*genotype interaction did emerge, with the choice latencies becoming longer in *Grin1*$^{\Delta PV}$ mice but not controls when challenged with MK-801 (effect of genotype: $F(1,11) = 2.599$, $P = 0.135$; effect of drug: $F(1,11) = 1.942$, $P = 0.191$; drug*genotype interaction: $F(1,11) = 9.777$, $P = 0.010$).

At a dose of 0.4 mg/kg the same analysis revealed a significant effect of genotype, drug and a significant drug*genotype interaction with longer choice latencies in *Grin1*$^{\Delta PV}$ mice and following MK-801 challenge (effect of genotype: $F(1,12) = 4.880$, $P = 0.047$; effect of drug: $F(1,12) = 15.695$, $P = 0.002$; drug*genotype interaction: $F(1,12) = 20.124$, $P = 0.001$). However, the significant effect of genotype and drug is being driven by the increase in choice latencies in *Grin1*$^{\Delta PV}$ mice and not controls following MK-801 challenge. Together these results indicate that at doses of 0.2 and 0.4 mg/kg MK-801 can increase the choice latency and that this increase is larger in *Grin1*$^{\Delta PV}$ mice compared to controls.

The increase in choice latency in *Grin1*$^{\Delta PV}$ mice could be a consequence of their increased sensitivity to the cognitive impairing effects of MK-801. It is possible that the choice latency in *Grin1*$^{\Delta PV}$ mice following MK-801 is greater as they are taking longer to try and make a decision. However, this is unlikely to be the case as there was a similar, selective increase in sample trial latencies in *Grin1*$^{\Delta PV}$ mice following MK-801 challenge under conditions where there was no memory load (**data not shown**).

It is possible that the increase in choice latency with MK-801 is due to impaired motor coordination (particularly in *Grin1*$^{\Delta PV}$ mice) which could somewhat confound the inferred cognitive impairing effects of MK-801 that appeared more pronounced in *Grin1*$^{\Delta PV}$ mice. However, it is worth noting that there was no significant effect of MK-

801 on choice latencies at a dose of 0.15 mg/kg despite the fact *Grin1*$^{\Delta PV}$ mice do become impaired at this dose. This argues against a simple explanation that the cognitive impairing effects of MK-801 are due to increased running latencies.

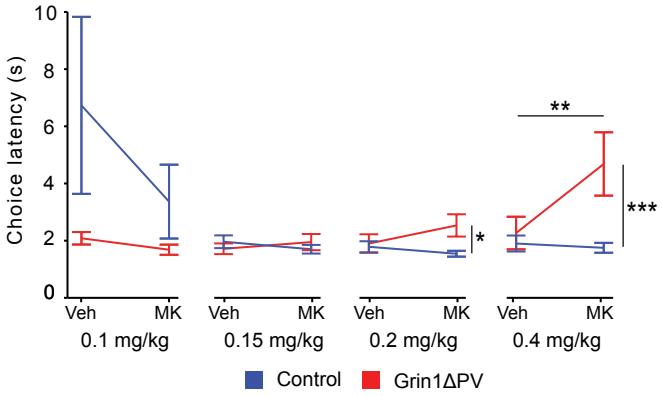

Figure 7.2: Choice trial latencies on the T-maze following MK-801 challenge
The average latency for the choice trial in control (blue) and *Grin1*$^{\Delta PV}$ mice (red) following MK-801 (MK) or vehicle (Veh) challenge. Lines display the mean and error bars display the SEM. Horizontal line and stars indicate a significant effect of drug on choice latency (** $P < 0.01$). Vertical line and stars indicate significant drug*genotype interactions (* $P < 0.05$, *** $P < 0.001$).

7.2.2 Location of electrodes in *Grin1*$^{\Delta PV}$ mice

To assess the effects of MK-801 on network activity in *Grin1*$^{\Delta PV}$ mice, LFPs were recorded from the prefrontal cortex of *Grin1*$^{\Delta PV}$ and control mice (see **3.3.6**). Recording sites were electrically lesioned to determine the location of electrodes in prefrontal cortex of *Grin1*$^{\Delta PV}$ mice (see **figure 7.3**).

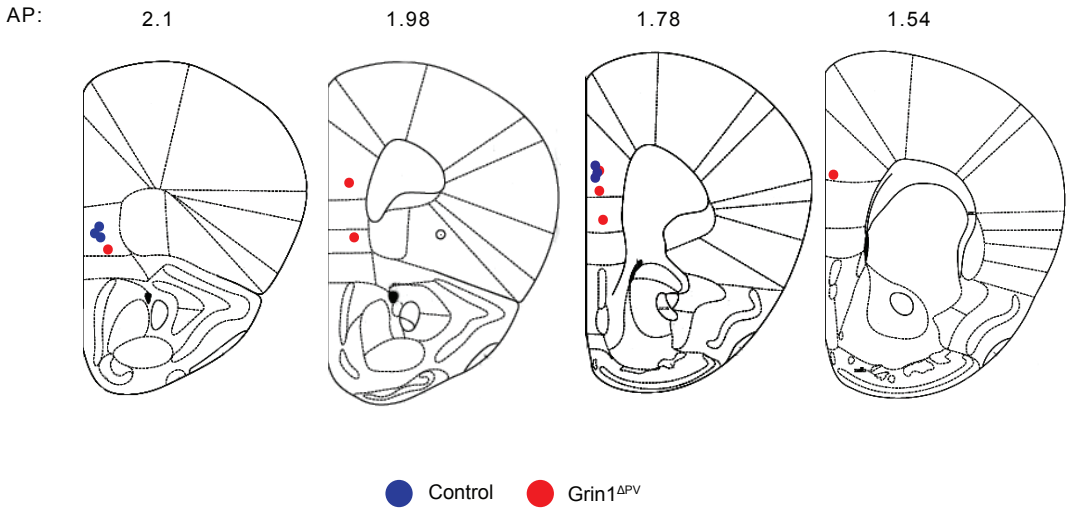

Figure 7.3: Estimates of electrode placement in control and *Grin1*$^{\Delta PV}$ mice
Location of electrodes in prefrontal cortex superimposed onto a schematic representation taken from the mouse brain atlas (adapted from Franklin and Paxinos). Numbers indicate the relative anterior/posterior location relative to bregma. Each dot represents a recording site from control (blue) or *Grin1*$^{\Delta PV}$ mice (red).

7.3 Electrophysiology and behaviour in *Gria1* KO mice

7.3.1 Electrode placements in prefrontal cortex and ventral hippocampus

The location of ventral hippocampus and prefrontal cortex electrodes was more variable than those in the dorsal hippocampus. In the ventral hippocampus, electrode placements varied across the hippocampal subfields. In particular, many electrode sites were located in the DG in posterior slices (**figure 7.4**; top panel). In the prefrontal cortex, electrode placements were more anterior than expected. In the most anterior slices (AP: + 1.2) electrodes were located in the anterior cingulate cortex.

Previous studies assessing prefrontal to hippocampal coherence have recorded LFPs from area CA1 in the hippocampus and infralimbic or prelimbic cortex (Jones and Wilson, 2005; Sigurdsson et al., 2010). It is not known how variations in electrode placements in the prefrontal cortex (and ventral hippocampus) will influence coherence. Therefore, at this stage coherence between prefrontal cortex and either dorsal or ventral hippocampus was not analysed.

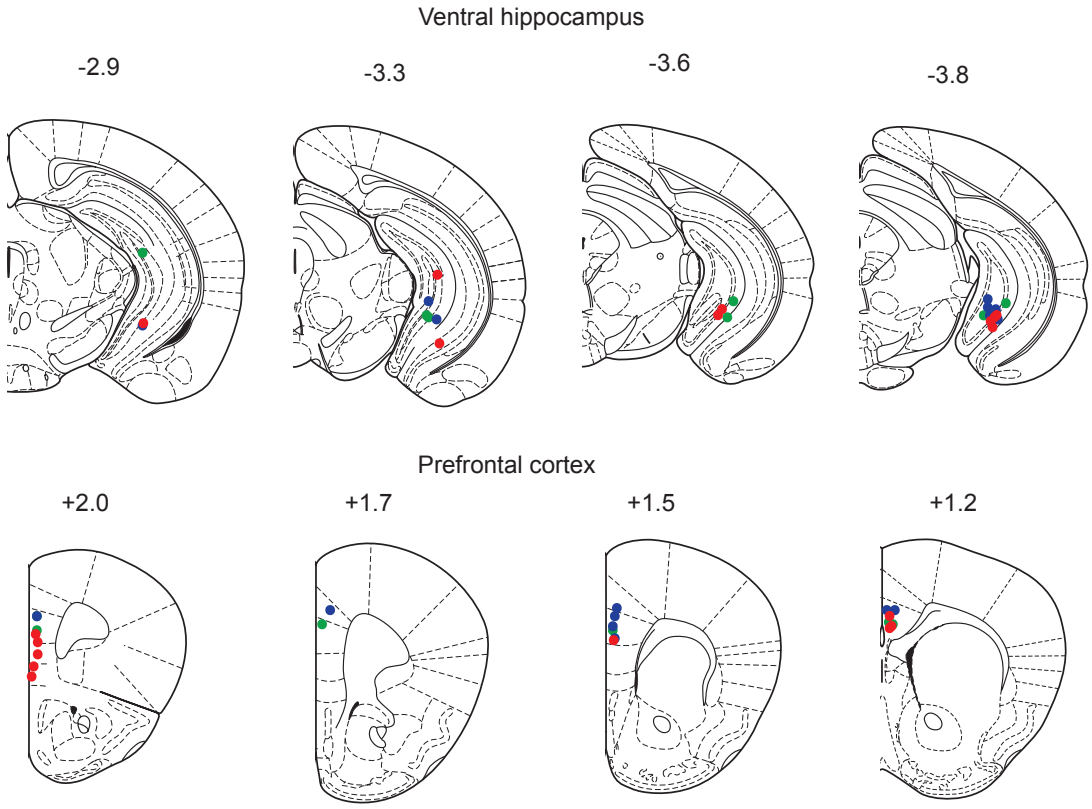

Figure 7.4: Estimates of electrode placement in control and *Gria1* KO mice
Schematic representation of electrode sites in the ventral hippocampus and prefrontal cortex, superimposed onto a schematic representation taken from the mouse brain atlas (adapted from Franklin and Paxinos). Numbers indicate the relative anterior/posterior location relative to bregma. Each dot represents a recording site from Gria1 WT (blue) or *Gria1* KO (red) or Gria1 KO with rescue virus (green).

7.3.2 Potential rescue of SWM in female *Gria1* KO rescue animals

In all analyses of locomotor activity, rewarded alternation on the T-maze (SWM) and spatial novelty preference on the Y-maze there was no significant sex*group interaction (i.e. *Gria1* WT, *Gria1* KO and *Gria1* KO rescue). Thus, strictly speaking there is no statistical rationale for analysing data separately based on sex. However, it appeared that the T-maze alternation performance of female *Gria1* KO rescue animals was partially rescued (when compared to both male and female *Gria1* KO and *Gria1* WT animals; **figure 7.5**)

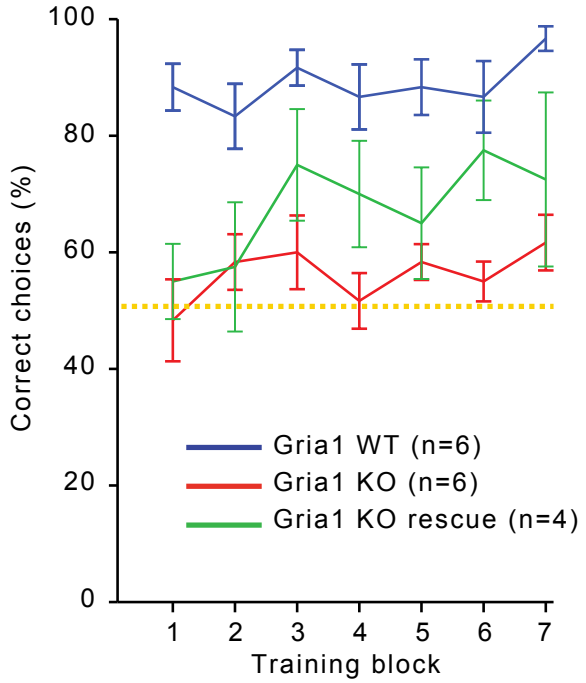

Figure 7.5: SWM could be partially rescued in female *Gria1* KO rescue animals
Correct choices made by *Gria1* WT (blue), *Gria1* KO (red) and *Gria1* KO rescue animals (green; female only). Note data from male and female *Gria1* WT and *Gria1* KO mice is compared to data from only female *Gria1* KO rescue. Yellow dashed line indicates chance level performance. Error bars display SEM.

Although not strictly appropriate, a repeated measure ANOVA with training block as a within subject factor and group (*Gria1* WT, *Gria1* KO and *Gria1* KO rescue) as a between subject factor revealed an overall significant effect of group on alternation performance (effect of group: $F(2,13) = 29.652$, $P = 0.001$). But note in this instance female *Gria1* KO rescue animals were compared to male and female *Gria1* WT and *Gria1* KO animals.

Post hoc analysis (LSD) revealed that *Gria1* WT animals made significantly more correct choices than *Gria1* KO and *Gria1* KO rescue animals (% correct choices in *Gria1* WT vs. *Gria1* KO: $F(1,13) = 57.943$, $P = 0.001$; *Gria1* WT vs. *Gria1* KO rescue: $F(1,14) = 19.784$, $P = 0.001$). However, *Gria1* KO rescue animals made significantly

more correct choices than Gria1 KO animals (% correct choices in *Gria1* KO rescue vs. *Gria1* KO: $F(1,13) = 5.573$, $P = 0.035$).

This indicated a partial rescue of alternation performance in female *Gria1* KO rescue animals. However it is important to stress that statistically there was no rationale for splitting the *Gria1* KO rescue group by sex. Thus, this thesis will discuss the phenotype of *Gria1* KO rescue animals based on the assumption that there is **no** rescue of SWM (see **figure 5.5b**; clearly demonstrating no rescue when all animals *Gria1* KO rescue animals were included). Future experiments, with larger cohorts will be required to follow up the interesting possibility of a subtle rescue of SWM in a sex specific manner.

8 Bibliography

Akbarian, S., Kim, J.J., Potkin, S.G., Jennifer, O., Bunney, W.E., Jones, E.G., 1995. Gene Expression for Glutamic Acid Decarboxylase Is Reduced Without Loss of Neurons in Prefrontal Cortex of Schizophrenics. Arch. Gen. Psychiatry 52, 258–266.

Alexander, G.M., Rogan, S.C., Abbas, A.I., Armbruster, B.N., Pei, Y., Allen, J. a, Nonneman, R.J., Hartmann, J., Moy, S.S., Nicolelis, M. a, McNamara, J.O., Roth, B.L., 2009. Remote control of neuronal activity in transgenic mice expressing evolved G protein-coupled receptors. Neuron 63, 27–39.

Andersen, P., Morris, R., Amaral, D., Bliss, T., O'Keefe, J., The Hippocampus Book. 2007. Oxford University Press.

Arguello, P.A., Gogos, J. a, 2006. Modeling madness in mice: one piece at a time. Neuron 52, 179–96.

Armbruster, B.N., Li, X., Pausch, M.H., Herlitze, S., Roth, B.L., 2007. Evolving the lock to fit the key to create a family of G protein-coupled receptors potently activated by an inert ligand. Proc. Natl. Acad. Sci. U. S. A. 104, 5163–8.

Atasoy, D., Aponte, Y., Su, H.H., Sternson, S.M., 2008. A FLEX switch targets Channelrhodopsin-2 to multiple cell types for imaging and long-range circuit mapping. J. Neurosci. 28, 7025–30.

Bannerman, D.M., Bus, T., Taylor, A., Sanderson, D.J., Schwarz, I., Jensen, V., Hvalby, Ø., Rawlins, J.N.P., Seeburg, P.H., Sprengel, R., 2012. Dissecting spatial knowledge from spatial choice by hippocampal NMDA receptor deletion. Nat. Neurosci. 15, 1153–9.

Bannerman, D.M., Deacon, R.M., Offen, S., Friswell, J., Grubb, M., Rawlins, J.N.P., 2002. Double dissociation of function within the hippocampus: spatial memory and hyponeophagia. Behav. Neurosci. 116, 884-901.

Bannerman, D.M., Deacon, R.M.J., Brady, S., Bruce, A., Sprengel, R., Seeburg, P.H., Rawlins, J.N.P., 2004. A comparison of GluR-A-deficient and wild-type mice on a test battery assessing sensorimotor, affective, and cognitive behaviors. Behav. Neurosci. 118, 643–647.

Bannerman, D.M., Grubb, M., Deacon, R.M.J., Yee, B.K., Feldon, J., Rawlins, J.N.P., 2003. Ventral hippocampal lesions affect anxiety but not spatial learning. Behav. Brain Res. 139, 197–213.

Bannerman, D.M., Sprengel, R., Sanderson, D.J., McHugh, S.B., Rawlins, J.N.P., Monyer, H., Seeburg, P.H., 2014. Hippocampal synaptic plasticity, spatial memory and anxiety. Nat. Rev. Neurosci. 15, 181–192.

Barkus, C., Dawson, L.A., Sharp, T., Bannerman, D.M., 2012. GluN1 hypomorph mice exhibit wide-ranging behavioral alterations. Genes, Brain Behav. 11, 342–351.

Barkus, C., Feyder, M., Graybeal, C., Wright, T., Wiedholz, L., Izquierdo, A., Kiselycznyk, C., Schmitt, W., Sanderson, D.J., Rawlins, J.N.P., Saksida, L.M., Bussey, T.J., Sprengel, R., Bannerman, D., Holmes, A., 2012. Do GluA1 knockout mice exhibit behavioral abnormalities relevant to the negative or cognitive symptoms of schizophrenia and schizoaffective disorder? Neuropharmacology 62, 1263–72.

Barkus, C., McHugh, S.B., Sprengel, R., Seeburg, P.H., Rawlins, J.N.P., Bannerman, D.M., 2010. Hippocampal NMDA receptors and anxiety: at the interface between cognition and emotion. Eur. J. Pharmacol. 626, 49–56.

Barkus, C., Sanderson, D.J., Rawlins, J.N.P., Walton, M.E., Harrison, P.J., Bannerman, D.M., 2014. What causes aberrant salience in schizophrenia ? A role for impaired short-term habituation and the GRIA1 (GluA1) AMPA receptor subunit 1–11.

Belforte, J.E., Zsiros, V., Sklar, E.R., Jiang, Z., Yu, G., Li, Y., Quinlan, E.M., Nakazawa, K., 2010a. Postnatal NMDA receptor ablation in corticolimbic interneurons confers schizophrenia-like phenotypes. Nat. Neurosci. 13, 76–83.

Belforte, J.E., Zsiros, V., Sklar, E.R., Jiang, Z., Yu, G., Li, Y., Quinlan, E.M., Nakazawa, K., 2010b. Postnatal NMDA receptor ablation in corticolimbic interneurons confers schizophrenia-like phenotypes. Nat. Neurosci. 13, 76–83.

Bender, F., Gorbati, M., Cadavieco, M.C., Denisova, N., Gao, X., Holman, C., Korotkova, T., Ponomarenko, A., 2015. Theta oscillations regulate the speed of locomotion via a hippocampus to lateral septum pathway. Nat. Commun. 6, 8521.

Benes, F.M., Lim, B., Matzilevich, D., Walsh, J.P., Subburaju, S., Minns, M., 2007. Regulation of the GABA cell phenotype in hippocampus of schizophrenics and bipolars. Proc. Natl. Acad. Sci. U. S. A. 104, 10164–10169.

Bernstein, J.G., Boyden, E.S., 2011. Optogenetic tools for analyzing the neural circuits of behavior. Trends Cogn. Sci. 15, 592–600.

Betley, J.N., Sternson, S.M., 2011. Adeno-associated viral vectors for mapping, monitoring, and

manipulating neural circuits. Hum. Gene Ther. 22, 669–677.
Bienemann, C., 2002. Adenoviral-Mediated, High-Level, Cell-Specific Transgene Expression: A SYN1-WPRE Cassette Mediates Increased Transgene Expression with No Loss of Neuron Specificity. Mol. Ther. 5, 509–516.
Billingslea, E.N., Tatard-Leitman, V.M., Anguiano, J., Jutzeler, C.R., Suh, J., Saunders, J. a, Morita, S., Featherstone, R.E., Ortinski, P.I., Gandal, M.J., Lin, R., Liang, Y., Gur, R.E., Carlson, G.C., Hahn, C.-G., Siegel, S.J., 2014. Parvalbumin cell ablation of NMDA-R1 causes increased resting network excitability with associated social and self-care deficits. Neuropsychopharmacology 39, 1603–13.
Bird, C.M., Burgess, N., 2008. The hippocampus and memory : insights from spatial processing 9.
Bitanihirwe, B.K.Y., Lim, M.P., Kelley, J.F., Kaneko, T., Woo, T.U.W., 2009. Glutamatergic deficits and parvalbumin-containing inhibitory neurons in the prefrontal cortex in schizophrenia. BMC Psychiatry 9, 71.
Bliss, T., Collingridge, G.L., 1993. A synaptic model of memory: long-term potentiation in the hippocampus. Nature 361, 31–39.
Bliss, T.V.P., Lomo, T., 1973. Long-Lasting Potentiation of Synaptic Transmission in the Dentate Area of the Anaesthetized Rabbit Following Stimulation of the Perforant Path. J. Physiol. 331–356.
Boutros, N.N., Arfken, C., Galderisi, S., Warrick, J., Pratt, G., Iacono, W., 2008. The status of spectral EEG abnormality as a diagnostic test for schizophrenia. Schizophr. Res. 99, 225–237.
Boyden, E.S., Zhang, F., Bamberg, E., Nagel, G., Deisseroth, K., 2005. Millisecond-timescale, genetically targeted optical control of neural activity. Nat. Neurosci. 8, 1263–8.
Brigman, J.L., Graybeal, C., Holmes, A., 2010. Predictably irrational: Assaying cognitive inflexibility in mouse models of schizophrenia. Front. Neurosci. 4, 19–28.
Bubeníková-Valesová, V., Horácek, J., Vrajová, M., Höschl, C., 2008. Models of schizophrenia in humans and animals based on inhibition of NMDA receptors. Neurosci. Biobehav. Rev. 32, 1014–23.
Bugarski-Kirola, D., Wang, A., Abi-Saab, D., Blättler, T., 2014. A phase II/III trial of bitopertin monotherapy compared with placebo in patients with an acute exacerbation of schizophrenia - results from the CandleLyte study. Eur. Neuropsychopharmacol. J. Eur. Coll. Neuropsychopharmacol. 24, 1024–1036.
Buzsáki, G., 2002. Theta Oscillations in the Hippocampus. Neuron 33, 325–340.
Buzsáki, G., Anastassiou, C. a., Koch, C., 2012. The origin of extracellular fields and currents — EEG, ECoG, LFP and spikes. Nat. Rev. Neurosci. 13, 407-420

Cardin, J. a, Carlén, M., Meletis, K., Knoblich, U., Zhang, F., Deisseroth, K., Tsai, L.-H., Moore, C.I., 2009. Driving fast-spiking cells induces gamma rhythm and controls sensory responses. Nature 459, 663–7.
Carlén, M., Meletis, K., Siegle, J.H., Cardin, J. a, Futai, K., Vierling-Claassen, D., Rühlmann, C., Jones, S.R., Deisseroth, K., Sheng, M., Moore, C.I., Tsai, L.-H., 2012. A critical role for NMDA receptors in parvalbumin interneurons for gamma rhythm induction and behavior. Mol. Psychiatry 17, 537–48.
Carpenter, W.T., Davis, J.M., 2012. Another view of the history of antipsychotic drug discovery and development. Mol. Psychiatry 17, 1168–1173.
Carroll, L.S., Owen, M.J., 2009. Genetic overlap between autism , schizophrenia and bipolar disorder 1–7.

Chatterton, J.E., Awobuluyi, M., Premkumar, L.S., Takahashi, H., Talantova, M., Shin, Y., Cui, J., Tu, S., Sevarino, K. a, Nakanishi, N., Tong, G., Lipton, S. a, Zhang, D., 2002. Excitatory glycine receptors containing the NR3 family of NMDA receptor subunits. Nature 415, 793–8.
Cho, K.K.A., Hoch, R., Lee, A.T., Patel, T., Rubenstein, J.L.R., Sohal, V.S., 2015. Gamma Rhythms Link Prefrontal Interneuron Dysfunction with Cognitive Inflexibility in Dlx5/6+/− Mice. Neuron 85, 1332–1343.
Chow, B.Y., Han, X., Dobry, A.S., Qian, X., Chuong, A.S., Li, M., Henninger, M. a, Belfort, G.M., Lin, Y., Monahan, P.E., Boyden, E.S., 2010. High-performance genetically targetable optical neural silencing by light-driven proton pumps. Nature 463, 98–102.
Claridge-Chang, A., Roorda, R.D., Vrontou, E., Sjulson, L., Li, H., Hirsh, J., Miesenböck, G., 2009. Writing memories with light-addressable reinforcement circuitry. Cell 139, 405–15.
Cohen, S.J., Munchow, A.H., Rios, L.M., 2013. Report The Rodent Hippocampus Is Essential for Nonspatial Object Memory 1685–1690.
Colgin, L.L., Denninger, T., Fyhn, M., Hafting, T., Bonnevie, T., Jensen, O., Moser, M.-B., Moser, E.I., 2009. Frequency of gamma oscillations routes flow of information in the hippocampus. Nature

462, 353–357.
Collingridge, G.L., Kehl, S.J., McLennan, H., 1983. The antagonism of amino acid-induced excitations of rat hippocampal CA1 neurones in vitro. J. Physiol. 334, 19–31.
Coyle, J.T., 2012. NMDA receptor and schizophrenia: A brief history. Schizophr. Bull. 38, 920–926.
Crabtree, G.W., Gogos, J.A., 2014. Synaptic plasticity , neural circuits , and the emerging role of altered short-term information processing in schizophrenia. Frontiers in Synaptic Neuroscience 6, 1–27.
Craig, M.T., McBain, C.J., 2015. Fast Gamma Oscillations Are Generated Intrinsically in CA1 without the Involvement of Fast-Spiking Basket Cells. J. Neurosci. 35, 3616–3624.
Curley, A.A., Arion, D., Volk, D.W., Asafu-Adjei, J.K., Sampson, A.R., Fish, K.N., Lewis, D.A., 2011. Cortical deficits of glutamic acid decarboxylase 67 expression in schizophrenia: Clinical, protein, and cell type-specific features. Am. J. Psychiatry 168, 921–929.
Davis, K.L., Kahn, R.S., KO, G., Davidson, M., 1991. Dopamine in Schiziophrenia: a review and reconceptualization. Am. J. psychiatry 148, 1474–1486.
Deacon, R.M.J., 2013. Measuring motor coordination in mice. J. Vis. Exp. e2609. doi:10.3791/2609
Deacon, R.M.J., 2006. Assessing nest building in mice. Nat. Protoc. 1, 1117–9.
Deacon, R.M.J., Bannerman, D.M., Kirby, B., Croucher, A., Rawlins, J.N.P., 2002. Effects of cytotoxic hippocampal lesions in mice on a cognitive test battery. Behav. Brain Res. 133, 57–68.
Deacon, R.M.J., Rawlins, J.N.P., 2006. T-maze alternation in the rodent. Nat. Protoc. 1, 7–12.
Deakin, J., Lees, J., McKie, S., Hallak, J., Williams, S., Dursun, S., 2008. Glutamate and the Neural Basis of the Subjective Effects of Ketamine 65, 154–164.
del Pino, I., García-Frigola, C., Dehorter, N., Brotons-Mas, J.R., Alvarez-Salvado, E., Martínez de Lagrán, M., Ciceri, G., Gabaldón, M.V., Moratal, D., Dierssen, M., Canals, S., Marín, O., Rico, B., 2013. Erbb4 Deletion from Fast-Spiking Interneurons Causes Schizophrenia-like Phenotypes. Neuron 79, 1152–1168.
Dickerson, D.D., Overeem, K. a, Wolff, a R., Williams, J.M., Abraham, W.C., Bilkey, D.K., 2014. Association of aberrant neural synchrony and altered GAD67 expression following exposure to maternal immune activation, a risk factor for schizophrenia. Transl. Psychiatry 4, e418.
Dickerson, D.D., Wolff, A.R., Bilkey, D.K., 2010. Abnormal long-range neural synchrony in a maternal immune activation animal model of schizophrenia. J. Neurosci. 30, 12424–31.
Donato, F., Rompani, S.B., Caroni, P., 2013. Parvalbumin-expressing basket-cell network plasticity induced by experience regulates adult learning. Nature 504, 272–6.
Eastwood, S.L., Kerwin, R.W., Harrison, P.J., 1997. Immunoautoradiographic evidence for a loss of alpha-amino-3-hydroxy-5-methyl-4-isoxazole propionate-preferring non-N-methyl-D-aspartate glutamate receptors within the medial temporal lobe in schizophrenia. Biol. Psychiatry 41, 636–643.
Eastwood, S.L., McDonald, B., Burnet, P.W., Beckwith, J.P., Kerwin, R.W., Harrison, P.J., 1995. Decreased expression of mRNAs encoding non-NMDA glutamate receptors GluR1 and GluR2 in medial temporal lobe neurons in schizophrenia. Brain Res. Mol. Brain Res. 29, 211–23.
Erickson, M. a, Maramara, L. a, Lisman, J., 2010. A single brief burst induces GluR1-dependent associative short-term potentiation: a potential mechanism for short-term memory. J. Cogn. Neurosci. 22, 2530–40.
Fisahn, a, Pike, F.G., Buhl, E.H., Paulsen, O., 1998. Cholinergic induction of network oscillations at 40 Hz in the hippocampus in vitro. Nature 394, 186–9.
Fitzgerald, P.J., Barkus, C., Feyder, M., Wiedholz, L.M., Chen, Y.C., Karlsson, R.M., Machado-Vieira, R., Graybeal, C., Sharp, T., Zarate, C., Harvey-White, J., Du, J., Sprengel, R., Gass, P., Bannerman, D., Holmes, A., 2010. Does gene deletion of AMPA GluA1 phenocopy features of schizoaffective disorder? Neurobiol. Dis. 40, 608–621.
Floresco, S.B., Seamans, J., Phillips, A.G., 1997. Selective Roles for Hippocampal, Prefrontal Cortical, and Ventral Striatal Circuits in Radial-Arm Maze Tasks With or Without a delay. J. Neurosci. 17, 1880–1890.
Floresco, S.B., Todd, C.L., Grace, a a, 2001. Glutamatergic afferents from the hippocampus to the nucleus accumbens regulate activity of ventral tegmental area dopamine neurons. J. Neurosci. 21, 4915–22.
Ford, J.M., Mathalon, D.H., Whitfield, S., Faustman, W.O., Roth, W.T., 2002. Reduced communication between frontal and temporal lobes during talking in schizophrenia. Biol. Psychiatry 51, 485–92.
Forrest, D., Yuzaki, M., Soares, H.D., Ng, L., Luk, D.C., Sheng, M., Stewart, C.L., Morgan, J.I., Connor, J. a, Curran, T., 1994. Targeted disruption of NMDA receptor 1 gene abolishes NMDA response and results in neonatal death. Neuron 13, 325–38.
Freudenberg, F., Marx, V., Seeburg, P.H., Sprengel, R., Celikel, T., 2013. Circuit mechanisms of GluA1-dependent spatial working memory. Hippocampus 23, 1359–1366.

Freudenberg, F., Resnik, E., Kolleker, A., Celikel, T., Sprengel, R., Seeburg, P.H., 2016. Hippocampal GluA1 expression in Gria1–/– mice only partially restores spatial memory performance deficits. Neurobiol. Learn. Mem. 1–8.
Fries, P., 2005. A mechanism for cognitive dynamics: neuronal communication through neuronal coherence. Trends Cogn. Sci. 9, 474–80.
Fuchs, E.C., Zivkovic, A.R., Cunningham, M.O., Middleton, S., Lebeau, F.E.N., Bannerman, D.M., Rozov, A., Whittington, M. a, Traub, R.D., Rawlins, J.N.P., Monyer, H., 2007. Recruitment of parvalbumin-positive interneurons determines hippocampal function and associated behavior. Neuron 53, 591–604.
Fukaya, M., Kato, A., Lovett, C., Tonegawa, S., Watanabe, M., 2003. Retention of NMDA receptor NR2 subunits in the lumen of endoplasmic reticulum in targeted NR1 knockout mice. Proc. Natl. Acad. Sci. U. S. A. 100, 4855–60.
Fung, S.J., Webster, M.J., Sivagnanasundaram, S., Duncan, C., Elashoff, M., Weickert, C.S., 2010. Expression of interneuron markers in the dorsolateral prefrontal cortex of the developing human and in schizophrenia. Am. J. Psychiatry 167, 1479–1488.
G.Tsai; Passani. L; Slushe. B; Carter. R; Baer. L; Kleinman. J; Coyle, J., 1995. Abnormal Excitatory Neurotransmitter Metabolism in Schizophrenic Brains. Arch. Gen. Psychiatry 52, 829–836.
Galderisi, S., Mucci, A., Volpe, U., Boutros, N., 2009. Evidence-Based Medicine and Electrophysiology in Schizophrenia 40, 62–77.
Gandal, M.J., Edgar, J.C., Klook, K., Siegel, S.J., 2012. Gamma synchrony: towards a translational biomarker for the treatment-resistant symptoms of schizophrenia. Neuropharmacology 62, 1504–18.
Geiger, J.R.P., Melcher, T., Koh, D.S., Sakmann, B., Seeburg, P.H., Jonas, P., Monyer, H., 1995. Relative abundance of subunit mRNAs determines gating and Ca2+ permeability of AMPA receptors in principal neurons and interneurons in rat CNS. Neuron 15, 193–204.
Gerlai, R., 1998. A new continuous alternation task in T-maze detects hippocampal dysfunction in mice: A strain comparison and lesion study. Behav. Brain Res. 95, 91–101.
Gilmour, G., Dix, S., Fellini, L., Gastambide, F., Plath, N., Steckler, T., Talpos, J., Tricklebank, M., 2012. NMDA receptors, cognition and schizophrenia--testing the validity of the NMDA receptor hypofunction hypothesis. Neuropharmacology 62, 1401–12.
Gilmour, G., Pioli, E.Y., Dix, S.L., Smith, J.W., Conway, M.W., Jones, W.T., Loomis, S., Mason, R., Shahabi, S., Tricklebank, M.D., 2009. Diverse and often opposite behavioural effects of NMDA receptor antagonists in rats: Implications for “nMDA antagonist modelling” of schizophrenia. Psychopharmacology (Berl). 205, 203–216.
Gloveli, T., Dugladze, T., Saha, S., Monyer, H., Heinemann, U., Traub, R.D., Whittington, M.A., Buhl, E.H., 2005. Differential involvement of oriens/pyramidale interneurones in hippocampal network oscillations in vitro. J. Physiol. 562, 131–47.
Gray, J.A. and McNaughton, N. 1982. The Neuropsychology of Anxiety. Oxford University Press.
Gray, J.A. and McNaughton, N. 200. The Neuropsychology of Anxiety, second edition. Oxford University Press.
Greger, I.H., Esteban, J. a, 2007. AMPA receptor biogenesis and trafficking. Curr. Opin. Neurobiol. 17, 289–97.
Gu, X., Zhou, L., Lu, W., 2015. An NMDA Receptor-Dependent Mechanism Underlies Inhibitory Synapse Development. Cell Rep. 14, 471–478.
Hall, B., Limaye, A., Kulkarni, A.B., 2009. Overview: Generation of Gene Knockout Mice. Curr. Protoc. Cell Biol. 1–17.
Harrison, P.J., 2004. The hippocampus in schizophrenia: a review of the neuropathological evidence and its pathophysiological implications. Psychopharmacology (Berl). 174, 151–62.
Harrison, P.J., Weinberger, D.R., 2005. Schizophrenia genes, gene expression, and neuropathology: on the matter of their convergence. Mol. Psychiatry 10, 40–68
Harrison, P.J., 2015. Recent genetic findings in schizophrenia and their therapeutic relevance. Journal of Psychopharmacology. 25, 85-96.
Harvey, R.J., Yee, B.K., 2013. Glycine transporters as novel therapeutic targets in schizophrenia , alcohol dependence and pain. Nat. Publ. Gr. 12, 866–885.
Hashimoto, T., 2005. Relationship of Brain-Derived Neurotrophic Factor and Its Receptor TrkB to Altered Inhibitory Prefrontal Circuitry in Schizophrenia. J. Neurosci. 25, 372–383.
Hashimoto, T., Bazmi, H.H., Mirnics, K., Wu, Q., Sampson, A.R., Lewis, D.A., 2008. Conserved regional patterns of GABA-related transcript expression in the neocortex of subjects with schizophrenia. Am. J. Psychiatry 165, 479–489.
Hashimoto, T., Volk, D.W., Eggan, S.M., Mirnics, K., Pierri, J.N., Sun, Z., Sampson, A.R., Lewis, D. a,

2003. Gene expression deficits in a subclass of GABA neurons in the prefrontal cortex of subjects with schizophrenia. J. Neurosci. 23, 6315–6326.
Henley, J.M., Wilkinson, K.A., 2016. Synaptic AMPA receptor composition in development, plasticity and disease. Nat. Rev. Neurosci. 17, 337–350.
Henson, M.A., Roberts, A.C., P??rez-Ota??o, I., Philpot, B.D., 2010. Influence of the NR3A subunit on NMDA receptor functions. Prog. Neurobiol. 91, 23–37.
Higuchi, M., Maas, S., Single, F.N., Hartner, J., Rozov, a, Burnashev, N., Feldmeyer, D., Sprengel, R., Seeburg, P.H., 2000. Point mutation in an AMPA receptor gene rescues lethality in mice deficient in the RNA-editing enzyme ADAR2. Nature 406, 78–81.
Hill, S.K., Bishop, R.J., Palumbo, D., Sweeney, A.J., 2010. Effect of second-generation antipsychotics on cognition: current issues and future challenges. Expert Rev Neurother 10, 43–57.
Hinman, J.R., Penley, S.C., Long, L.L., Escabí, M.A., Chrobak, J.J., 2011. Septotemporal variation in dynamics of theta : speed and habituation. J Neurophysiol 105, 2675–2686.
Hippenmeyer, S., Vrieseling, E., Sigrist, M., Portmann, T., Laengle, C., Ladle, D.R., Arber, S., 2005. A Developmental Switch in the Response of DRG Neurons to ETS Transcription Factor Signaling. PLoS Biol 3, e159.
Hoffman, D. a, Sprengel, R., Sakmann, B., 2002. Molecular dissection of hippocampal theta-burst pairing potentiation. Proc. Natl. Acad. Sci. U. S. A. 99, 7740–5.
Hollmann, M., Boulter, J., Maron, C., Beasley, L., Sullivan, J., Pecht, G., Heinemann, S., 1993. Zinc potentiates agonist-induced currents at certain splice variants of the NMDA receptor. Neuron 10, 943–954.
Holt, D.J., Weiss, A.P., Rauch, S.L., Wright, C.I., Zalesak, M., Goff, D.C., Ditman, T., Welsh, R.C., Heckers, S., 2005. Sustained Activation of the Hippocampus in Response to Fearful Faces in Schizophrenia.
Homayoun, H., Moghaddam, B., 2007. NMDA receptor hypofunction produces opposite effects on prefrontal cortex interneurons and pyramidal neurons. J. Neurosci. 27, 11496–500.
Howard, M.W., Rizzuto, D.S., Caplan, J.B., Madsen, J.R., Lisman, J., Aschenbrenner-Scheibe, R., Schulze-Bonhage, A., Kahana, M.J., 2003. Gamma Oscillations Correlate with Working Memory Load in Humans. Cereb. Cortex 13, 1369–1374.
Howes, O.D., Kapur, S., 2009. The dopamine hypothesis of schizophrenia: Version III - The final common pathway. Schizophr. Bull. 35, 549–562.
Hu, H., Gan, J., Jonas, P., 2014. Interneurons. Fast-spiking, parvalbumin^{+} GABAergic interneurons: from cellular design to microcircuit function. Science 345, 1255263.
Huganir, R.L., Nicoll, R.A., 2013. AMPARs and Synaptic Plasticity: The Last 25 Years. Neuron 80, 704–717.
Hyman, S.E., 2012. Revolution Stalled. Sci. Transl. Med. 155, 1-5.
Jackson, M.E., Homayoun, H., Moghaddam, B., 2004. NMDA receptor hypofunction produces concomitant firing rate potentiation and burst activity reduction in the prefrontal cortex. Proc. Natl. Acad. Sci. U. S. A. 101, 8467–72.
Jacob, T.C., Moss, S.J., Jurd, R., 2008. GABA(A) receptor trafficking and its role in the dynamic modulation of neuronal inhibition. Nat Rev Neurosci 9, 331–343. doi:10.1038/nrn2370
Javitt, C., Zukin, S., 1991. Recent Advances in the Phencyclidine Model of Schizophrenia. Am J Psychiatry 148, 1301–1308.
Jiang, Z., Cowell, R.M., Nakazawa, K., 2013. Convergence of genetic and environmental factors on parvalbumin-positive interneurons in schizophrenia. Front. Behav. Neurosci. 7, 116.
Jiang, Z., Rompala, G.R., Zhang, S., Cowell, R.M., Nakazawa, K., 2013. Social isolation exacerbates schizophrenia-like phenotypes via oxidative stress in cortical interneurons. Biol. Psychiatry 73, 1024–34.
Jiang, Z., Rompala, G.R., Zhang, S., Cowell, R.M., Nakazawa, K., 2013c. Social isolation exacerbates schizophrenia-like phenotypes via oxidative stress in cortical interneurons. Biol. Psychiatry 73, 1024–34.
Johnson, J., Ascher, P., 1987. Glycine potentiates the NMDA response in cultured mouse brain neurons. Nature 325, 529–531.
Jones, M.W., Wilson, M. a, 2005. Theta rhythms coordinate hippocampal-prefrontal interactions in a spatial memory task. PLoS Biol. 3, e402.
Kapur, S., 2003. Psychosis as a State of Aberrant Salience : and Pharmacology in Schizophrenia. Am J Psychiatry 160, 13–23.
Kätzel, D., Nicholson, E., Schorge, S., Walker, M.C., Kullmann, D.M., 2014. Chemical-genetic attenuation of focal neocortical seizures. Nat. Commun. 5, 3847.

Kellendonk, C., Simpson, E.H., Kandel, E.R., 2009. Modeling cognitive endophenotypes of schizophrenia in mice. Trends Neurosci. 32, 347–58.
Kellendonk, C., Simpson, E.H., Polan, H.J., Malleret, G., Vronskaya, S., Winiger, V., Moore, H., Kandel, E.R., 2006. Transient and selective overexpression of dopamine D2 receptors in the striatum causes persistent abnormalities in prefrontal cortex functioning. Neuron 49, 603–15.
Kendler, K.S., Mcguire, M., Gruenberg, A.M., Hare, A.O., Spellman, M., Walsh, D., 1993. The Roscommon Family Study. Arch. Gen. Psychiatry 50, 527–540.
Kim, H., Ährlund-Richter, S., Wang, X., Deisseroth, K., Carlén, M., 2016. Prefrontal Parvalbumin Neurons in Control of Attention. Cell 164, 208–218.
King, D.J., 1998. Drug treatment of the negative symptoms of schizophrenia. European Neuropsychopharmacology 8, 33–42.

Klausberger, T., Somogyi, P., 2008. Neuronal diversity and temporal dynamics: the unity of hippocampal circuit operations. Science 321, 53–7.
Korotkova, T., Fuchs, E.C., Ponomarenko, A., von Engelhardt, J., Monyer, H., 2010. NMDA receptor ablation on parvalbumin-positive interneurons impairs hippocampal synchrony, spatial representations, and working memory. Neuron 68, 557–69.
Krystal, J, Karper, L, Siebyl, J, Freeman, G, Delaney, R, Bremmer, J, Heninger, G, Bowers, M, Charney, D., 1994. Subanaesthetic Effects of the Noncompetititive NMDA Antagonist, Ketamine, in Humans. Arch. Gen. Psychiatry 51, 199–214.
Kügler, S., Kilic, E., Bähr, M., 2003. Human synapsin 1 gene promoter confers highly neuron-specific long-term transgene expression from an adenoviral vector in the adult rat brain depending on the transduced area. Gene Ther. 10, 337–347.
Kuryatov, A., Laube, B., Betz, H., Kuhse, J., 1994. Mutational analysis of the glycine-binding site of the NMDA receptor: Structural similarity with bacterial amino acid-binding proteins. Neuron 12, 1291–1300.
Lahti, A, Koffel, B, LaPorte, D, Tamminga, C., 1995. Suanaesthetic Doses of Ketamine Stimulate Psychosis in Schizophrenia. Neuropharmacology 13, 9–19.
Lau, C.G., Murthy, V.N., 2012. Activity-dependent regulation of inhibition via GAD67. J. Neurosci. 32, 8521–8531.
Laube, B., Hirai, H., Sturgess, M., Betz, H., Kuhse, J., 1997. Molecular determinants of agonist discrimination by NMDA receptor subunits: Analysis of the glutamate binding site on the NR2B subunit. Neuron 18, 493–503.
Laurie, D.J., Seeburg, P.H., 1994. Regional and developmental heterogeneity in splicing of the rat brain NMDAR1 mRNA. J. Neurosci. 14, 3180–3194.
Lee, C.-H., Lü, W., Michel, J.C., Goehring, A., Du, J., Song, X., Gouaux, E., 2014. NMDA receptor structures reveal subunit arrangement and pore architecture. Nature 511, 191–197.
Lee, H., Takamiya, K., Han, J., Man, H., Kim, C., Rumbaugh, G., Yu, S., Ding, L., He, C., Petralia, R.S., Wenthold, R.J., Gallagher, M., Huganir, R.L., 2003. Phosphorylation of the AMPA Receptor GluR1 Subunit Is Required for Synaptic Plasticity and Retention of Spatial Memory 112, 631–643.
Lewis, D. a, Curley, A. a, Glausier, J.R., Volk, D.W., 2012. Cortical parvalbumin interneurons and cognitive dysfunction in schizophrenia. Trends Neurosci. 35, 57–67.
Lewis, D. a, Hashimoto, T., Volk, D.W., 2005. Cortical inhibitory neurons and schizophrenia. Nat. Rev. Neurosci. 6, 312–24.
Lieberman, J.A., Dunbar, G., Segreti, A.C., Girgis, R.R., Seoane, F., Beaver, J.S., Duan, N., Hosford, D.A., 2013. A randomized exploratory trial of an α-7 nicotinic receptor agonist (TC-5619) for cognitive enhancement in schizophrenia. Neuropsychopharmacology 38, 968–75.
Lima, S.Q., Miesenböck, G., 2005. Remote control of behavior through genetically targeted photostimulation of neurons. Cell 121, 141–52.
Lipska, B.K., Lerman, D.N., Khaing, Z.Z., Weickert, C.S., Weinberger, D.R., 2003. Gene expression in dopamine and GABA systems in an animal model of schizophrenia: Effects of antipsychotic drugs. Eur. J. Neurosci. 18, 391–402.
Lisman, J., 2012. Excitation, inhibition, local oscillations, or large-scale loops: What causes the symptoms of schizophrenia? Curr. Opin. Neurobiol. 22, 537–544.
Lisman, J., 2005. The theta/gamma discrete phase code occuring during the hippocampal phase precession may be a more general brain coding scheme. Hippocampus 15, 913–922.
Lisman, J.E., Coyle, J.T., Green, R.W., Javitt, D.C., Benes, F.M., Heckers, S., Grace, A. a, 2008. Circuit-based framework for understanding neurotransmitter and risk gene interactions in schizophrenia. Trends Neurosci. 31, 234–42.
Lisman, J.E., Jensen, O., 2013. The Theta-Gamma Neural Code. Neuron 77, 1002–1016.

Liu, J., Moghaddam, B., 1995. Regulationof Glutamate Effluxby Excitatory AminoAcid Receptors : Evidencefor Tonic Inhibitory and Phasic Excitatory Regulation. Pharmacology 274, 1209-1215.
Lodge, D.J., Grace, A.A., 2009. Gestational methylazoxymethanol acetate administration: A developmental disruption model of schizophrenia. Behav. Brain Res. 204, 306–312.
Lodge, D.J., Grace, A.A., 2007. Aberrant hippocampal activity underlies the dopamine dysregulation in an animal model of schizophrenia. J. Neurosci. 27, 11424–30.
Lou, A.H, Tahsili-Fahadan, P., Wise, R.A., Lupica. C.R., Aston-Jones. G., 2011. Linking Context with Reward: A Functional Circuit from Hippocampal CA3 to Ventral Tegmental Area. Science 333, 353-357.
Lu, W., Shi, Y., Jackson, A.C., Bjorgan, K., During, M.J., Sprengel, R., Seeburg, P.H., Nicoll, R.A., 2009. Subunit Composition of Synaptic AMPA Receptors Revealed by a Single-Cell Genetic Approach. Neuron 62, 254–268.
Luby, D.E., Cohen, D.B., Rosenbaum, G., Gottlieb, S.J., Kelley, R., 1959. Study of a New Schizophrenomimetic Drug—Sernyl. AMA Arch NeurPsych. 81, 363–369.

Ludewig, K., Geyer, M., Vollenweider, F., 2003. Deficits in Prepulse Inhibition and Habituation in Never-Medicated, First-Episode Schizophrenia. Biol. Psychiatry 3223, 121–128.
Mack, V., Burnashev, N., Kaiser, K.M., Rozov, a, Jensen, V., Hvalby, O., Seeburg, P.H., Sakmann, B., Sprengel, R., 2001. Conditional restoration of hippocampal synaptic potentiation in Glur-A-deficient mice. Science 292, 2501–4.
Malinow, R., Malenka, R.C., 2002. AMPA Receptor Trafficking and Synaptic Plasticity. Annu. Rev. Neurosci. 25, 103–126.
Mann, E.O., Suckling, J.M., Hajos, N., Greenfield, S. a, Paulsen, O., 2005. Perisomatic feedback inhibition underlies cholinergically induced fast network oscillations in the rat hippocampus in vitro. Neuron 45, 105–17.
Mattson, M.P., Magnus, T., 2006. Ageing and neuronal vulnerability. Nat. Rev. Neurosci. 7, 278–94.
Mayer, M.L., Westbrook, G.L., Guthrie, P.B., 1984. Voltage-dependent block by Mg2+ of NMDA responses in spinal cord neurones. Nature 309, 261–263.
McCown, T.J., Xiao, X., Li, J., Breese, G.R., Samulski, R.J., 1996. Differential and persistent expression patterns of CNS gene transfer by an adeno-associated virus (AAV) vector. Brain Res. 713, 99–107.
McFarland, W.L., Teitelbaum, H., Hedges, E.K., 1975. Relationship between hippocampal theta activity and running speed in the rat. J. Comp. Physiol. Psychol. 88, 324–328.
McHugh, S.B., Niewoehner, B., Rawlins, J.N.P., Bannerman, D.M., 2008. Dorsal hippocampal N-methyl-d-aspartate receptors underlie spatial working memory performance during non-matching to place testing on the T-maze. Behav. Brain Res. 186, 41–47.
Meyer, U., Feldon, J., Schedlowski, M., Yee, B.K., 2005. Towards an immuno-precipitated neurodevelopmental animal model of schizophrenia. Neurosci. Biobehav. Rev. 29, 913–947.
Miyake, K., Miyake, N., Shimada, T., 2015. Gene Delivery into the Central Nervous System (CNS) Using AAV Vectors. Gene Ther. - Princ. Challenges.
Miyake, N., Miyake, K., Yamamoto, M., Hirai, Y., Shimada, T., 2011. Global gene transfer into the CNS across the BBB after neonatal systemic delivery of single-stranded AAV vectors. Brain Res. 1389, 19–26.
Moghaddam, B., Adams, B., Verma, a, Daly, D., 1997. Activation of glutamatergic neurotransmission by ketamine: a novel step in the pathway from NMDA receptor blockade to dopaminergic and cognitive disruptions associated with the prefrontal cortex. J. Neurosci. 17, 2921–2927.
Mohn, A.R., Gainetdinov, R.R., Caron, M.G., Koller, B.H., Hill, C., Carolina, N., Hughes, H., 1999. Mice with Reduced NMDA Receptor Expression Display Behaviors Related to Schizophrenia. Cell 98, 427–436.
Monyer, H., Burnashev, N., Laurie, D.J., Sakmann, B., Seeburg, P.H., 1994. Developmental and regional expression in the rat brain and functional properties of four NMDA receptors. Neuron 12, 529–540.
Monyer, H., Seeburg, P.H., Wisden, W., 1991. Glutamate-operated channels: Developmentally early and mature forms arise by alternative splicing. Neuron 6, 799–810.
Monyer, H., Sprengel, R., Schoepfer, R., Herb, A., Higuchi, M., Lomeli, H., Burnashev, N., Sakmann, B., Seeburg, P.H., 1992. Heteromeric NMDA Receptors: Molecular and Functional Distinction of Subtypes. Science. 256, 1217–1221.
Morris, R.G.M., Garrud, P., Rawlins, J.N.P., O'Keefe, J., 1982. Place navigation impaired in rats with hippocampal lesions. Nature. 297, 681–683.
Morris, R.G.M., Anderson, E., Lunch, G.S., Baudry, M. 1986. Selective impairment of learning and

blockade of long-term potentiation by an N-methyl-D-aspartate receptor antagonist, AP5. Nature. 319, 774-776.
Moser, E.I., Kropff, E., Moser, M., 2008. Place Cells , Grid Cells , and the Brain ' s Spatial Representation System.
Moy, S.S., Nadler, J.J., Perez, A., Barbaro, R.P., Johns, J.M., Magnuson, T.R., Piven, J., Crawley, J.N., 2004. Sociability and preference for social novelty in five inbred strains: An approach to assess autistic-like behavior in mice. Genes, Brain Behav. 3, 287–302.
Mueser, K.T., McGurk, S.R., 2004. Schizophrenia. Lancet 363, 2063–72.
Murray, A.J., Sauer, J.-F., Riedel, G., McClure, C., Ansel, L., Cheyne, L., Bartos, M., Wisden, W., Wulff, P., 2011. Parvalbumin-positive CA1 interneurons are required for spatial working but not for reference memory. Nat. Neurosci. 14, 297–9.
Murray, A.J., Woloszynowska-Fraser, M.U., Ansel-Bollepalli, L., Cole, K.L.H., Foggetti, A., Crouch, B., Riedel, G., Wulff, P., 2015. Parvalbumin-positive interneurons of the prefrontal cortex support working memory and cognitive flexibility. Sci. Rep. 5, 16778.
Nakazawa, K., Quirk, M.C., Chitwood, R.A., Watanabe, M., Yeckel, M.F., Sun, L.D., Kato, A., Carr, C.A., Johnston, D., Wilson, M.A., Tonegawa, S., 2002. Requirement for Hippocampal CA3 NMDA Receptors in Associative Memory Recall. Science. 297, 211–297.
Nakazawa, K., Zsiros, V., Jiang, Z., Nakao, K., Kolata, S., Zhang, S., Belforte, J.E., 2012. GABAergic interneuron origin of schizophrenia pathophysiology. Neuropharmacology 62, 1574–83.
Nassar, M., Simonnet, J., Lofredi, R., Cohen, I., Savary, E., Yanagawa, Y., Miles, R., Fricker, D., 2015. Diversity and overlap of parvalbumin and somatostatin expressing interneurons in mouse presubiculum. Front. Neural Circuits 9, 20.
Nathanson, J.L., Yanagawa, Y., Obata, K., Callaway, E.M., 2009. Preferential labeling of inhibitory and excitatory cortical neurons by endogenous tropism of adeno-associated virus and lentivirus vectors. Neuroscience 161, 441–450.
Nguyen, R., Morrissey, M.D., Mahadevan, V., Cajanding, J., Woodin, M. a, Yeomans, J.S., Takehara-Nishiuchi, K., Kim, J., 2014. Parvalbumin and GAD65 Interneuron Inhibition in the Ventral Hippocampus Induces Distinct Behavioral Deficits Relevant to Schizophrenia. J. Neurosci. 34, 14948–14960.
Nicoll, R.A., Kauer, J.A., Malenka, R.C., 1988. The current excitement in long term potentiation. Neuron 1, 97–103.
Niewoehner, B., Single, F.N., Hvalby, Ø., Jensen, V., Meyer zum Alten Borgloh, S., Seeburg, P.H., Rawlins, J.N.P., Sprengel, R., Bannerman, D.M., 2007. Impaired spatial working memory but spared spatial reference memory following functional loss of NMDA receptors in the dentate gyrus. Eur. J. Neurosci. 25, 837–46.
Nusser, Z., Sieghart, W., Benke, D., Fritschy, J.M., Somogyi, P., 1996. Differential synaptic localization of two major gamma-aminobutyric acid type A receptor alpha subunits on hippocampal pyramidal cells. Proc.Natl.Acad.Sci.U.S.A. 93, 11939–11944.
O'Keefe, J., Dostrovsky, J., 1971. The hippocampus as a spatial map . Preliminary evidence from unit activity in the freely-moving rat. Brain Research. 34, 171–175.
O'Neill, P.-K., Gordon, J. a., Sigurdsson, T., 2013. Theta Oscillations in the Medial Prefrontal Cortex Are Modulated by Spatial Working Memory and Synchronize with the Hippocampus through Its Ventral Subregion. J. Neurosci. 33, 14211–14224.
O'neill, S.K., Bolger, G.T., 1989. Phencyclidine and MK-801: A behavioral and neurochemical comparison of their interactions with dihydropyridine calcium antagonists. Brain Res. Bull. 22, 611–616.
O`Carroll, R., 2000. Cognitive impairment in schizophrenia. Adv. Psychiatr. Treat. 6, 161–168.
Okabe, S., Miwa, a, Okado, H., 1999. Alternative splicing of the C-terminal domain regulates cell surface expression of the NMDA receptor NR1 subunit. J. Neurosci. 19, 7781–92.
Olney, J.W., Ikonomidou, C., Mosinger, J.L., Frierdich, G., 1989. MK-801 prevents hypobaric-ischemic neuronal degeneration in infant rat brain. J. Neurosci. 9, 1701–4.
Pedersen, C.S., Sørensen, D.B., Parachikova, A.I., Plath, N., 2014. PCP-induced deficits in murine nest building activity: Employment of an ethological rodent behavior to mimic negative-like symptoms of schizophrenia. Behav. Brain Res. 273, 63–72.
Penn, A.C., Balik, A., Wozny, C., Cais, O., Greger, I.H., 2012. Activity-mediated AMPA receptor remodeling, driven by alternative splicing in the ligand-binding domain. Neuron 76, 503–10.
Perova, Z., Delevich, K., Li, B., 2015. Depression of Excitatory Synapses onto Parvalbumin Interneurons in the Medial Prefrontal Cortex in Susceptibility to Stress. J. Neurosci. 35, 3201–3206.
Perry, W., Geyer, M. a, Braff, D.L., 1999. Sensorimotor gating and thought disturbance measured in

close temporal proximity in schizophrenic patients. Arch. Gen. Psychiatry 56, 277–281.
Picchioni, M.M., Murray, R.M., 2007. Schizophrenia. Bmj 335, 91–95.
Powell, C.M., Miyakawa, T., 2006. Schizophrenia-Relevant Behavioral Testing in Rodent Models: A Uniquely Human Disorder? Biol. Psychiatry 59, 1198–1207.
Pozzi, L., Dorocic, I.P., Wang, X., Carlén, M., Meletis, K., 2014. Mice Lacking NMDA Receptors in Parvalbumin Neurons Display Normal Depression-Related Behavior and Response to Antidepressant Action of NMDAR Antagonists. PLoS One 9, e83879.
Pratt, J., Winchester, C., Dawson, N., Morris, B., 2012. Advancing schizophrenia drug discovery: optimizing rodent models to bridge the translational gap. Nat. Rev. Drug Discov. 11, 560–79.
Procaccini, C., Aitta-aho, T., Jaako-Movits, K., Zharkovsky, A., Panhelainen, A., Sprengel, R., Linden, A.-M., Korpi, E.R., 2011. Excessive novelty-induced c-Fos expression and altered neurogenesis in the hippocampus of GluA1 knockout mice. Eur. J. Neurosci. 33, 161–74.
Procaccini, C., Maksimovic, M., Aitta-Aho, T., Korpi, E.R., Linden, a-M., 2013. Reversal of novelty-induced hyperlocomotion and hippocampal c-Fos expression in GluA1 knockout male mice by the mGluR2/3 agonist LY354740. Neuroscience 250C, 189–200.
Ralph-Williams, R.J., Lehmann-Masten, V., Otero-Corchon, V., Low, M.J., Geyer, M. a, 2002. Differential effects of direct and indirect dopamine agonists on prepulse inhibition: a study in D1 and D2 receptor knock-out mice. J. Neurosci. 22, 9604–11.
Reisel, D., Bannerman, D.M., Schmitt, W.B., Deacon, R.M.J., Flint, J., Borchardt, T., Seeburg, P.H., Rawlins, J.N.P., 2002. Spatial memory dissociations in mice lacking GluR1. Nat. Neurosci. 5, 868–73.
Resnik, E., McFarland, J.M., Sprengel, R., Sakmann, B., Mehta, M.R., 2012. The effects of GluA1 deletion on the hippocampal population code for position. J. Neurosci. 32, 8952–68.
Ripke, S., Dushlaine, C.O., Chambert, K., Moran, J.L., Kähler, A.K., Akterin, S., Bergen, S.E., Collins, A.L., Crowley, J.J., Fromer, M., Kim, Y., Lee, S.H., Magnusson, P.K.E., Sanchez, N., Stahl, E.A., Williams, S., Wray, N.R., Xia, K., Bettella, F., Borglum, A.D., Bulik-sullivan, B.K., Golimbet, V., Hamshere, M.L., Holmans, P., Hougaard, D.M., Kendler, K.S., Lin, K., Morris, D.W., Mors, O., Mortensen, P.B., Neale, B.M., Neill, F.A.O., Owen, M.J., Milovancevic, M.P., Posthuma, D., Powell, J., Bramon, E., Corvin, A.P., Donovan, M.C.O., Stefansson, K., Scolnick, E., 2013. Genome-wide association analysis identifies 13 new risk loci for schizophrenia. Nat. Publ. Gr. 45, 1150–1159.
Ripke, S., Neale, B.M., Corvin, A., Walters, J.T.R., Farh, K.-H., Holmans, P. a., Lee, P., Bulik-Sullivan, B., Collier, D. a., Huang, H., Pers, T.H., Agartz, I., Agerbo, E., Albus, M., Alexander, M., Amin, F., Bacanu, S. a., Begemann, M., Belliveau Jr, R. a., Bene, J., Bergen, S.E., Bevilacqua, E., Bigdeli, T.B., Black, D.W., Bruggeman, R., Buccola, N.G., Buckner, R.L., Byerley, W., Cahn, W., Cai, G., Campion, D., Cantor, R.M., Carr, V.J., Carrera, N., Catts, S. V., Chambert, K.D., Chan, R.C.K., Chen, R.Y.L., Chen, E.Y.H., Cheng, W., Cheung, E.F.C., Ann Chong, S., Robert Cloninger, C., Cohen, D., Cohen, N., Cormican, P., Craddock, N., Crowley, J.J., Curtis, D., Davidson, M., Davis, K.L., Degenhardt, F., Del Favero, J., Demontis, D., Dikeos, D., Dinan, T., Djurovic, S., Donohoe, G., Drapeau, E., Duan, J., Dudbridge, F., Durmishi, N., Eichhammer, P., Eriksson, J., Escott-Price, V., Essioux, L., Fanous, A.H., Farrell, M.S., Frank, J., Franke, L., Freedman, R., Freimer, N.B., Friedl, M., Friedman, J.I., Fromer, M., Genovese, G., Georgieva, L., Giegling, I., Giusti-Rodríguez, P., Godard, S., Goldstein, J.I., Golimbet, V., Gopal, S., Gratten, J., de Haan, L., Hammer, C., Hamshere, M.L., Hansen, M., Hansen, T., Haroutunian, V., Hartmann, A.M., Henskens, F. a., Herms, S., Hirschhorn, J.N., Hoffmann, P., Hofman, A., Hollegaard, M. V., Hougaard, D.M., Ikeda, M., Joa, I., Julià, A., Kahn, R.S., Kalaydjieva, L., Karachanak-Yankova, S., Karjalainen, J., Kavanagh, D., Keller, M.C., Kennedy, J.L., Khrunin, A., Kim, Y., Klovins, J., Knowles, J. a., Konte, B., Kucinskas, V., Ausrele Kucinskiene, Z., Kuzelova-Ptackova, H., Kähler, A.K., Laurent, C., Lee Chee Keong, J., Hong Lee, S., Legge, S.E., Lerer, B., Li, M., Li, T., Liang, K.-Y., Lieberman, J., Limborska, S., Loughland, C.M., Lubinski, J., Lönnqvist, J., Macek Jr, M., Magnusson, P.K.E., Maher, B.S., Maier, W., Mallet, J., Marsal, S., Mattheisen, M., Mattingsdal, M., McCarley, R.W., McDonald, C., McIntosh, A.M., Meier, S., Meijer, C.J., Melegh, B., Melle, I., Mesholam-Gately, R.I., Metspalu, A., Michie, P.T., Milani, L., Milanova, V., Mokrab, Y., Morris, D.W., Mors, O., Murphy, K.C., Murray, R.M., Myin-Germeys, I., Müller-Myhsok, B., Nelis, M., Nenadic, I., Nertney, D. a., Nestadt, G., Nicodemus, K.K., Nikitina-Zake, L., Nisenbaum, L., Nordin, A., O'Callaghan, E., O'Dushlaine, C., O'Neill, F.A., Oh, S.-Y., Olincy, A., Olsen, L., Van Os, J., Endophenotypes International Consortium, P., Pantelis, C., Papadimitriou, G.N., Papiol, S., Parkhomenko, E., Pato, M.T., Paunio, T., Pejovic-Milovancevic, M., Perkins, D.O., Pietiläinen, O., Pimm, J., Pocklington, A.J., Powell, J., Price, A., Pulver, A.E., Purcell, S.M., Quested, D., Rasmussen, H.B., Reichenberg, A., Reimers, M. a., Richards, A.L., Roffman, J.L., Roussos, P., Ruderfer, D.M.,

Salomaa, V., Sanders, A.R., Schall, U., Schubert, C.R., Schulze, T.G., Schwab, S.G., Scolnick, E.M., Scott, R.J., Seidman, L.J., Shi, J., Sigurdsson, E., Silagadze, T., Silverman, J.M., Sim, K., Slominsky, P., Smoller, J.W., So, H.-C., Spencer, C. a., Stahl, E. a., Stefansson, H., Steinberg, S., Stogmann, E., Straub, R.E., Strengman, E., Strohmaier, J., Scott Stroup, T., Subramaniam, M., Suvisaari, J., Svrakic, D.M., Szatkiewicz, J.P., Söderman, E., Thirumalai, S., Toncheva, D., Tosato, S., Veijola, J., Waddington, J., Walsh, D., Wang, D., Wang, Q., Webb, B.T., Weiser, M., Wildenauer, D.B., Williams, N.M., Williams, S., Witt, S.H., Wolen, A.R., Wong, E.H.M., Wormley, B.K., Simon Xi, H., Zai, C.C., Zheng, X., Zimprich, F., Wray, N.R., Stefansson, K., Visscher, P.M., Trust Case-Control Consortium, W., Adolfsson, R., Andreassen, O. a., Blackwood, D.H.R., Bramon, E., Buxbaum, J.D., Børglum, A.D., Cichon, S., Darvasi, A., Domenici, E., Ehrenreich, H., Esko, T., Gejman, P. V., Gill, M., Gurling, H., Hultman, C.M., Iwata, N., Jablensky, A. V., Jönsson, E.G., Kendler, K.S., Kirov, G., Knight, J., Lencz, T., Levinson, D.F., Li, Q.S., Liu, J., Malhotra, A.K., McCarroll, S. a., McQuillin, A., Moran, J.L., Mortensen, P.B., Mowry, B.J., Nöthen, M.M., Ophoff, R. a., Owen, M.J., Palotie, A., Pato, C.N., Petryshen, T.L., Posthuma, D., Rietschel, M., Riley, B.P., Rujescu, D., Sham, P.C., Sklar, P., St Clair, D., Weinberger, D.R., Wendland, J.R., Werge, T., Daly, M.J., Sullivan, P.F., O'Donovan, M.C., 2014. Biological insights from 108 schizophrenia-associated genetic loci. Nature 511, 421–427.

Rogan, S.C., Roth, B.L., 2011. Remote Control of Neuronal Signaling 63, 291–315.

Romberg, C., Raffel, J., Martin, L., Sprengel, R., Seeburg, P.H., Rawlins, J.N.P., Bannerman, D.M., Paulsen, O., 2009. Induction and expression of GluA1 (GluR-A)-independent LTP in the hippocampus. Eur. J. Neurosci. 29, 1141–52.

Rondi-Reig, L., 2006. Impaired Sequential Egocentric and Allocentric Memories in Forebrain-Specific-NMDA Receptor Knock-Out Mice during a New Task Dissociating Strategies of Navigation. J. Neurosci. 26, 4071–4081.

Rotaru, D.C., Lewis, D.A., Gonzalez-Burgos, G., 2013. The role of glutamatergic inputs onto parvalbumin-positive interneurons: relevance for schizophrenia. Rev Neurosci. 23, 97–109.

Rotaru, D.C., Yoshino, H., Lewis, D. a, Ermentrout, G.B., Gonzalez-Burgos, G., 2011. Glutamate receptor subtypes mediating synaptic activation of prefrontal cortex neurons: relevance for schizophrenia. J. Neurosci. 31, 142–56.

Salgado, S., Kaplitt, M.G., 2015. The nucleus accumbens: A comprehensive review. Stereotact. Funct. Neurosurg. 93, 75–93.

Samulski, R.J., Chang, L.S., Shenk, T., 1989. Helper-free stocks of recombinant adeno-associated viruses: normal integration does not require viral gene expression. J. Virol. 63, 3822–8.

Sanderson, D.J., Gray, A., Simon, A., Taylor, A.M., Deacon, R.M.J., Seeburg, P.H., Sprengel, R., Good, M.A., Rawlins, J.N.P., Bannerman, D.M., 2007. Deletion of Glutamate Receptor-A (GluR-A) AMPA Receptor Subunits Impairs One-Trial Spatial Memory. Behavioural Neuroscience, 121, 559-569.

Sanderson, D.J., Bannerman, D.M., 2012. The role of habituation in hippocampus-dependent spatial working memory tasks: evidence from GluA1 AMPA receptor subunit knockout mice. Hippocampus 22, 981–94.

Sanderson, D.J., Good, M. a, Skelton, K., Sprengel, R., Seeburg, P.H., Rawlins, J.N.P., Bannerman, D.M., 2009. Enhanced long-term and impaired short-term spatial memory in GluA1 AMPA receptor subunit knockout mice: evidence for a dual-process memory model. Learn. Mem. 16, 379–86.

Sanderson, D.J., Hindley, E., Smeaton, E., Denny, N., Taylor, A., Barkus, C., Sprengel, R., Seeburg, P.H., Bannerman, D.M., 2011a. Deletion of the GluA1 AMPA receptor subunit impairs recency-dependent object recognition memory. Learn. Mem. 18, 181–90.

Sanderson, D.J., Sprengel, R., Seeburg, P.H., Bannerman, D.M., 2011b. Deletion of the GluA1 AMPA receptor subunit alters the expression of short-term memory. Learn. Mem. 18, 128–31.

Sauer, B., Henderson, N., 1988. Site-specific DNA recombination in mammalian cells by the Cre recombinase of bacteriophage P1. Proc. Natl. Acad. Sci. U. S. A. 85, 5166–70.

Saunders, J.A., Tatard-Leitman, V.M., Suh, J., Billingslea, E.N., Roberts, T.P., Siegel, S.J., 2013. Knockout of NMDA Receptors in Parvalbumin Interneurons Recreates Autism-Like Phenotypes. Autism Res. 6, 69–77.

Schmitt, W.B., Deacon, R.M.J., Seeburg, P.H., Rawlins, J.N.P., Bannerman, D.M., 2003. A within-subjects, within-task demonstration of intact spatial reference memory and impaired spatial working memory in glutamate receptor-A-deficient mice. J. Neurosci. 23, 3953–9.

Schmitt, W.B., Sprengel, R., Mack, V., Draft, R.W., Seeburg, P.H., Deacon, R.M.J., Rawlins, J.N.P., Bannerman, D.M., 2005. Restoration of spatial working memory by genetic rescue of GluR-A-deficient mice. Nat. Neurosci. 8, 270–2.

Schmidt-kastner, R., 2015. Review Genomic Approach to Selective Vulnerability of the Hippocampus

in Brain Ischemia – Hypoxia. Neuroscience 309, 259–279.

Schobel, S.A., Chaudhury, N.H., Khan, U.A., Paniagua, B., Styner, M.A., Asllani, I., Inbar, B.P., Corcoran, C.M., Lieberman, J.A., Moore, H., Small, S.A., 2013. Article Imaging Patients with Psychosis and a Mouse Model Establishes a Spreading Pattern of Hippocampal Dysfunction and Implicates Glutamate as a Driver. Neuron 78, 81–93.

Schulman, J.J., Cancro, R., Lowe, S., Lu, F., Walton, K.D., Llinás, R.R., Ridder, D. De, 2011. Imaging of thalamocortical dysrhythmia in neuropsychiatry. Frontiers in Human Neuroscience. 5, 1–11.

Schwarcz, R., Rassoulpour, A., Wu, H.Q., Medoff, D., Tamminga, C.A., Roberts, R.C., 2001. Increased cortical kynurenate content in schizophrenia. Biol. Psychiatry 50, 521–530.

Scoviille, W.B., Milner, B., 1957. Loss of Recent Memory After Bilateral Hippocampal Lesions. J Neurol. Neurosurg. Psychiaty 20, 11–21.

Seeman, P., Lee, T., 1975. Antipsychotic Drugs: Direct Correllation between Clinical Potency and Presynaptic Action on Dopamine Neurons. Science. 188, 1217–1219.

Seeman, P., Lee, T., Chau-Wong, M., Wong, K., 1976. Antipsychotic drugs doses and neuroleptic / dopamine receptors. Nature. 261, 717–719.

Shepherd, J.D., Huganir, R.L., 2007. The cell biology of synaptic plasticity: AMPA receptor trafficking. Annu. Rev. Cell Dev. Biol. 23, 613–643.

Sigurdsson, T., Stark, K.L., Karayiorgou, M., Gogos, J. a, Gordon, J. a, 2010. Impaired hippocampal-prefrontal synchrony in a genetic mouse model of schizophrenia. Nature 464, 763–7.

Sohal, V.S., Zhang, F., Yizhar, O., Deisseroth, K., 2009. Parvalbumin neurons and gamma rhythms enhance cortical circuit performance. Nature 459, 698–702.

Sommer, B., Keinanen, K., Verdoorn, T.A., Wisden, W., Burnashev, N., Herb, A., Kohler, M., Takagi, T., Sakmann, B., Seeburgt, P.H., 1989. Flip and Flop : A Cell-Specific Functional Switch in Glutamate-Operated Channels of the CNS. Science. 249, 1580-1585.

Somogyi, P., Freund, T.F., Hodgson, A.J., Somogyi, J., Beroukas, D., Chubb, I.W., 1985. Identified axo-axonic cells are immunoreactive for GABA in the hippocampus and visual cortex of the cat. Brain Res. 332, 143–149.

Stachniak, T.J., Ghosh, A., Sternson, S.M., 2014. Chemogenetic Synaptic Silencing of Neural Circuits Localizes a Hypothalamus→Midbrain Pathway for Feeding Behavior. Neuron 82, 797–808.

Stujenske, J.M., Spellman, T., Gordon, J.A., 2015. Modeling the Spatiotemporal Dynamics of Light and Heat Propagation for In Vivo Optogenetics. Cell Rep. 12, 525–534.

Sucher, N.J., Akbarian, S., Chi, C.L., Leclerc, C.L., Awobuluyi, M., Deitcher, D.L., Wu, M.K., Yuan, J.P., Jones, E.G., Lipton, S.A., 1995. Developmental and regional expression pattern of a novel NMDA receptor-like subunit (NMDAR-L) in the rodent brain. J. Neurosci. 15, 6509–6520.

Tamura, M., Mukai, J., Gordon, J.A., Gogos, J.A., 2016. Developmental Inhibition of Gsk3 Rescues Behavioral and Neurophysiological Deficits in a Mouse Model of Schizophrenia Predisposition. Neuron 89, 1100–1109.

Tatard-Leitman, V.M., Jutzeler, C.R., Suh, J., Saunders, J. a, Billingslea, E.N., Morita, S., White, R., Featherstone, R.E., Ray, R., Ortinski, P.I., Banerjee, A., Gandal, M.J., Lin, R., Alexandrescu, A., Liang, Y., Gur, R.E., Borgmann-Winter, K.E., Carlson, G.C., Hahn, C.-G., Siegel, S.J., 2014. Pyramidal Cell Selective Ablation of N-Methyl-D-Aspartate Receptor 1 Causes Increase in Cellular and Network Excitability. Biol. Psychiatry 1–12.

Tsien, J., Chen, D., Gerber, D., Anderson, D., Mayford, M., Kandel, E., Tonegawa, S., 1996a. Subregion and cell type restricted gene knockout in mouse brain. Cell 87, 1317–1324.

Tsien, J., Huerta, P., Tonegawa, S., 1996b. The essential role of hippocampal CA1 NMDA receptor-dependent synaptic plasticity in spatial memory. Cell 87, 1327–1338.

Tye, K.M., Mirzabekov, J.J., Warden, M.R., Ferenczi, E. a., Tsai, H.-C., Finkelstein, J., Kim, S.-Y., Adhikari, A., Thompson, K.R., Andalman, A.S., Gunaydin, L. a., Witten, I.B., Deisseroth, K., 2012. Dopamine neurons modulate neural encoding and expression of depression-related behaviour. Nature 493, 537–541.

Uhlhaas, P.J., Singer, W., 2010. Abnormal neural oscillations and synchrony in schizophrenia. Nat. Rev. Neurosci. 11, 100–13.

Umbricht, D., Alberati, D., Martin-Facklam, M., Borroni, E., Youssef, E.A., Ostland, M., Wallace, T.L., Knoflach, F., Dorflinger, E., Wettstein, J.G., Bausch, A., Garibaldi, G., Santarelli, L., 2014. Effect of bitopertin, a glycine reuptake inhibitor, on negative symptoms of schizophrenia: a randomized, double-blind, proof-of-concept study. JAMA Psychiatry 71, 637–646.

Vardigan, J.D., Huszar, S.L., McNaughton, C.H., Hutson, P.H., Uslaner, J.M., 2010. MK-801 produces a deficit in sucrose preference that is reversed by clozapine, d-serine, and the metabotropic glutamate 5 receptor positive allosteric modulator CDPPB: Relevance to negative symptoms

associated with schizophrenia? Pharmacol. Biochem. Behav. 95, 223–229.
Volk, D.W., Austin, M.C., Pierri, J.N., Sampson, A.R., Lewis, D.A., 2001. GABA transporter-1 mRNA in the prefrontal cortex in schizophrenia: Decreased expression in a subset of neurons. Am. J. Psychiatry 158, 256–265.
Volk, D.W., Pierri, J.N., Fritschy, J.-M., Auh, S., Sampson, A.R., Lewis, D.A., 2002. Reciprocal alterations in pre- and postsynaptic inhibitory markers at chandelier cell inputs to pyramidal neurons in schizophrenia. Cereb. Cortex 12, 1063–1070.
von Engelhardt, J., Doganci, B., Jensen, V., Hvalby, Ø., Göngrich, C., Taylor, A., Barkus, C., Sanderson, D.J., Rawlins, J.N.P., Seeburg, P.H., Bannerman, D.M., Monyer, H., 2008. Contribution of hippocampal and extra-hippocampal NR2B-containing NMDA receptors to performance on spatial learning tasks. Neuron 60, 846–60.
Vyazovskiy, V. V, Riedner, B.A., Cirelli, C., Tononi, G., 2007. Sleep homeostasis and cortical synchronization: II. A local field potential study of sleep slow waves in the rat. Sleep 30, 1631–42.
Walters, J.T.R., Owen, M.J., 2007. Endophenotypes in psychiatric genetics. Mol. Psychiatry 12, 886–90.
Wang, H.-X., Gao, W.-J., 2010. Development of calcium-permeable AMPA receptors and their correlation with NMDA receptors in fast-spiking interneurons of rat prefrontal cortex. J. Physiol. 588, 2823–38.
Wang, G-W and Cai, J-X., 2006. Disconnection of the hippocampal-prefrontal cortical circuits impairs spatial working memory performance in rats. Behavioural Brain Research. 175, 329-336.
Weickert, C.S., Hyde, T.M., Lipska, B.K., Herman, M.M., Weinberger, D.R., Kleinman, J.E., 2003. Reduced brain-derived neurotrophic factor in prefrontal cortex of patients with schizophrenia. Mol. Psychiatry 8, 592–610.
Weinberger, D.R., 1999. Cell biology of the hippocampal formation in schizophrenia. Biol. Psychiatry 45, 395–402.
Wiedholz, L.M., Owens, W. a, Horton, R.E., Feyder, M., Karlsson, R.-M., Hefner, K., Sprengel, R., Celikel, T., Daws, L.C., Holmes, a, 2008. Mice lacking the AMPA GluR1 receptor exhibit striatal hyperdopaminergia and “schizophrenia-related” behaviors. Mol. Psychiatry 13, 631–40.
Wolff, A.R., Bilkey, D.K., 2010. The maternal immune activation (MIA) model of schizophrenia produces pre-pulse inhibition (PPI) deficits in both juvenile and adult rats but these effects are not associated with maternal weight loss. Behav. Brain Res. 213, 323–327.
Wolff, A.R., Cheyne, K.R., Bilkey, D.K., 2011. Behavioural deficits associated with maternal immune activation in the rat model of schizophrenia. Behav. Brain Res. 225, 382–387.
Wright, I., Rabe-Hesketh, S., Woodruff, P.W.R., David, A.S., Murray, R.M., Bullmore, E.T., 2000. Meta-Analysis of Regional Brain Volumes in Schizophrenia 157, 16–25.
Wu, J., Zou, H., Strong, J. a, Yu, J., Zhou, X., Xie, Q., Zhao, G., Jin, M., Yu, L., 2005. Bimodal effects of MK-801 on locomotion and stereotypy in C57BL/6 mice. Psychopharmacology (Berl). 177, 256–63.
Wu, E.Q., Birnbaum, H.G., Shi, L., Ball, D.E., Kessler, R.C., Moulis, M., Aggarwal, J., 2005. The Economic Burden of Schizophrenia in the United States in 2002. J. Clin. Psychiatry 66, 1122–1129.
Yamada, M.K., Nakanishi, K., Ohba, S., Nakamura, T., Ikegaya, Y., Nishiyama, N., Matsuki, N., 2002. Brain-derived neurotrophic factor promotes the maturation of GABAergic mechanisms in cultured hippocampal neurons. J. Neurosci. 22, 7580–5.
Yang, Y., Lee, P., Sternson, S.M., 2015. Cell type-specific pharmacology of NMDA receptors using masked MK801. Elife 4, 1–12.
Yang, H., Wang, H., Jaenisch, R., 2014. Generating genetically modified mice using CRISPR / Cas-mediated genome engineering 11. 1956-1968

Yates, J.W., Meij, J.T.A., Sullivan, J.R., Richtand, N.M., Yu, L., 2007. Bimodal effect of amphetamine on motor behaviors in C57BL/6 mice. Neurosci. Lett. 427, 66–70.
Yizhar, O., Fenno, L.E., Prigge, M., Schneider, F., Davidson, T.J., Shea, D.J.O., Sohal, V.S., Goshen, I., Finkelstein, J., Paz, J.T., Stehfest, K., Fudim, R., Ramakrishnan, C., Huguenard, J.R., Hegemann, P., Deisseroth, K., 2011. Neocortical excitation / inhibition balance in information processing and social dysfunction. Nature 477, 171–178.
Zamanillo, D., Sprengel, R., Hvalby, Ø., Jensen, V., Burnashev, N., Rozov, A., Kaiser, K.M.M., Koster, H., Borchardt, T., Worley, P., Lubke, J., Frotscher, M., Kelly, P., Sommer, B., Andersen, P., Seeburg, P.H., Sakmann, B., 1999. Importance of AMPA Receptors for Hippocampal Synaptic Plasticity But Not for Spatial Learning. Science 284, 1805–1811.
Zang, Y., Llinas, R., Lisman, J., 2009. Inhibition of NMDARs in the nucleus reticularis of the thalamus

produces delta frequency bursting. Front. Neural Circuits 3, 1–9.
Zemelman, B. V., Lee, G.A., Ng, M., Miesenböck, G., 2002. Selective photostimulation of genetically chARGed neurons. Neuron 33, 15–22.
Zhu, J.J., Esteban, J. a, Hayashi, Y., Malinow, R., 2000. Postnatal synaptic potentiation: delivery of GluR4-containing AMPA receptors by spontaneous activity. Nat. Neurosci. 3, 1098–106.